Integrable Anderson impurities in pseudogap systems

Dissertation

to obtain the degree of a

Doctor of Natural Sciences (Dr. rer. nat.)

of the Faculty of Mathematics and Natural Sciences

(Department of Physics)

of the Bergische Universität Wuppertal

presented by

Yahya Öz

30th November 2017

This dissertation can be cited as follows:

Die Dissertation kann wie folgt zitiert werden:

urn:nbn:de:hbz:468-20180109-152128-5
[http://nbn-resolving.de/urn/resolver.pl?urn=urn%3Anbn%3Ade%3Ahbz%3A468-20180109-152128-5]

Contents

1 Introduction

The goal of theoretical physics is to formulate statements from microscopic contexts, which can be tested experimentally. For example, in quantum field theory, starting from the fundamental interactions between the elementary particles, one computes cross sections, which can be measured in scattering experiments. An example from solid-state physics is the calculation of the electrical resistance or similar transport variables of a given material based on its composition. Within the framework of the linear response theory such measurable quantities are given by the correlation functions of the model. In practice the calculation of correlation functions even in the simplest interacting systems is problematic, because the Hilbert space of an N-particle problem grows exponentially with the number of particles N. An obvious strategy is to simplify the models so far that an exact solution is possible. The simplest approximations include effective single-particle models like the band model of solid state physics, with which many fundamental properties of a solid can be understood. However, such approximations are limited and cannot explain many collective phenomena in strongly correlated systems.

In today's research, two approaches (or a combination of both) are used in the investigation of many-particle problems. These are, on the one hand, calculations done with perturbation theory and, on the other hand, the use of large computers and sophisticated algorithms. However, both methods have a limited range of validity and typically fail in one-dimensional models [47].

A further possibility is to search for multi-particle systems whose properties are exactly calculable. At first sight this may be a strong limitation, however, one can expect that the study of exactly solvable ("integrable") models makes a better understanding of generic interacting multi-particle systems possible. This assumption is supported by the result that systems of statistical mechanics can be classified into universality classes. Models of the same class may be very different microscopically, but they can show similar macroscopic behaviour in the vicinity of a critical point. Although there exists a well-defined notion of integrability in classical mechanics due to Liouville's theorem, no such general notion is known for quantum mechanical systems. Still, certain classes of systems have been found that admit an exact solution.

Of particular interest are integrable models, which are related to solutions of the Yang-Baxter equation. This class includes the one-dimensional anisotropic spin-$\frac{1}{2}$ Heisenberg model (XXZ chain) as well as the Hubbard model. Another integrable model is the Anderson impurity model (AIM), which can be solved with coordiante Bethe ansatz. These models are investigated in this work. An overview of these models as well as their applications in solid-state physics can be found in the book [36] and in the review[124].

The one-dimensional anisotropic spin-$\frac{1}{2}$ Heisenberg model is a prototype of an integrable model and has been studied intensively for a long time. Hans Bethe first succeeded in

calculating the spectrum (not explicitly) and the eigenvectors of the isotropic spin-$\frac{1}{2}$ Heisenberg model with the coordinate Bethe ansatz for finite L [18]. Further important steps to a better understanding of the model were the discovery of the link to vertex models of statistical physics [12] and the abstraction of the method of the Bethe ansatz ("algebraic" Bethe ansatz) [75]. The underlying structure can be identified as a scattering problem of two particles. The scattering matrix of the many-particle problem is reduced to a product of scattering matrices of two particles with arbitrary succession. The consistency equation of the two-particle scattering matrix is the Yang-Baxter equation. The Yang-Baxter equation for triple R-matrices forms the basis for all Bethe ansatz approachable models, because, remarkably, the same equation also applies to the local Boltzmann weights of the solvable two-dimensional classical models, where it gives rise to a commuting family of transfer matrices. As a consequence of this mutual relationship between both types of models, it follows that the logarithmic derivative of the row-to-row transfer matrix of a given solvable two-dimensional model taken at some special spectral parameter also defines the Hamiltonian of an integrable quantum chain.

Since Lieb and Wu found the coordinate Bethe ansatz solution for the Hubbard model [79], it "has become a laboratory for theoretical studies of non-perturbative effects in strongly correlated electron systems" [36, p. iii]. Lieb and Wu calculated "the ground state energy and demonstrated that the Hubbard model undergoes a Mott metal-insulator transition at half filling (one electron per site) with critical interaction strength $U = 0$" [36, p. 9]. To supply "complementary insights to what is [...] [to be discovered] from the exact solution or as an ultimate test of their quality" [36, p. iii], many of the approximative tools existing for the analysis of such systems were used on this model. Simultaneously, "due to the synthesis of new quasi one-dimensional materials and the [...] [improvement] of experimental techniques, the Hubbard model [...] [is not considered as a toy model anymore, instead it is regarded as a paragon] of experimental relevance for strongly correlated electron systems" [36, p. iii]. Due to the continuous endeavor to enhance our knowledge of one-dimensional correlated electron systems, there are many review articles and books available covering several facets of the general theory and also theoretical methods and the Bethe ansatz.

Takahashi suggested that the solutions of the Lieb and Wu equations are classified in terms of a "string hypothesis" [117]. The Bethe ansatz roots corresponding to excited states of the model mold into certain string patterns in the complex plane. Takahashi takes advantage of this observation. To replace the equations of Lieb and Wu by more elementary ones Takahashi used this string hypothesis in the thermodynamical limit and then cotinued to deduce an infinite "set of non-linear integral equations, which determine the Gibbs free energy of the Hubbard model. These integral equations are known as thermodynamic Bethe ansatz (TBA) equations" [36, p. 9]. Physical quantities "that pertain[...] to the energy spectrum of the Hubbard model" [36, p. 9] can be determined with Takahashi's

equations, in combination with the thermodynamic Bethe ansatz equations [142, 117]. "By placing it into the [...] [scheme] of the quantum inverse scattering method" [36, p. 11] Shastry developed a novel way for investigating the Hubbard model. By the use of "a Jordan-Wigner transformation he mapped the Hubbard model to a spin model[. He showed that the arising] [...] spin Hamiltonian commutes with the row-to-row transfer matrix of a related covering vertex model" [36, p. 11] [112]. Shastry embedded the spin model "into the general classification of "integrable models" [36, p. 11] by deriving the R-matrix [111]. "This result was of crucial importance for the [...] [column-to-column] transfer matrix approach to the thermodynamics [63] of the Hubbard model [...]. This approach allows for a drastically simplified description of the thermodynamics in terms of the solution of a finite set of non-linear integral equations, rather than the infinite set originally obtained by Takahashi in 1972 [117]. Within the [...] [column-to-column] transfer matrix approach thermodynamic quantities can be calculated numerically with a very high precision. The approach can be extended to the calculation of correlation lengths at finite temperature [120, 129]" [36, p. 11].
The subject of the Anderson impurity model "is a microscopic theory of dilute magnetic alloys. [...] A small amount of magnetic impurities dissolved in a non-magnetic meta [...] [influences its features extremely]. [...] The perturbation theory in the impurity-conduction electron exchange interaction is not applicable at low temperatures" [124, p. 457]. This is the issue encountered in the theory of this phenomenon. "The exchange interaction [...] [among] the magnetic impurity and the electrons, which is responsible for those outstanding effects in [...] [the dilute magnetic] alloys, can be [...] [characterized] by a simple model Hamiltonian. It is the [...] s-d exchange model of the Kondo physics [74], which is [...] one of the first and [...] simplest quantum field theories with a growth of coupling at low energies" [124, p. 457]. Many of the models, which have been used for the "description of dilute magnetic alloys[, especially the s-d exchange Kondo model and the Anderson impurity model,] [...] are integrable" [124, p. 453] and the solutions were derived [124]. It is noteworthy that both the s-d exchange Kondo model and the Anderson impurity model are models in the continuum and not lattice models like the one-dimensional anisotropic spin-$\frac{1}{2}$ Heisenberg model or the Hubbard model.

1.1 Experimental results

Numerous experimental realizations of three-dimensional solids can be found, which show structures of quasi-one-dimensional subsystems. Since the interactions between the chains in such materials are often negligibly small, the substructures determine the behaviour of the three-dimensional body. For the first time spin-chain-like systems were investigated in experimental solid state physics in the early 1970s. One of the classic examples is the early neutron scattering experiments of Tetramethyl-Trichloro-Manganate (TMMC,

$(CH_3)_4NMnCl_3$) [60]. One of the qualitative Heisenberg chains was first considered by Heilmann et. al. ($CuCl_2 \cdot 2N(C_5D_5)$) [59].
Another, recent example of a very well-established spin-$\frac{1}{2}$ chain system is Copper pyrazine dinitrate ($CuPzN$). In this system, copper atoms are doubly positively ionized by the neighboring nitrate groups. The Pyrazin rings lying between the copper atoms mediate the interaction of the spin moments. This material belongs to one of the best implementations of an antiferromagnetic spin-$\frac{1}{2}$ Heisenberg chain and has a phase transition as a function of an external magnetic field [76].
Also chain models, which can be well described by higher spin models $\left(\text{e.g. } s = 1, \frac{3}{2}, 2, \frac{5}{2}\right)$ like the antiferromagnetic spin-s Heisenberg chain, were implemented experimentally [87].
There are also spin-chain models, which cannot be described only by bilinear next-neighbor coupling terms, but also by necessary biquadratic next-neighbor coupling terms, for example Lithium-vanadium metagermanate ($LiVGe_2O_6$) [88].
It should be noted that one-dimensional models are relevant under two conditions: Either the structure of a crystal indicates its one-dimensionality, or a three-dimensional system can be mapped on one dimension.

1.2 Pseudogap systems

The physics of diluted magnetic interference in electronic hosts has been an established discipline of electronic correlation physics since Kondo's work [74]. Although the interaction of the band electrons is irrelevant among each other, the studied systems show a resistance minimum at low temperatures instead of a monotonous decrease of the resistance while lowering the temperature. Furthermore, the susceptibility contribution of the impurity shows not the expected paramagnetic value, instead it shows the value of a screened impurity spin. The size of the screening, as well as a possibly remaining entropy at temperature zero depend on the ratio of the number of energetically degenerate charge channels and the value of the impurity spins (one-channel vs. multi-channel Kondo physics).
The complexity of the phenomena is due to the correlation of the host electrons, which do not interact directly with each other, but via the impurity spin. The modeling is typically performed by the Anderson impurity model [3], which gives in the limit of strong Coulomb interaction in the local d- or f-orbitals the s-d exchange Kondo model [108]. Both models describe an (anti-ferromagnetic) coupling of band electrons to a local impurity with spin degree of freedom, which in the case of the Anderson impurity model also has a charge degree of freedom. The observed phenomena are abundant and the theory is as intricate as the theory of the one-dimensional spin-$\frac{1}{2}$ Heisenberg or the Hubbard model. In fact, very similar Bethe ansatz techniques were successfully used on bulk properties and impurity contributions of the above-mentioned models. The Kondo

effect in metals is well understood due to analytical results (perturbative: [74], exactly: [7, 9, 138, 40, 99, 33, 124, 121], conformal field theory: [2, 1]) as well as numerical results (renormalization group (RG): [140]).

The Kondo physics in metalloids and in pseudogap systems is current research area, especially in graphene, a system whose low-temperature physics in the charge-neutral case is dominated by two-dimensional Dirac electrons [93, 92, 91, 103]. Here the host density of states disappears linearly with the energy while it approaches the Fermi level. The screening, which is known from metallic systems, is strongly repressed, so that it occurs only for Kondo couplings, which are stronger than a finite critical coupling strength [141, 131]. In fact, in the case of graphene, the question for the most promising candidates of magnetic impurities with Kondo physics is only insufficiently answered [30, 127, 135, 148, 126, 125, 128]. Possible candidates are adatoms, for example Co [135, 62, 136, 101], but also simple molecules such as NiH [136] on highly symmetrical positions (centers of the C-hexagon, edges, C-sites). Also defects due to radiation [90, 85] or due to H and F adatoms are interesting candidates.

Graphene is a two-dimensional hexagonal formation of carbon atoms. "The sp^2 orbitals hybridize to yield the σ orbitals. [...] [These] are electrically inert and responsible for the [...] [noteworthy] mechanical robustness. [...] The p_z orbitals, which form the π-bonds" [44, p. 3], determine the electronic structure of graphene. Therefore electron hopping between neighboring atoms is allowed and yields a kinetic energy. Graphene has two sublattices A and B. Two dispersive bands (π^* and π) are formed, which "touch at the two inequivalent wavevectors $\vec{K} = \left(\frac{2\pi}{3a_1}, \frac{2\pi}{3\sqrt{3}a_1}\right)^t$ and $\vec{K}' = \left(\frac{2\pi}{3a_1}, -\frac{2\pi}{3\sqrt{3}a_1}\right)^t$" [44, p. 3], where $a_1 = 1.42 \cdot 10^{-10}$ m is the bond length, i.e. the distance between adjacent carbon atoms.

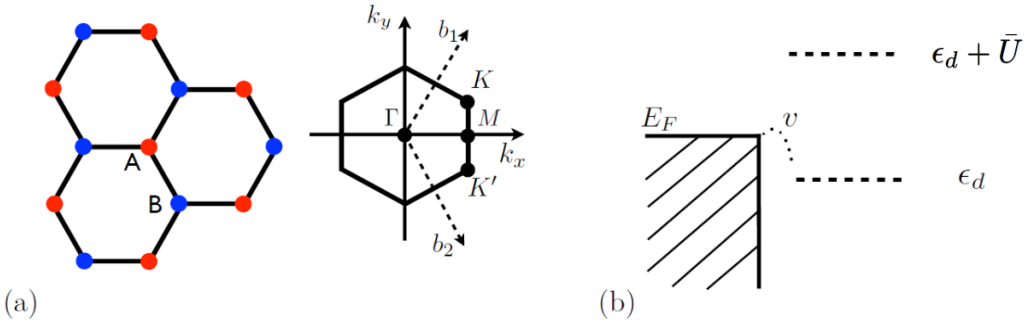

Figure 1: (a) Illustration of the honeycomb lattice of graphene: There are two inequivalent carbon atoms per unit cell, A and B. The hexagonal Brillouin zone is also shown. The touching points of the bands are K and K'.
(b) Illustration of the Anderson impurity model: "A local spin-degenerate state with energy ϵ_d is hybridized via v with a sea of conduction electrons. Local double occupancy costs the Coulomb energy $\bar{U}$" [44, p. 4].

The fundamental description of the interaction of the electronic host and the impurity spin is again the Anderson impurity model or in the limit of vanishing charge fluctuations the *s-d* exchange Kondo model.
To understand this, we consider the general form of the Anderson model [124]. The magnetic characteristics of the impurity depend on the host and on the occurrence of $3d\,(4f)$ elements. Essentially two interactions determine the behaviour of the impurity: "atomic Coulomb interactions and [...] [spin-orbit coupling] in a free atom and the interaction of the wavefunctions with the conduction electron band of the host" [124, p. 481]. The form of the metal-impurity interaction is given by

$$\mathcal{H} = \mathcal{H}_0 + \sum_{j=1}^{L} V_{\mathrm{i}}\left(r_j\right) + \frac{1}{2}\sum_{\substack{j=1\\ j\neq k}}^{L} \frac{e^2}{r_{jk}} + \frac{1}{mc}\sum_{j=1}^{L} \frac{1}{r_j}\frac{\mathrm{d}}{\mathrm{d}r_j} V_{\mathrm{i}}\left(r_j\right)\left(\vec{L}_j \cdot \vec{S}_j\right). \tag{1}$$

"$\mathcal{H}_0$ is a Hamiltonian of electrons in the potential of a crystal lattice, $r_j = |\vec{r}_j|$ and $r_{jk} = |\vec{r}_j - \vec{r}_k|$; m, $\vec{L}$, $\vec{S}$ and L are the mass, orbital moment, spin and the number of electrons[.] [...] $V_{\mathrm{i}}\left(r\right)$ is a potential of the impurity [...] [without any] electrons [...] [in] the outer shell." [124, p. 481]. We assume $V_{\mathrm{i}}\left(r\right)$ to be spherically symmetric. "The third term [...] is a Coulomb interaction, [...] [whereas] the fourth term [...] [is] the spin-orbit coupling [generated] by the impurity" [124, p. 481]. The important observation is that the $l = 2$ states of $V_{\mathrm{i}}\left(r\right)$ are near the Fermi surface and build the small resonance. The discrepancy among "the interatomic distance $\frac{1}{k_F}$ and the Bohr radius r_B of the d shell, $k_F r_B \ll 1$" [124, p. 481], yields the narrow width. In fact, the wavefunction of electrons with energies close to the Fermi-surface consist of "both localized and delocalized components" [124, p. 481]. Therefore "using as a basis the orbital and band wavefunctions" [124, p. 481] the eigenstates of $\mathcal{H}$ can be expanded. For the band wavefunctions we select "a spherical wave with the centre at the impurity site" [124, p. 481]. In second quantization we have

$$\begin{aligned}
\Psi^{\dagger}\left(\vec{r}\right) &= \sum_{k<\frac{1}{r_B},l,m,\sigma} \Psi_{lm}\left(k,\vec{r}\right) c^{\dagger}_{k,l,m,\sigma} + \sum_{m,\sigma} \Psi_d\left(\vec{r}\right) d^{\dagger}_{m,\sigma},\\
\Psi_{lm}\left(k,\vec{r}\right) &= r_l\left(kr\right) Y_{lm}\left(\frac{\vec{r}}{r}\right),\\
\Psi_d\left(\vec{r}\right) &= R_{l_0}\left(\frac{r}{r_B}\right) Y_{l_0 m}\left(\frac{\vec{r}}{r}\right),
\end{aligned}$$

where $r = |\vec{r}|$ and $c^{\dagger}_{k,l,m,\sigma}$ "is a creation operator for the spherical wave with the centre at the impurity" [124, p. 481] site. The creation "operator $d^{\dagger}_{m,\sigma}$ corresponds to the localized [...] [parts] of the state with $l = 2$. [...] For transition and rare-earth impurities" [124, p. 481 - 482] we have $l_0 = 2$ and $l_0 = 3$, m is a z-component of the angular momentum, $m = -l_0, \ldots, l_0$. The set of chosen functions is not orthogonal, but the corresponding

overlap integral

$$\int_0^\infty \mathrm{d}r r^2 r_{l_0}(kr) R_{l_0}\left(\frac{r}{r_B}\right)$$

is small, since r_B and $\frac{1}{k_F}$ differ greatly in scale. Therefore the non-orthogonality is negligible. Rewritten in terms of $c^\dagger_{k,l,m,\sigma}$, $c_{k,l,m,\sigma}$, $d^\dagger_{m,\sigma}$ and $d_{m,\sigma}$ the Hamiltonian $\mathcal{H}$ in (1) contains a high number of terms.

- Terms containing only $c^\dagger_{k,l,m,\sigma}$ and $c_{k,l,m,\sigma}$: They characterize the Hamiltonian of the host metal. For the description of the conduction band "we neglect the many particle corrections to the band spectrum. [...] [We suppose] "that the spectrum of electrons near the Fermi surface is spherically symmetric" [124, p. 483].

- The terms with $d^\dagger_{m,\sigma}$ and $d_{m,\sigma}$ operators characterize "the Hamiltonian of a $3d\,(4f)$ ion in a crystal field" [124, p. 483].

- The one-electron mixing interaction in $\mathcal{H}_0$ is off-diagonal in the number of $3d\,(4f)$ electrons. We neglect the crystal field and spin-orbit effects. We just keep terms "invariant under rotation in the coordinate space" [124, p. 483].

- There are also terms containing $c^\dagger_{k,l,m,\sigma}$, $c_{k,l,m,\sigma}$, $d^\dagger_{m,\sigma}$ and $d_{m,\sigma}$ operators:

$$c^\dagger d^\dagger c d$$
$$c^\dagger c^\dagger d d, d^\dagger d^\dagger c c$$
$$c^\dagger c^\dagger c d, d^\dagger d^\dagger d c$$

  We neglect all these terms.
  The first term characterizes the contact exchange coupling. This term rivals the virtual-mixing coupling. "For $3d$ impurities strong Kondo effect [...] [indicates] that the virtual-mixing mechanism is [...] stronger. For $4f$ ions we must distinguish between normal ions and ions near a valence instability. [...] [For a normal ion there is no Kondo effect and for an ion near] a valence instability, the virtual-mixing coupling becomes large.[Since we are] only interested in alloys [...] [that show] the Kondo effect we [...] neglect the contact exchange coupling. [...]
  States with $n_{d_0} \pm 2$ (corresponding to two additional orbital electrons or holes) [...] [are located] sufficiently high" [124, p. 483 - 484]. The second terms result therefore in the renormalization of the Coulomb interaction.
  The third terms give only trivial renormalizations of virtual-mixing coupling.

Thus the characteristics "of a magnetic impurity in a metal [...] [can] be described by the semiphenomenological Anderson Hamiltonian" [124, p. 484]:

$$\begin{aligned}
\mathcal{H}_A = & \sum_{k,m,\sigma} \epsilon\left(k\right) c^{\dagger}_{k,m,\sigma} c_{k,m,\sigma} + \frac{1}{L} \sum_{k,m,\sigma} v_k \left(c^{\dagger}_{k,m,\sigma} d_{m,\sigma} + d^{\dagger}_{m,\sigma} c_{k,m,\sigma} \right) \\
& + \sum_{m,m',\sigma} \epsilon_{mm'} d^{\dagger}_{m,\sigma} d_{m',\sigma} \\
& + \sum_{\substack{m_1,m_2,m_3,m_4,\sigma_1,\sigma_2,\sigma_3,\sigma_4 \\ m_1+m_2=m_3+m_4 \\ \sigma_1+\sigma_2=\sigma_3+\sigma_4}} \Gamma^{m_3,\sigma_3;m_4,\sigma_4}_{m_1,\sigma_1;m_2,\sigma_2} d^{\dagger}_{m_1,\sigma_1} d^{\dagger}_{m_2,\sigma_2} d_{m_3,\sigma_3} d_{m_4,\sigma_4} - A \left(\vec{L}_d \cdot \vec{S}_d \right), \quad (2) \\
c^{\dagger}_{k,l_0,m,\sigma} = & \, c^{\dagger}_{k,m,\sigma}, \\
\epsilon_{mm'} = & \, \delta_{mm'} \int_0^{\infty} \mathrm{d}r r^2 R_{l_0}\left(\frac{r}{r_B}\right) \left(R_{l_0}\left(\frac{r}{r_B}\right) \left(V_{\mathrm{i}}\left(r\right) + \frac{l_0\left(l_0+1\right)}{2mr^2} \right) \right. \\
& \left. - \frac{1}{2mr} \partial_r^2 r R_{l_0}\left(\frac{r}{r_B}\right) \right) + (\text{crystal field}), \\
v_k = & \int \mathrm{d}^3 r r_{l_0}\left(kr\right) Y^{*}_{l_0 m}\left(\frac{\vec{r}}{r}\right) \left(\mathcal{H}_0 + V_{\mathrm{i}}\left(r\right)\right) R_{l_0}\left(\frac{r}{r_B}\right) Y_{l_0 m}\left(\frac{\vec{r}}{r}\right), \\
\vec{L}_d = & \sum_{m,m',\sigma} d^{\dagger}_{m,\sigma} \vec{I}_{m,m'} d_{m',\sigma}, \\
\vec{S}_d = & \sum_{m,m',\sigma} d^{\dagger}_{m,\sigma} \vec{S}_{m,m'} d_{m',\sigma}.
\end{aligned}$$

$\epsilon_{mm'}$ is the one-electron atomic energy. "The non-relativistic [component] of interaction between $d\left(f\right)$ electrons" [124, p. 482] can be seen in the fourth term in $\mathcal{H}_A$. The matrix $\mathbf{\Gamma}$ is determined by $l+1$ Slater coefficients. The last term in $\mathcal{H}_A$ describes the spin-orbit coupling. $\vec{L}_d$ is the angular momentum and $\vec{S}_d$ the total spin of the $d\left(f\right)$ shell. I^x, I^y and I^z are the matrices of the $j = l_0$ representation. The core of $\mathcal{H}_A$ is that it describes a one-dimensional system. All quantities in $\mathcal{H}_A$ depend only on $\left|\vec{k}\right| = k$. The assumption "about a spherical Fermi surface and impurity-ion potential" [124, p. 484] yields the one-dimensionality. Note that we have to "consider impurities as independent scatterers" [124, p. 484]. This means that a three-dimensional system with one impurity can be mapped to a one-dimensional system with one impurity. This is not possible for a system with more than one impurity.
To find the Anderson impurity model from (2) we can choose $\epsilon\left(k\right) = k$, $\epsilon_{mm'} = \delta_{mm'}\epsilon_d$, $\Gamma^{m_3,\sigma_3;m_4,\sigma_4}_{m_1,\sigma_1;m_2,\sigma_2} = \bar{U}$ and $v_k = V$.

In the case of graphene, the Anderson impurity model or in the limit of vanishing charge fluctuations the *s*-*d* exchange Kondo model has a pseudogap low-energy density of states [44]

$$\rho\left(\omega\right) = \rho_0 \left|\omega\right|^r \Theta\left(D - \left|\omega\right|\right), \quad (3)$$

where ρ_0 is a constant, ω is the energy and D is the bandwidth. An arbitrary value of $r > 0$, but especially $r = 1$ is of interest. In addition, compared to the metallic Kondo system which is particle-hole symmetric, there are relevant particle-hole symmetry breaking terms, which can be modeled with a potential scattering with certain strength V_0 [44].
J_0 and V_0 are a reparameterization of the parameters V, ϵ_d and $\bar{U}$ of the Anderson impurity model. "It is supposed that no more than two electrons with spins $\sigma =\uparrow,\downarrow$, can simultaneously occupy the impurity level ϵ_d. The [...] [intra-atomic] Coulomb interaction is given by the term $\bar{U}$, and V is the admixture of the d level with conduction band states" [124, p. 462]

$$J_0 = 2V^2 \left(\frac{1}{|\epsilon_d|} + \frac{1}{|\epsilon_d + \bar{U}|} \right), \qquad V_0 = \frac{V^2}{2} \left(\frac{1}{|\epsilon_d|} - \frac{1}{|\epsilon_d + \bar{U}|} \right). \tag{4}$$

Depending on r, V_0 and the Kondo coupling J_0 between the electronic spins and the impurity spin, there are rich phase diagrams, which are completely understood for one-channel systems [44]. They follow from numerical renormalization group studies.

- Local-moment phase (LM): "The impurity moment is [...] [decoupled asymptotically] from the host and [...] [acts] like a free local moment" [44, p. 10], i.e. the residual entropy is given by $S_\mathrm{i} = \ln 2$.
- Symmetric strong-coupling phase (SSC): This phase "is the generalization of the metallic Kondo-screened phase to finite r" [44, p. 10]. It matches to Kondo screening with particle-hole symmetry, $\bar{U} = -2\epsilon_d$, i.e. $V_0 = 0$. The residual entropy is $S_\mathrm{i} = 2r \ln 2$. Therefore the impurity moment is screened only partially.
- Asymmetric strong-coupling phase (ASC): Without particle-hole symmetry, full screening with $S_\mathrm{i} = 0$ is obtained.
- Symmetric and asymmetric critical points (SCR) and (ACR): There are "two distinct critical fixed points" [44, p. 10]. Their difference lies in their symmetry under particle-hole transformation.

"The topology of the phase diagram changes [...] as [...] the exponent r [in (3)] is varied. Different phase diagram topologies are [...] [known] in [...] [four] regimes" [44, p. 10] [56]:

1. $0 < r < r^* = 0.375 \pm 0.002$:
   a) At particle-hole symmetry the local-moment phase is separated from the symmetric strong-coupling phase by a critical coupling J_c. It belongs to a symmetric critical point. For starting values $J < J_c$ the flow points to the local-moment phase, while for $J > J_c$ it points to the symmetric strong-coupling phase.
   b) For particle-hole asymmetry the flow to the local-moment phase is separated from the flow to the asymmetric strong-coupling phase by a separatrix.

c) In the local-moment phase and at the symmetric critical point particle-hole asymmetry is irrelevant, whereas it is important in the strong-coupling phase where it pushes the flow to the asymmetric critical point. The symmetric critical point is therefore a multicritical fixed point.

2. $r^* < r < r_{\max} = \frac{1}{2}$:
   a) There is a critical coupling which separates the local-moment phase from the symmetric strong-coupling phase for particle-hole symmetry.
   b) "The symmetric critical point is unstable with respect to particle-hole asymmetry and a new asymmetric critical fixed point [...] [arises, regulating] the transition between the local-moment phase and the asymmetric strong-coupling phase" [44, p. 10].

3. $r > r_{\max}$
   a) The symmetric critical point melts together with the symmetric strong-coupling phase. There is no Kondo screening at particle-hole symmetry.
   b) For particle-hole asymmetry screening is possible. The asymmetric critical point still regulates the local-moment - symmetric strong-coupling phase transition.
   c) "The critical exponents are [trivial] at the asymmetric critical point for $r > 1$" [44, p. 11]. $r = 1$ (corresponding to charge-neutral graphene) is an upper-critical dimension.

4. $-1 < r < 0$:
   a) The symmetric strong-coupling phase is stable.
   b) The symmetric strong-coupling phase is separated "from a newly [...] arising fixed asymmetric local moment point, located at $J_0 = 0$ and $V_0 = \infty$" [44, p. 11], by an asymmetric critical point [132]. In the following we will, however, not discuss $r < 0$ in any detail.

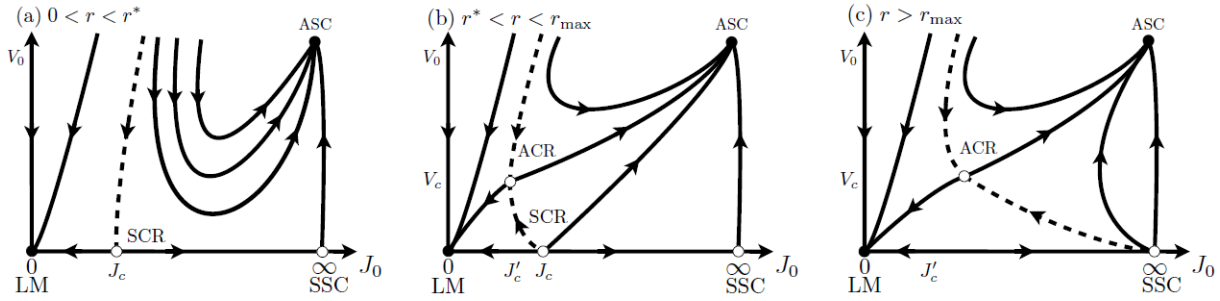

Figure 2: "Schematic renormalization group flow diagrams for the pseudogap Kondo model in the plane [...]. The flow topology [...] [varies] as a function of r, as [...] [demonstrated] in the three panels. [...] Full dots [...] [indicate] stable fixed points, [...] [whereas] open dots are critical fixed points. Dashed lines [...] [imply separatrices], i.e. phase boundaries" [44, p. 10].

(Two-channel systems were investigated [56, 107], but less well understood due to the more complicated relations.) The phase diagrams were determined with numerical (NRG)

[26, 56, 25, 61] and perturbative renormalization group studies [133, 43]. The vicinities of the critical fixed points were investigated with effective field theories [133, 43], but not with exact Bethe ansatz methods.

1.3 Integrability

A more detailed overview of this chapter can be found in the book [36].
The basis of the integrability in the sense of this thesis is the R-matrix. The R-matrix $R(\lambda,\mu) \in \mathrm{End}\left(\mathbb{C}^d \otimes \mathbb{C}^d\right)$ is a $d^2 \times d^2$ matrix. R-matrices can be illustrated by graphs. Relations among products of R-matrices become relations between graphs. The application of these graphical conventions sometimes clarifies complicated algebraic proofs. We shall utilize the graphical representation in the next chapters.

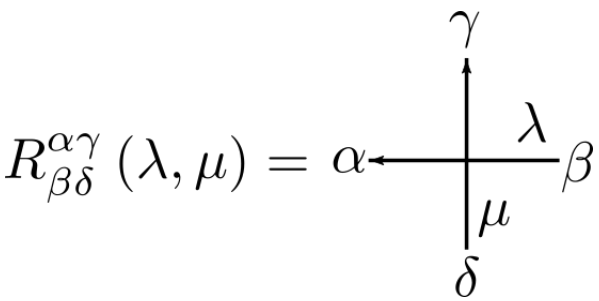

Figure 3: Graphical representation of the R-matrix.

"The R-matrix fixes the structure of the associative quadratic Yang-Baxter algebra $\mathcal{T}_R$"[36, p. 427] "defined in terms of its generators $T^{\alpha}_{\beta}(\lambda)$ (monodromy matrix), $\alpha,\beta = 1,\ldots,d$, $\lambda \in \mathbb{C}$, by the relation" [36, p. 426]

$$R(\lambda,\mu)\, T_1(\lambda)\, T_2(\mu) = T_2(\mu)\, T_1(\lambda)\, R(\lambda,\mu). \tag{5}$$

With the definition of the row-to-row transfer matrix

$$t(\lambda) = T^{\alpha}_{\alpha}(\lambda) = \mathrm{tr}_{\mathrm{aux}} T(\lambda) \tag{6}$$

we find the important result

$$[t(\lambda), t(\mu)] = 0. \tag{7}$$

Therefore the row-to-row transfer matrix $t(\lambda)$ "is a generating function of a commutative subalgebra of $\mathcal{T}_R$" [36, p. 427].
Note that the elements of the monodromy matrix are operators in a Hilbert space. This space is called quantum space. The row-to-row "transfer matrix is [...] [derived] by taking the trace with respect to the auxiliary space of the monodromy matrix" [36, p. 531].

This yields an operator, which acts on the quantum space. Taking a trace in quantum / auxiliary space is depicted by tr / $\mathrm{tr}_{\mathrm{aux}}$.
Under the assumption that we have "a given representation of $\mathcal{T}_R$ on the space of states of some physical system[,] [...] $t(\lambda)$ generates a set of mutually commuting operators[: These operators are] by construction [...] embedded into the quadratic algebra $\mathcal{T}_R$. [...] [Therefore we have an oppurtunity to fulfill the conditions] of Liouville's theorem in the classical limit (if it exists)[.] [...] [Furthermore] the quadratic relations of the algebra $\mathcal{T}_R$ [...] [could deliver a possibility] to simultaneously diagonalize the quantum integrals of motion [...] generated by $t(\lambda)$" [36, p. 427].
Another way to "the defining relations of the Yang-Baxter algebra [...] [is the matrix] $\check{R}(\lambda,\mu)$ with matrix elements $\check{R}^{\alpha\beta}_{\gamma\delta}(\lambda,\mu) = R^{\beta\alpha}_{\gamma\delta}(\lambda,\mu)$" [36, p. 428]. We find

$$\check{R}(\lambda,\mu)\left(T(\lambda)\otimes T(\mu)\right) = \left(T(\mu)\otimes T(\lambda)\right)\check{R}(\lambda,\mu). \tag{8}$$

The Yang-Baxter equation

$$R_{12}(\lambda,\mu)\,R_{13}(\lambda,\nu)\,R_{23}(\mu,\nu) = R_{23}(\mu,\nu)\,R_{13}(\lambda,\nu)\,R_{12}(\lambda,\mu) \tag{9}$$

or

$$\check{R}_{23}(\lambda,\mu)\,\check{R}_{12}(\lambda,\nu)\,\check{R}_{23}(\mu,\nu) = \check{R}_{12}(\mu,\nu)\,\check{R}_{23}(\lambda,\nu)\,\check{R}_{12}(\lambda,\mu)$$

"is a sufficient requirement for the consistency of the Yang-Baxter algebra $\mathcal{T}_R$" [36, p. 428]. It also secures the existence of nontrivial representations of $\mathcal{T}_R$.

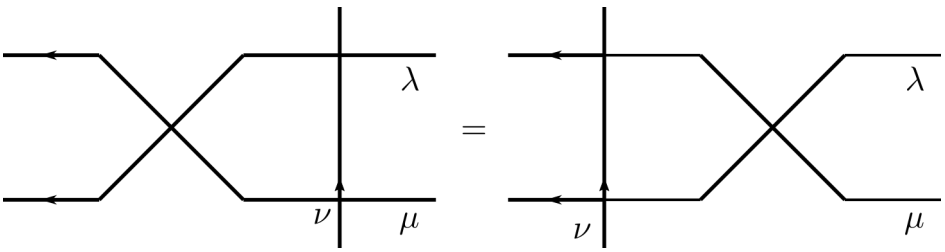

Figure 4: Graphical representation of the Yang-Baxter equation.

"We denote by $e_\gamma \in \mathbb{C}^d$, $\gamma = 1,\ldots,d$ a column vector with only non-vanishing entry 1 in row γ. The set $\left\{e_\gamma \in \mathbb{C}^d \mid \gamma = 1,\ldots,d\right\}$ is a basis of $\mathbb{C}^d$. Let $e^\beta_\alpha \in \mathrm{End}\left(\mathbb{C}^d\right)$, such that $e^\beta_\alpha e_\gamma = \delta^\beta_\gamma e_\alpha$. Then $\left\{e^\beta_\alpha \in \mathrm{End}\left(\mathbb{C}^d\right) \mid \alpha,\beta = 1,\ldots,d\right\}$ is a basis of $\mathrm{End}\left(\mathbb{C}^d\right)$. e^β_α is a $d\times d$ matrix with only non-vanishing entry 1 in row α and column β" [36, p. 429].
"Representations of the Yang-Baxter algebra [...] [are considered], where the quantum space is a L-fold tensor product of auxiliary spaces $\mathbb{C}^d$" [36, p. 429]. The L-matrix at site j is introduced by defining its matrix elements

$$L_{j\beta}^{\alpha}(\lambda,\mu) = R_{\beta\delta}^{\alpha\gamma}(\lambda,\mu)\, e_{j\gamma}^{\delta}. \tag{10}$$

These matrix elements are operators in $\left(\mathrm{End}\left(\mathbb{C}^d\right)\right)^{\otimes L}$. This yields

$$\check{R}(\lambda,\mu)\left(L_j(\lambda,\nu)\otimes L_j(\mu,\nu)\right) = \left(L_j(\mu,\nu)\otimes L_j(\lambda,\nu)\right)\check{R}(\lambda,\mu), \tag{11}$$

which implies "that the L-fold product of ordered L-matrices

$$T(\lambda) = L_L(\lambda,\nu_L)\ldots L_1(\lambda,\nu_1) \tag{12}$$

is a representation of the Yang-Baxter algebra (8)" [36, p. 431]. The row-to-row transfer matrix $t(\lambda)$ and "every appropriately [...] [selected] differentiable function of $t(\lambda)$ [...] [can be viewed] as a generating function of a set of mutually commuting operators" [36, p. 432]. A beneficial selection of a generating function is $\tau(\lambda) = \ln\left(t^{-1}(\lambda_0)\, t(\lambda)\right)$. Since "the nth coefficient [in the series expansion of $\tau(\lambda)$] is a sum over local densities [...] [operating] non-trivially at $n+1$ neighboring sites at most" if $\nu_j = \nu_0$, $j = 1,\ldots,L$ and $R(\lambda_0,\lambda_0) = P$ [36, p. 532], the coefficients in the series expansion of $\tau(\lambda)$ are local [81]. The two-site term

$$H = t^{-1}(\lambda_0)\, t'(\lambda_0) \tag{13}$$

can be interpreted as a Hamiltonian. Corresponding with the R-matrix $R(\lambda,\mu)$ equation (12) defines the fundamental model. If all the ν_j, $j = 1,\ldots,L$ are equal, the model is called homogeneous, otherwise inhomogeneous. The homogeneous model yields the local Hamiltonian H (13). A result is the expansion of $t(\lambda)$ for small λ and $\nu_j = 0$, $j = 1,\ldots,L$

$$t(\lambda) = e^{i\Pi - \lambda H + \mathcal{O}\left(\lambda^2\right)}, \tag{14}$$

where Π is the momentum operator.

1.3.1 Column-to-column transfer matrix

An extraordinary state of affair follows in the framework of the derivation of the partition function from the spectrum of an integrable Hamiltonian. In spite of "the validity of the Bethe ansatz equations for all energy eigenvalues of the model the [...] [calculation] of the partition function is [...] [quite] difficult. The eigenstates are not explicitly known. The Bethe ansatz equations yield just implicit descriptions. In the thermodynamical Bethe ansatz the grandcanonical partition function is calculated in the thermodynamic limit by identifying the leading energy states. "The macro-state for [...] temperature T is [...] [determined] by a set of root densities satisfying integral equations, [...] [which are derived] from the Bethe ansatz equations" [36, p. 526]. The energy and the entropy are expressed

in terms of the density functions. The minimization of the free energy functional yields the thermodynamical Bethe ansatz equations [142, 117].
There are some problems in the explained procedure: The determination of the spectrum of the Heisenberg model uses the string hypothesis, which was "criticized [quite] a number of times and led [...] to a lattice path-integral" [36, p. 527] representation of the partition function and the definition of a column-to-column transfer matrix (quantum transfer matrix) [116, 69].
"Quantum systems at finite temperatures [...] [are therefore considered] in terms of classical systems on lattices in one dimension higher" [36, p. 527]. Quantum systems are typically viewed "as the original objects and the classical systems as derived objects" [36, p. 527]. The classical system is primary for us and the quantum system is secondary. This yields "classical systems on lattices that are partially staggered with alternating rows, but identical columns" [36, p. 527].
We introduce "$\bar{R}(\lambda,\mu)$ and $\tilde{R}(\lambda,\mu)$ by clockwise and anticlockwise 90° rotations of $R(\lambda,\mu)$" [36, p. 528]

$$\bar{R}^{\alpha\gamma}_{\beta\delta}(\lambda,\mu) = R^{\gamma\beta}_{\delta\alpha}(\mu,\lambda), \qquad \tilde{R}^{\alpha\gamma}_{\beta\delta}(\lambda,\mu) = R^{\delta\alpha}_{\gamma\beta}(\mu,\lambda). \tag{15}$$

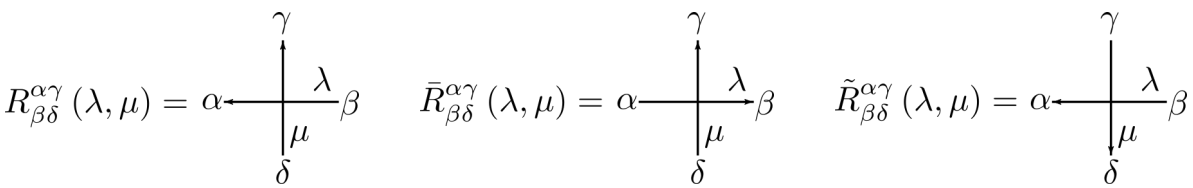

Figure 5: Graphical illustration of the fundamental R-matrix $R(\lambda,\mu)$ and the associated $\bar{R}(\lambda,\mu)$ and $\tilde{R}(\lambda,\mu)$.

We define an auxiliary transfer matrix $\bar{t}(\lambda)$ consisting of Boltzmann weights $\bar{R}(-\lambda,0)$ and find

$$\begin{aligned}\bar{t}(\lambda) :&= \mathrm{tr}_{\mathrm{aux}}\left(\bar{R}(-\lambda,0)\right)^{\otimes L}\\ &= e^{-i\Pi-\lambda H+\mathcal{O}(\lambda^2)},\end{aligned}$$

so that we have for the partition function

$$\begin{aligned}Z_L &= \mathrm{tr}e^{-\beta H}\\ &= \lim_{N\to\infty}\mathrm{tr}\left(t(\tau)\,\bar{t}(\tau)\right)^{\frac{N}{2}}\Big|_{\tau=\frac{\beta}{N}}.\end{aligned} \tag{16}$$

"We consider [the resulting system as a [...] [notional] two-dimensional model on a $L\times N$

square lattice. [...] N is the extension in the [...] [notional] imaginary time direction" [36, p. 529], which we call Trotter direction. There are alternating rows on the lattice. "Each of which is a product of only R weights or of only $\bar{R}$ weights" [36, p. 529]. The columns consist of alternating R and $\bar{R}$ weights.

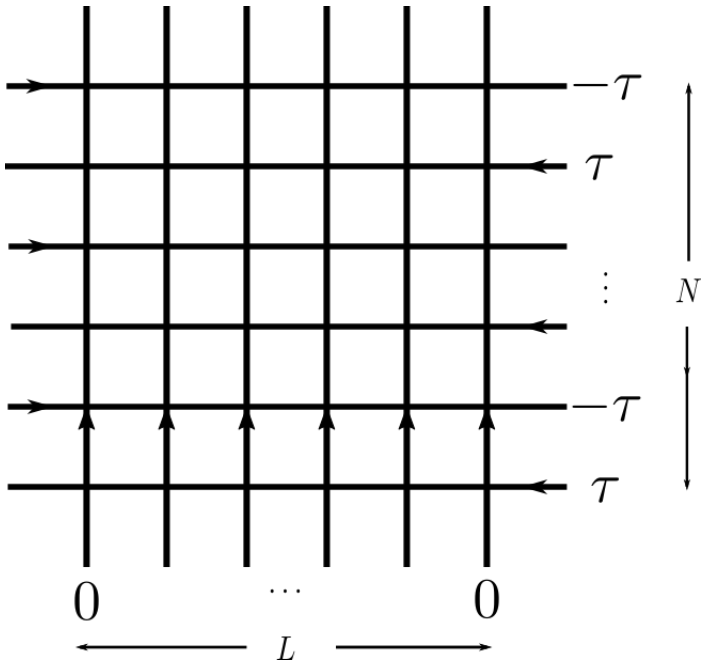

Figure 6: The quantum chain is mapped onto this two-dimensional classical model at finite temperature. The lattice has width L and height N. The rows belong to the transfer matrices $t(\tau)$ and $\bar{t}(\tau)$, $\tau = \frac{\beta}{N}$. The column-to-column transfer matrix is crucial for the thermodynamics.

It is reasonable to introduce a new transfer matrix procedure "based on the transfer direction along the horizontal axis [...] [and to study] the column-to-column transfer matrix" [36, p. 529], which we will denote by t^{QTM}.
By considering "the system in a 90° rotated frame[, we] define a [...] column-to-column transfer matrix with arbitrary spectral parameter λ on the vertical line" [36, p. 529]

$$\begin{aligned} t^{\mathrm{QTM}}(\lambda,\tau) &:= \mathrm{tr}_{\mathrm{aux}}\left(\bigotimes^{\frac{N}{2}} R(\lambda,-\tau)\otimes\tilde{R}(\lambda,\tau)\right) \\ &= \mathrm{tr}_{\mathrm{aux}}\left(L_N^{\mathrm{QTM}}(\lambda,-\tau)\,L_{N-1}^{\mathrm{QTM}}(\lambda,\tau)\ldots L_2^{\mathrm{QTM}}(\lambda,-\tau)\,L_1^{\mathrm{QTM}}(\lambda,\tau)\right). \end{aligned} \tag{17}$$

The L^{QTM}-matrices are defined by

$$\left(L_j^{\mathrm{QTM}}\right)_{\beta}^{\alpha}(\lambda,\mu) := \begin{cases} R_{\beta\delta}^{\alpha\gamma}(\lambda,\mu)\,e_{j\gamma}^{\delta}, & \text{for } j \text{ even},\\ \tilde{R}_{\beta\delta}^{\alpha\gamma}(\lambda,\mu)\,e_{j\gamma}^{\delta}, & \text{for } j \text{ odd}. \end{cases} \tag{18}$$

Using the column-to-column transfer yields

$$Z_L = \lim_{N\to\infty} \operatorname{tr}\left(t^{\mathrm{QTM}}(0,\tau)\right)^L\Big|_{\tau=\frac{\beta}{N}}. \tag{19}$$

The free energy f per lattice site is given by

$$f := -\frac{1}{\beta}\lim_{L\to\infty}\lim_{N\to\infty}\frac{1}{L}\ln\operatorname{tr}\left(t^{\mathrm{QTM}}(0,\tau)\right)^L\Big|_{\tau=\frac{\beta}{N}} \tag{20}$$

The two limits are interchangeable [116, 115].
We are interested in the spectrum of eigenvalues $\Lambda^{\mathrm{QTM}}(\lambda,\tau)$. There is a gap between the largest and the second largest eigenvalue of the column-to-column transfer matrix for finite β [116]. Hence the free energy per site can be written in terms of the leading eigenvalue $\Lambda_0^{\mathrm{QTM}}(0,\tau)$

$$f = -\frac{1}{\beta}\lim_{N\to\infty}\ln\Lambda_0^{\mathrm{QTM}}(0,\tau)\Big|_{\tau=\frac{\beta}{N}}. \tag{21}$$

Note that the "second largest" eigenvalue may be non-real, but its absolute value is smaller than $\Lambda_0^{\mathrm{QTM}}(0,\tau)$.
The calculation of the free energy is shortened to that of the eigenvalue $\Lambda_0^{\mathrm{QTM}}(0,\tau)$. Of course, a demanding treatment is required for the Trotter limit $N\to\infty$.

1.3.2 External fields

We consider "the thermodynamics of the quantum chain [...] [with] an external field that couples to a conserved quantity, e.g. a magnetic field h acting on the spin $S=\sum_{j=1}^{L}S_j$, where S_j [...] [is] a component of the jth spin, for [...] [example] S_j^z" [36, p. 531]. This changes (16) only in an obvious way

$$\begin{aligned} Z_L &= \operatorname{tr} e^{-\beta(H-hS)}. \\ &= \lim_{N\to\infty}\operatorname{tr}\left(\left(t(\tau)\,\bar{t}(\tau)\right)^{\frac{N}{2}}e^{\beta hS}\right)\Big|_{\tau=\frac{\beta}{N}}. \end{aligned}$$

"The equivalent two-dimensional $L\times N$ lattice is modified [...] by a horizontal seam" [36, p. 532]. Corresponding to that, the column-to-column transfer matrix is changed "by a field dependent boundary operator D" [36, p. 532], where D is in the case of a spin-$\frac{1}{2}$ model with $S_j=\frac{1}{2}\sigma_j^z$

$$D = \begin{pmatrix} e^{\frac{\beta h}{2}} & \\ & e^{-\frac{\beta h}{2}} \end{pmatrix}. \tag{22}$$

This modification can be handled "exactly as the additional operators acting on the bonds belong[ing] to symmetries of the model" [36, p. 532]. Consequently, within a

"grandcanonical ensemble for general magnetic fields and chemical potentials" [36, p. 532] the properties of many-particle systems can be investigated.

1.4 Structure and goal of this work

The aim of this thesis is the construction of a pseudogap Anderson impurity model, i.e. an Anderson impurity model with the dispersion relation $\epsilon(k) = k^z$, $z > 0$ for the host instead of the standard Anderson impurity model with dispersion relation $\epsilon(k) = k$ for the host. Such a dispersion relation leads to a density of states of the host like (3). We note that the Anderson impurity model is an integrable continuum model for which the coordinate Bethe approach is known so far [124]. Since the column-to-column transfer matrix does not exist in the continuum, the finitely many non-linear integral equations for the description of thermodynamics could not be directly determined. In [22] Bortz, Klümper and Scheeren showed that there is a different lattice model with the same regimes as in the phase diagram of the Anderson impurity model [124]. With respect to the regimes the models were considered as equivalent and the finitely many non-linear integral equations for the lattice model were derived.
In this thesis, our first goal is to embed the standard Anderson impurity model into a lattice model. As an appropriate model, the Hubbard model with integrable impurity emerges. For this reason, we generalize known results of the Hubbard model [36].
After that our goal is that this lattice model yields the Anderson impurity model with all parameters in a continuum limit. Then we want to use the limit for the description of the thermodynamics by performing it for the infinite set of thermodynamic Bethe ansatz equations as well as for the finitely many non-linear integral equations. The latter represents a new result. In this thesis, we also develop a method to perform the limit for the Hamiltonian.
By embedding the Anderson impurity model in a lattice model, it is now possible to perform modifications on the lattice that serve to change the dispersion relation of the host. These modifications are thus carried out at the level of the Hubbard model. After performing the established continuum limit, this provides the desired pseudogap Anderson impurity model, whose Hamiltonian we can specify. Through the generalization on the lattice, it is possible to fully describe the thermodynamics of this newly constructed model with a finite number of non-linear integral equations.
Therefore the aim of this thesis is the construction of a Anderson impurity model with modified density of states and the exact description of the thermodynamics with Bethe ansatz techniques.

In chapter 2 we introduce the one-dimensional anisotropic spin-$\frac{1}{2}$ Heisenberg model and consider it as a toy model. We show how to modify this model so that it contains an impurity

and the dispersion relation is changed. This novel model is subsequently investigated. We derive the Bethe ansatz equations for the row-to-row and column-to-column transfer matrices and the finitely many non-linear integral equations for the complete description of the thermodynamics. We study the thermodynamics for low temperatures T depending on the magnetic field h.

In chapter 3, an integrable impurity is added to the Hubbard model by additionally introduced spectral lines. The Bethe ansatz equations of the row-to-row transfer matrix change as a result. We describe the thermodynamics both with the thermodynamic Bethe ansatz and with the finitely many non-linear integral equations. In both cases the contribution of the impurity to the free energy is determined.

In chapter 4 we modify the density of states of the Hubbard model with integrable impurity and describe the thermodynamics of this new model completely with the finitely many non-linear integral equations. We show that the host still behaves like a free fermion gas in the limit $U \to 0$. Furthermore we analyze the low-temperature asymptotics.

In chapter 5 we demonstrate that the well-known Anderson impurity model can be derived from the Hubbard model with integrable impurity from chapter 3 by use of a combined continuum limit. We apply the continuum limit to the Bethe ansatz equations, the thermodynamic Bethe ansatz, the finitely many non-linear integral equations, the creation and annihilation operators and the Hamiltonian. We also derive the low-temperature asymptotics.

In chapter 6 we use the combined continuum limit established in chapter 5 to derive a novel pseudogap Anderson impurity model from the modified Hubbard model with integrable impurity in Chapter 4. We compute the corresponding Hamiltonian, describe the thermodynamics through the finitely many non-linear integral equations, consider the low-temperature asymptotics and the screening of the impurity.

In chapter 7 we comment on the most important results as well as further unresolved questions and the outlook.

2 One-dimensional anisotropic spin-$\frac{1}{2}$ Heisenberg model with spin-$\frac{1}{2}$ impurity and modification of the density of states

In this section we consider the one-dimensional anisotropic spin-$\frac{1}{2}$ Heisenberg model and outline how an integrable spin-$\frac{1}{2}$ impurity is incorporated and the density of states of the model is modified.

Our starting point is the one-dimensional anisotropic spin-$\frac{1}{2}$ Heisenberg model

$$H_{\mathrm{XXZ}} = J \sum_{j=1}^{L} \left(\sigma_{j-1}^{x} \sigma_{j}^{x} + \sigma_{j-1}^{y} \sigma_{j}^{y} + \Delta \left(\sigma_{j-1}^{z} \sigma_{j}^{z} - 1 \right) \right) - \frac{h}{2} \sum_{j=1}^{L} \sigma_{j}^{z}, \tag{23}$$

with periodic boundary conditions on a chain of length L, where h denotes the magnetic field. $J > 0$ fixes the energy scale and Δ is the (real) anisotropy parameter. "Apparently, for $\Delta = 1$ the system specializes to the isotropic antiferromagnetic Heisenberg chain, for $\Delta = -1$ (and applying a simple unitary transformation) the system reduces to the isotropic ferromagnetic case. The classical counterpart of the one-dimensional anisotropic spin-$\frac{1}{2}$ Heisenberg model is the six-vertex model" [70, p. 11]. We use the following parametrization of the Boltzmann weights

$$a(\lambda, \mu) = 1, \qquad b(\lambda, \mu) = \frac{\sin(\lambda - \mu)}{\sin(\lambda - \mu + \gamma)}, \qquad c(\lambda, \mu) = \frac{\sin \gamma}{\sin(\lambda - \mu + \gamma)}, \tag{24}$$

where $\Delta = \cos \gamma$. In the following we consider $0 \leq \gamma \leq \pi$. The integrable structure encoded in the R-matrix is given by

$$R(\lambda, \mu) = \begin{pmatrix} a(\lambda, \mu) & & & \\ & b(\lambda, \mu) & c(\lambda, \mu) & \\ & c(\lambda, \mu) & b(\lambda, \mu) & \\ & & & a(\lambda, \mu) \end{pmatrix}. \tag{25}$$

It is well known how to diagonalize the row-to-row transfer matrix and the column-to-column transfer matrix by means of the algebraic Bethe ansatz [70].

However, we would like to modify the model in two ways:

First, we introduce an integrable spin-$\frac{1}{2}$ impurity on the site $L + 1$ with the spectral parameter ν.

Next we introduce shifts $\theta_1, \ldots, \theta_{\frac{N}{2}}$ and $\vartheta_1, \ldots, \vartheta_L$ on the horizontal and vertical lines. These shifts are, however, not intended to be arbitrary, but are intended to follow predetermined distribution densities ρ_h and ρ_v. These distribution densities depend on the parameters α_h and α_v ($\alpha_h, \alpha_v > 0$). These shifts serve to modify the dispersion relation of

the host.

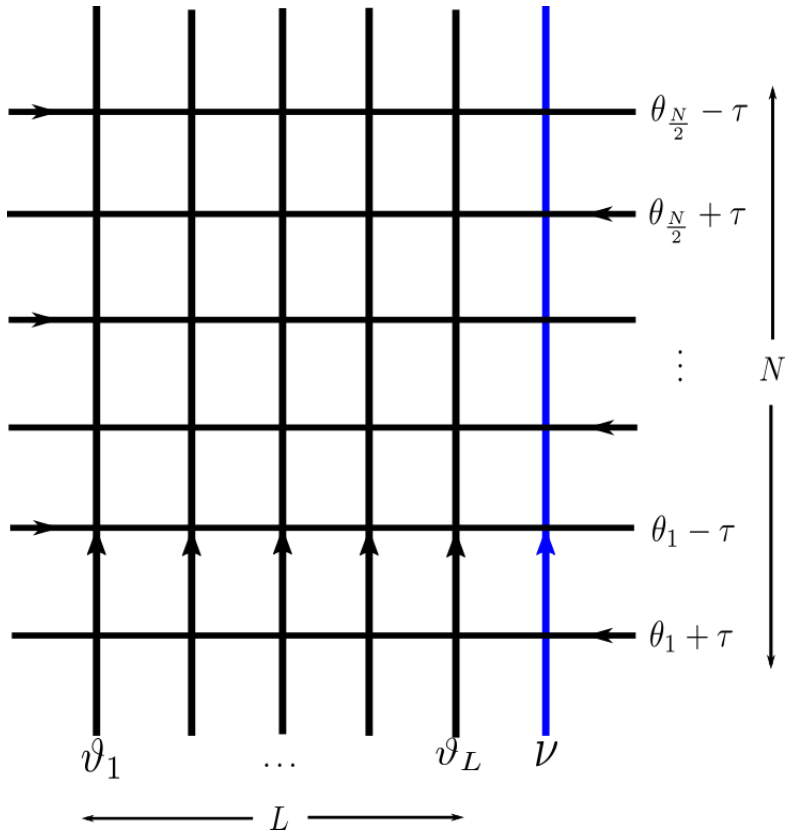

Figure 7: The quantum chain at finite temperature is mapped onto this two-dimensional classical model. The lattice has width $L+1$, and height N. The rows of the lattice belong to the row-to-row transfer matrices with $\tau = \sin\gamma\frac{\beta}{N}$. The column-to-column transfer matrix is crucial for the thermodynamics. The blue line is intended to illustrate the integrable spin-$\frac{1}{2}$ impurity.

The column-to-column transfer matrix with arbitrary spectral parameter λ on the vertical line is according to (17) and (22)

$$t^{\mathrm{QTM}}(\lambda,\tau) = \mathrm{tr}_{\mathrm{aux}}\left(D\cdot\bigotimes_{j=1}^{\frac{N}{2}} R(\lambda,\theta_j-\tau)\otimes\tilde{R}(\lambda,\theta_j+\tau)\right)$$

"The L-matrices are defined differently for even and odd indices" [36, p. 530]

$$\left(L_j^{\mathrm{QTM}}\right)_{\beta}^{\alpha}(\lambda,\mu) := \begin{cases} R_{\beta\delta}^{\alpha\gamma}(\lambda,\mu)\, e_{j\gamma}^{\delta}, & \text{for } j \text{ even},\\ \tilde{R}_{\beta\delta}^{\alpha\gamma}(\lambda,\mu)\, e_{j\gamma}^{\delta} & \text{for } j \text{ odd}\ . \end{cases}$$

The free energy F is

$$F = -\frac{1}{\beta}\lim_{N\to\infty}\ln\mathrm{tr}\left(t^{\mathrm{QTM}}(\nu,\tau)\prod_{j=1}^{L}t^{\mathrm{QTM}}(\vartheta_j,\tau)\right)\Bigg|_{\tau=\sin\gamma\frac{\beta}{N}}. \tag{26}$$

"Of particular interest is the spectrum of eigenvalues" [36, p. 532] of $t^{\mathrm{QTM}}(\lambda,\tau)$. There is a gap between the largest and the absolute value of the second largest eigenvalue of the column-to-column transfer matrix for finite β [116, 115]. Therefore, with the right choice of the parameters $\vartheta_1,\ldots,\vartheta_L$ the free energy per site is given just in terms of the largest eigenvalue $\Lambda_0^{\mathrm{QTM}}(\lambda,\tau)$.
"The diagonalization of the column-to-column transfer matrix is achieved by the algebraic Bethe ansatz very much like for the homogeneous case of the row-to-row transfer matrix" [70, p. 5]. In our case we find

$$\begin{aligned}\Lambda_0^{\mathrm{QTM}}(\lambda,\tau) = e^{\frac{\beta h}{2}}&\left(\prod_{j=1}^{\frac{N}{2}} b(\tau+\theta_j,\lambda)\right)\left(\prod_{k=1}^{M}\frac{1}{b(\mu_k,\lambda)}\right)\\ &+ e^{-\frac{\beta h}{2}}\left(\prod_{j=1}^{\frac{N}{2}} b(\lambda,-\tau+\theta_j)\right)\left(\prod_{k=1}^{M}\frac{1}{b(\lambda,\mu_k)}\right)\end{aligned}$$

with

$$e^{\beta h}\prod_{j=1}^{\frac{N}{2}}\frac{\mathrm{sh}(\mu_k+i(\tau+\theta_j-\gamma))\,\mathrm{sh}(\mu_k-i(\tau-\theta_j))}{\mathrm{sh}(\mu_k-i(\tau-\theta_j-\gamma))\,\mathrm{sh}(\mu_k+i(\tau+\theta_j))} = -\prod_{l=1}^{M}\frac{\mathrm{sh}(\mu_k-\mu_l-i\gamma)}{\mathrm{sh}(\mu_k-\mu_l+i\gamma)}. \tag{27}$$

"The last constraints are nothing but the famous Bethe ansatz equations" [70, p. 16] here formulated for our model and determine $\{\mu_k\}_{k=1}^{M}$.
After the substitutions $\lambda\to i\tilde{\lambda}$, $\mu_k\to i\tilde{\mu}_k$ and "factorization of common terms of the vacuum functions we" [36, p. 535] get

$$\Lambda_0^{\mathrm{QTM}}\left(\tilde{\lambda},\tau\right) = \frac{\lambda_+\left(\tilde{\lambda}\right)+\lambda_-\left(\tilde{\lambda}\right)}{\prod_{j=1}^{\frac{N}{2}}\mathrm{sh}\left(\tilde{\lambda}-i(\gamma-\tau-\theta_j)\right)\mathrm{sh}\left(\tilde{\lambda}+i(\gamma-\tau+\theta_j)\right)}.$$

$\lambda_\pm\left(\tilde{\lambda}\right)$ are given by

$$\lambda_\pm\left(\tilde{\lambda}\right) = e^{\pm\frac{\beta h}{2}}\phi\left(\tilde{\lambda}\mp i\frac{\gamma}{2}\right)\frac{q\left(\tilde{\lambda}\pm i\gamma\right)}{q\left(\tilde{\lambda}\right)}. \tag{28}$$

The function $\phi\left(\tilde{\lambda}\right)$ is

$$\phi\left(\tilde{\lambda}\right) = \prod_{j=1}^{\frac{N}{2}}\mathrm{sh}\left(\tilde{\lambda}-i\left(\frac{\gamma}{2}-\tau-\theta_j\right)\right)\mathrm{sh}\left(\tilde{\lambda}+i\left(\frac{\gamma}{2}-\tau+\theta_j\right)\right) \tag{29}$$

and $q\left(\tilde{\lambda}\right)$ is defined by

$$q\left(\tilde{\lambda}\right) := \prod_{k=1}^{M} \mathrm{sh}\left(\tilde{\lambda} - \tilde{\mu}_k\right). \tag{30}$$

In the following we let the tilde fall.

"The unknown zeroes of $q(\lambda)$ are the Bethe ansatz rapidities" [36, p. 536] and are determined by the Bethe ansatz equations, which are reformulated

$$\mathfrak{a}(\mu_k) = -1, \tag{31}$$

where the function $\mathfrak{a}(\lambda)$ is given by

$$\begin{aligned} \mathfrak{a}(\lambda) &= \frac{\lambda_+(\lambda)}{\lambda_-(\lambda)} \\ &= e^{\beta h} \frac{\phi\left(\lambda - i\frac{\gamma}{2}\right) q(\lambda + i\gamma)}{\phi\left(\lambda + i\frac{\gamma}{2}\right) q(\lambda - i\gamma)}. \end{aligned} \tag{32}$$

2.1 Bethe ansatz equations of the one-dimensional anisotropic spin-$\frac{1}{2}$ Heisenberg model with spin-$\frac{1}{2}$ impurity and modification of the density of states

The Bethe ansatz equations for the column-to-column transfer matrix can be written as (27) or (31).

In the same way, it is possible to derive the Bethe ansatz equations of the row-to-row transfer matrix. That leads to

$$\frac{\mathrm{sh}\left(\nu_k - \nu + i\frac{\gamma}{2}\right)}{\mathrm{sh}\left(\nu_k - \nu - i\frac{\gamma}{2}\right)} \prod_{j=1}^{L} \frac{\mathrm{sh}\left(\nu_k - \vartheta_j + i\frac{\gamma}{2}\right)}{\mathrm{sh}\left(\nu_k - \vartheta_j - i\frac{\gamma}{2}\right)} = -\prod_{l=1}^{M} \frac{\mathrm{sh}\left(\nu_k - \nu_l + i\gamma\right)}{\mathrm{sh}\left(\nu_k - \nu_l - i\gamma\right)}. \tag{33}$$

Due to the shift on the vertical and horizontal lines and the spin-$\frac{1}{2}$ impurity, we have modified Bethe ansatz equations. Note that these shifts do not change the particle-particle or particle-impurity scattering phases. There is just a phase-shift of the particle wave function in the Bethe ansatz equations of the row-to-row transfer matrix due to the presence of the spin-$\frac{1}{2}$ impurity. "This is consistent with the understanding that the number of scattering channels in a Bethe ansatz-solvable Hamiltonian is conserved" [35, p. 5].

Furthermore the shifts $\theta_1, \ldots, \theta_{\frac{N}{2}}$ on the horizontal lines can only be seen in the Bethe ansatz equations of the column-to-column transfer matrix, whereas the shifts $\vartheta_1, \ldots, \vartheta_L$ on the vertical lines and the spin-$\frac{1}{2}$ impurity manifest themselves in the other set of Bethe ansatz equations.

2.2 Thermodynamics of the of the one-dimensional anisotropic spin-$\frac{1}{2}$ Heisenberg model with spin-$\frac{1}{2}$ impurity and modification of the density of states

Note that it is relatively easy to derive the Bethe ansatz equations of this new model. The thermodynamics can be explicitly determined. The derivation of the Hamiltonian, however, is much more complicated and is discussed in Chapter 2.4.
"We are dealing with a set of coupled non-linear equations" [36, p. 536] for the derivation of the thermodynamics. For the treatment of the thermodynamics of the anisotropic Heisenberg chain with spin-$\frac{1}{2}$ impurity and the further introduced modifications we derive a set of non-linear integral equations for the function $\mathfrak{a}(\lambda)$ (32). Hence we define the associated auxiliary function

$$\mathfrak{A}(\lambda) := 1 + \mathfrak{a}(\lambda). \tag{34}$$

The poles of $\mathfrak{A}(\lambda)$ are identical to those of $\mathfrak{a}(\lambda)$. However, the set of zeroes is different. The derivation of the non-linear integral equations follows the usual scheme [49, 70]. "There are, however, variants of these integral equations that are somewhat more convenient for the analysis" [70, p. 22]. Using $\mathfrak{b}(\lambda) = \mathfrak{a}\left(\lambda + i\frac{\gamma}{2}\right)$ and $\bar{\mathfrak{b}}(\lambda) = \frac{1}{\mathfrak{a}\left(\lambda - i\frac{\gamma}{2}\right)}$ yields

$$\ln \mathfrak{b}(\lambda) = -\beta (\rho_h * \epsilon)(\lambda) + \frac{\pi\beta h}{2(\pi-\gamma)} + (\kappa * \ln \mathfrak{B})(\lambda) - \left(\kappa * \ln \bar{\mathfrak{B}}\right)(\lambda + i\gamma), \tag{35}$$

$$\ln \bar{\mathfrak{b}}(\lambda) = -\beta (\rho_h * \epsilon)(\lambda) - \frac{\pi\beta h}{2(\pi-\gamma)} + \left(\kappa * \ln \bar{\mathfrak{B}}\right)(\lambda) - (\kappa * \ln \mathfrak{B})(\lambda - i\gamma), \tag{36}$$

$$\mathfrak{B}(\lambda) = 1 + \mathfrak{b}(\lambda), \tag{37}$$

$$\bar{\mathfrak{B}}(\lambda) = 1 + \bar{\mathfrak{b}}(\lambda). \tag{38}$$

The symbol $*$ denotes the convolution $(f * g)(x) = \int_{-\infty}^{\infty} \mathrm{d}y f(x-y) g(y)$ and the functions $\epsilon(\lambda)$ and $\kappa(x)$ are defined by

$$\epsilon(\lambda) := \frac{2\pi J \sin\gamma}{\gamma \mathrm{ch}\left(\frac{\pi}{\gamma}\lambda\right)}, \tag{39}$$

$$\kappa(x) := \int_{-\infty}^{\infty} \mathrm{d}k e^{ikx} \frac{\mathrm{sh}\left(k\left(\frac{\pi}{2}-\gamma\right)\right)}{2\mathrm{ch}\left(\frac{\gamma}{2}k\right)\mathrm{sh}\left(\frac{k}{2}(\pi-\gamma)\right)}. \tag{40}$$

"Note that the integrals in (35) and (36) are well-defined with integration paths just below and above the real axis" [70, p. 22].
The integral expression for Λ_0^{QTM} in the limit $N \to \infty$ reads

$$\ln \Lambda_0^{\mathrm{QTM}}(\lambda) = -\beta e_0(\lambda) + \left(K * \ln\left(\mathfrak{B}\bar{\mathfrak{B}}\right)\right)(\lambda), \tag{41}$$

where the functions $e_0(\lambda)$ and $K(\lambda)$ are defined by

$$e_0(\lambda) := J \sin\gamma \int_{-\infty}^{\infty} \mathrm{d}k e^{ik\lambda} \frac{\mathrm{sh}\left(\frac{k}{2}(\pi-\gamma)\right)}{\mathrm{sh}\left(\frac{\pi}{2}k\right)\mathrm{ch}\left(\frac{\gamma}{2}k\right)}, \tag{42}$$

$$K(\lambda) := \frac{1}{2\gamma \mathrm{ch}\left(\frac{\pi}{\gamma}\lambda\right)}. \tag{43}$$

Note that in the next chapter we will see that shifts $\vartheta_1, \ldots, \vartheta_L$ on the vertical lines are not necessary for the desired change in the dispersion relation / density of states (3). Shifts $\theta_1, \ldots, \theta_{\frac{N}{2}}$ on the horizontal lines are sufficient. For this reason, we set the shifts $\vartheta_1, \ldots, \vartheta_L$ on the vertical lines in this remaining subsection equal to zero. The free energy per site of the host and the spin-$\frac{1}{2}$ impurity are therefore

$$f_{\mathrm{h}} = -\frac{1}{\beta} \ln \Lambda_0^{\mathrm{QTM}}(0), \tag{44}$$

$$f_{\mathrm{i}} = -\frac{1}{\beta} \ln \Lambda_0^{\mathrm{QTM}}(\nu), \tag{45}$$

$$f = f_{\mathrm{h}} + \frac{1}{L} f_i. \tag{46}$$

Note that $\rho_h(\lambda)$ only enters into the non-linear integral equations of $\mathfrak{b}(\lambda)$ and $\bar{\mathfrak{b}}(\lambda)$ in the dressing term (35) and (36), while $\rho_v(\lambda)$ can only occur in the integral expression for the free energy of the host (26). The Hamiltonian of the model is derived in chapter 2.4.

2.3 Dispersion relation

In the following, we determine the new dispersion relation of the host. Since we are interested in pseudogap systems (3), we first consider (39)

$$\begin{aligned} \epsilon(\lambda) &= \frac{2\pi J \sin\gamma}{\gamma \mathrm{ch}\left(\frac{\pi}{\gamma}\lambda\right)} \\ \Rightarrow \left(\mathcal{F}\epsilon\right)(k) &= \int_{-\infty}^{\infty} \mathrm{d}\lambda e^{-ik\lambda} \epsilon(\lambda) \\ &= \frac{2\pi J \sin\gamma}{\mathrm{ch}\left(\frac{\gamma}{2}k\right)}, \end{aligned}$$

where $\epsilon(\lambda)$ denotes the energy of the low-lying excitation of the antiferromagnet. The corresponding momentum is the integral of $\epsilon(\lambda)$ with respect to the spectral parameter ($\epsilon(\lambda) = p'(\lambda)$).
The function $(\mathcal{F}\epsilon)(k)$ has poles at $\frac{\pi i}{\gamma}(\pm 1 + 2m)$ with $m \in \mathbb{Z}$.
There are many different distribution densities ρ_h and ρ_v that could be used to describe shifts on the horizontal and vertical lines. Since we are interested in pseudogap systems (3), we use the following distribution densities

$$\begin{aligned} \rho_h(\lambda) &= \frac{\alpha_h}{\gamma \mathrm{ch}\left(\frac{\pi}{\gamma}\alpha_h \lambda\right)}, \qquad \tilde{\rho}_v(\lambda) = \frac{\alpha_v}{\gamma \mathrm{ch}\left(\frac{\pi}{\gamma}\alpha_v \lambda\right)}, \\ \Rightarrow (\mathcal{F}\rho_h)(k) &= \frac{1}{\mathrm{ch}\left(\frac{\gamma}{2\alpha_h}k\right)}, \qquad (\mathcal{F}\tilde{\rho}_v)(k) = \frac{1}{\mathrm{ch}\left(\frac{\gamma}{2\alpha_v}k\right)}. \end{aligned} \tag{47}$$

The functions $(\mathcal{F}\rho_h)(k)$ and $(\mathcal{F}\rho_v)(k)$ have poles at $\frac{\pi i}{\gamma}\alpha_h(\pm 1 + 2m_h)$ and $\frac{\pi i}{\gamma}\alpha_v(\pm 1 + 2m_v)$ with $m_h, m_v \in \mathbb{Z}$. The distribution densities also satisfy

$$\int_{-\infty}^{\infty} \mathrm{d}\lambda \rho_h(\lambda) = \int_{-\infty}^{\infty} \mathrm{d}\lambda \rho_v(\lambda) = 1. \tag{48}$$

$\rho_h(\lambda)$ only enters into the non-linear integral equations of $\mathfrak{b}(\lambda)$ and $\bar{\mathfrak{b}}(\lambda)$ (35) and (36) in the dressing term and changes the energy. If there were no shifts $\theta_1, \ldots, \theta_{\frac{N}{2}}$ on the horizontal lines, this dressing term would be $-\beta\epsilon(\lambda)$. With shifts it is $-\beta(\rho_h * \epsilon)(\lambda)$. We consider therefore $(\rho_h * \epsilon)(\lambda)$ and use the convolution theorem

$$(\rho_h * \epsilon)(\lambda) = \int_{-\infty}^{\infty} \frac{\mathrm{d}k}{2\pi} e^{ik\lambda} (\mathcal{F}\rho_h)(k) (\mathcal{F}\epsilon)(k). \tag{49}$$

The poles of the two functions $(\mathcal{F}\rho_h)(k)$ and $(\mathcal{F}\epsilon)(k)$ determine the behaviour of the function $(\rho_{\alpha_h} * \epsilon)(\lambda)$ for large λ

$$\begin{aligned} \epsilon_{\mathrm{new}}(\lambda) &:= (\rho_h * \epsilon)(\lambda) \\ &\underset{\text{large } \lambda}{\simeq} \begin{cases} \mathrm{cst}.e^{-\frac{\pi}{\gamma}\alpha_h|\lambda|}, & \text{for } \alpha_h < 1, \\ \mathrm{cst}.e^{-\frac{\pi}{\gamma}|\lambda|}, & \text{for } \alpha_h \geq 1. \end{cases} \end{aligned} \tag{50}$$

We consider (43)

$$K(\lambda) = \frac{1}{2\gamma \mathrm{ch}\left(\frac{\pi}{\gamma}\lambda\right)}$$
$$\Rightarrow (\mathcal{F}K)(k) = \frac{1}{2\mathrm{ch}\left(\frac{\gamma}{2}k\right)}.$$

The function $(\mathcal{F}K)(k)$ has poles at $\frac{\pi i}{\gamma}(\pm 1 + 2n)$ with $n \in \mathbb{Z}$.
The "momentum" of the low-lying excitation of the system with shifts $\vartheta_1, \ldots, \vartheta_L$ on the vertical lines is $p_{\mathrm{new}}(\lambda) = (\rho_v * p)(\lambda)$ or in differential form

$$\begin{aligned} p'_{\mathrm{new}}(\lambda) &= (\rho_v * K)(\lambda) \\ &\overset{\text{large } \lambda}{\simeq} \begin{cases} \mathrm{cst}.e^{-\frac{\pi}{\gamma}\alpha_v|\lambda|}, & \text{for } \alpha_v < 1, \\ \mathrm{cst}.e^{-\frac{\pi}{\gamma}|\lambda|}, & \text{for } \alpha_v \geq 1. \end{cases} \end{aligned} \tag{51}$$

Note that the system is no longer translationally invariant, but $p_{\mathrm{new}}(\lambda)$ is a "appropriate quantum number" that is uniformly distributed in the interval $[-\pi, \pi]$.
Since obviously large λ corresponds to small momenta, the following new dispersion relation follows

$$\epsilon_{\mathrm{new}}(p_{\mathrm{new}}) \overset{\text{small } p_{\mathrm{new}}}{\simeq} \begin{cases} \mathrm{cst}.\,|p_{\mathrm{new}}|^{\frac{\alpha_h}{\alpha_v}}, & \text{for } \alpha_h, \alpha_v < 1, \\ \mathrm{cst}.\,|p_{\mathrm{new}}|^{\alpha_h}, & \text{for } \alpha_h < 1, \alpha_v \geq 1, \\ \mathrm{cst}.\,|p_{\mathrm{new}}|^{\frac{1}{\alpha_v}}, & \text{for } \alpha_h \geq 1, \alpha_v < 1, \\ \mathrm{cst}.\,|p_{\mathrm{new}}|, & \text{for } \alpha_h, \alpha_v \geq 1. \end{cases} \tag{52}$$

The exponent of p_{new} is always positive. In the first case, the exponent is arbitrary, in the second smaller than 1 and in the third larger than 1. Finally we have a linear dispersion relation in the last case.
The parameters α_h and α_v can thus be selected so that they correspond to a pseudogap system, because the density of states of the host is given by

$$\rho(\epsilon) = \frac{1}{2\pi |\partial_k \epsilon(k)|}. \tag{53}$$

Assuming $\epsilon(k) = Ak^z$ yields

$$\rho(\epsilon) = \frac{|\epsilon|^{\frac{1}{z}-1}}{2\pi \left| zA^{\frac{1}{z}} \right|}. \tag{54}$$

In the case $0 < \alpha_h, \alpha_v < 1$ follows

$$\rho(\epsilon) = \frac{|\epsilon|^{\frac{\alpha_v}{\alpha_h}-1}}{2\pi\frac{\alpha_h}{\alpha_v}|A_{h,v}|^{\frac{\alpha_v}{\alpha_h}}}.$$

For $\alpha_v > \alpha_h$ follows a positive exponent, which is fitting for a pseudogap system. For $\alpha_v = 2\alpha_h$ we find the case of charge-neutral graphene. (Note that, of course, this model is not yet used to study graphene, it is a toy model.) It is also noteworthy that shifts $\vartheta_1, \ldots, \vartheta_L$ on the vertical lines are not necessary. Shifts $\theta_1, \ldots, \theta_{\frac{N}{2}}$ on the horizontal lines are sufficient, since then follows a density of states with positive exponent

$$\rho(\epsilon) = \frac{|\epsilon|^{\frac{1}{\alpha_h}-1}}{2\pi\alpha_h|A_h|^{\frac{1}{\alpha_h}}}, \qquad 0 < \alpha_h < 1.$$

A, $A_{h,v}$ and A_h are constants.

2.4 Hamiltonian

In the following section, we sketch a way to calculate the Hamiltonian of the one-dimensional anisotropic spin-$\frac{1}{2}$ Heisenberg chain with spin-$\frac{1}{2}$ impurity and modified density of states.

2.4.1 Hamiltonian of the one-dimensional spin-$\frac{1}{2}$ anisotropic Heisenberg model with spin-$\frac{1}{2}$ impurity

Setting all shifts $\theta_1 = ... = \theta_{\frac{N}{2}} = \vartheta_1 = \ldots = \vartheta_L = 0$, which means that we only consider the one-dimensional spin-$\frac{1}{2}$ anisotropic Heisenberg model with an integrable spin-$\frac{1}{2}$ impurity, yields the Hamiltonian

$$\mathcal{H} = 2iJ\sin\gamma\,\frac{\mathrm{d}}{\mathrm{d}\lambda}\ln t(\lambda,\nu)\Big|_{\lambda=0}, \tag{55}$$

where $t(\lambda,\nu)$ is the row-to-row transfer matrix. Through a direct but straightforward calculation we obtain the following compact expression. We remark that the XXZ Hamiltonian with the spin-$\frac{1}{2}$ impurity, given in (56) is hermitian when the spin-$\frac{1}{2}$ impurity spectral parameter ν is real.

$$\begin{aligned}\mathcal{H} = & J\sum_{j=1}^{L-1}\left(\sigma_j^x\sigma_{j+1}^x+\sigma_j^y\sigma_{j+1}^y+\Delta\left(\sigma_{j-1}^z\sigma_j^z-1\right)\right)-J\Delta-\frac{h}{2}\sum_{j=1}^{L}\sigma_j^z\\ & +Jc\left(i\nu\right)c\left(-i\nu\right)\left(\mathrm{ch}\nu\left(\sigma_L^x\sigma_{L+1}^x+\sigma_L^y\sigma_{L+1}^y\right)+\Delta\left(\sigma_L^z\sigma_{L+1}^z-1\right)\right)\\ & +Jc\left(i\nu\right)c\left(-i\nu\right)\left(\mathrm{ch}\nu\left(\sigma_{L+1}^x\sigma_1^x+\sigma_{L+1}^y\sigma_L^y\right)+\Delta\sigma_{L+1}^z\sigma_1^z\right)\\ & +Jb\left(i\nu\right)b\left(-i\nu\right)\Delta\left(\sigma_L^x\sigma_1^x+\sigma_L^y\sigma_1^y+\sigma_L^z\sigma_1^z\right)\\ & +iJb\left(i\nu\right)c\left(-i\nu\right)\left(\mathrm{ch}\nu\left(\sigma_L^y\sigma_1^x-\sigma_L^x\sigma_1^y\right)\sigma_{L+1}^z-\Delta\left(\sigma_L^y\sigma_{L+1}^x-\sigma_L^x\sigma_{L+1}^y\right)\sigma_1^z\right.\\ & \left.-\Delta\left(\sigma_{L+1}^y\sigma_1^x-\sigma_{L+1}^x\sigma_1^y\right)\sigma_L^z\right).\end{aligned} \tag{56}$$

By putting $\nu = 0$, the Hamiltonian reduces to the standard homogeneous spin-$\frac{1}{2}$ anisotropic Heisenberg model on $L+1$ sites, which has no impurity.

2.4.2 Hamiltonian of the one-dimensional spin-$\frac{1}{2}$ anisotropic Heisenberg model with spin-$\frac{1}{2}$ impurity and shifts on the horizontal and vertical lines

If we want to calculate the Hamiltonian of the one-dimensional spin-$\frac{1}{2}$ anisotropic Heisenberg model with spin-$\frac{1}{2}$ impurity and shifts $\theta_1,\ldots,\theta_{\frac{N}{2}}$ and $\vartheta_1,\ldots,\vartheta_L$ on the horizontal and vertical lines we have to pay attention to two aspects.
First, we have to perform a Jordan-Wigner transformation for the host in the Hamiltonian in (56) and switch to the momentum space via Fourier transformation. Since we know the effect of the shifts $\theta_1,\ldots,\theta_{\frac{N}{2}}$ and $\vartheta_1,\ldots,\vartheta_L$ on the horizontal and vertical lines on the host (these change the dispersion relation), the old dispersion relation can now be exchanged with the new one. Nothing else changes in the host.
The Jordan-Wigner transformation for the host in (56) yields

$$H_{\mathrm{h}} = J\sum_{j=1}^{L}\left(2\left(c_{j-1}^\dagger c_j+c_j^\dagger c_{j-1}\right)+\Delta\left(\left(1-2n_{j-1}\right)\left(1-2n_j\right)-1\right)\right)-\frac{h}{2}\sum_{j=1}^{L}\left(2n_j-1\right),$$

and after the Fourier transformation we find

$$\begin{aligned}H_{\mathrm{h}} = & 4J\left(\sum_{k=0}^{L-1}\left(\cos\left(\frac{2\pi}{L}k\right)-\Delta\right)c_k^\dagger c_k+\frac{\Delta}{L}\sum_{k,k',q=0}^{L-1}\cos\left(\frac{2\pi}{L}q\right)c_{k-q}^\dagger c_{k'+q}^\dagger c_{k'}c_k\right)\\ & -\frac{h}{2}\sum_{k=0}^{L-1}\left(2c_k^\dagger c_k-1\right).\end{aligned}$$

The more complicated question is how the shifts $\theta_1,\ldots,\theta_{\frac{N}{2}}$ and $\vartheta_1,\ldots,\vartheta_L$ on the horizontal and vertical lines affect the interaction with the spin-$\frac{1}{2}$ impurity. With the inhomogenities

on the vertical lines there is a priori no local Hamiltonian. Since we saw in Chapter 2.3 that shifts $\vartheta_1, \ldots, \vartheta_L$ on the vertical lines are not necessary for the desired modification of the dispersion relation, we set these inhomogenities equal to zero, as in Chapter 2.2.
In principle, there are three cases of the interaction of one plane wave with the spin-$\frac{1}{2}$ impurity which must be observed.

1. A plane wave with spectral parameter Θ can interact with the spin-$\frac{1}{2}$ impurity so that the impurity spin changes from $\uparrow$ to $\downarrow$. The impurity spin can also change from $\downarrow$ to $\uparrow$ and a plane wave is emitted. The transition rate for this we call $A_{\uparrow\downarrow}(\Theta) = A_{\downarrow\uparrow}(\Theta)$.

2. A plane wave with spectral parameter Θ can interact with the spin-$\frac{1}{2}$ impurity so that a plane wave with spectral parameter $\tilde{\Theta}$ goes out. The impurity spin remains fixed. The transition for these two cases we call $A_{\uparrow\uparrow}\left(\Theta, \tilde{\Theta}\right)$ and $A_{\downarrow\downarrow}\left(\Theta, \tilde{\Theta}\right)$.

Note that the spectral parameters Θ and $\tilde{\Theta}$ can be converted in momenta k_{in} and k_{out} before and after the interaction. The transition rates occur in the Hamiltonian and must be calculated.
The exact evaluation is based on the fact that the local objects

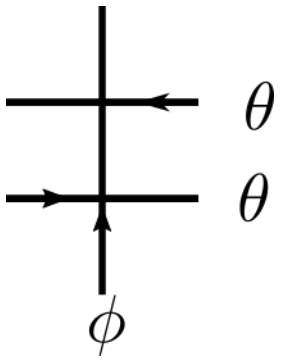

Figure 8: Product of L-matrices with spectral parameters θ and ϕ, which are used for calculations.

leave right hand-sided singlets

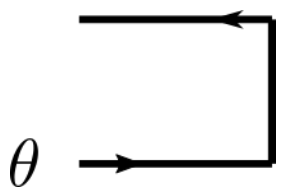

Figure 9: "Ket" singlets.

and "bra" states (which are orthogonal to the right hand-sided singlet) invariant,

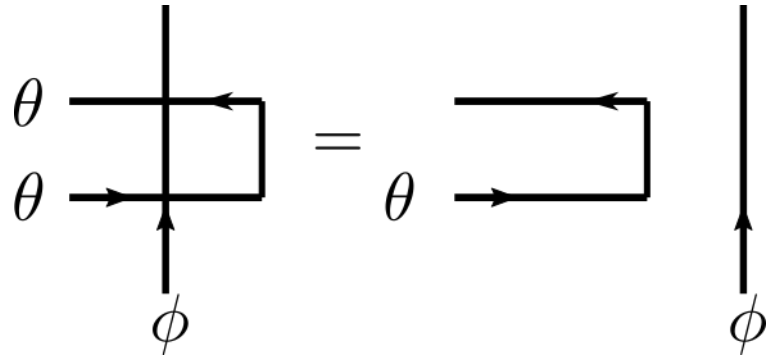

Figure 10: Invariance.

but other states (orthogonal to the right hand-sided singlet) have very small eigenvalues. That reads

$$\begin{aligned} t(\theta)\,\bar{t}(\theta) &= \mathrm{id} + \mathcal{O}\left(e^{-\mathrm{cst}.L}\right), \\ t(\theta)\,\bar{t}(\theta+\epsilon) &= e^{-\epsilon H} + \mathcal{O}\left(e^{-\mathrm{cst}.L}\right). \end{aligned} \tag{57}$$

For L lattice sites of the host we consider the row-to-row transfer matrix with open boundary conditions left and right. An incoming or outgoing plane wave with spectral parameter k and $\sigma = 1$ can be written down graphically.

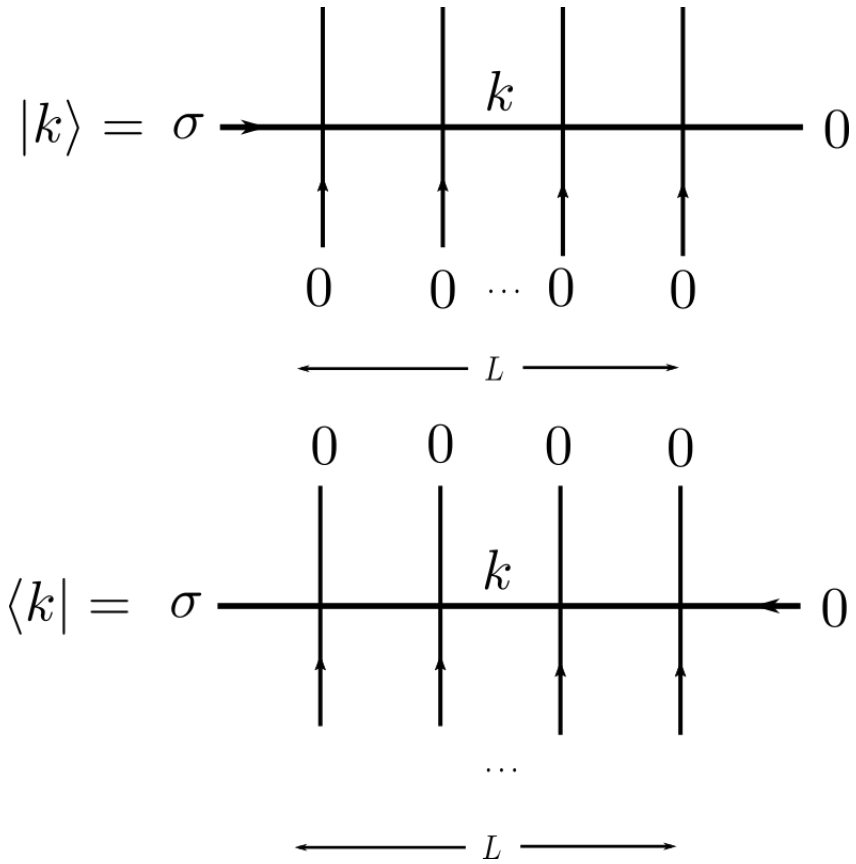

Figure 11: Incoming and outgoing plane wave with $\sigma = 1$. The spectral parameters can be converted into momenta as required. σ on the horizontal line means that there is a spinless fermion, 0 means there is none.

Due to equation (57), we consider two horizontal lines, i.e. the product of two row-to-row transfer matrices. Now we consider the interaction with a plane wave which is generated. Putting everything together we get

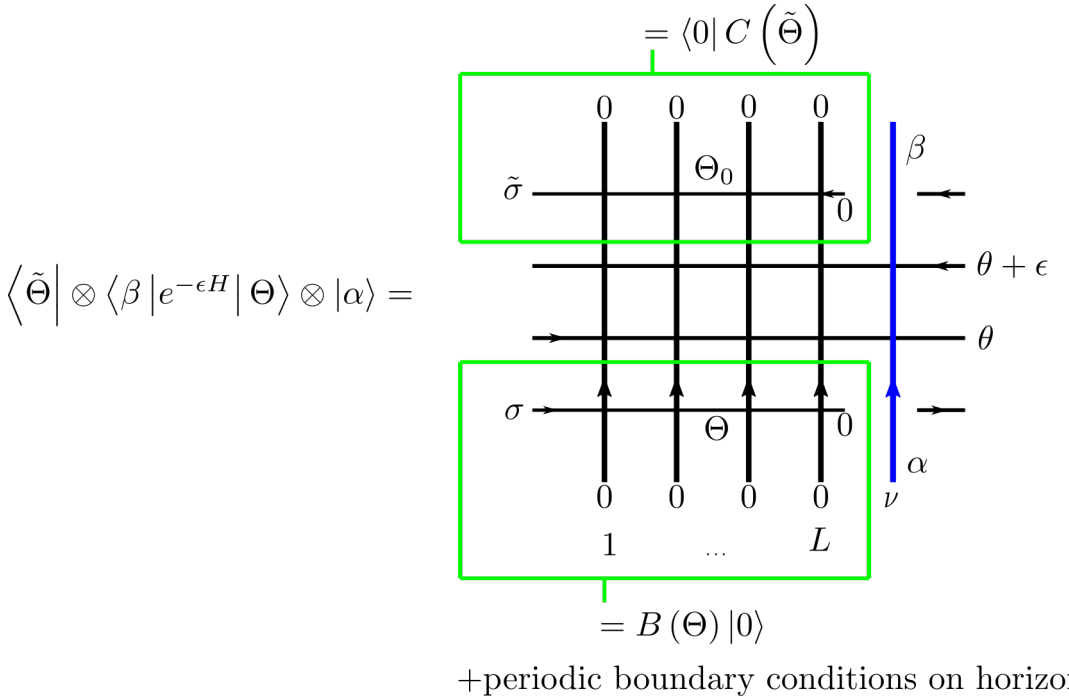

Figure 12: The "effective" partition function on a $(L+1) \times 4$ lattice. Here we can also add a twist angle. We can see two kinds of column-to-column transfer matrices, T for the host and T_{i} for the impurity. Note that we use open boundary conditions on vertical lines.

The matrix element has a natural interpretation as the partition function on a $(L+1) \times 4$ lattice. The derivative with respect to ϵ at $\epsilon = 0$ yields the desired matrix element of H. As $L \to \infty$ we intend to apply a transfer matrix approach. For this, we define the transfer matrices.

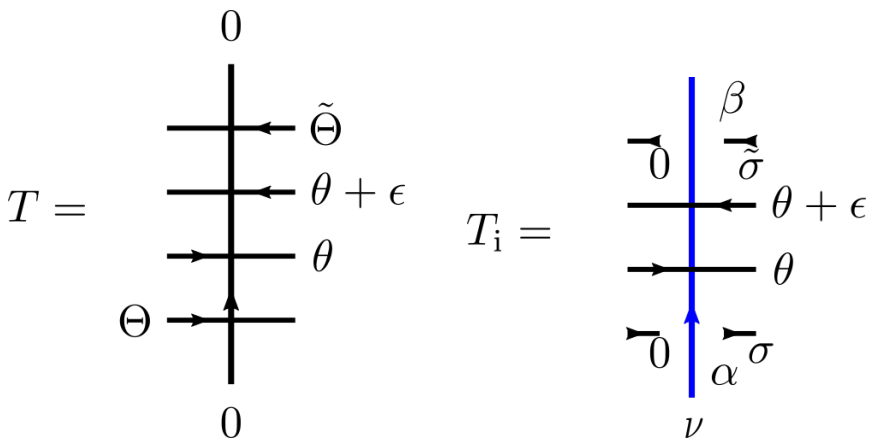

Figure 13: Transfer matrices of the bulk and the impurity.

These calculations were performed on Maple and the results for $\Delta = 1$ are

$$A_{\uparrow\downarrow}(\Theta) = A_{\downarrow\uparrow}(\Theta) = \frac{2\Theta(3\theta - 2\Theta - 1 - \nu)}{(1+\theta-\nu)(-1+\theta-\nu)(-1+\theta-\Theta)(\theta-\Theta)},$$

$$A_{\uparrow\uparrow}(\Theta,\Theta_0) = 2\Theta\left(1+\tilde{\Theta}\right) \cdot \frac{1 - 3\theta + 4\theta^2 + \nu - 2\theta\nu - 3\theta\left(\Theta+\tilde{\Theta}\right) + \tilde{\Theta} + \Theta + 2\Theta\tilde{\Theta} + \left(\Theta+\tilde{\Theta}\right)\nu}{(1+\theta-\nu)(-1+\theta-\nu)(-1+\theta-\Theta)\left(-1+\theta-\tilde{\Theta}\right)(\theta-\Theta)\left(\theta-\tilde{\Theta}\right)},$$

$$A_{\downarrow\downarrow}(\Theta,\Theta_0) = -2\Theta\left(1+\tilde{\Theta}\right) \cdot \frac{-1 - 3\theta + 4\theta^2 + \nu - 2\theta\nu - 3\theta\left(\Theta+\tilde{\Theta}\right) + \tilde{\Theta} + \Theta + 2\Theta\tilde{\Theta} + \left(\Theta+\tilde{\Theta}\right)\nu}{(1+\theta-\nu)(-1+\theta-\nu)\left(-1+\theta-\tilde{\Theta}\right)\left(-1+\theta-\tilde{\Theta}\right)(\theta-\Theta)\left(\theta-\tilde{\Theta}\right)}.$$

All transition rates are real and show physical behaviour. This means that the shifts on the horizontal do not create a problem and the Hamiltonian can now simply be specified. Notice that all transition rates depend on θ, which corresponds to the horizontal shifts. The calculations can also be done for $\Delta \neq 1$, but require a higher computation time. Therefore the results are not listed here. The spectral parameters Θ and $\tilde{\Theta}$ can be converted into momenta k and $\tilde{k}$.
The hybridization is given by

$$V_k = J \int_{-\infty}^{\infty} \mathrm{d}\theta \rho_h(\theta) A_{\uparrow\downarrow}\left(\frac{\gamma}{\pi}\ln\frac{2\pi^2 k}{L}\right). \tag{58}$$

The Hamiltonian of the one-dimensional spin-$\frac{1}{2}$ isotropic Heisenberg model with spin-$\frac{1}{2}$ impurity and shifts on the horizontal lines for the case $\alpha_h < 1$ is therefore given by

$$H = \sum_{k=0}^{L-1}\left(\left(4J\left(\left(\frac{2\pi k}{L}\right)^{\alpha_h} - 1\right) - h\right)c_k^\dagger c_k + V_k\left(c_k^\dagger d + d^\dagger c_k\right)\right) + \frac{4J}{L}\sum_{k,k',q=0}^{L-1}\cos\left(\frac{2\pi}{L}q\right)c_{k-q}^\dagger c_{k'+q}^\dagger c_{k'}c_k + \frac{hL}{2} + \text{many particle terms.} \tag{59}$$

We determined the Hamiltonian of this new model, where we neglected additional many-body terms. Naturally, terms of this kind exist because of the shifts $\theta_1, \ldots, \theta_{\frac{N}{2}}$ on the horizontal lines. The calculation of the additional many-body terms becomes more and more complicated and reaches its limits. It should also be noted that this is a special impurity lattice model with an impurity interacting with an interacting host.
From this model we have therefore learned that it is possible to introduce an impurity in an integrable lattice model and to modify the dispersion relation. On the lattice, however,

there are relevant many-particle terms that cannot be neglected.

2.5 Low temperature asymptotics

In this section we will consider the low-temperature asymptotics of our model and we will determine critical exponents for the host and the impurity.
There are two cases for the low-temperature analysis. The case $h = 0$ and the case $h > 0$ (which is analogous to $h < 0$).

2.5.1 Case $h = 0$

In the case of $h = 0$ we consider

$$\begin{aligned}
\ln \Lambda_0^{\mathrm{QTM}}(\lambda) &= -\beta e_0(\lambda) + \left(K * \ln\left(\mathfrak{B}\bar{\mathfrak{B}}\right)\right)(\lambda) \\
&= -\beta e_0(\lambda) + \int\limits_{\mu > \frac{\gamma \ln \beta}{\pi \alpha_h}}^{\infty} \mathrm{d}\mu K\left(\lambda - \mu - \frac{\gamma \ln \beta}{\pi \alpha_h}\right) \ln\left(\mathfrak{B}\bar{\mathfrak{B}}\right)\left(\mu + \frac{\gamma \ln \beta}{\pi \alpha_h}\right) \\
&\quad + \int\limits_{\mu > \frac{\gamma \ln \beta}{\pi \alpha_h}}^{\infty} \mathrm{d}\mu K\left(\lambda + \mu + \frac{\gamma \ln \beta}{\pi \alpha_h}\right) \ln\left(\mathfrak{B}\bar{\mathfrak{B}}\right)\left(-\mu - \frac{\gamma \ln \beta}{\pi \alpha_h}\right) \\
&= -\beta e_0(\lambda) + \frac{1}{\gamma \beta^{\frac{1}{\alpha_h}}} \int\limits_{\mu > \frac{\gamma \ln \beta}{\pi \alpha_h}}^{\infty} \mathrm{d}\mu \left(e^{\frac{\pi}{\gamma}(\lambda - \mu)} + e^{-\frac{\pi}{\gamma}(\lambda - \mu)}\right) \ln\left(\mathfrak{B}\bar{\mathfrak{B}}\right)\left(\mu + \frac{\gamma \ln \beta}{\pi \alpha_h}\right).
\end{aligned}$$

Defining the functions

$$B(\lambda) := \mathfrak{B}\left(\lambda + \frac{\gamma \ln \beta}{\pi \alpha_h}\right), \qquad \bar{B}(\lambda) := \bar{\mathfrak{B}}\left(\lambda + \frac{\gamma \ln \beta}{\pi \alpha_h}\right) \tag{60}$$

yields

$$\ln \Lambda_0^{\mathrm{QTM}}(\lambda) = -\beta e_0(\lambda) + \frac{2}{\gamma \beta^{\frac{1}{\alpha_h}}} \int\limits_{\frac{\gamma \ln \beta}{\pi \alpha_h}}^{\infty} \mathrm{d}\mu \mathrm{ch}\left(\frac{\pi}{\gamma}(\lambda - \mu)\right) \ln\left(B^+ \bar{B}^+\right)(\mu)$$

This means that for the case $0 < \alpha_h, \alpha_v < 1$ (the case with the positive but otherwise arbitrary exponent in the dispersion relation) the free energy of the host shows a $T^{1+\frac{\alpha_v}{\alpha_h}}$ and the spin-$\frac{1}{2}$ impurity shows a $T^{1+\frac{1}{\alpha_h}}$ behaviour. In the case of no shifts $\vartheta_1, \ldots, \vartheta_L$ on the vertical lines we find $T^{1+\frac{1}{\alpha_h}}$ behaviour for the contribution to the free energy for both the host and the impurity.

2.5.2 Case $h > 0$

In the case of $h > 0$ and $T \to 0$, the dressing terms of the non-linear integral equations for $\mathfrak{b}(\lambda)$ and $\bar{\mathfrak{b}}(\lambda)$ (35) and (36) are dominant and $\mathfrak{b}(\lambda) \gg \bar{\mathfrak{b}}(\lambda)$ and also $1 \gg \bar{\mathfrak{b}}(\lambda)$. Therefore we consider

$$\mathfrak{B}(\lambda) = 1 + e^{-\beta\left((\rho_h * \epsilon)(\lambda) - \frac{\pi h}{2(\pi-\gamma)}\right)}. \tag{61}$$

and

$$\begin{aligned} \left|\ln \bar{\mathfrak{B}}(\lambda)\right| &\propto e^{-\mathrm{cst.}\beta} \\ &\to 0. \end{aligned}$$

For $\lambda = \lambda_0$ let

$$(\rho_h * \epsilon)(\lambda_0) - \frac{\pi h}{2(\pi - \gamma)} = 0. \tag{62}$$

This equation defines λ_0 for temperature $T = 0$. Note that $\rho_h(\lambda)$ and $\epsilon(\lambda)$ are real and symmetric functions. Therefore, $(\rho_h * \epsilon)(\lambda)$ is also real and symmetric. A numerical analysis shows that points $\pm\lambda_0$ that satisfy (62) exist. In general for $T \neq 0$ $\pm\lambda_0$ are zeroes of the function $-\frac{\ln \mathfrak{b}(\lambda)}{\beta}$.
The driving term of $\mathfrak{b}(\lambda)$ is real and symmetric and has the property, that the function $\mathfrak{b}(\lambda)$ shows "steep crossover behaviour" [36, p. 593] at λ_0 for low temperatures

$$\begin{aligned} \mathfrak{b}(\lambda) &\ll 1 \qquad \text{for } |\lambda| < \lambda_0, \\ \mathfrak{b}(\lambda) &\gg 1 \qquad \text{for } |\lambda| > \lambda_0. \end{aligned}$$

"The slopes at the crossover points are steep, allowing" [36, p. 593] some approximations to the integral equation.
Then we find

$$\begin{aligned}
\ln \Lambda_0^{\mathrm{QTM}}(\lambda) &= -\beta e_0(\lambda) + (K * \ln \mathfrak{B})(\lambda) \\
&= -\beta e_0(\lambda) + \int_{-\infty}^{\infty} \mathrm{d}\mu K(\lambda-\mu) \ln \mathfrak{B}(\mu) \\
&\simeq -\beta e_0(\lambda) - \beta \int_{|\mu|>\lambda_0} \mathrm{d}\mu K(\lambda-\mu) \left((\rho_h * \epsilon)(\mu) - \frac{\pi h}{2(\pi-\gamma)} \right) \\
&\quad + \int_{|\mu|<\lambda_0} \mathrm{d}\mu K(\lambda-\mu) \ln\left(1 + e^{-\beta\left((\rho_h*\epsilon)(\lambda) - \frac{\pi h}{2(\pi-\gamma)}\right)}\right) \\
&\quad + \int_{|\mu|>\lambda_0} \mathrm{d}\mu K(\lambda-\mu) \ln\left(1 + e^{\beta\left((\rho_h*\epsilon)(\lambda) - \frac{\pi h}{2(\pi-\gamma)}\right)}\right).
\end{aligned}$$

The slope $-\beta(\rho_h * \epsilon)'(\lambda)$ is of order $\mathcal{O}(\beta)$ and thus "steep at low temperatures" [36, p. 593], therefore we approximate $e^{\pm\beta\left((\rho_h*\epsilon)(\lambda) - \frac{\pi h}{2(\pi-\gamma)}\right)}$ for $|\lambda| > \lambda_0$ and $|\lambda| < \lambda_0$ by $e^{\beta(\rho_h*\epsilon)'(\lambda_0)|\lambda\pm\lambda_0|}$ in the vicinity of the Fermi rapidities $\pm\lambda_0$. Thus the last two terms in the integral yield

$$\begin{aligned}
\ln \Lambda_0^{\mathrm{QTM}}(\lambda) &= -\beta e_0(\lambda) \\
&\quad - \beta \int_{\lambda_0}^{\infty} \mathrm{d}\mu \left(K(\lambda-\mu) + K(\lambda+\mu)\right) \left((\rho_h * \epsilon)(\mu) - \frac{\pi h}{2(\pi-\gamma)} \right) \\
&\quad + 2\left(K(\lambda-\lambda_0) + K(\lambda+\lambda_0)\right) \int_0^{\infty} \mathrm{d}\mu \ln\left(1 + e^{\beta(\rho_h*\epsilon)'(\lambda_0)\mu}\right) + o\left(\frac{1}{\beta}\right) \\
&= -\beta e_0(\lambda) - \frac{\pi^2}{6\beta(\rho_{\alpha_h} * \epsilon)'(\lambda_0)} \left(K(\lambda-\lambda_0) + K(\lambda+\lambda_0)\right) \\
&\quad - \beta \int_{\lambda_0}^{\infty} \mathrm{d}\mu \left(K(\lambda-\mu) + K(\lambda+\mu)\right) \left((\rho_h * \epsilon)(\mu) - \frac{\pi h}{2(\pi-\gamma)} \right), \qquad (63)
\end{aligned}$$

where we have evaluated the integral

$$\int_0^{\infty} \mathrm{d}x \ln(1 + e^x) = \frac{\pi^2}{12}.$$

This means that regardless of the choice of the parameters α_h and α_v, the free energy of the host and the impurity show a T^2 behaviour in this case.
The exponents for the low temperature asymptotics therefore depend on h.

Combining the results from the chapters 2.5.1 and 2.5.2 leads with a very similar calculation to the scaling behaviour and we see that the free energy behaves essentially like a function g of $\frac{h}{T}$

$$f = T^2 \left(\text{cst.} + g\left(\frac{h}{T}\right)\right).$$

3 Hubbard model with integrable impurity

In this section the history of the one-dimensional Hubbard model is summarized by following and quoting the excellent textbook [36].

"One of the main motivations for studying the Hubbard model is that it is the simplest generalization beyond the band theory description of solids, yet still appears to capture the gross physical features of many systems characterized by more general interaction parameters. The Hubbard model has been used in attempts to describe

- the electronic properties of solids with narrow bands,
- band magnetism in iron, cobalt, nickel,
- the Mott metal-insulator transition,
- electronic properties of high-T_c cuprates in the normal state.

Despite its apparent simplicity, no fully consistent treatment of the Hubbard model is available in general. However, there are two cases in which one is more fortunate and many properties are calculable, namely the extremes of lattice coordination numbers two and infinity. One might naively expect that the latter case can be easily understood by means of a mean-field approximation. Surprisingly, there is a particular way of performing the limit of infinite lattice dimension $d \to \infty$ [86], in which the behaviour of the Hubbard model does not become mean-field like, but the model remains tractable. A striking result obtained in this approach is an understanding of the Mott transition between a paramagnetic metal and a correlated insulator [46, 45].

[...] Here we are concerned with the first case, which corresponds to a one-dimensional lattice" [36, p. 6].

"The history of the [...] Hubbard model as an exactly solvable model began in 1968 with [...] Lieb and [...] Wu's article [79]. Lieb and Wu discovered that Bethe's ansatz can be applied to the Hubbard model and reduced the spectral problem of the Hamiltonian to solving a set of algebraic equations, nowadays known as the Lieb-Wu equations [...]. They succeeded in calculating the ground state energy and demonstrated that the Hubbard model undergoes a Mott metal-insulator transition at half filling (one electron per site) with critical interaction strength $U = 0$. [...] In 1972 [...] Takahashi [117] proposed a classification of the solutions of the Lieb-Wu equations in terms of a string hypothesis. He employed this hypothesis to replace the Lieb-Wu equations by simpler ones and then proceeded to derive a set of non-linear integral equations, which determine the Gibbs free energy of the Hubbard model [...]. These integral equations are known as thermodynamic Bethe ansatz [...] equations. Solving them in the limit of small temperatures Takahashi calculated the specific heat [118]. Later on a more complete picture of the thermodynamics of the Hubbard model was obtained from numerical solutions of the thermodynamic Bethe ansatz equations

[68, 130]. In fact, Takahashi's equations, in conjunction with the thermodynamic Bethe ansatz equations, can be used to calculate any physical quantity that pertains to the energy spectrum of the Hubbard model. In particular, the dispersion curves of all elementary excitations can be obtained from the thermodynamic Bethe ansatz equations in the limit $T \to 0$ [32]. Constraints on the quantum numbers in Takahashi's equations imply certain selection rules that determine the allowed combinations of elementary excitations and therefore the physical excitation spectrum [32]. [...] Takahashi's equations may also serve as starting point for the calculation of the scattering matrix of the elementary excitations. For the half-filled Hubbard model in vanishing magnetic field the S-matrix was calculated [38, 39]. It was shown that the excitation spectrum at half filling is given by scattering states of four elementary excitations: holon and antiholon with spin 0 and charge $\pm e$ and charge neutral spinons with spin up or down respectively. This is remarkable, since away from half filling, or at finite magnetic field, the number of elementary excitations is infinite [32]. It was further shown that the four particles can only be excited in $SO(4)$ multiplets [38, 39]" [36, p. 9 - 10].

"In 1986 B. S. Shastry opened up a new way for studying the Hubbard model by placing it into the framework of the quantum inverse scattering method. Using a Jordan-Wigner transformation he mapped the Hubbard model to a spin model and then demonstrated that the resulting spin Hamiltonian commutes with the row-to-row transfer matrix of a related covering vertex model [112]. Shastry first obtained the R-matrix of the spin model, thus embedding it into the general classification of integrable models [111]. [...] It was shown that Shastry's R-matrix satisfies the Yang-Baxter equation [114]. An algebraic Bethe ansatz for the Hubbard model was constructed [...] and expressions for the eigenvalues of the [row-to-row] transfer matrix of the two-dimensional statistical covering model were obtained [100, 144, 84]. This result was of crucial importance for the [...] [column-to-column] transfer matrix approach to the thermodynamics [63] of the Hubbard model [...]. This approach allows for a drastically simplified description of the thermodynamics in terms of the solution of a finite set of non-linear integral equations, rather than the infinite set originally obtained by Takahashi in 1972 [117]. Within the [...] [column-to-column] transfer matrix approach thermodynamic quantities can be calculated numerically with a very high precision. The approach can be extended to the calculation of correlation lengths at finite temperature [120, 129]" [36, p. 11].

First of all we consider the essential characteristics "of the Hamiltonian of the Hubbard model and its exactly solvable classical" [36, p. 548] analogue in two dimensions [36]. The Hubbard model characterizes a lattice fermion system on L sites with an electron hopping term, on-site Coulomb repulsion U and external fields μ and B:

$$H_{\text{Hubbard}} = -\sum_{j=1}^{L}\left(\sum_{a=\uparrow,\downarrow}\left(c_{j+1,a}^{\dagger}c_{j,a} + c_{j,a}^{\dagger}c_{j+1,a}\right) - U\left(n_{j,\uparrow} - \frac{1}{2}\right)\left(n_{j,\downarrow} - \frac{1}{2}\right)\right.$$
$$\left. +\mu\left(n_{j,\uparrow} + n_{j,\downarrow}\right) + B\left(n_{j,\uparrow} - n_{j,\downarrow}\right)\right) \tag{64}$$

In two dimensions we view at a double-layer square lattice, consisting of $\uparrow$- and $\downarrow$-sublattices, for the classical analogue. "Each local Hilbert space corresponding to a [...] [specific] site of the lattice is indexed by an integer j, the sublattice is [...] [labeled] by the additional $a = \uparrow, \downarrow$" [36, p. 549]. The following local vertex weights are found [113]

$$\begin{aligned} R\left(\lambda,\mu\right) &= \cos\left(\lambda+\mu\right)\mathrm{ch}\left(h\left(\lambda\right)-h\left(\mu\right)\right)r\left(\lambda-\mu\right) \\ &\quad +\cos\left(\lambda-\mu\right)\mathrm{sh}\left(h\left(\lambda\right)-h\left(\mu\right)\right)r\left(\lambda+\mu\right)\sigma_{1,\uparrow}^{z}\sigma_{1,\downarrow}^{z}, \\ r_a\left(\lambda\right) &= \frac{\cos\lambda+\sin\lambda}{2} + \frac{\cos\lambda-\sin\lambda}{2}\sigma_{1,a}^{z}\sigma_{2,a}^{z} + \sigma_{1,a}^{+}\sigma_{2,a}^{-} + \sigma_{1,a}^{-}\sigma_{2,a}^{+}, \\ r\left(\lambda\right) &= r_{\uparrow}\left(\lambda\right)r_{\downarrow}\left(\lambda\right), \\ \mathrm{sh}\left(2h\left(\lambda\right)\right) &:= \frac{U}{4}\sin\left(2\lambda\right). \end{aligned} \tag{65}$$

"This R-matrix satisfies the Yang-Baxter relation for triple R matrices" [36, p. 549] (9). We may replace U by $-U$. We define state vectors by

$$|1\rangle = |+,-\rangle, \qquad |2\rangle = |+,+\rangle, \qquad |3\rangle = |-,-\rangle, \qquad |4\rangle = |-,+\rangle.$$

We start with the parametrization of λ in terms of

$$e^{2x} = \tan\lambda$$

and consider the functions

$$z_{\pm}\left(x\right) := e^{2h(x)\pm 2x}, \qquad 2h\left(x\right) = -\mathrm{arsinh}\frac{U}{4\mathrm{ch}\left(2x\right)}. \tag{66}$$

3.1 Bethe ansatz equations of the Hubbard model with integrable impurity

We now proceed in the same way as in Chapter 2. First of all, for our purposes we introduce an integrable impurity on the site $L+1$ with the spectral parameter ν.

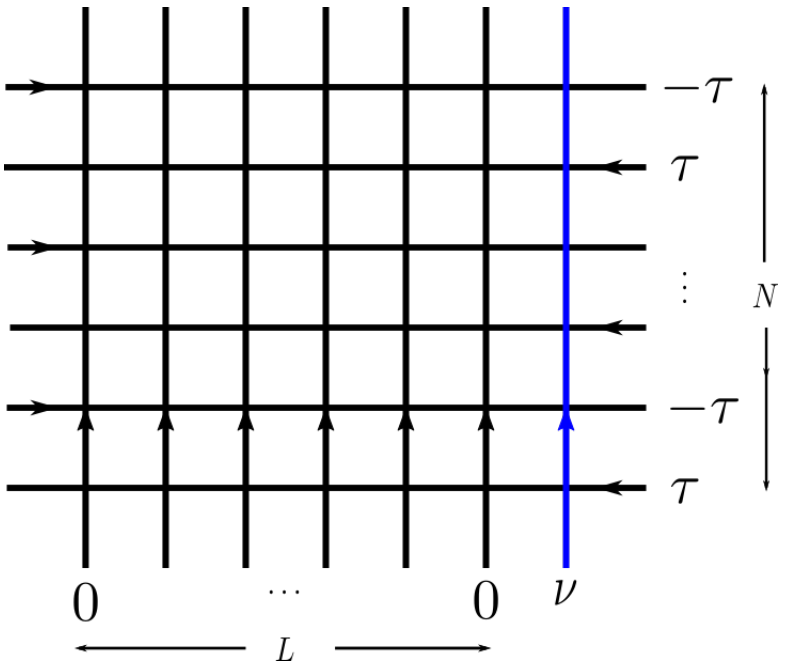

Figure 14: The quantum chain is mapped onto this two-dimensional classical model at finite temperature T. The square lattice has width $L+1$ and height N. The rows of the lattice belong to the row-to-row transfer matrices with $\tau = \frac{\beta}{N}$. The column-to-column transfer matrix is crucial for the thermodynamics. The blue line is intended to illustrate the integrable impurity.

The Bethe ansatz eigenstates for the row-to-row transfer matrix of the Hubbard model (64) for K electrons and M down spins are characterized by two sets of quantum numbers $\{k_j\}_{j=1}^{K}$ and $\{\Lambda_l\}_{l=1}^{M}$, $2M \leq K \leq L$. The quantum numbers $\{k_j\}_{j=1}^{K}$ and $\{\Lambda_l\}_{l=1}^{M}$, may in general be complex. They are known as charge momenta and spin rapidities, respectively. They have to be calculated from the Lieb-Wu equations [79]

$$e^{ik_jL} = \prod_{l=1}^{M} \frac{\Lambda_l - \sin k_j - i\frac{U}{4}}{\Lambda_l - \sin k_j + i\frac{U}{4}},$$
$$\prod_{j=1}^{K} \frac{\Lambda_l - \sin k_j - i\frac{U}{4}}{\Lambda_l - \sin k_j + i\frac{U}{4}} = -\prod_{m=1}^{M} \frac{\Lambda_l - \Lambda_m - i\frac{U}{2}}{\Lambda_l - \Lambda_m + i\frac{U}{2}}.$$

We confine our discussion to solutions with finite values for $\{k_j\}_{j=1}^{K}$ and $\{\Lambda_l\}_{l=1}^{M}$.
The relations between the spectral parameters λ and μ (65) and the charge momentum k and the spin rapidity Λ is

$$e^{ik(\lambda)} = -e^{2h(\lambda)} \cot \lambda, \qquad \Lambda = \sin k\,(\mu) - i\frac{U}{4}. \tag{67}$$

As in the case of the one-dimensional anisotropic spin-$\frac{1}{2}$ Heisenberg model with spin-$\frac{1}{2}$ impurity, the integrable impurity changes the Lieb-Wu equations. The additional vertex

$R_{22}^{22}(\lambda_j, \nu) =$ 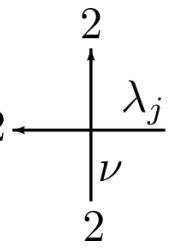

$R_{12}^{12}(\lambda_j, \nu) =$ 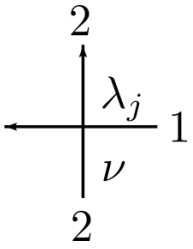

Figure 15: Additional vertex, where "2" corresponds to the local vacuum state.

provides only additional vacuum eigenvalue factors [100, 144, 84]

$$\begin{aligned}
\frac{R_{22}^{22}(\lambda_j,\nu)}{R_{12}^{12}(\lambda_j,\nu)} &= \big(\cos(\lambda_j+\nu)\,\mathrm{ch}\,(h(\lambda_j)-h(\nu))\cos^2(\lambda_j-\nu) \\
&\quad + \cos(\lambda_j-\nu)\,\mathrm{sh}\,(h(\lambda_j)-h(\nu))\cos^2(\lambda_j+\nu)\big) \\
&\quad \cdot (\cos(\lambda_j+\nu)\,\mathrm{ch}\,(h(\lambda_j)-h(\nu))\cos(\lambda_j-\nu)\sin(\lambda_j-\nu) \\
&\quad - \cos(\lambda_j-\nu)\,\mathrm{sh}\,(h(\lambda_j)-h(\nu))\cos(\lambda_j+\nu)\sin(\lambda_j+\nu))^{-1} \\
&= \frac{\mathrm{ch}\,(h(\lambda_j)-h(\nu))\cos(\lambda_j-\nu)+\mathrm{sh}\,(h(\lambda_j)-h(\nu))\cos(\lambda_j+\nu)}{\mathrm{ch}\,(h(\lambda_j)-h(\nu))\sin(\lambda_j-\nu)-\mathrm{sh}\,(h(\lambda_j)-h(\nu))\sin(\lambda_j+\nu)} \\
&= \frac{\mathrm{ch}\,(h(\lambda_j)-h(\nu))(\cot\lambda_j\cot\nu+1)+\mathrm{sh}\,(h(\lambda_j)-h(\nu))(\cot\lambda_j\cot\nu-1)}{\mathrm{ch}\,(h(\lambda_j)-h(\nu))(\cot\nu-\cot\lambda_j)-\mathrm{sh}\,(h(\lambda_j)-h(\nu))(\cot\lambda_j+\cot\nu)} \\
&= \frac{e^{h(\lambda_j)-h(\nu)}\cot\lambda_j\cot\nu+e^{h(\nu)-h(\lambda_j)}}{e^{h(\nu)-h(\lambda_j)}\cot\nu-e^{h(\lambda_j)-h(\nu)}\cot\lambda_j} \\
&= \frac{e^{h(\nu)-h(\lambda_j)}}{e^{-h(\nu)-h(\lambda_j)}}\frac{e^{2(h(\lambda_j)-h(\nu))}\cot\lambda_j\cot\nu+1}{e^{2h(\nu)}\cot\nu-e^{2h(\lambda_j)}\cot\lambda_j} \\
&= e^{2h(\nu)}\frac{\frac{z_-(\lambda_j)}{z_+(\nu)}+1}{z_-(\nu)-z_-(\lambda_j)}.
\end{aligned}$$

Since λ_j is related to k_j (67), we now write $z_-(k_j)$ instead of $z_-(\lambda_j)$.
The Bethe ansatz equations for the row-to-row transfer matrix of the Hubbard model with impurity are thus

$$e^{ik_jL}e^{2h(\nu)}\frac{\frac{z_-(k_j)}{z_+(\nu)}+1}{z_-(\nu)-z_-(k_j)}=\prod_{l=1}^{M}\frac{\Lambda_l-\sin k_j-i\frac{U}{4}}{\Lambda_l-\sin k_j+i\frac{U}{4}},$$
$$\prod_{j=1}^{K}\frac{\Lambda_l-\sin k_j-i\frac{U}{4}}{\Lambda_l-\sin k_j+i\frac{U}{4}}=-\prod_{m=1}^{M}\frac{\Lambda_l-\Lambda_m-i\frac{U}{2}}{\Lambda_l-\Lambda_m+i\frac{U}{2}}. \tag{68}$$

3.2 Gibbs free energy per site of the Hubbard model with integrable impurity via thermodynamic Bethe Ansatz

The tridiagonal form of the thermodynamic Bethe Ansatz equations of the Hubbard model (64) are [117]

$$\begin{aligned}
\ln\zeta(k)&=-\frac{2\cos k}{T}-\frac{4}{T}\int_{-\infty}^{\infty}\mathrm{d}y s(\sin k-y)\,\mathrm{Re}\sqrt{1-\left(y-i\frac{U}{4}\right)^2}\\
&\quad+\left(s*\ln\frac{1+\eta_1'}{1+\eta_1}\right)(\sin k),\\
\eta_0(\Lambda)&=\eta_0'(\Lambda)=0,\\
\ln\eta_n(\Lambda)&=\left(s*\ln\left((1+\eta_{n-1})(1+\eta_{n+1})\right)\right)(\Lambda)-\delta_{1n}\left(s*\ln\left(1+\zeta^{-1}\right)\right)(\Lambda),\\
\ln\eta_n'(\Lambda)&=\left(s*\ln\left((1+\eta_{n-1})(1+\eta_{n+1})\right)\right)(\Lambda)-\delta_{1n}\left(s*\ln\left(1+\zeta\right)\right)(\Lambda),
\end{aligned} \tag{69}$$

with $n=1,2,\ldots$ and where

$$s(x)=\frac{1}{U\mathrm{ch}\frac{2\pi x}{U}}.$$

These equations are completed by the boundary conditions

$$\lim_{n\to\infty}\frac{\ln\eta_n}{n}=\frac{2B}{T},\qquad\lim_{n\to\infty}\frac{\ln\eta_n'}{n}=-\frac{2\mu}{T}.$$

The derivation of these equations are explained in the course of this subsection.
The Gibbs free energy of the host per site is given in terms of solutions of (69) as

$$\begin{aligned}
f_\mathrm{h}&=\frac{U}{4}-T\int_{-\pi}^{\pi}\frac{\mathrm{d}k}{2\pi}\ln\left(1+\frac{1}{\zeta(k)}\right)\\
&\quad-T\sum_{n=1}^{\infty}\int_{-\infty}^{\infty}\frac{\mathrm{d}\Lambda}{\pi}\ln\left(1+\frac{1}{\eta_n'(\Lambda)}\right)\mathrm{Re}\frac{1}{\sqrt{1-\left(\Lambda-in\frac{U}{4}\right)^2}}
\end{aligned} \tag{70}$$

Since we introduced an impurity, there is a corresponding contribution to the free energy, which we now calculate here. To this end we formulate the string hypothesis:
"Three different classes of strings" [36, p. 137] are composed in all finite solutions of $\{k_j\}_{j=1}^{K}$ and $\{\Lambda_l\}_{l=1}^{M}$ of (68).

- "A single real momentum k_j.
- m Λ's combining into a Λ string. [...]
- $2m$ k's and m Λ's combining into a k-Λ string." [36, p. 137]

"For large lattices ($L \gg 1$) and a large number of electrons ($K \gg 1$), [...] [nearly for all strings[the imaginary parts of the k's and Λ's" [36, p. 138] are spaced evenly.
Solving the equations (68) is uncomplicated with the string hypothesis . "For some particular, fixed values" [36, p. 138] of K electrons and M down spins we consider solutions of the equations (68). Any solution can be displayed "in terms of a particular configuration of strings" [36, p. 138]: Any solution includes M_n Λ-strings and M'_n k-Λ strings of length n ($n = 1, 2, \ldots$) and $\mathcal{M}_e$ single k_j's . $\mathcal{M}_e$, M_n and M'_n are called occupation numbers of the string configuration. "The occupation numbers $\mathcal{M}_e$, M_n and M'_n satisfy the sum rules" [36, p. 138]

$$M = \sum_{n=1}^{\infty} n \left(M_n + M'_n\right),$$
$$K = \mathcal{M}_e + \sum_{n=1}^{\infty} 2n M'_n.$$

Exerting this procedure to the equations (68), using

$$e^{i\hat{\delta}(k_j)} := e^{2h(\nu)} \frac{\frac{z_-(k_j)}{z_+(\nu)} + 1}{z_-(\nu) - z_-(k_j)}$$

and then taking the logarithm, we find for even L the following "equations for the real centers of the strings" [36, p. 138]

$$k_j L + \hat{\delta}(k_j) = 2\pi I_j - \sum_{n=1}^{\infty} \sum_{\alpha=1}^{M_n} \theta\left(\frac{\sin k_j - \Lambda_\alpha^n}{n\frac{U}{4}}\right) - \sum_{n=1}^{\infty} \sum_{\alpha=1}^{M_n} \theta\left(\frac{\sin k_j - \Lambda_\alpha'^n}{n\frac{U}{4}}\right), \tag{71}$$

$$\sum_{j=1}^{N-2M'} \theta\left(\frac{\Lambda_\alpha^n - \sin k_j}{n\frac{U}{4}}\right) = 2\pi J_\alpha^n + \sum_{m=1}^{\infty} \sum_{\beta=1}^{M_m} \Theta_{nm}\left(\frac{\Lambda_\alpha^n - \Lambda_\beta^m}{\frac{U}{4}}\right), \tag{72}$$

$$2L\mathrm{Re}\left(\arcsin\left(\Lambda_\alpha'^n+in\frac{U}{4}\right)\right)+2\hat{\delta}\left(\mathrm{Re}\left(\arcsin\left(\Lambda_\alpha'^n+in\frac{U}{4}\right)\right)\right)$$
$$=2\pi J_\alpha'^n+\sum_{j=1}^{K-2M'}\theta\left(\frac{\Lambda_\alpha'^n-\sin k_j}{n\frac{U}{4}}\right)+\sum_{m=1}^{\infty}\sum_{\beta=1}^{M_m'}\Theta_{nm}\left(\frac{\Lambda_\alpha'^n-\Lambda_\beta'^m}{\frac{U}{4}}\right). \tag{73}$$

The functions $\theta(x)$ and $\Theta_{nm}(x)$ are defined as

$$\theta(x):=2\arctan x,$$
$$\Theta_{nm}(x):=\begin{cases}\theta\left(\frac{x}{|n-m|}\right)+2\theta\left(\frac{x}{|n-m|+2}\right)+\ldots+2\theta\left(\frac{x}{n+m-2}\right)+\theta\left(\frac{x}{n+m}\right), & \text{if } n\neq m,\\ 2\theta\left(\frac{x}{2}\right)+2\theta\left(\frac{x}{4}\right)+\ldots+2\theta\left(\frac{x}{2n-2}\right)+\theta\left(\frac{x}{2n}\right), & \text{if } n=m.\end{cases}$$

I_j, J_α^n and $J_\alpha'^n$ are integer or half-odd integer numbers. They exist due "to the multivaluedness of the logarithm" [36, p. 139]. We have

$$I_j \text{ is } \begin{cases}\text{integer} & \text{if } \sum_{n=1}^{\infty}(M_n+M_n') \text{ is even},\\ \text{half - odd integer}, & \text{if } \sum_{n=1}^{\infty}(M_n+M_n') \text{ is odd},\end{cases}$$
$$J_\alpha^n \text{ is } \begin{cases}\text{integer} & \text{if } K-M_n \text{ is odd},\\ \text{half - odd integer}, & \text{if } K-M_n \text{ is even},\end{cases}$$
$$J_\alpha'^n \text{ is } \begin{cases}\text{integer} & \text{if } L-K+M_n' \text{ is odd},\\ \text{half - odd integer}, & \text{if } L-K+M_n' \text{ is even}.\end{cases}$$

"M' is the [...] number of Λ's involved in k-Λ strings" [36, p. 139]

$$M'=\sum_{n=1}^{\infty}nM_n'.$$

In the thermodynamical limit $L\to\infty$, $\frac{K}{L}$ and $\frac{M}{L}$ fixed, solutions of equations (72) k_j, Λ_α^n and $\Lambda_\alpha'^n$ should be expressed in terms of distributions of particles $\rho^p(k)$, $\sigma_n^p(\Lambda)$, $\sigma_n'^p(\Lambda)$ and the appropriate $\rho^h(k),\sigma_n^h(\Lambda),\sigma_n'^h(\Lambda)$.
"In the thermodynamic limit the equations (71), (72) and (73) [...] [can be expressed as] coupled integral equations involving [...] the root densities" [36, p. 168] for particles and holes

$$\rho^p(k)+\rho^h(k)=\frac{1}{2\pi}+\frac{\hat{\Delta}(k)}{L}+\cos k\sum_{n=1}^{\infty}\int_{-\infty}^{\infty}\mathrm{d}\Lambda a_n(\Lambda-\sin k)\left(\sigma_n'^p(\Lambda)+\sigma_n'^p(\Lambda)\right),$$

$$\sigma_n^h(\Lambda)=-\sum_{m=1}^{\infty}A_{nm}*\sigma_m^p|_\Lambda+\int_{-\pi}^{\pi}\mathrm{d}k a_n(\Lambda-\sin k)\rho^p(k),$$

$$\sigma_n'^h(\Lambda)=\frac{1}{\pi}\mathrm{Re}\frac{1}{\sqrt{1-\left(\Lambda-ni\frac{U}{4}\right)^2}}+\frac{2}{\pi L}\partial_\Lambda\hat{\delta}\left(\mathrm{Re}\frac{1}{\sqrt{1-\left(\Lambda-ni\frac{U}{4}\right)^2}}\right)$$
$$-\sum_{m=1}^{\infty}A_{nm}*\sigma_m'^p|_\Lambda-\int_{-\pi}^{\pi}\mathrm{d}k a_n(\sin k-\Lambda)\rho^p(k),\tag{74}$$

where

$$\hat{\Delta}(k)=\frac{1}{2\pi}\partial_k\hat{\delta}(k),$$

$a_n(x)$ is a shorthand notation

$$a_n(x)=\frac{1}{2\pi}\frac{n\frac{U}{2}}{\left(n\frac{U}{4}\right)^2+x^2},$$

and A_{nm} is an integral operator that acts on a function $f(x)$

$$A_{nm}*f|_x=\delta_{nm}f(x)+\int_{-\infty}^{\infty}\frac{\mathrm{d}y}{2\pi}\frac{\mathrm{d}}{\mathrm{d}x}\Theta_{nm}\left(\frac{x-y}{\frac{U}{4}}\right)f(y).$$

For further transformations of (74) the following relation is of great use

$$\int_{-\pi}^{\pi}\frac{\mathrm{d}k}{2\pi}a_n(\sin k-\Lambda)=\frac{1}{\pi}\mathrm{Re}\frac{1}{\sqrt{1-\left(\Lambda-ni\frac{U}{4}\right)^2}}.$$

"To find the [state of thermodynamic] equilibrium [...] one should, [...] [corresponding] to the statistical mechanics principles, [...] [locate] the minimum of the thermodynamical potential" [124, p. 672] per site

$$f=e-\mu n_c-2Bm-Ts.$$

μ is a chemical potential, B is a magnetic field, T is the temperature, n_c is the particle density, m the magnetization and s the total entropy per site. We restrict ourselve to a magnetic field $B\geq 0$ and to a chemical potential $\mu\leq 0$.
The distribution of Bethe ansatz roots describe a corresponding general state. "In the

thermodynamic limit[, we can instead use] the root densities of particles and holes" [36, p. 169]. Therefore we consider the entropy as a functional in terms of root densities.
For k in the interval $[k, k+\Delta k]$ "the number of vacancies" [36, p. 169] is obviously $L\left(\rho^p(k)+\rho^h(k)\right)\Delta k$. $L\rho^p(k)\,\Delta k$ of them are occupied. For such k the number of states is

$$\frac{\left(L\left(\rho^p(k)+\rho^h(k)\right)\Delta k\right)!}{(L\rho^p(k)\,\Delta k)!(L\rho^h(k)\,\Delta k)!}.$$

We use Stirling's formula to approximate the factorials in the contribution $\mathrm{d}S$ to the entropy, since it is the logarithm of this number of states and it is large in the thermodynamic limit. This yields the following expression for the total entropy per site

$$\begin{aligned} s = &\int_{-\pi}^{\pi} \mathrm{d}k \left(\left(\rho^p(k)+\rho^h(k)\right)\ln\left(\rho^p(k)+\rho^h(k)\right) - \rho^p(k)\ln\rho^p(k) - \rho^h(k)\ln\rho^h(k)\right) \\ &+ \sum_{n=1}^{\infty}\int_{-\infty}^{\infty} \mathrm{d}\Lambda \left(\left(\sigma_n^p(\Lambda)+\sigma_n^h(\Lambda)\right)\ln\left(\sigma_n^p(\Lambda)+\sigma_n^h(\Lambda)\right) - \sigma_n^p(\Lambda)\ln\sigma_n^p(\Lambda)\right. \\ &\qquad \left. -\sigma_n^h(\Lambda)\ln\sigma_n^h(\Lambda)\right) \\ &+ \sum_{n=1}^{\infty}\int_{-\infty}^{\infty} \mathrm{d}\Lambda \left(\left(\sigma_n'^p(\Lambda)+\sigma_n'^h(\Lambda)\right)\ln\left(\sigma_n'^p(\Lambda)+\sigma_n'^h(\Lambda)\right) - \sigma_n'^p(\Lambda)\ln\sigma_n'^p(\Lambda)\right. \\ &\qquad \left. -\sigma_n'^h(\Lambda)\ln\sigma_n'^h(\Lambda)\right). \end{aligned}$$

The thermodynamical potential per site f is a functional in terms of the root densities. "With respect to variations in a maximal set of independent root densities" [36, p. 170]" the state of thermodynamic equilibrium must be a stationary" [36, p. 170] point. The densities of holes are given in terms of densities of particles with the equations (74). There we find the condition

$$0 = \delta f,$$

where (74) are constraint equations. For the ratios

$$\zeta(k) = \frac{\rho^h(k)}{\rho^p(k)}, \qquad \eta_n(\Lambda) = \frac{\sigma_n^h(\Lambda)}{\sigma_n^p(\Lambda)}, \qquad \eta_n'(\Lambda) = \frac{\sigma_n'^h(\Lambda)}{\sigma_n'^p(\Lambda)}$$

we find the thermodynamical Bethe ansatz equations (69). The Gibbs free energy per site in terms of $\zeta(k)$, $\eta_n(\Lambda)$ and $\eta_n'(\Lambda)$ is of the form

$$f = f_{\mathrm{h}} + \frac{1}{L} f_{\mathrm{i}}, \tag{75}$$

where f_{i} is the impurity part of the thermodynamical potential

$$f_i = \frac{U}{4} - T\int_{-\pi}^{\pi} \mathrm{d}k \hat{\Delta}(k) \ln\left(1+\frac{1}{\zeta(k)}\right) - \frac{4T}{\pi}\sum_{n=1}^{\infty}\int_{-\infty}^{\infty} \mathrm{d}\Lambda \left(\partial_\Lambda \hat{\delta}\left(\mathrm{Re}\frac{1}{\sqrt{1-\left(\Lambda - ni\frac{U}{4}\right)^2}}\right)\right) \ln\left(1+\frac{1}{\eta_n'(\Lambda)}\right). \tag{76}$$

Equations (69), (70), (76) and (75) completely describe the thermodynamical properties of the Hubbard model with impurity.

3.3 Diagonalization of the column-to-column transfer matrix of the Hubbard model

In the last subsection, we used the infinite number of thermodynamic equations for the description of thermodynamics. In this chapter, on the other hand, we use the finitely many non-linear integral equations. The equivalence of both sets of equations was shown in [27]. Since we introduced an impurity, there is now a corresponding contribution to the free energy, which we want to calculate.

In this chapter we want to use the column-to-column transfer matrix approach. In principle, we proceed as in chapter 2 and we use known results [63, 36].

We introduce the column-to-column transfer matrix (17)

$$t^{\mathrm{QTM}}(\lambda,\tau) = \mathrm{tr}_{\mathrm{aux}}\left(\bigotimes^{\frac{N}{2}} R(\lambda,-\tau)\otimes\tilde{R}(\lambda,\tau)\right).$$

We will diagonalize the column-to-column transfer matrix by the Quantum Inverse Scattering Method. The diagonalization of the column-to-column transfer matrix appears to be fairly different in comparison with the row-to-row case. However the main point is that column-to-column transfer matrices "have the same intertwining operator" [36, p. 550] as row-to-row transfer matrices. We use "periodic or twisted boundary conditions in the Trotter direction" [36, p. 550], since we consider external magnetic field B and chemical potential μ.

A convenient vacuum for the purposes of this thesis is

$$|\Omega\rangle = |1,4,1,4,\ldots,1,4\rangle$$

The vacuum expectation values are given by

$$\langle\Omega|\, t_{j,j}^{\mathrm{QTM}}\, |\Omega\rangle = A_j e^{\beta\mu_j}, \qquad j = 1,\ldots,4 \tag{77}$$

with

$$\mu_1 = \mu + B, \qquad \mu_2 = 2\mu, \qquad \mu_3 = 0, \qquad \mu_4 = \mu - B.$$

We write for λ, τ

$$e^{2x} = \tan\lambda, \qquad e^{2w} = \tan\tau \tag{78}$$

and consider the functions

$$z_\pm(x) := e^{2h(x)\pm 2x}, \qquad 2h(x) := -\mathrm{arsinh}\frac{U}{4\mathrm{ch}\,(2x)}.$$

The vacuum expectation values are

$$\begin{aligned}
\frac{A_1}{A_2} &= \left(\frac{(1 - z_-(w)\, z_+(x))\,(1 - z_+(w)\, z_+(x))}{(1 + z_-(w)\, z_+(x))\,(1 + z_+(w)\, z_+(x))}\right)^{\frac{N}{2}}, \\
\frac{A_4}{A_2} &= \left(\frac{\left(1 + \frac{z_-(w)}{z_-(x)}\right)\left(1 + \frac{z_+(w)}{z_-(x)}\right)}{\left(1 - \frac{z_-(w)}{z_-(x)}\right)\left(1 - \frac{z_+(w)}{z_-(x)}\right)}\right)^{\frac{N}{2}}, \\
A_2 &= \left(\cos^2\lambda\cos^2\tau\cos^2(\lambda-\tau)\cos^2(\lambda+\tau)\, e^{2h(w)}\left(\frac{1}{z_-(w)} - \frac{1}{z_-(x)}\right)\right. \\
&\quad \left.\cdot\left(z_+(x) + \frac{1}{z_-(w)}\right)\right)^{\frac{N}{2}}, \\
A_3 &= A_2.
\end{aligned} \tag{79}$$

The leading eigenvalue of the column-to-column transfer matrix is given by [63, 36]

$$\begin{aligned}
\frac{\Lambda_0^{\mathrm{QTM}}(\lambda)}{A_2} &= e^{\beta(\mu+B)}\frac{A_1}{A_2}\prod_{j=1}^{m} e^{2x}\frac{1 + z_j z_-(x)}{1 - z_j z_+(x)} \\
&\quad + e^{2\beta\mu}\prod_{j=1}^{m}\left(-e^{2x}\frac{1 + z_j z_-(x)}{1 - z_j z_+(x)}\right)\prod_{\alpha=1}^{l}\left(-\frac{z_-(x) - \frac{1}{z_-(x)} - 2iw_\alpha + \frac{3U}{2}}{z_-(x) - \frac{1}{z_-(x)} - 2iw_\alpha + \frac{U}{2}}\right) \\
&\quad + \prod_{j=1}^{m}\left(-e^{-2x}\frac{1 + \frac{z_+(x)}{z_j}}{1 - \frac{z_-(x)}{z_j}}\right)\prod_{\alpha=1}^{l}\left(-\frac{z_-(x) - \frac{1}{z_-(x)} - 2iw_\alpha - \frac{U}{2}}{z_-(x) - \frac{1}{z_-(x)} - 2iw_\alpha + \frac{U}{2}}\right) \\
&\quad + e^{\beta(\mu-B)}\frac{A_4}{A_2}\prod_{j=1}^{m} e^{-2x}\frac{1 + \frac{z_+(x)}{z_j}}{1 - \frac{z_-(x)}{z_j}}
\end{aligned} \tag{80}$$

with $z_j := z_- (\lambda_j)$.
The parameters $\{z_j\}_{j=1}^m$ and $\{w_\alpha\}_{\alpha=1}^l$ are determined by the Bethe ansatz equations

$$e^{\beta(\mu-B)} \left(\frac{\left(1+\frac{z_-(w)}{z_j}\right)\left(1+\frac{z_+(w)}{z_j}\right)}{\left(1-\frac{z_-(w)}{z_j}\right)\left(1-\frac{z_+(w)}{z_j}\right)} \right)^{\frac{N}{2}} = (-1)^{1+m+l} \prod_{\alpha=1}^{l} \left(\frac{z_j - \frac{1}{z_j} - 2iw_\alpha - \frac{U}{2}}{z_j - \frac{1}{z_j} - 2iw_\alpha + \frac{U}{2}} \right),$$
$$e^{2\beta\mu} \prod_{j=1}^{m} \frac{z_j - \frac{1}{z_j} - 2iw_\alpha + \frac{U}{2}}{z_j - \frac{1}{z_j} - 2iw_\alpha - \frac{U}{2}} = -\prod_{\beta=1}^{l} \frac{2i\left(w_\alpha - w_\beta\right) - U}{2i\left(w_\alpha - w_\beta\right) + U}. \tag{81}$$

In the limit $U \to 0$ we find the free-fermion partition function. Using another vacuum $|\Omega'\rangle = |2,3,2,3,\ldots,2,3\rangle$, we can find another formula for $\Lambda_0^{\mathrm{QTM}}(\lambda)$. This formula is the same as in equation (80) after changing the sign of U and swapping $B \longleftrightarrow \mu$. This alternative expression is equivalent to equation (80) due "to a partial particle-hole transformation" [36, p. 552]. The solutions of the Bethe ansatz equations of the column-to-column transfer matrix (81) for the leading eigenvalue $\Lambda_0^{\mathrm{QTM}}(\lambda)$ have "a characteristic temperature dependence" [36, p. 552]. For large temperatures T all z_j satisfy $\mathrm{Re} z_j = 0$ and $|z_j| > 1$. Lowering the temperature T yields a decrease of the z_j and they converge to the origin. For "low temperatures T a certain number of the z_j's" [36, p. 553] satisfy $|z_j| < 1$. The w_α parameters behave alike on the real axis.
This behaviour has strong consequences. By use of a double valued function $s(z)$ (with a branch cut from -1 to 1) we will express the z_j's in terms of s_j parameters. Therefore z, that satisfy $\mathrm{Re} z = 0$, "with $|z| > 1$ and those with $|z| < 1$ are mapped onto the same [...] [area] of the real axis with $|s| > 1$" [36, p. 553]. Accordingly there is a motion of s_j from the first branch to the second branch. At high temperatures T all parameters s_j lie on the first sheet. At low temperatures T parameters s_j lie on the first and on the second sheet. Therefore obviously there is a flow from the first to the second sheet [63, 36].

3.3.1 Associated auxiliary problem of difference type

In analogy to chapter 2 we want to reformulate the Bethe ansatz equations (81) for the leading eigenvalue of the column-to-column transfer matrix in the limit $N \to \infty$ as a system of non-linear integral equations. We introduce the variables

$$s_j = \frac{1}{2i}\left(z_j - \frac{1}{z_j}\right),$$
$$s = s(x) = \frac{1}{2i}\left(z_-(x) - \frac{1}{z_-(x)}\right). \tag{82}$$

Equations (81) can be written "in a difference form in the rapidities $\{s_j\}_{j=1}^m$ and $\{w_\alpha\}_{\alpha=1}^l$"

[36, p. 555]

$$
\begin{aligned}
e^{-\beta(\mu-B)}\Phi\left(s_j\right) &= -\frac{q_2\left(s_j - i\frac{U}{4}\right)}{q_2\left(s_j + i\frac{U}{4}\right)}, \\
e^{-2\beta\mu}\frac{q_2\left(w_\alpha + i\frac{U}{2}\right)}{q_2\left(w_\alpha - i\frac{U}{2}\right)} &= -\frac{q_1\left(w_\alpha + i\frac{U}{4}\right)}{q_1\left(w_\alpha - i\frac{U}{4}\right)},
\end{aligned} \tag{83}
$$

where we have defined

$$
q_1\left(s\right) := \prod_{j=1}^{m}\left(s - s_j\right), \qquad q_2 := \prod_{\alpha=1}^{l}\left(s - w_\alpha\right), \tag{84}
$$

$$
\Phi\left(s\right) := \left(\frac{\left(1 - \frac{z_-(w)}{z(s)}\right)\left(1 - \frac{z_+(w)}{z(s)}\right)}{\left(1 + \frac{z_-(w)}{z(s)}\right)\left(1 + \frac{z_+(w)}{z(s)}\right)}\right)^{\frac{N}{2}}, \tag{85}
$$

$$
z\left(s\right) := is\left(1 + \sqrt{1 - \frac{1}{s^2}}\right). \tag{86}
$$

Note that the functions $\Phi\left(s\right)$ and $z\left(s\right)$ have two branches: The requirement $z\left(s\right) \simeq 2is$ for large values of s defines the standard first branch of $z\left(s\right)$. The branch cut of $z\left(s\right)$ for "values of z on the unit circle" [36, p. 555] is along $[-1, 1]$. Thus "the first branch of the function $z\left(s\right)$ maps the complex plane without $[-1, 1]$ [...] [to the outer area] of the complex plane of the unit circle. [Vice versa] the second branch of $z\left(s\right)$ maps the complex plane without $[-1, 1]$ [...]to the inner area of the unit circle" [36, p. 555]. On the branch cut we have

$$
z\left(x \pm i0\right) = ix \mp \sqrt{1 - x^2}, \qquad x \in [-1, 1]\,.
$$

The two branches of the function $\Phi\left(s\right)$ defined in (85) are denoted by $\Phi^{\pm}\left(s\right)$. "The function $\Phi^{+}\left(s\right)$ has a zero (pole) of order $\frac{N}{2}$ at the point s_0 $(-s_0)$. [...] $\Phi^{-}\left(s\right)$ has a zero (pole) of order $\frac{N}{2}$ at the point $-s_0 + i\frac{U}{2}$ $(s_0 - i\frac{U}{2})$" [36, p. 557]. The point s_0 is defined by

$$
z\left(s_0\right) := z_-\left(w\right).
$$

The general formula for the leading eigenvalue $\Lambda_0^{\mathrm{QTM}}\left(\lambda\right)$ (80) is complicated, but simplifies, if

$$
\begin{aligned}
\operatorname{sh}(2h(x))\operatorname{ch}(2x) &= -\frac{U}{4} \\
\Leftrightarrow z_+(x) - \frac{1}{z_+(x)} + z_-(x) - \frac{1}{z_-(x)} &= -U, \\
\left(1+\frac{z_+(x)}{z_j}\right)(1-z_j z_+(x)) &= 2iz_+(x)\left(s-s_j-i\frac{U}{2}\right), \\
(1+z_j z_-(x))\left(1-\frac{z_-(x)}{z_j}\right) &= 2iz_-(x)(s_j-s)
\end{aligned}
$$

and the functions

$$
\begin{aligned}
\lambda_1(s) &= e^{\beta(\mu+B)}\frac{\Phi\left(s-i\frac{U}{4}\right)}{q_1\left(s-i\frac{U}{4}\right)}, \qquad \lambda_2(s) = e^{2\beta\mu}\frac{q_2\left(s-i\frac{U}{2}\right)}{q_1\left(s-i\frac{U}{4}\right)q_2(s)}, \\
\lambda_3(s) &= \frac{q_2\left(s+i\frac{U}{2}\right)}{q_1\left(s+i\frac{U}{4}\right)q_2(s)}, \qquad \lambda_4(s) = \frac{e^{\beta(\mu-B)}}{\Phi\left(s+i\frac{U}{4}\right)q_1\left(s+i\frac{U}{4}\right)}, \\
\Lambda^{\text{aux}}(s) &= \lambda_1(s)+\lambda_2(s)+\lambda_3(s)+\lambda_4(s)
\end{aligned} \tag{87}
$$

are used

$$
\begin{aligned}
\frac{\Lambda_0^{\mathrm{QTM}}(\lambda)}{A_2} &= e^{\beta(\mu+B)}\frac{A_1}{A_2}\prod_{j=1}^{m} e^{2x}\frac{1+z_j z_-(x)}{1-z_j z_+(x)} \\
&\quad + e^{2\beta\mu}\prod_{j=1}^{m}\left(-e^{2x}\frac{1+z_j z_-(x)}{1-z_j z_+(x)}\right)\prod_{\alpha=1}^{l}\left(-\frac{z_-(x)-\frac{1}{z_-(x)}-2iw_\alpha+\frac{3U}{2}}{z_-(x)-\frac{1}{z_-(x)}-2iw_\alpha+\frac{U}{2}}\right) \\
&\quad + \prod_{j=1}^{m}\left(-e^{-2x}\frac{1+\frac{z_+(x)}{z_j}}{1-\frac{z_-(x)}{z_j}}\right)\prod_{\alpha=1}^{l}\left(-\frac{z_-(x)-\frac{1}{z_-(x)}-2iw_\alpha-\frac{U}{2}}{z_-(x)-\frac{1}{z_-(x)}-2iw_\alpha+\frac{U}{2}}\right) \\
&\quad + e^{\beta(\mu-B)}\frac{A_4}{A_2}\prod_{j=1}^{m} e^{-2x}\frac{1+\frac{z_+(x)}{z_j}}{1-\frac{z_-(x)}{z_j}} \\
&= \prod_{j=1}^{m}\left((1+z_j z_-(x))\left(1+\frac{z_+(x)}{z_j}\right)\right) \\
&\quad \cdot\left(e^{\beta(\mu+B)}\left(\frac{e^{2x}}{2iz_+(x)}\right)^m\frac{A_1}{A_2}\frac{1}{q_1\left(s-i\frac{U}{2}\right)}\right. \\
&\quad\quad + (-1)^{m+l}e^{2\beta\mu}\left(\frac{e^{2x}}{2iz_+(x)}\right)^m\frac{q_2\left(s-i\frac{3U}{4}\right)}{q_1\left(s-i\frac{U}{2}\right)q_2\left(s-i\frac{U}{4}\right)} \\
&\quad\quad + (-1)^{l}\left(\frac{e^{-2x}}{2iz_-(x)}\right)^m\frac{q_2\left(s+i\frac{U}{4}\right)}{q_1(s)\,q_2\left(s-i\frac{U}{4}\right)} \\
&\quad\quad \left. + (-1)^{m}e^{\beta(\mu-B)}\left(\frac{e^{-2x}}{2iz_-(x)}\right)^m\frac{A_4}{A_2}\frac{1}{q_1(s)}\right) \\
&= \left(\frac{e^{-2h(x)}}{2i}\right)^m\prod_{j=1}^{m}\left((1+z_j z_-(x))\left(1+\frac{z_+(x)}{z_j}\right)\right) \\
&\quad \cdot\left(\lambda_1\left(s-i\frac{U}{4}\right)+(-1)^{m+l}\lambda_2\left(s-i\frac{U}{4}\right)+(-1)^{l}\lambda_3\left(s-i\frac{U}{4}\right)\right. \\
&\quad\quad \left. +(-1)^{m}\lambda_4\left(s-i\frac{U}{4}\right)\right)
\end{aligned}
$$

Choosing m and l even results in

$$
\frac{\Lambda_0^{\mathrm{QTM}}(\lambda)}{A_2} = \left(\frac{e^{-2h(x)}}{2i}\right)^m\Lambda^{\mathrm{aux}}\left(s-i\frac{U}{4}\right)\prod_{j=1}^{m}\left((1+z_j z_-(x))\left(1+\frac{z_+(x)}{z_j}\right)\right). \tag{88}
$$

Note that on the right-hand side x and s depend on λ via (78) and (82).
The requirement of analyticity of $\Lambda^{\mathrm{aux}}(s)$ yields the equations (83), which are the Bethe ansatz equations of the leading eigenvalue $\Lambda_0^{\mathrm{QTM}}(\lambda)$. Note "that while $\Lambda_0^{\mathrm{QTM}}(\lambda)$ is analytic everywhere [...] $\Lambda^{\mathrm{aux}}(s)$ is analytic on the first [...] branch, but may have singularities on the other three branches" [36, p. 557]. To understand this we consider the first set of the Bethe ansatz equations (83). They arise from the requirement "that the zeroes $s_j + i\frac{U}{4}$ in

the denominators of $\lambda_1(s)$ and $\lambda_2(s)$ [...] [cancel each other] in the sum $(\lambda_1+\lambda_2)(s)$ ([...] the zeroes $s_j - i\frac{U}{4}$ in the denominators of $\lambda_3(s)$ and $\lambda_4(s)$ [...] [also have to cancel each other] in the sum $(\lambda_3+\lambda_4)(s)$)" [36, p. 557]:

$$\frac{\lambda_1\left(s_j + i\frac{U}{4}\right)}{\lambda_2\left(s_j + i\frac{U}{4}\right)} = -1 \tag{89}$$

In the limit $N \to \infty$ there is "an infinite number of rapidities on the first branch of the function $\frac{\lambda_1}{\lambda_2}(s)$" [36, p. 558] that fulfill this requirement. On the second branch there is "a finite number of rapidities" [36, p. 558]. At high temperature T all rapidities s_j satisfy equation (89) on the first branch. "All poles with imaginary part $\frac{U}{4}$ [...] [are] on the second branch and [cannot exist] on the first one" [36, p. 558]. We have two cuts of this type, so the total number of branches is four.

We remark that the functions $(\lambda_1+\lambda_2)(s)$, $(\lambda_3+\lambda_4)(s)$ and $\Lambda^{\text{aux}}(s)$ around their branch cuts have "no non-zero winding number [, because the] [...] number of poles on the first branch is [...] N and the asymptotic[s] of the functions [behaves like] $\frac{1}{s^N}$" [36, p. 558]. Isolated singularities may move "from one branch to the other [...] [through] the branch cuts" [36, 558] for lower temperatures T, but our arguments are still correct if the loop encircles the branch cut and the arising singularities.

3.3.2 Finitely many non-linear integral equations of the Hubbard model

We consider the integral equations equivalent to the nested Bethe ansatz equations for the leading eigenvalue of the column-to-column transfer matrix for $U > 0$. The case $U < 0$ can be found "via a particle-hole transformation" [36, p. 558]. We use a set of auxiliary functions satisfying a set of non-linear integral equations. The following definitions are very useful:

$$
\begin{aligned}
l_j(s) &:= e^{2\beta B}\lambda_j\left(s - i\frac{U}{4}\right)\Phi^+(s)\,\Phi^-(s), \qquad j = 1,\ldots,4,\\
\bar{l}_j(s) &:= \lambda_j\left(s + i\frac{U}{4}\right), \qquad j = 1,\ldots,4,\\
\mathfrak{b}(s) &:= \frac{\bar{l}_1 + \bar{l}_2 + \bar{l}_3 + \bar{l}_4}{l_1 + l_2 + l_3 + l_4}(s),\\
\bar{\mathfrak{b}}(s) &:= \frac{1}{\mathfrak{b}}(s),\\
\mathfrak{c}(s) &:= \frac{(l_1 + l_2)\left(\bar{l}_1 + \bar{l}_2 + \bar{l}_3 + \bar{l}_4\right)}{(l_3 + l_4)\left(l_1 + l_2 + l_3 + l_4 + \bar{l}_1 + \bar{l}_2 + \bar{l}_3 + \bar{l}_4\right)}(s),\\
\bar{\mathfrak{c}}(s) &:= \frac{\left(\bar{l}_3 + \bar{l}_4\right)(l_1 + l_2 + l_3 + l_4)}{\left(\bar{l}_1 + \bar{l}_2\right)\left(l_1 + l_2 + l_3 + l_4 + \bar{l}_1 + \bar{l}_2 + \bar{l}_3 + \bar{l}_4\right)}(s)\\
\mathfrak{B}(s) &:= 1 + \mathfrak{b}(s),\\
\bar{\mathfrak{B}}(s) &:= 1 + \bar{\mathfrak{b}}(s),\\
\mathfrak{C}(s) &:= 1 + \mathfrak{c}(s),\\
\bar{\mathfrak{C}}(s) &:= 1 + \bar{\mathfrak{c}}(s).
\end{aligned}
\tag{90}
$$

We note that "any analytic function on the complex plane is [...] [settled] by its singularities [...] [and its] asymptotic behaviour at infinity" [36, p. 561]. All of the above defined auxiliary functions $\mathfrak{b}(s)$, $\mathfrak{c}(s)$ and $\bar{\mathfrak{c}}(s)$ show constant asymptotics for finite N. They are products like $\left(\ldots + l_3 + l_4 + \bar{l}_1 + \bar{l}_2 + \ldots\right)(s)$. Poles exist only if "such a string does not begin with $l_1(s)$ or does not end with $\bar{l}_4(s)$" [36, p. 562], because of the reasoning in the previous subsection. There are cuts, since the function $\Phi(s)$ shows up in the definition of $\lambda_1(s)$ and $\lambda_4(s)$. Therefore terms like $(l_1 + l_2 + \ldots)(s)$ and $\left(\ldots + \bar{l}_3 + \bar{l}_4\right)(s)$ have "branch cuts along $[-1,1] + i\frac{U}{2}$ and $[-1,1] - i\frac{U}{2}$, respectively" [36, p. 563]. On top of that, "terms like $(\ldots + l_3 + l_4)(s)$ and $\left(\bar{l}_1 + \bar{l}_2 + \ldots\right)$ have branch cuts along $[-1,1]$" [36, p. 563]. In terms like $\left(\ldots + l_4 + \bar{l}_1 + \ldots\right)(s)$ the branch cut vanishes, because

$$
\left(l_4 + \bar{l}_1\right)(s) = e^{\beta(\mu+B)}\frac{\Phi^+ + \Phi^-}{q_1}(s)
$$

"and $(\Phi^+ + \Phi^-)(s)$ is analytic everywhere" [36, p. 563], since passing the line $[-1,1]$ yields an exchange $\Phi^+(s) \longleftrightarrow \Phi^-(s)$, hence the sum remains invariant.
By investigating "the function $\lambda_1(s) + \lambda_2(s) + \lambda_3(s) + \lambda_4(s)$ [...] we find poles of order $\frac{N}{2}$ at $s_0 - i\frac{U}{4}$ and $i\frac{U}{4} - s_0$. [...] [We also have] zeroes and branch cuts on the lines $\operatorname{Im} s = \pm\frac{U}{4}$" [36, p. 563]. This yields the following expression

$$\ln\left(l_1(s)+l_2(s)+l_3(s)+l_4(s)\right) \equiv_s -\frac{N}{2}\ln\left((s-s_0)\left(s+s_0-i\frac{U}{2}\right)\right) + \ln\left(\Phi^+(s)\,\Phi^-(s)\right) + L_-(s) + L_+\left(s-i\frac{U}{2}\right),$$

"where $\equiv_s$ indicates that the left and right hand side[...] have the same singularities on the entire plane" [36, p. 563] and

$$L_\pm(s) = (k\circ l_\pm)(s),$$
$$k(s) = \frac{1}{2\pi i s}, \tag{91}$$
$$(g\circ f)(s) = \int_{\mathcal{L}} \mathrm{d}t\, g(s-t)\, f(t), \tag{92}$$
$$l_\pm(s) = (\lambda_1+\lambda_2+\lambda_3+\lambda_4)\left(s\pm i\frac{U}{4}\right).$$

The "contour $\mathcal{L}$ is surrounding the real axis at infinitesimal distance above and below in anticlockwise manner" [36, p. 564].
Furthermore using

$$\Phi^+(s)\,\Phi^-(s) = \left(\frac{(s-s_0)\left(s+s_0-i\frac{U}{2}\right)}{(s+s_0)\left(s-s_0+i\frac{U}{2}\right)}\right)^{\frac{N}{2}}$$

and the singularities

$$L_-(s) \equiv_s -(k\circ\ln\mathfrak{B})(s)$$
$$L_-(s)-L_+(s) \equiv_s \left(k\circ\left(\ln\bar{\mathfrak{c}}-\ln\bar{\mathfrak{C}}\right)\right)(s)$$

we get

$$\ln\left(l_1(s)+l_2(s)+l_3(s)+l_4(s)\right) \equiv_s -\frac{N}{2}\ln\left((s+s_0)\left(s-s_0+i\frac{U}{2}\right)\right) - (k\circ\ln\mathfrak{B})(s) + \left(k\circ\left(\ln\bar{\mathfrak{C}}-\ln\bar{\mathfrak{c}}-\ln\mathfrak{B}\right)\right)\left(s-i\frac{U}{2}\right). \tag{93}$$

The asymptotic behaviour at infinity is given by

$$\begin{aligned}
\ln\left(l_1(s)+l_2(s)+l_3(s)+l_4(s)\right) &\overset{s\to\infty}{\longrightarrow} \ln\left(e^{\beta(\mu+3B)}+e^{2\beta(\mu+B)}+e^{2\beta B}+e^{\beta(\mu+B)}\right),\\
\ln\mathfrak{b}(s) &\overset{s\to\infty}{\longrightarrow} -2\beta B\\
\ln\mathfrak{B}(s) &\overset{s\to\infty}{\longrightarrow} \ln\left(1+e^{-2\beta B}\right),\\
\ln\bar{\mathfrak{b}}(s) &\overset{s\to\infty}{\longrightarrow} 2\beta B,\\
\ln\bar{\mathfrak{B}}(s) &\overset{s\to\infty}{\longrightarrow} \ln\left(1+e^{2\beta B}\right),\\
\ln\bar{\mathfrak{c}}(s) &\overset{s\to\infty}{\longrightarrow} -\beta(\mu-B)-\ln\left(1+e^{2\beta B}\right)\\
\ln\bar{\mathfrak{C}}(s) &\overset{s\to\infty}{\longrightarrow} \ln\left(1+\frac{e^{-\beta(\mu-B)}}{1+e^{2\beta B}}\right).
\end{aligned}$$

Using the functions

$$\begin{aligned}
K_1(s) &= k\left(s-i\frac{U}{4}\right)-k\left(s+i\frac{U}{4}\right)\\
&= \frac{U}{4\pi}\frac{1}{s^2+\left(\frac{U}{4}\right)^2},\\
\hat{K}_1(s) &= K_1\left(s+i\frac{U}{4}\right),\\
\bar{K}_1(s) &= K_1\left(s-i\frac{U}{4}\right),\\
K_2(s) &= k\left(s-i\frac{U}{2}\right)-k\left(s+i\frac{U}{2}\right)\\
&= \frac{U}{2\pi}\frac{1}{s^2+\left(\frac{U}{2}\right)^2},
\end{aligned} \tag{94}$$

and the notation

$$(g\,\square\, f)(s) = (g\circ f)(s)+f(s),$$

which indicates the convolution with an integration contour with a "wide loop [around the real axis] consisting of the two horizontal lines $\mathrm{Im}s=\pm\alpha$ with $0<\alpha\leq\frac{U}{4}$" [36, p. 565], we find the non-linear integral equations for the auxiliary functions $\mathfrak{b}(s)$, $\mathfrak{c}(s)$ and $\bar{\mathfrak{c}}(s)$

$$\begin{aligned}
\ln \mathfrak{b}(s) &= -2\beta B + (K_2 \circ \ln \mathfrak{B})(s) + \left(\bar{K}_1 \circ \left(\ln \bar{\mathfrak{c}} - \ln \bar{\mathfrak{C}}\right)\right)(s), \\
\ln \mathfrak{c}(s) &= \beta(\mu + B) + \frac{N}{2} \ln \frac{s + s_0}{s + s_0 - i\frac{U}{2}} + \ln \Phi(s) - \left(\bar{K}_1 \square \ln \bar{\mathfrak{B}}\right)(s) \\
&\quad - \left(\bar{K}_1 \circ \ln \bar{\mathfrak{C}}\right)(s), \\
\ln \bar{\mathfrak{c}}(s) &= -\beta(\mu + B) + \frac{N}{2} \ln \frac{s + s_0}{s + s_0 - i\frac{U}{2}} - \ln \Phi(s) + \left(\hat{K}_1 \square \ln \mathfrak{B}\right)(s) \\
&\quad + \left(\hat{K}_1 \circ \ln \mathfrak{C}\right)(s).
\end{aligned} \tag{95}$$

The Trotter limit $N \to \infty$ yields

$$\begin{aligned}
\ln \mathfrak{b}(s) &= -2\beta B + (K_2 \square \ln \mathfrak{B})(s) + \left(\bar{K}_1 \circ \left(\ln \bar{\mathfrak{c}} - \ln \bar{\mathfrak{C}}\right)\right)(s), \\
\ln \mathfrak{c}(s) &= -\frac{\beta U}{2} + \beta(\mu + B) - 2i\beta s\sqrt{1 - \frac{1}{s^2}} - \left(\bar{K}_1 \square \ln \bar{\mathfrak{B}}\right)(s) - \left(\bar{K}_1 \circ \ln \bar{\mathfrak{C}}\right)(s), \\
\ln \bar{\mathfrak{c}}(s) &= -\frac{\beta U}{2} - \beta(\mu + B) + 2i\beta s\sqrt{1 - \frac{1}{s^2}} + \left(\hat{K}_1 \square \ln \mathfrak{B}\right)(s) + \left(\hat{K}_1 \circ \ln \mathfrak{C}\right)(s).
\end{aligned} \tag{96}$$

We note that the function $\mathfrak{b}(s)$ will be calculated on $\mathrm{Im} s = \pm\alpha$, especially $\alpha = \frac{U}{4}$. The functions $\mathfrak{c}(s)$ and $\bar{\mathfrak{c}}(s)$ will be "calculated on the real axis infinitesimally above and below the interval $[-1, 1]$" [36, p. 566]. Note furthermore that "these functions are analytic outside" [36, p. 566] of $[-1, 1]$. Therefore convolutions with these functions $\mathfrak{c}(s)$ and $\bar{\mathfrak{c}}(s)$ can be reduced to contours surrounding $[-1, 1]$. We have to solve the set of non-linear integral equations (96) for the auxiliary functions $\mathfrak{b}(s)$, $\mathfrak{c}(s)$ and $\bar{\mathfrak{c}}(s)$ before calculating the free energy.

For the handling of equations (96) we express them as convolutions with a real variable

$$(K * f)(x) = \int_{-\infty}^{\infty} \mathrm{d}y K(x - y) f(y). \tag{97}$$

We use the notations

$$
\begin{aligned}
\mathfrak{b}^{\pm}(s) &= \mathfrak{b}\left(s \pm i\frac{U}{4}\right), \\
\mathfrak{c}^{\pm}(s) &= \mathfrak{c}(s \pm i0), \\
\bar{\mathfrak{c}}^{\pm}(s) &= \bar{\mathfrak{c}}(s \pm i0), \\
\mathfrak{B}^{\pm}(s) &= 1 + \mathfrak{b}^{\pm}(s), \\
\bar{\mathfrak{B}}^{\pm}(s) &= 1 + \frac{1}{\mathfrak{b}^{\pm}(s)}, \\
\mathfrak{C}^{\pm}(s) &= 1 + \mathfrak{c}^{\pm}(s), \\
\bar{\mathfrak{C}}^{\pm}(s) &= 1 + \bar{\mathfrak{c}}^{\pm}(s), \\
f_{\alpha}(s) &= f(s + i\alpha)
\end{aligned}
\tag{98}
$$

and rewrite the equations (96) as

$$
\begin{aligned}
\ln \mathfrak{b}^{+}(s) = &-2\beta B - \left(K_2 * \ln \mathfrak{B}^{+}\right)(s) + \left(K_{2,\frac{U}{2}} * \ln \mathfrak{B}^{-}\right)(s) \\
&- \left(K_1 * \ln \frac{\bar{\mathfrak{c}}^{+}\bar{\mathfrak{C}}^{-}}{\bar{\mathfrak{c}}^{-}\bar{\mathfrak{C}}^{+}}\right)(s), \\
\ln \mathfrak{b}^{-}(s) = &-2\beta B - \left(K_{2,-\frac{U}{2}} * \ln \mathfrak{B}^{+}\right)(s) + \left(K_2 * \ln \mathfrak{B}^{-}\right)(s) \\
&- \left(K_{1,-\frac{U}{2}} * \ln \frac{\bar{\mathfrak{c}}^{+}\bar{\mathfrak{C}}^{-}}{\bar{\mathfrak{c}}^{-}\bar{\mathfrak{C}}^{+}}\right)(s), \\
\ln \mathfrak{c}^{\pm}(s) = &-\frac{\beta U}{2} + \beta(\mu + B) \pm 2\beta\sqrt{1 - s^2} + \left(K_{1,-\frac{U}{2}} * \ln \bar{\mathfrak{B}}^{+}\right)(s) \\
&- \left(K_1 * \ln \bar{\mathfrak{B}}^{-}\right)(s) + \left(K_{1,-\frac{U}{4}} * \ln \frac{\bar{\mathfrak{C}}^{+}}{\bar{\mathfrak{C}}^{-}}\right)(s) \pm \frac{1}{2} \ln \frac{\bar{\mathfrak{C}}^{+}}{\bar{\mathfrak{C}}^{-}}(s), \\
\ln \bar{\mathfrak{c}}^{\pm}(s) = &-\frac{\beta U}{2} - \beta(\mu + B) \mp 2\beta\sqrt{1 - s^2} - \left(K_1 * \ln \mathfrak{B}^{+}\right)(s) \\
&+ \left(K_{1,\frac{U}{2}} * \ln \mathfrak{B}^{-}\right)(s) - \left(K_{1,\frac{U}{4}} * \ln \frac{\mathfrak{C}^{+}}{\mathfrak{C}^{-}}\right)(s) \pm \frac{1}{2} \ln \frac{\mathfrak{C}^{+}}{\mathfrak{C}^{-}}(s).
\end{aligned}
\tag{99}
$$

"Note that the convolutions of $K_{1,\pm\frac{U}{4}}$ with $\ln \frac{\mathfrak{C}^{+}}{\mathfrak{C}^{-}}$ and $\ln \frac{\bar{\mathfrak{C}}^{+}}{\bar{\mathfrak{C}}^{-}}$ are [...] [calculated] by Cauchy's principal value [...] [and take into account] that these functions [...] [disappear] outside the interval $[-1, 1]$" [36, p. 578].

3.3.3 Integral expression for the leading eigenvalue $\Lambda_0^{\mathsf{QTM}}(\lambda)$

Here we go back "to the derivation [...] [of the leading eigenvalue $\Lambda_0^{\mathrm{QTM}}(\lambda)$ of the column-to-column] transfer matrix in terms of the [...] auxiliary functions (96)" [36, p. 566]. This eigenvalue is known for $\lambda = 0$ [63]. "We use a contour $\mathcal{L}_0$ encircling the [rapidities] s_j anticlockwise" [36, p. 566]. The rapidities s_j are not placed on the branch cut of

$\ln\left(\left(1+z\left(s\right)z_{-}\left(x\right)\right)\left(1+\frac{z_{+}(x)}{z(s)}\right)\right)$. Therefore $\mathcal{L}_0$ has two partitions. For zero external fields the contours are surrounding $]-\infty,-1]$ and $[1,\infty[$. For non-zero external fields they are deformed. For the general case we use Cauchy's integral and write

$$f\left(s\right):=\ln\underbrace{\left(\left(1+z\left(s\right)z_{-}\left(x\right)\right)\left(1+\frac{z_{+}\left(x\right)}{z\left(s\right)}\right)\right)}_{=:g(s)}\left[\ln\left(1+\frac{l_4}{l_3}\left(s\right)\right)\right]', \tag{100}$$

$$2\pi i\sum_{i=1}^{m}\ln\left(\left(1+z_jz_{-}\left(x\right)\right)\left(1+\frac{z_{+}\left(x\right)}{z_j}\right)\right)=\underbrace{\int\limits_{\mathcal{L}_0}\mathrm{d}s\;f\left(s\right)|_{\text{1st branch}}}_{=\Sigma_1}+\underbrace{\int\limits_{\mathcal{L}_0}\mathrm{d}s\;f\left(s\right)|_{\text{2nd branch}}}_{=\Sigma_2}, \tag{101}$$

where Σ_1 and Σ_2 will be calculated below.

3.3.4 Integral expression for the leading eigenvalue $\Lambda_0^{\mathsf{QTM}}(\lambda)$ in terms of auxiliary functions

The function $\frac{l_4}{l_3}\left(s\right)$ for $s\to\infty$ shows the behaviour

$$\frac{l_4}{l_3}\left(s\right)\overset{s\to\infty}{\longrightarrow}e^{\beta(\mu-B)}+\mathcal{O}\left(\frac{1}{s}\right).$$

$z\left(s\right)$ is of order $\mathcal{O}\left(s\right)$. Therefore we find the asymptotic behavior of $f\left(s\right)$ as $\mathcal{O}\left(\frac{\ln s}{s^2}\right)$. Hence we add two semi-circles to the contour $\mathcal{L}_0$.

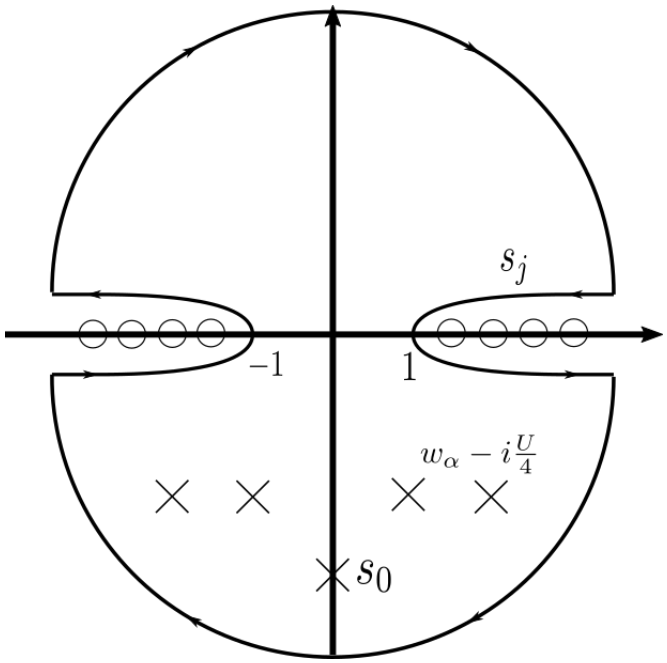

Figure 16: Zeroes and poles of $1 + \frac{l_4}{l_3}(s)$. "Zeroes (poles) are [...] [illustrated] by open circles (crosses)" [36, p. 567]. We add two semi-circles.

We deform the integration contour. We do this without changing the integral. If the contour does not run over singularities of $f(s)$ we can do that. This yields a contour with three parts

$$\Sigma_1 = \int_{(a)} \mathrm{d}s\, f(s)|_{\text{1st branch}} + \int_{(b)} \mathrm{d}s\, f(s)|_{\text{1st branch}} + \int_{(c)} \mathrm{d}s\, f(s)|_{\text{1st branch}}$$

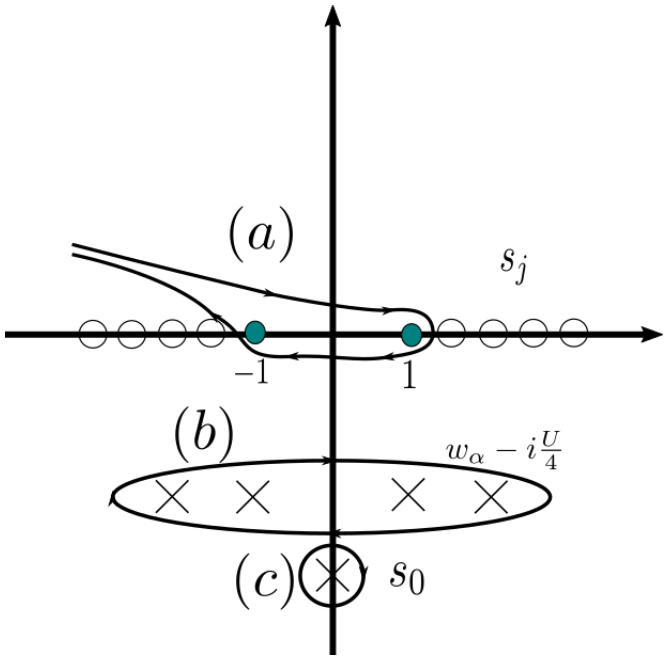

Figure 17: Contour with three parts equal to the last figure. (a) is beginning and ending at $-\infty$. (b) is surrounding all $w_\alpha - i\frac{U}{4}$ and (c) surrounds s_0.

Contour (a) contains a path (a_1) from $-\infty$ to -1, a loop (a_2) around the interval $[-1, 1]$ and a path (a_3) from -1 back to $-\infty$. The paths (a_1) and (a_3) obviously cancel each other.

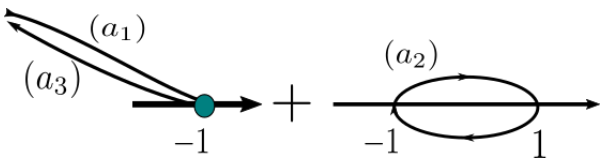

Figure 18: Illustration of (a).

For the integrals on (b) and (c) we find

$$\Sigma_1 = 2\pi i \left(\sum_{\alpha=1}^{l} \ln g \left(w_\alpha - i\frac{U}{4} \right) + \frac{N}{2} \ln g \left(s_0 \right) \right) + \int\limits_{(a_2)} \mathrm{d}s \; f\left(s\right)|_{\text{1st branch}} \, .$$

Now we consider Σ_2. The deformation of the integration contour is analogous to as above. "The integral of $f\left(s\right)|_{\text{1st branch}}$ [...] [on the part (a_2) is equal] to the integral of $f\left(s\right)|_{\text{2nd branch}}$" [36, p. 569] on the reversed part (a_2). Therefore we get

$$\Sigma_2 = \int\limits_{\mathcal{L}} \mathrm{d}s \; f\left(s\right)|_{\text{2nd branch}} - \int\limits_{(a_2)} \mathrm{d}s \; f\left(s\right)|_{\text{1st branch}} \, .$$

Now we join this results and obtain

$$\Sigma_1 + \Sigma_2 = 2\pi i \left(\sum_{\alpha=1}^{l} \ln g \left(w_\alpha - i\frac{U}{4} \right) + \frac{N}{2} \ln g \left(s_0 \right) \right) + \int\limits_{\mathcal{L}} \mathrm{d}s \; f\left(s\right)|_{\text{2nd branch}} \,. \tag{102}$$

Now we are considering

$$\Sigma := \int\limits_{\mathcal{L}} \mathrm{d}s \left[\ln g \left(s - i\frac{U}{2} \right) \right]' \ln \mathfrak{C}\left(s\right) + \int\limits_{\mathcal{L}} \mathrm{d}s \left[\ln g \left(s \right) \right]' \ln \frac{1 + \mathfrak{c} + \bar{\mathfrak{c}}}{\bar{\mathfrak{c}}} \left(s\right) \tag{103}$$

First of all we are integrating by parts and use that $\ln g \left(s - i\frac{U}{2} \right)$ and $\ln g \left(s \right)$ show no jump after surrounding the real axis. Therefore the surface terms vanish

$$\Sigma = - \int\limits_{\mathcal{L}} \mathrm{d}s \ln g \left(s - i\frac{U}{2} \right) \left[\ln \mathfrak{C}\left(s\right) \right]' - \int\limits_{\mathcal{L}} \mathrm{d}s \ln g \left(s \right) \left[\ln \frac{1 + \mathfrak{c} + \bar{\mathfrak{c}}}{\bar{\mathfrak{c}}} \left(s\right) \right]' .$$

Now we are using

$$\begin{aligned} \mathfrak{C}\left(s\right) &= \left(\frac{\sum_{j=1}^{4} l_j}{l_3 + l_4} \frac{l_3 + l_4 + \sum_{j=1}^{4} \bar{l}_j}{\sum_{j=1}^{4} \left(l_j + \bar{l}_j \right)} \right) \left(s\right) , \\ \frac{\mathfrak{1} + \mathfrak{c} + \bar{\mathfrak{c}}}{\bar{\mathfrak{c}}} \left(s\right) &= \frac{\sum_{j=1}^{4} \bar{l}_j}{\bar{l}_3 + \bar{l}_4} \left(s\right) \cdot \underbrace{\frac{l_3 + l_4 + \bar{l}_1 + \bar{l}_2}{l_3 + l_4} \left(s\right)}_{= 1 + \frac{l_4}{l_3}(s)\big|_{\text{2nd branch}}} , \end{aligned}$$

$$\Rightarrow \Sigma = - \int\limits_{\mathcal{L}} \mathrm{d}s \ln g \left(s - i\frac{U}{2} \right) \left[\ln \frac{\sum_{j=1}^{4} l_j}{l_3 + l_4} \left(s\right) \right]' - \int\limits_{\mathcal{L}} \mathrm{d}s \ln g \left(s \right) \left[\ln \frac{1 + \mathfrak{c} + \bar{\mathfrak{c}}}{\bar{\mathfrak{c}}} \left(s\right) \right]' . \tag{104}$$

We deform the integration contour $\mathcal{L}$. This yields a contour with three parts.

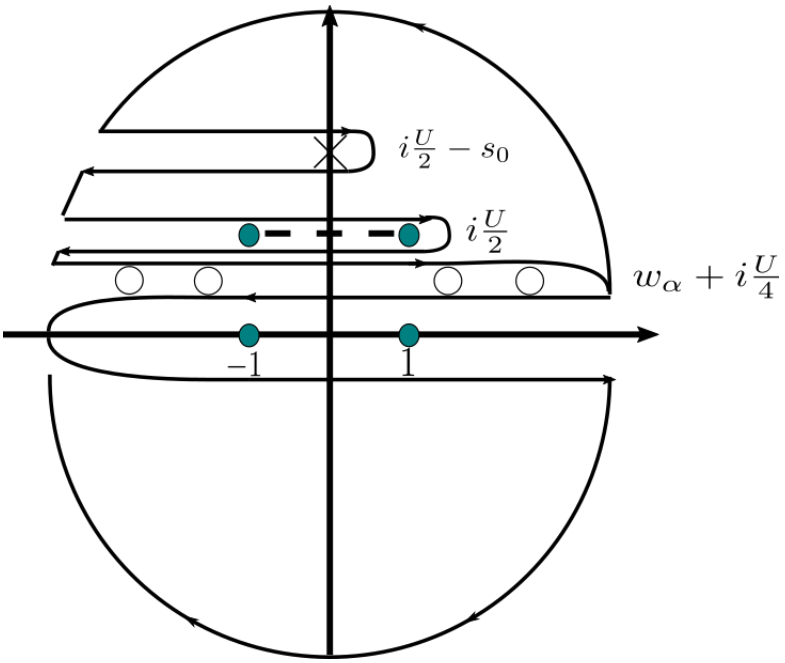

Figure 19: Zeroes and Singularities of $\frac{l_1+l_2+l_3+l_4}{l_3+l_4}(s)$: Zeroes are illustrated by open circles, the pole by a cross and branch cuts by dashed lines. The integration contour $\mathcal{L}$ can be seen. We "add a large semi-circle with radius R" [36, p. 572] to the lower half-plane. The integrand behaves like $\mathcal{O}\left(\frac{\ln R}{R^2}\right)$. Therefore this path does not contribute to the integral (104). We add up a path to the upper part. Without moving over the singularities this path can be closed to a point. Therefore this path does also not contribute to the integral (104).

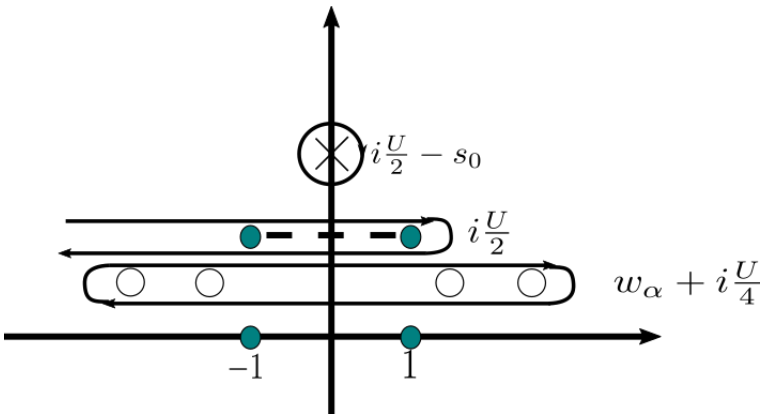

Figure 20: Illustration of the three contours remaining from the contour in figure (19). The contours are around the zeroes $w_\alpha + i\frac{U}{4}$, the branch cut $[-1, 1] + i\frac{U}{2}$, and the pole $i\frac{U}{2} - s_0$ of $\frac{l_1+l_2+l_3+l_4}{l_3+l_4}(s)$ in clockwise manner. The first and third contour integrals can be calculated easily.

The second contour is equal to the contour $\mathcal{L} + i\frac{U}{2}$ in clockwise manner. We rewrite this contour integral by the use of a shift of the integration variable from s to $s + i\frac{U}{2}$. Then we have to exchange "$l_j(s)$ functions by $\bar{l}_j(s)$ functions" [36, p. 571]. Furthermore we are using

$$\frac{1+\mathfrak{c}+\bar{\mathfrak{c}}}{\bar{\mathfrak{c}}}(s)=\frac{\sum_{j=1}^{4}\bar{l}_j}{\bar{l}_3+\bar{l}_4}(s)\cdot\underbrace{\frac{l_3+l_4+\bar{l}_1+\bar{l}_2}{l_3+l_4}(s)}_{=1+\frac{l_4}{l_3}(s)\big|_{\text{2nd branch}}},$$

so that some integral contributions cancel each other

$$\begin{aligned}\Sigma&=2\pi i\left(\sum_{\alpha=1}^{l}\ln g\left(w_\alpha-i\frac{U}{4}\right)-\frac{N}{2}\ln g\left(-s_0\right)\right)+\int\limits_{\mathcal{L}}\mathrm{d}s\ln g\left(s\right)\left[\ln\frac{\sum_{j=1}^{4}\bar{l}_j}{\bar{l}_3+\bar{l}_4}(s)\right]'\\&\quad-\int\limits_{\mathcal{L}}\mathrm{d}s\ln g\left(s\right)\left[\ln\frac{1+\mathfrak{c}+\bar{\mathfrak{c}}}{\bar{\mathfrak{c}}}(s)\right]'\\&=2\pi i\left(\sum_{\alpha=1}^{l}\ln g\left(w_\alpha-i\frac{U}{4}\right)-\frac{N}{2}\ln g\left(-s_0\right)\right)\\&\quad-\int\limits_{\mathcal{L}}\mathrm{d}s\ln g\left(s\right)\left[\ln\left(1+\frac{l_4}{l_3}(s)\right)\Big|_{\text{2nd branch}}\right]'.\end{aligned}\tag{105}$$

Comparing (102) with (105) and using

$$z\left(s\right)|_{\text{2nd branch}}=-\frac{1}{z\left(s\right)|_{\text{1st branch}}}$$

yields

$$\begin{aligned}\Sigma_1+\Sigma_2&=\Sigma+2\pi i\left(\frac{N}{2}\left(\ln g\left(s_0\right)+\ln g\left(-s_0\right)\right)\right)\\&\quad+\int\limits_{\mathcal{L}}\mathrm{d}s\left(f\left(s\right)|_{\text{2nd branch}}+\ln g\left(s\right)\left[\ln\left(1+\frac{l_4}{l_3}(s)\right)\Big|_{\text{2nd branch}}\right]'\right)\\&=\Sigma+2\pi i\left(\frac{N}{2}\left(\ln g\left(s_0\right)+\ln g\left(-s_0\right)\right)\right)\\&\quad+\int\limits_{\mathcal{L}}\mathrm{d}s\ln\left(\left(1-z_-^2\left(x\right)+2iz_-\left(x\right)s\right)\left(1-z_+^2\left(x\right)+2iz_+\left(x\right)s\right)\right)\\&\qquad\cdot\left[\ln\left(1+\frac{l_4}{l_3}(s)\right)\Big|_{\text{2nd branch}}\right]'\end{aligned}\tag{106}$$

Inserting (101) in (88) with respect to (106) and (103) we get

$$
\begin{aligned}
2\pi i \ln \frac{\Lambda_0^{\mathrm{QTM}}(\lambda)}{A_2} &= -2\pi i m\left(2h(x)+\ln(2i)\right)+2\pi i\left(\frac{N}{2}\left(\ln g(s_0)+\ln g(-s_0)\right)\right). \\
&\quad + 2\pi i \ln \Lambda^{\mathrm{aux}}\left(s-i\frac{U}{4}\right)+\int\limits_{\mathcal{L}} \mathrm{d}s\left[\ln g\left(s-i\frac{U}{2}\right)\right]' \ln \mathfrak{C}(s) \\
&\quad + \int\limits_{\mathcal{L}} \mathrm{d}s\left[\ln g(s)\right]' \ln \frac{1+\mathfrak{c}+\bar{\mathfrak{c}}}{\bar{\mathfrak{c}}}(s) \\
&\quad + \int\limits_{\mathcal{L}} \mathrm{d}s \ln\left(\left(1-z_-^2(x)+2iz_-(x)s\right)\left(1-z_+^2(x)+2iz_+(x)s\right)\right) \\
&\qquad \cdot \left[\ln\left(1+\frac{l_4}{l_3}(s)\right)\Big|_{\text{2nd branch}}\right]'.
\end{aligned}
$$

The expression $\left(1-z_-^2(x)+2iz_-(x)s\right)\left(1-z_+^2(x)+2iz_+(x)s\right)$ has zeroes at

$$
\begin{aligned}
s &= -\frac{i}{2}\left(z_\pm(x)-\frac{1}{z_\pm(x)}\right) \\
&= -i\mathrm{sh}\left(2h(x)\pm 2x\right).
\end{aligned}
$$

Using

$$
\begin{aligned}
\frac{l_3+l_4+\bar{l}_1+\bar{l}_2}{l_3+l_4}(s) &= \frac{1+\mathfrak{c}+\bar{\mathfrak{c}}}{\bar{\mathfrak{c}}}(s)\,\frac{\bar{l}_3+\bar{l}_4}{\sum_{j=1}^4 \bar{l}_j}(s) \\
&= \frac{1+\mathfrak{c}+\bar{\mathfrak{c}}}{\bar{\mathfrak{c}}}(s)\,\frac{\bar{\mathfrak{c}}\mathfrak{B}}{1+\bar{\mathfrak{c}}\mathfrak{B}}(s)
\end{aligned}
$$

yields

$$
\begin{aligned}
&\int\limits_{\mathcal{L}} \mathrm{d}s \ln\left(\left(1-z_-^2(x)+2iz_-(x)s\right)\left(1-z_+^2(x)+2iz_+(x)s\right)\right)\left[\ln\left(1+\frac{l_4}{l_3}(s)\right)\Big|_{\text{2nd branch}}\right]' \\
&= \int\limits_{\mathcal{L}} \mathrm{d}s \ln\left(\left(1-z_-^2(x)+2iz_-(x)s\right)\left(1-z_+^2(x)+2iz_+(x)s\right)\right)\left[\ln\frac{l_3+l_4+\bar{l}_1+\bar{l}_2}{l_3+l_4}(s)\right]' \\
&= \int\limits_{\mathcal{L}} \mathrm{d}s \ln\left(\left(1-z_-^2(x)+2iz_-(x)s\right)\left(1-z_+^2(x)+2iz_+(x)s\right)\right)\left[\ln\left(\frac{1+\mathfrak{c}+\bar{\mathfrak{c}}}{\bar{\mathfrak{c}}}\frac{\bar{\mathfrak{c}}\mathfrak{B}}{1+\bar{\mathfrak{c}}\mathfrak{B}}\right)(s)\right]'.
\end{aligned}
$$

Inserting (93) we get

$$\begin{aligned}\ln\frac{\Lambda_0^{\mathrm{QTM}}(\lambda)}{A_2} &= -m\left(2h(x)+\ln(2i)\right)+\frac{N}{2}\left(\ln g(s_0)+\ln g(-s_0)\right)\\ &+\frac{N}{2}\ln\frac{(s-s_0)\left(s+s_0-i\frac{U}{2}\right)}{(s+s_0)^2\left(s-s_0+i\frac{U}{2}\right)^2}-(k\circ\ln\mathfrak{B})(s)\\ &+\left(k\circ\left(\ln\bar{\mathfrak{C}}-\ln\bar{\mathfrak{c}}-\ln\mathfrak{B}\right)\right)\left(s-i\frac{U}{2}\right)+\int\limits_{\mathcal{L}}\frac{\mathrm{d}s'}{2\pi i}\left[\ln g\left(s'-i\frac{U}{2}\right)\right]'\ln\mathfrak{C}(s')\\ &+\int\limits_{\mathcal{L}}\frac{\mathrm{d}s'}{2\pi i}\left[\ln g(s')\right]'\ln\frac{1+\mathfrak{c}+\bar{\mathfrak{c}}}{\bar{\mathfrak{c}}}(s')\\ &+\int\limits_{\mathcal{L}}\frac{\mathrm{d}s'}{2\pi i}\ln\left(\left(1-z_-^2(x)+2iz_-(x)s'\right)\left(1-z_+^2(x)+2iz_+(x)s'\right)\right)\\ &\qquad\cdot\left[\ln\left(\frac{1+\mathfrak{c}+\bar{\mathfrak{c}}}{\bar{\mathfrak{c}}}\frac{\bar{\mathfrak{c}}\mathfrak{B}}{1+\bar{\mathfrak{c}}\mathfrak{B}}\right)(s')\right]'.\end{aligned}$$

Performing the Trotter limit $N\to\infty$ yields

$$\begin{aligned}\ln\Lambda_0^{\mathrm{QTM}}(\lambda) &= \frac{3N}{2}\ln(-1)+3N\ln\cos\lambda+\left(\frac{1}{2z_+(x)}-\frac{z_-(x)}{2}-\frac{U}{4}\right)\beta\\ &-\frac{1}{2\pi i}(k\circ\ln\mathfrak{B})(s)+\frac{1}{2\pi i}\left(k\circ\left(\ln\bar{\mathfrak{C}}-\ln\bar{\mathfrak{c}}-\ln\mathfrak{B}\right)\right)\left(s-i\frac{U}{2}\right)\\ &+\int\limits_{\mathcal{L}}\frac{\mathrm{d}s'}{2\pi i}\left[\ln g\left(s'-i\frac{U}{2}\right)\right]'\ln\mathfrak{C}(s')+\int\limits_{\mathcal{L}}\frac{\mathrm{d}s'}{2\pi i}\left[\ln g(s')\right]'\ln\frac{1+\mathfrak{c}+\bar{\mathfrak{c}}}{\bar{\mathfrak{c}}}(s')\\ &+\int\limits_{\mathcal{L}}\frac{\mathrm{d}s'}{2\pi i}\ln\left(\left(1-z_-^2(x)+2iz_-(x)s'\right)\left(1-z_+^2(x)+2iz_+(x)s'\right)\right)\\ &\qquad\cdot\left[\ln\left(\frac{1+\mathfrak{c}+\bar{\mathfrak{c}}}{\bar{\mathfrak{c}}}\frac{\bar{\mathfrak{c}}\mathfrak{B}}{1+\bar{\mathfrak{c}}\mathfrak{B}}\right)(s')\right]'.\end{aligned}$$

We have to drop the term $\frac{3N}{2}\ln(-1)$ since it does not contribute to $\ln\Lambda_0^{\mathrm{QTM}}(\lambda)$. Furthermore we also have to drop the term $3N\ln\cos\lambda$ because our R-matrix (65) is not normalized

$$\check{R}(\lambda,0)\,\check{R}(0,\lambda)\neq 1,$$

therefore we find

$$\begin{aligned}\ln \Lambda_0^{\mathrm{QTM}}(\lambda) = &\left(\frac{1}{2z_+(x)} - \frac{z_-(x)}{2} - \frac{U}{4}\right)\beta \\ &- \frac{1}{2\pi i}\left(k \circ \ln \mathfrak{B}\right)(s) + \frac{1}{2\pi i}\left(k \circ \left(\ln \bar{\mathfrak{C}} - \ln \bar{\mathfrak{c}} - \ln \mathfrak{B}\right)\right)\left(s - i\frac{U}{2}\right) \\ &+ \int_{\mathcal{L}} \frac{\mathrm{d}s'}{2\pi i}\left[\ln g\left(s' - i\frac{U}{2}\right)\right]' \ln \mathfrak{C}(s') \\ &+ \int_{\mathcal{L}} \frac{\mathrm{d}s'}{2\pi i}\left[\ln g(s')\right]' \ln \frac{1+\mathfrak{c}+\bar{\mathfrak{c}}}{\bar{\mathfrak{c}}}(s') \\ &+ \int_{\mathcal{L}} \frac{\mathrm{d}s'}{2\pi i} \ln\left(\left(1 - z_-^2(x) + 2iz_-(x)s'\right)\left(1 - z_+^2(x) + 2iz_+(x)s'\right)\right) \\ &\cdot \left[\ln \frac{(1+\mathfrak{c}+\bar{\mathfrak{c}})\mathfrak{B}}{1+\bar{\mathfrak{c}}\mathfrak{B}}(s')\right]'. \end{aligned} \tag{107}$$

Note that on the right-hand side x and s depend on λ via (78) and (82) and that $g(s)$ also depends on x (100).
Furthermore note that for $\lambda = 0$ the expression for $\ln \Lambda_0^{\mathrm{QTM}}(\lambda)$ simplifies to the well-known result [63, 36], which yields the host's contribution to the thermodynamics of our impurity model

$$f_{\mathrm{h}} = -\frac{1}{\beta}\ln \Lambda_0^{\mathrm{QTM}}(0), \tag{108}$$

$$\begin{aligned}\ln \Lambda_0^{\mathrm{QTM}}(0) = &-\frac{\beta U}{4} + \int_{\mathcal{L}} \frac{\mathrm{d}s}{2\pi i}\left[\ln z\left(s - i\frac{U}{2}\right)\right]' \ln \mathfrak{C}(s) \\ &+ \int_{\mathcal{L}} \frac{\mathrm{d}s}{2\pi i}\left[\ln z(s)\right]' \ln \frac{1+\mathfrak{c}+\bar{\mathfrak{c}}}{\bar{\mathfrak{c}}}(s). \end{aligned} \tag{109}$$

The impurity contribution to the free energy per site is given by

$$f_{\mathrm{i}} = -\frac{1}{\beta}\ln \Lambda_0^{\mathrm{QTM}}(\nu), \tag{110}$$

$$f = f_{\mathrm{h}} + \frac{1}{L} f_{\mathrm{i}}. \tag{111}$$

Equations (96),(107), (108), (109), (110) and (111) completely describe the thermodynamical properties of the Hubbard model with impurity.
We note that we found alternative formulas for $\ln \Lambda_0^{\mathrm{QTM}}(\lambda)$. The alternative expressions are given in the appendix.
At this point, we furthermore note that we have not calculated the Hamiltonian of the

Hubbard model with integrable impurity. In principle, it is possible to calculate this Hamiltonian. In chapter 6.1 the procedure for the calculation is explained. However, the calculation requires a high computing time and has therefore not been carried out. Note that the result should contain additional manybody terms like in chapter 2.4.2. Notice also that this is a special impurity lattice model with an impurity interacting with an interacting host.

4 Modified Hubbard model with integrable impurity

In this section we consider the Hubbard model with integrable impurity and modify the density of states similar to chapter 2.
We introduce shifts $\theta_1, \ldots, \theta_{\frac{N}{2}}$ on the horizontal lines. These shifts are, however, not intended to be arbitrary, but are intended to follow a predetermined distribution density ρ_α. This distribution density depends on the parameter α. Note that, unlike Chapter 2, we have no shifts on the vertical lines.

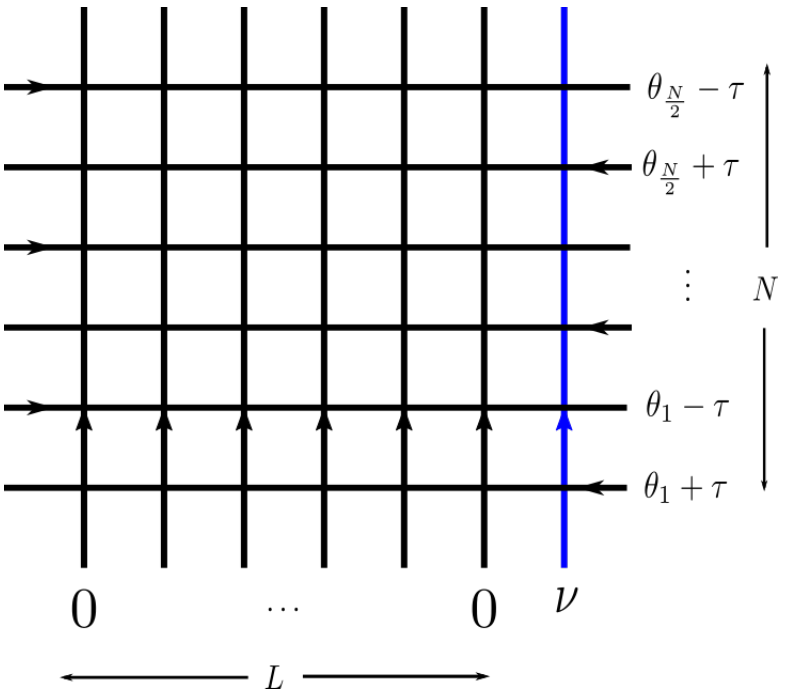

Figure 21: The quantum chain is mapped to this two-dimensional classical model at finite temperature. The lattice has width $L+1$ and height N. The rows of the lattice belong to the row-to-row transfer matrices with $\theta_j \pm \tau$, $\tau = \frac{\beta}{N}$. The column-to-column transfer matrix is crucial for the thermodynamics. The blue line is intended to illustrate the integrable spin-$\frac{1}{2}$ impurity.

The way of dealing with the shifts $\theta_1, \ldots, \theta_{\frac{N}{2}}$ is again similar to chapter 2. The Bethe ansatz equations of the row-to-row transfer matrix (68) do not depend on shifts on the horizontal lines and do not change.

$$
\begin{aligned}
e^{ik_jL}e^{2h(\nu)}\frac{\frac{z_-(k_j)}{z_+(\nu)}+1}{z_-(\nu)-z_-(k_j)} &= \prod_{l=1}^{M}\frac{\Lambda_l-\sin k_j-i\frac{U}{4}}{\Lambda_l-\sin k_j+i\frac{U}{4}}, \\
\prod_{j=1}^{K}\frac{\Lambda_l-\sin k_j-i\frac{U}{4}}{\Lambda_l-\sin k_j+i\frac{U}{4}} &= -\prod_{m=1}^{M}\frac{\Lambda_l-\Lambda_m-i\frac{U}{2}}{\Lambda_l-\Lambda_m+i\frac{U}{2}}.
\end{aligned}
\tag{112}
$$

In contrast, the Bethe ansatz equations of the column-to-column transfer matrix change.

We introduce the column-to-column transfer matrix (17)

$$t^{\mathrm{QTM}}(\lambda,\tau)=\mathrm{tr}_{\mathrm{aux}}\left(\bigotimes_{j=1}^{\frac{N}{2}}R(\lambda,\theta_j-\tau)\otimes\tilde{R}(\lambda,\theta_j+\tau)\right),$$

where the R-matrix is given by (65).
The column-to-column transfer matrix is again diagonalized by the Quantum Inverse Scattering Method [100, 63]. The diagonalization scheme is similar to that in chapter 3. We use the parametrizations of λ,τ in terms of

$$e^{2x}=\tan\lambda,\qquad e^{2w_n^{\pm}}=\tan(\theta_n\pm\tau)$$

and consider the functions

$$z_{\pm}(x):=e^{2h(x)\pm 2x},\qquad 2h(x):=-\mathrm{arsinh}\frac{U}{4\mathrm{ch}\ (2x)}.$$

Furthermore we use the definition $z_j:=z_-(\lambda_j)$.
The parameters $\{z_j\}_{j=1}^m$ and $\{w_\alpha\}_{\alpha=1}^l$ satisfy the Bethe ansatz equations of the column-to-column transfer matrix

$$\begin{aligned}&(-1)^{\frac{N}{2}}e^{\beta(\mu-B)}\prod_{n=1}^{\frac{N}{2}}e^{2\left(w_n^--w_n^+\right)}\frac{\left(1-\frac{1}{z_jz_+\left(w_n^-\right)}\right)\left(1+\frac{z_+\left(w_n^+\right)}{z_j}\right)}{\left(1-\frac{z_-\left(w_n^+\right)}{z_j}\right)\left(1+\frac{1}{z_jz_-\left(w_n^-\right)}\right)}\\&=(-1)^{1+m+l}\prod_{\alpha=1}^{l}\frac{z_j-\frac{1}{z_j}-2iw_\alpha-\frac{U}{2}}{z_j-\frac{1}{z_j}-2iw_\alpha+\frac{U}{2}},\end{aligned}$$

$$e^{2\beta\mu}\prod_{j=1}^{m}\frac{z_j-\frac{1}{z_j}-2iw_\alpha+\frac{U}{2}}{z_j-\frac{1}{z_j}-2iw_\alpha-\frac{U}{2}}=-\prod_{\beta=1}^{l}\frac{2i(w_\alpha-w_\beta)-U}{2i(w_\alpha-w_\beta)+U}.\tag{113}$$

The derivation of the non-linear integral equations is analogous to [63, 36] (see chapter 3). We find

$$\begin{aligned}
\ln \mathfrak{b}^+(s) &= -2\beta B - \left(K_2 * \ln \mathfrak{B}^+\right)(s) + \left(K_{2,\frac{U}{2}} * \ln \mathfrak{B}^-\right)(s) \\
&\quad - \left(K_1 * \ln \frac{\bar{\mathfrak{c}}^+ \bar{\mathfrak{C}}^-}{\bar{\mathfrak{c}}^- \bar{\mathfrak{C}}^+}\right)(s), \\
\ln \mathfrak{b}^-(s) &= -2\beta B - \left(K_{2,-\frac{U}{2}} * \ln \mathfrak{B}^+\right)(s) + \left(K_2 * \ln \mathfrak{B}^-\right)(s) \\
&\quad - \left(K_{1,-\frac{U}{2}} * \ln \frac{\bar{\mathfrak{c}}^+ \bar{\mathfrak{C}}^-}{\bar{\mathfrak{c}}^- \bar{\mathfrak{C}}^+}\right)(s), \\
\ln \mathfrak{c}^\pm(s) &= -\frac{\beta U}{2} + \beta(\mu + B) \pm \beta e_{\text{new}}(s) + \left(K_{1,-\frac{U}{2}} * \ln \bar{\mathfrak{B}}^+\right)(s) \\
&\quad - \left(K_1 * \ln \bar{\mathfrak{B}}^-\right)(s) + \left(K_{1,-\frac{U}{4}} * \ln \frac{\bar{\mathfrak{C}}^+}{\bar{\mathfrak{C}}^-}\right)(s) \pm \frac{1}{2} \ln \frac{\bar{\mathfrak{C}}^+}{\bar{\mathfrak{C}}^-}(s), \\
\ln \bar{\mathfrak{c}}^\pm(s) &= -\frac{\beta U}{2} - \beta(\mu + B) \mp \beta e_{\text{new}}(s) - \left(K_1 * \ln \mathfrak{B}^+\right)(s) \\
&\quad + \left(K_{1,\frac{U}{2}} * \ln \mathfrak{B}^-\right)(s) - \left(K_{1,\frac{U}{4}} * \ln \frac{\mathfrak{C}^+}{\mathfrak{C}^-}\right)(s) \pm \frac{1}{2} \ln \frac{\mathfrak{C}^+}{\mathfrak{C}^-}(s),
\end{aligned} \tag{114}$$

where the integration kernels are given by (94). The shifts $\theta_1, \ldots, \theta_{\frac{N}{2}}$ do not change the form of the Gibbs free energy (the value changes obviously). Therefore it is still given by (111). Note that $e_{\text{new}}(s)$ depends on the choice of the distribution density function ρ_α. The next subsection explains how ρ_α has to be selected for our goals (3). Then $e_{\text{new}}(s)$ is given by (124). Note that the functions $\mathfrak{c}^\pm(s)$ and $\bar{\mathfrak{c}}^\pm(s)$ can be restricted to the interval $[-1, 1]$ as these functions vanish outside.

4.1 Distribution density function $\rho_\alpha(s)$

There are many different distribution densities that can be selected, for example

- the normal distribution with $\mu, \sigma \geq 0$

$$\begin{aligned}
\rho_{\mu,\sigma}(x) &= \frac{e^{-\frac{(x-\mu)^2}{2\sigma^2}}}{\sqrt{2\pi}\sigma} \\
\Rightarrow \left(\mathcal{F}\rho_{\mu,\sigma}\right)(k) &= e^{-\frac{\sigma^2}{2}k^2 - i\mu k}.
\end{aligned}$$

- the gamma distribution with $\alpha, \beta > 0$

$$\begin{aligned}
\rho_{\alpha,\beta}(x) &= \frac{\beta^\alpha}{\Gamma(\alpha)} x^{\alpha-1} e^{-\beta x} \Theta(x) \\
\Rightarrow \left(\mathcal{F}\rho_{\alpha,\beta}\right)(k) &= \left(\frac{\beta}{\beta + ik}\right)^\alpha.
\end{aligned}$$

- the beta distribution with $\alpha, \beta > 0$ and for $0 \leq x \leq 1$

$$\begin{aligned}\rho_{\alpha,\beta}(x) &= \frac{\Gamma(\alpha+\beta)}{\Gamma(\alpha)\Gamma(\beta)} x^{\alpha-1}(1-x)^{\beta-1} \\ \Rightarrow (\mathcal{F}\rho_{\mu,\sigma})(k) &= \frac{\sqrt{\pi}\Gamma(\alpha+\beta)}{2^{\alpha+\beta-1}\Gamma\left(\frac{\alpha+\beta}{2}\right)\Gamma\left(\frac{1+\alpha+\beta}{2}\right)} \\ &\quad \cdot \left({}_2F_3\left(\frac{1+\alpha}{2}, \frac{\alpha}{2}; \frac{1}{2}, \frac{\alpha+\beta}{2}, \frac{1+\alpha+\beta}{2}; -\frac{k^2}{4}\right)\right. \\ &\quad \left. -\frac{i\alpha k}{\alpha+\beta} {}_2F_3\left(\frac{1+\alpha}{2}, 1+\frac{\alpha}{2}; \frac{3}{2}, \frac{1+\alpha+\beta}{2}, 1+\frac{\alpha+\beta}{2}; -\frac{k^2}{4}\right)\right),\end{aligned}$$

  where ${}_pF_q(a_1,\ldots,a_p; b_1,\ldots,b_q; z)$ is the generalized hypergeometric function.

- the Lorentz distribution for $\alpha > 0$

$$\begin{aligned}\rho_\alpha(x) &= \frac{1}{\pi\alpha}\frac{1}{1+\left(\frac{x}{\alpha}\right)^2} \\ \Rightarrow (\mathcal{F}\rho_\alpha)(k) &= e^{-\alpha|k|}.\end{aligned}$$

- for $\alpha > 0$ the distribution

$$\begin{aligned}\rho_\alpha(x) &= \frac{\alpha}{\pi \mathrm{ch}(\alpha x)} \\ \Rightarrow (\mathcal{F}\rho_\alpha)(k) &= \frac{1}{\mathrm{ch}\left(\frac{\pi k}{2\alpha}\right)}.\end{aligned}$$

Unfortunately, all these densities do not show the desired behaviour (3)! To understand this, we consider the known result for any eigenvalue of the row-to-row transfer matrix for the host of the Hubbard model from [113]:

$$\begin{aligned}\Lambda(\lambda) &= a^{2L}(\lambda) e^{Lh(\lambda)} \prod_{n=1}^{M} \sigma_-\left(\lambda, e^{ik_n}\right) + (-1)^M b^{2L}(\lambda) e^{Lh(\lambda)} \prod_{n=1}^{M} \sigma_+\left(\lambda, e^{ik_n}\right) \\ &\quad + (-1)^{M-K} a^L(\lambda) b^L(\lambda) e^{-Lh(\lambda)} \prod_{n=1}^{M} \sigma_-\left(\lambda, e^{ik_n}\right) \\ &\quad \cdot \prod_{m=1}^{K} \frac{z_-(\lambda) - \frac{1}{z_-(\lambda)} - 2i\Lambda_m + \frac{U}{2}}{z_-(\lambda) - \frac{1}{z_-(\lambda)} - 2i\Lambda_m - \frac{U}{2}} \\ &\quad + (-1)^K a^L(\lambda) b^L(\lambda) e^{-Lh(\lambda)} \prod_{n=1}^{M} \sigma_+\left(\lambda, e^{ik_n}\right) \\ &\quad \cdot \prod_{m=1}^{K} \frac{\frac{1}{z_+(\lambda)} - z_+(\lambda) - 2i\Lambda_m - \frac{U}{2}}{\frac{1}{z_+(\lambda)} - z_+(\lambda) - 2i\Lambda_m + \frac{U}{2}},\end{aligned} \tag{115}$$

where

$$a(\lambda) = \frac{1}{\sqrt{1+e^{4x}}}, \qquad b(\lambda) = \frac{e^{2x}}{\sqrt{1+e^{4x}}}, \qquad \sigma_\pm(\lambda, z) = \frac{e^{2x} + ze^{\pm 2h(x)}}{1 - ze^{2x \pm 2h(x)}}.$$

Note that x depends on λ via (66). Note furthermore that $\{k_n\}_{n=1}^M$ and $\{\Lambda_m\}_{m=1}^K$ are given by (112).

4.1.1 Procedure for the row-to-row transfer matrix

To understand the way forward, let's first look at the XX model, which corresponds to the case $U = 0$. First we consider the momentum and the energy

$$\begin{aligned} e^{ip(\lambda)} &= \tan\lambda, \\ e(\lambda) &= \frac{1}{\sin(2\lambda)}. \end{aligned}$$

At the free fermion point $p = \frac{\pi}{2}$ we have to choose $\lambda = i\infty$. Parameterizing $\lambda = \frac{\pi}{4} + iy$ we have

$$e\left(\frac{\pi}{4} + iy\right) = \frac{1}{\mathrm{ch}(2y)} \in \mathbb{R}.$$

If we work at the free fermion point or directly for a XX model and then take the logarithmic derivative at some point θ instead of 0, then we find the energy as a function of the difference in λ and θ

$$\begin{aligned} e^{ip(\lambda)} &= \tan\lambda, \\ e(\lambda) &= \frac{1}{\sin(2(\lambda-\theta))}. \end{aligned} \tag{116}$$

For $b \simeq 0$ and large L in equation (115) follows the momentum and the energy of the one-particle excitations from $\sigma_-(\lambda, z)$. It is easy to see that

$$\begin{aligned} \sigma_-(\theta, z)|_{\theta=0} &= z, \\ \partial_\theta \ln \sigma_-(\theta, z)|_{\theta=0} &= z + \frac{1}{z} - \frac{U}{2}. \end{aligned}$$

Inserting $z = e^{ip(\lambda)} = \tan\lambda$, we find

$$\partial_\theta \ln \sigma_-(\theta, z)|_{\theta=0} = \frac{2}{\sin(2\lambda)} - \frac{U}{2},$$

which corresponds essentially to (116). So here, for $\theta = 0$, everything still corresponds to the expectation. Now we perform the same calculation for $\theta \neq 0$. Then we have

$$\partial_\theta \ln \sigma_-(\theta, z) = \left(1 + e^{4x}\right) \frac{e^{4h(x)} + z^2 + z\frac{Ue^{2h(x)}\mathrm{th}(2x)}{2\mathrm{ch}(2h(x))}}{\left(z + e^{2x+2h(x)}\right)\left(e^{2h(x)} - ze^{2x}\right)}, \tag{117}$$

but this can not be brought into the form (116). This is a consequence of Shastry's R-matrix, which is not of difference type.

To solve this problem, one can try to choose z such that $\partial_\theta \ln \sigma_-(\theta, z)$ is independent of θ. For example at $U = 0$ we find

$$\partial_\theta \ln \sigma_-(\theta, z)|_{U=0} = \left(1 + e^{4x}\right) \frac{1 + z^2}{\left(z + e^{2x}\right)\left(1 - ze^{2x}\right)},$$
$$\sigma_-(\theta, \pm i)|_{U=0} = \pm i,$$

which means, that for $U = 0$ $z = \pm i$ is such a point. For $U \neq 0$ there is, however, no z which is independent of θ, satisfying the required condition that $\partial_\theta \ln \sigma_-(\theta, z)$ is independent of θ.

For this reason, we apply the following procedure:

We now consider $\partial_\theta \ln \sigma_-(\theta, z)|_{U=0}$ for $U = 0$, set $e^{2x} = -iy$ and multiply with $(1-y)^\alpha$. This factor will later be our distribution density function. Integrating this over y in the interval $[0, 1]$ and using $z = i + \epsilon$ (where ϵ will later be our energy) and $y = 1 - x'$ yields

$$\left(1 + z^2\right) \int_0^1 \mathrm{d}y \frac{i\left(1 - y^2\right)(1-y)^\alpha}{(iz + y)(1 + izy)} = -i\left(2i\epsilon + \epsilon^2\right) \int_0^1 \mathrm{d}x' \frac{x'^\alpha\left(1 - (1-x')^2\right)}{\epsilon^2 + x'^2 - \epsilon^2 x' - i\epsilon x'^2}$$

Assuming that ϵ and x' are small, i.e. $\alpha < 0$, follows

$$\left(1 + z^2\right) \int_0^1 \mathrm{d}y \frac{i\left(1 - y^2\right)(1-y)^\alpha}{(iz + y)(1 + izy)} \simeq 4\epsilon \int_0^1 \mathrm{d}x \frac{x^{\alpha+1}}{\epsilon^2 + x^2}$$
$$= 4\epsilon\,|\epsilon|^\alpha \int_0^{\frac{1}{\epsilon}} \mathrm{d}x \frac{x^{\alpha+1}}{1 + x^2}.$$

Note that the remaining integral is just a number for small ϵ. We see here the desired behaviour $\epsilon\,|\epsilon|^\alpha$ for the modified energy.

To use this for the case $U \neq 0$, we consider the factor $z + e^{2x+2h(x)}$ in the denominator of

$$\partial_\theta \ln \sigma_-(\theta, z) = \left(1 + e^{4x}\right) \frac{e^{4h(x)} + z^2 + z\frac{Ue^{2h(x)}\mathrm{th}(2x)}{2\mathrm{ch}(2h(x))}}{\left(z + e^{2x+2h(x)}\right)\left(e^{2h(x)} - ze^{2x}\right)}.$$

To set this factor to 0, the following selection for z and x

$$z = \pm i, \qquad \mathrm{ch}^2(2x) = \pm i\frac{U}{4} \tag{118}$$

can be made. The "full" calculation for small $U \neq 0$ shows that the same behaviour follows for the energy as for the case $U = 0$. Here we have to choose $e^{2x+2h(x)} = -iy$. Using the parametrization y the distribution density of the shifts $\theta_1, \ldots, \theta_{\frac{N}{2}}$ is then given by

$$\rho_\alpha(y) = (1+\alpha)(1-y)^\alpha \Theta(y)\Theta(1-y), \qquad -1 < \alpha < 0. \tag{119}$$

The distribution density satisfies

$$\int_{-\infty}^{\infty} \mathrm{d}y \rho_\alpha(y) = 1. \tag{120}$$

4.1.2 Procedure for the column-to-column transfer matrix

Up to now the row-to-row transfer matrix has been treated and the desired density function (119) for the modified density of states has been derived. Now this must be translated into the language of the column-to-column transfer matrix.
In section 3.3 without shifts $\theta_1, \ldots, \theta_{\frac{N}{2}}$ we considered (77) with

$$A_i = \left(R^{i,1}_{i,1}(\lambda, -\tau) R^{4.i}_{4,i}(\tau, \lambda)\right)^{\frac{N}{2}}.$$

In order to assess the influence of the shifts $\theta_1, \ldots, \theta_{\frac{N}{2}}$, the following combination

$$\left(R^{i,1}_{i,1}(\lambda, \tau) R^{4.i}_{4,i}(\tau + \Delta\tau, \lambda)\right)^{\frac{N}{2}} \tag{121}$$

must be considered. In (81) and (83) the occurring $z_\pm(w)$ must be decoupled. The singular point is $z_-(w) = \pm i$ and $z_+(w) = \mp i$. The τ should be distributed accordingly.
Therefore we use $e^{2w} = \tan\tau$ from (78) and consider $-\tau \to \tau$

$$\begin{aligned} z_\pm(w) &= e^{2h(w)\pm 2w} \\ &\to -\frac{1}{z_\mp(w)}. \end{aligned} \tag{122}$$

Analogously $\tau \to \tau + \Delta\tau$ yields

$$
\begin{aligned}
e^{\pm 2w} &= (\tan\tau)^{\pm 1} \\
&\to (\tan(\tau+\Delta\tau))^{\pm 1} \\
&= \begin{cases} \tan\tau + \frac{\Delta\tau}{\cos^2\tau} + \mathcal{O}(\Delta\tau^2) \\ \frac{1}{\tan\tau} - \frac{\Delta\tau}{\sin^2\tau} + \mathcal{O}(\Delta\tau^2) \end{cases} \\
&= \begin{cases} e^{2w} + \Delta\tau(1+e^{4w}) + \mathcal{O}(\Delta\tau^2) \\ e^{-2w} - \Delta\tau(1+e^{-4w}) + \mathcal{O}(\Delta\tau^2) \end{cases} \\
&= e^{\pm 2w} \pm \Delta\tau\left(1+e^{\pm 4w}\right) + \mathcal{O}\left(\Delta\tau^2\right), \\
2h(w) &= -\operatorname{arsinh}\frac{U}{4\operatorname{ch}(2w)} \\
&\to -\operatorname{arsinh}\frac{U}{2(e^{2w}+e^{-2w}) + 2\Delta\tau(1+e^{4w}-1-e^{-4w}) + \mathcal{O}(\Delta\tau^2)} \\
&= -\operatorname{arsinh}\frac{U}{4\operatorname{ch}(2w) + 4\Delta\tau\operatorname{sh}(4w) + \mathcal{O}(\Delta\tau^2)} \\
&= -\operatorname{arsinh}\frac{U}{4\operatorname{ch}(2w)} + \Delta\tau\frac{2U\operatorname{sh}(2w)}{\sqrt{U^2+16\operatorname{ch}^2(2w)}} + \mathcal{O}\left(\Delta\tau^2\right) \\
&= 2h(w) + \Delta\tau\frac{U\operatorname{th}(2w)}{2\operatorname{ch}(2h(w))} + \mathcal{O}\left(\Delta\tau^2\right), \\
\Rightarrow e^{2h(w)} &\to e^{2h(w)}\left(1+\Delta\tau\frac{U\operatorname{th}(2w)}{2\operatorname{ch}(2h(w))}\right) + \mathcal{O}\left(\Delta\tau^2\right), \\
\Rightarrow z_\pm(w) &\to e^{2h(w)}\left(1+\Delta\tau\frac{U\operatorname{th}(2w)}{2\operatorname{ch}(2h(w))}\right)\left(e^{\pm 2w} \pm \Delta\tau\left(1+e^{\pm 4w}\right)\right) + \mathcal{O}\left(\Delta\tau^2\right) \\
&= z_\pm(w) + \Delta\tau\left(\pm e^{2h(w)}\left(1+e^{\pm 4w}\right) + \frac{U\operatorname{th}(2w)}{2\operatorname{ch}(2h(w))} z_\pm(w)\right) + \mathcal{O}\left(\Delta\tau^2\right) \\
&= z_\pm(w) + \Delta\tau\left(\frac{U\operatorname{th}(2w)}{2\operatorname{ch}(2h(w))} z_\pm(w) \pm 2\operatorname{ch}(2w)\, z_\pm(w)\right) + \mathcal{O}\left(\Delta\tau^2\right) \\
&= z_\pm(w) + \Delta\tau z_\pm(w)\left(\frac{U\operatorname{th}(2w)}{2\operatorname{ch}(2h(w))} \pm 2\operatorname{ch}(2w)\right) + \mathcal{O}\left(\Delta\tau^2\right).
\end{aligned}
$$

If this is used in equation (83) for $\Phi(s)$, then it yields

$$
\begin{aligned}
&\frac{\left(1-\frac{z_-(w)}{z(s)}\right)\left(1-\frac{z_+(w)}{z(s)}\right)}{\left(1+\frac{z_-(w)}{z(s)}\right)\left(1+\frac{z_+(w)}{z(s)}\right)} \\
&\to -\left(1+2\Delta\tau \mathrm{ch}\left(2w\right)\right) \\
&\quad\cdot\frac{\left(1+\frac{1}{z(s)z_-(w)}\right)\left(1-\frac{z_-(w)}{z(s)}-\frac{\Delta\tau z_-(w)}{z(s)}\left(\frac{U\mathrm{th}(2w)}{2\mathrm{ch}(2h(w))}-2\mathrm{ch}\left(2w\right)\right)\right)}{\left(1-\frac{1}{z(s)z_+(w)}\right)\left(1+\frac{z_+(w)}{z(s)}+\frac{\Delta\tau z_+(w)}{z(s)}\left(\frac{U\mathrm{th}(2w)}{2\mathrm{ch}(2h(w))}+2\mathrm{ch}\left(2w\right)\right)\right)} \\
&= -\left(1+2\Delta\tau \mathrm{ch}\left(2w\right)\right) \\
&\quad\cdot\frac{\left(1+\frac{1}{z(s)z_-(w)}\right)\left(1-\frac{z_-(w)}{z(s)}\right)\left(1-\frac{\Delta\tau z_-(w)}{z(s)-z_-(w)}\left(\frac{U\mathrm{th}(2w)}{2\mathrm{ch}(2h(w))}-2\mathrm{ch}\left(2w\right)\right)\right)}{\left(1-\frac{1}{z(s)z_+(w)}\right)\left(1+\frac{z_+(w)}{z(s)}\right)\left(1+\frac{\Delta\tau z_+(w)}{z(s)+z_+(w)}\left(\frac{U\mathrm{th}(2w)}{2\mathrm{ch}(2h(w))}+2\mathrm{ch}\left(2w\right)\right)\right)}.
\end{aligned}
$$

Due to the shifts $\theta_1,\ldots,\theta_{\frac{N}{2}}$ a modified energy $e_{\mathrm{new}}(s)$ occurs in the driving term of the non-linear integral equation (114). This term follows from $\Phi(s)$ by using the logarithm. We therefore consider $\ln\Phi(s)$. Analogously to the procedure for the row-to-row transfer matrix $\ln\Phi(s)$ shows singular behaviour in the vicinity of $z_-(w)\to\pm i$, i.e. $\mathrm{ch}^2(2w)\to\pm i\frac{U}{4}$, and for

$$
\begin{aligned}
z(s) &= is\left(1+\sqrt{1-\frac{1}{s^2}}\right) \\
&= \pm i-\sqrt{2\left(1-|s|\right)}+\mathcal{O}\left(1-|s|\right). \qquad (123)
\end{aligned}
$$

Using the distribution density (119) and performing a procedure similar to that of the row-to-row transfer matrix, we derive the new energy $e_{\mathrm{new}}(s)$ occuring in the non-linear integral equations (114)

$$
e_{\mathrm{new}}(s) = (1+\alpha)\frac{\pi}{\sin\left(\frac{\pi\alpha}{2}\right)}\sqrt{2\left(1-|s|\right)}^{1+\alpha}\Theta\left(1+s\right)\Theta\left(1-s\right). \qquad (124)
$$

At this point, we furthermore note that we have not specified the Hamiltonian of the Hubbard model with integrable impurity. In principle, it is possible to calculate this Hamiltonian. In chapter 6.1 the procedure for the calculation is explained. However, the calculation requires a high computing time and has therefore not been carried out. Note that the result should contain additional manybody terms like in chapter 2.4.2. Notice also that this is a special impurity lattice model with an impurity interacting with an interacting host.

4.2 Free-Fermion limit for the host of the modified Hubbard model with impurity

We consider the limit $U \to 0$. The non-linear integral equations (114) yield an algebraic set of equations, because

$$K_1(s) \to \delta(s), \qquad K_{1,\pm\frac{U}{2}} \to 0, \qquad K_{1,\pm\frac{U}{4}} \to \frac{\delta(s)}{2}, \qquad K_{2,\alpha} \overset{|\alpha|<\frac{U}{2}}{\longrightarrow} \delta(s).$$

Therefore we get

$$\begin{aligned}
\ln \mathfrak{b}^{\pm}(s) &= -2\beta B - \ln \mathfrak{B}^{+}(s) + \ln \mathfrak{B}^{-}(s) - \frac{1 \pm 1}{2} \ln \frac{\bar{\mathfrak{c}}^{+}\bar{\mathfrak{C}}^{-}}{\bar{\mathfrak{c}}^{-}\bar{\mathfrak{C}}^{+}}(s), \\
\ln \mathfrak{c}^{\pm}(s) &= \beta(\mu + B) \pm \beta e_{\text{new}}(s) - \ln \bar{\mathfrak{B}}^{-}(s) + \frac{1 \pm 1}{2} \ln \frac{\bar{\mathfrak{C}}^{+}}{\bar{\mathfrak{C}}^{-}}(s), \\
\ln \bar{\mathfrak{c}}^{\pm}(s) &= -\beta(\mu + B) \mp \beta e_{\text{new}}(s) - \ln \mathfrak{B}^{+}(s) + \frac{-1 \pm 1}{2} \ln \frac{\mathfrak{C}^{+}}{\mathfrak{C}^{-}}(s),
\end{aligned} \tag{125}$$

and for the host

$$\ln \Lambda_0^{\text{QTM}}(0) = \int_{-1}^{1} \frac{\mathrm{d}s}{2\pi\sqrt{1-s^2}} \ln \frac{(1+\mathfrak{c}^{-})(1+\mathfrak{c}^{+}+\bar{\mathfrak{c}}^{+})(1+\mathfrak{c}^{-}+\bar{\mathfrak{c}}^{-})}{\bar{\mathfrak{c}}^{+}\bar{\mathfrak{c}}^{-}(1+\mathfrak{c}^{+})}.$$

The non-linear integral equations simplify to algebraic equations and are solved easily. Substituting $s = \sin k$ we get

$$\ln \Lambda_0^{\text{QTM}}(0) = \int_{-\pi}^{\pi} \frac{\mathrm{d}k}{2\pi} \left(\ln\left(1 + e^{\beta(\mu+B+e_{\text{new}}(\sin k))}\right) + \ln\left(1 + e^{\beta(\mu-B+e_{\text{new}}(\sin k))}\right) \right). \tag{126}$$

This is the result expected from ideal Fermi gases, which means that the host still behaves like an ideal Fermi gas for $U \to 0$ with the energy $e_{\text{new}}(s)$. This is an obvious, but important result for chapter 5 and 6.

4.3 Low-temperature asymptotics of the modified Hubbard model with impurity

We derive analytic expressions for the thermodynamics. For $T \ll 1$ we simplify the non-linear integral equations (114). For external fields we set $B > 0$, $\mu < 0$, such that $\mathfrak{b}^{-}(s) \to 0$ and $\mathfrak{c}^{\pm}(s) \to 0$ for $\beta \to \infty$. $\mathfrak{b}^{+}(s)$ and $\bar{\mathfrak{c}}^{\pm}(s)$ do not disappear. Then we find from equations (114)

$$\ln \mathfrak{b}^{+}(\lambda) = -2\beta B - \left(K_2 * \ln \mathfrak{B}^{+}\right)(\lambda) - \left(K_1 * \ln \frac{\bar{\mathfrak{c}}^{+}\bar{\mathfrak{C}}^{-}}{\bar{\mathfrak{c}}^{-}\bar{\mathfrak{C}}^{+}}\right)(\lambda),$$
$$\ln \bar{\mathfrak{c}}^{\pm}(s) = -\frac{\beta U}{2} - \beta(\mu + B) \mp \beta e_{\text{new}}(s) - \left(K_1 * \ln \mathfrak{B}^{+}\right)(s). \tag{127}$$

These formulas are justified at low temperatures T. There the corrections are exponentially small $\mathcal{O}\left(e^{-\text{cst.}\beta}\right)$. The constant is real and positive.
For the eigenvalue (109) and (107) we find

$$\ln \Lambda_0^{\text{QTM}}(0) = -\frac{\beta U}{4} + \int_{-1}^{1} \frac{\mathrm{d}s}{2\pi\sqrt{1-s^2}} \ln\left(\left(1 + \frac{1}{\bar{\mathfrak{c}}^{+}(s)}\right)\left(1 + \frac{1}{\bar{\mathfrak{c}}^{-}(s)}\right)\right), \tag{128}$$

$$\begin{aligned}
\ln \Lambda_0^{\text{QTM}}(\lambda) = {} & \left(\frac{1}{2z_{+}(x)} - \frac{z_{-}(x)}{2} - \frac{U}{4}\right)\beta + \frac{1}{2\pi i}\left(k * \ln \mathfrak{B}^{+}\right)(s) \\
& + \frac{1}{2\pi i}\left(k * \ln \mathfrak{B}^{+}\right)\left(s - i\frac{U}{2}\right) + \frac{1}{2\pi i}\left(k \circ \ln \frac{\bar{\mathfrak{C}}}{\bar{\mathfrak{c}}}\right)\left(s - i\frac{U}{2}\right) \\
& + \int_{\mathcal{L}} \frac{\mathrm{d}s'}{2\pi i}\left[\ln g(s')\right]' \ln \frac{\mathfrak{1} + \bar{\mathfrak{c}}}{\bar{\mathfrak{c}}}(s') \\
& + \int_{\mathcal{L}} \frac{\mathrm{d}s'}{2\pi i} \ln\left(\left(1 - z_{-}^2(x) + 2iz_{-}(x)s'\right)\left(1 - z_{+}^2(x) + 2iz_{+}(x)s'\right)\right) \\
& \qquad \cdot \left[\ln \frac{(\mathfrak{1} + \bar{\mathfrak{c}})\mathfrak{B}}{1 + \bar{\mathfrak{c}}\mathfrak{B}}(s')\right]'.
\end{aligned} \tag{129}$$

We note that it is easily possible to find a connection between auxiliary functions (127) and dressed energy functions. One just needs a similar linearization as in chapter 2.5.2. By the use of

$$\mathfrak{b}(\lambda) := \mathfrak{b}^{+}(\lambda), \qquad \mathfrak{c}(k) := \begin{cases} \frac{1}{\bar{\mathfrak{c}}^{+}(\sin k)}, & \text{for } k \in \left[-\frac{\pi}{2}, \frac{\pi}{2}\right], \\ \frac{1}{\bar{\mathfrak{c}}^{-}(\sin k)}, & \text{for } k \in \left[\frac{\pi}{2}, \frac{3\pi}{2}\right], \end{cases} \tag{130}$$

we find

$$\ln \mathfrak{b}(\lambda) = -2\beta B - \left(K_2 * \ln \mathfrak{B}\right)(\lambda) + \left(K_1 * \ln \mathfrak{C}\right)(\lambda),$$
$$\ln \mathfrak{c}(k) = \frac{\beta U}{2} + \beta(\mu + B) - \beta e_{\text{new}}(\sin k) + \left(K_1 * \ln \mathfrak{B}\right)(\sin k).$$

$\ln \mathfrak{b}(\lambda)$ and $\ln \mathfrak{c}(k)$ "are analytic functions of order $\mathcal{O}(\beta)$ [...], $\ln \mathfrak{b}(\lambda) = -\beta\epsilon_s(\lambda)$ and $\ln \mathfrak{c}(k) = -\beta\epsilon_c(k)$, with some analytic functions $\epsilon_s(\lambda)$ and $\epsilon_c(k)$" [36, p. 612]. These functions will be studied. They are real and symmetric. They have zeroes at $\pm\lambda_0$, $\pm k_0$

and the characteristics

$$\begin{aligned} \epsilon_s(\lambda), \epsilon_c(k) < 0 \qquad & \text{for } |\lambda| < \lambda_0, |k| < k_0, \\ \epsilon_s(\lambda), \epsilon_c(k) > 0 \qquad & \text{for } |\lambda| > \lambda_0, |k| > k_0, \end{aligned}$$

such that $\mathfrak{b}(\lambda)$ and $\mathfrak{c}(k)$ have "steep crossover behaviour at low temperatures" [36, p. 593]

$$\begin{aligned} |\mathfrak{b}(\lambda)|, |\mathfrak{c}(k)| \gg 1 \qquad & \text{for } |\lambda| < \lambda_0, |k| < k_0, \\ |\mathfrak{b}(\lambda)|, |\mathfrak{c}(k)| \ll 1 \qquad & \text{for } |\lambda| > \lambda_0, |k| > k_0. \end{aligned}$$

Therefore at low temperature T the functions $\ln \mathfrak{B}(\lambda)$ and $\ln \mathfrak{C}(k)$ are not analytic anymore: If the arguments λ and k are lesser than λ_0 and k_0 then these functions $\ln \mathfrak{B}(\lambda)$ and $\ln \mathfrak{C}(k)$ are equal to $-\beta\epsilon_s(\lambda)$ and $-\beta\epsilon_c(k)$, if the arguments λ and k are bigger than λ_0 and k_0 the functions $\ln \mathfrak{B}(\lambda)$ and $\ln \mathfrak{C}(k)$ are equal to zero. Still the convolutions yield analytic functions.
"The slopes at the crossover points are steep" [36, p. 593], therefore approximations to the integral equations similar to the linearization in chapter 2.5.2 are possible. We find

$$\begin{aligned} \ln \mathfrak{b}(\lambda) = {} & -2\beta B \\ & + \frac{\pi^2}{6}\left(\frac{K_2(\lambda - \lambda_0) + K_2(\lambda + \lambda_0)}{(\ln \mathfrak{b})'(\lambda_0)} \right. \\ & \qquad \left. - \cos k_0 \frac{K_1(\lambda - \sin k_0) + K_1(\lambda + \sin k_0)}{(\ln \mathfrak{c})'(k_0)} \right) \\ & - \int_{-\lambda_0}^{\lambda_0} \mathrm{d}\lambda' K_2(\lambda - \lambda') \ln \mathfrak{b}(\lambda') + \int_{-k_0}^{k_0} \mathrm{d}k' K_1(\lambda - \sin k') \cos k' \ln \mathfrak{c}(k'), \end{aligned} \tag{131}$$

$$\begin{aligned} \ln \mathfrak{c}(k) = {} & \frac{\beta U}{2} + \beta(\mu + B) - \beta e_{\text{new}}(\sin k) - \frac{\pi^2}{6} \frac{K_1(\sin k - \lambda_0) + K_1(\sin k + \lambda_0)}{(\ln \mathfrak{b})'(\lambda_0)} \\ & + \int_{-\lambda_0}^{\lambda_0} \mathrm{d}\lambda' K_1(\sin k - \lambda') \ln \mathfrak{b}(\lambda'). \end{aligned} \tag{132}$$

We find the connection among auxiliary functions and the dressed energy functions by keeping the leading terms in the integral equations

$$\ln \mathfrak{b}(\lambda) = -\beta\epsilon_s(\lambda) + \mathcal{O}\left(\frac{1}{\beta}\right), \qquad \ln \mathfrak{c}(k) = -\beta\epsilon_c(k) + \mathcal{O}\left(\frac{1}{\beta}\right).$$

5 Limit from the Hubbard model with integrable impurity to the Anderson impurity model

Localized magnetic moments in metals are typically described by the Anderson impurity model [3, 5]

$$H_{\mathrm{AIM}} = \frac{l}{2\pi} \sum_{\sigma=\uparrow,\downarrow} \int_{-\infty}^{\infty} \mathrm{d}k \left(k n_{k,\sigma} + V \left(c_{k,\sigma}^{\dagger} d_{\sigma} + d_{\sigma}^{\dagger} c_{k,\sigma} \right) \right) + \epsilon_d \sum_{\sigma=\uparrow,\downarrow} n_{d,\sigma} + \bar{U} n_{d,\uparrow} n_{d,\downarrow}. \quad (133)$$

It is the non-degenerate Anderson impurity model. Note that in comparison with the previous chapters this is a continuum model and not a lattice model. The "orbital degeneracy of the impurity shell is" [124, p. 462] negligible. The impurity level ϵ_d cannot be simultaneously occupied by more than two electrons with spins $\sigma =\uparrow,\downarrow$. $\bar{U}$ is the intra-atomic Coulomb interaction. The "admixture of the d level with conduction band states" [124, p. 462] is given by V.

The d level is widened since d and s states are mixed. The resonance level has the width $\frac{V^2}{2}$ for $\bar{U} \to 0$ and its center is located at ϵ_d. Adding one electron to the singly occupied impurity shell leads to the energy variation $-\epsilon_d$. Removing one from the doubly occupied shell leads to $\epsilon_d + \bar{U}$. The impurity "shell can be considered as singly occupied" [124, p. 11] if the energy variation is larger than the resonance width. Hence the impurity would have a magnetic moment. The exchange interaction among the host electrons and the impurity moment is arranged by virtual processes, which accordingly change particle number by ± 1 [6]. Schrieffer and Wolf [108] showed the equivalence of the s-d exchange Kondo model and the Anderson model in the limit

$$\frac{V^2}{2} \ll -\epsilon_d, \epsilon_d + \bar{U}.$$

This follows because the dispersion relation is obviously given by $\epsilon(k) = k$.

The impurity is occupied partially with electrons with $\sigma =\uparrow,\downarrow$ if a broad resonance level arises in the vicinity of the Fermi level $|\epsilon_d| \ll \frac{V^2}{2}$ and the Coulomb energy satisfies $\bar{U} \lesssim \frac{V^2}{2}$. This state is non-magnetic. The variation of the occupation numbers for different spins σ can yield a magnetic susceptibility. Therefore at temperatures $T \lesssim \frac{V^2}{2}$ all physical quantities can be expressed in integer powers of T [124].

"The non-magnetic regime goes over continuously [in]to the magnetic regime, but, simultaneously, the impurity magnetic moment is compensated by the conduction electrons due to the Kondo effect" [124, p. 463] if the relative values of $\bar{U}$, ϵ_d and V are changed. Due to that the Anderson impurity model is offering a unified picture of the narrow many-body and the broad single-particle resonances.

Coordinate Bethe ansatz techniques were applied to the Anderson impurity model and the infinitely many thermodynamic Bethe ansatz equations for characterising the thermodynamics were derived in a series of papers [40, 66, 67, 42, 94, 123, 122, 95, 139, 124]. In this chapter we will show that the Anderson impurity model can be described as the continuum limit of the Hubbard model with integrable impurity.

5.1 Bethe ansatz equations of the Anderson impurity model

All eigenstates of the Anderson impurity model Hamiltonian are described by the set of charge $\{k_j\}_{j=1}^K$ and spin $\{\lambda_\alpha\}_{\alpha=1}^M$ rapidities [124], which are restricted by the Bethe ansatz equations

$$\begin{aligned} e^{i\bar{k}_j l + i\delta(k_j)} &= \prod_{\alpha=1}^{M} \frac{g\left(\bar{k}_j\right) - \lambda_\alpha + \frac{i}{2}}{g\left(\bar{k}_j\right) - \lambda_\alpha - \frac{i}{2}}, \\ \prod_{j=1}^{K} \frac{\lambda_\alpha - g\left(\bar{k}_j\right) + \frac{i}{2}}{\lambda_\alpha - g\left(\bar{k}_j\right) - \frac{i}{2}} &= -\prod_{\beta=1}^{M} \frac{\lambda_\alpha - \lambda_\beta + i}{\lambda_\alpha - \lambda_\beta - i}, \end{aligned}$$

where

$$g\left(\bar{k}\right) = \frac{\left(\bar{k} - \epsilon_d - \frac{\bar{U}}{2}\right)^2}{\bar{U}V^2}, \qquad e^{i\delta\left(\bar{k}\right)} = \frac{\bar{k} - \epsilon_d - i\frac{V^2}{2}}{\bar{k} - \epsilon_d + i\frac{V^2}{2}}.$$

The eigenvalues of the Hamiltonian (133) are given by

$$E = \sum_{j=1}^{K} \bar{k}_j.$$

Consider the Bethe ansatz equations for the row-to-row transfer matrix of the Hubbard model with impurity (68)

$$\begin{aligned} e^{ik_j L} e^{2h(\nu)} \frac{\frac{z_-(k_j)}{z_+(\nu)} + 1}{z_-\left(\nu\right) - z_-\left(k_j\right)} &= \prod_{l=1}^{M} \frac{\Lambda_l - \sin k_j - i\frac{U}{4}}{\Lambda_l - \sin k_j + i\frac{U}{4}}, \\ \prod_{j=1}^{K} \frac{\Lambda_l - \sin k_j - i\frac{U}{4}}{\Lambda_l - \sin k_j + i\frac{U}{4}} &= -\prod_{m=1}^{M} \frac{\Lambda_l - \Lambda_m - i\frac{U}{2}}{\Lambda_l - \Lambda_m + i\frac{U}{2}}. \end{aligned} \tag{134}$$

First of all we introduce a lattice constant $\sqrt{U}$ with $U \to 0$. The temperature T is also sent to zero with order $\mathcal{O}\left(\sqrt{U}\right)$ in the combined continuum limit. Correspondingly, we set $L = \frac{\sqrt{\bar{U}}Vl}{\sqrt{U}}$. We now consider the neighborhood of the Fermi points $k = \pm\frac{\pi}{2}$ (In the following we perform the continuum limit for the $-$ case. The other case then follows

trivially by the interchange of the sign of U.)

$$\begin{aligned} k &= \tilde{k} - \frac{\pi}{2}, \\ \Rightarrow \cos k &= \tilde{k} + \mathcal{O}\left(\tilde{k}^3\right), \qquad \sin k = -1 + \frac{\tilde{k}^2}{2} + \mathcal{O}\left(\tilde{k}^4\right). \end{aligned} \tag{135}$$

Furthermore we set $\Lambda_l = \frac{U}{2}\lambda_l - 1$.
In the equations (134) $z_\pm(\nu)$ occurs, where ν is the spectral parameter of the impurity of the Hubbard model. We choose ν such that

$$z_\pm(\nu) = e^{\mp i\left(-\frac{\pi}{2} + l_\pm\right)}. \tag{136}$$

Furthermore we set $l_\pm = \pm a - ib$ and assume that $\tilde{k}$, a and b are of order $\mathcal{O}\left(\sqrt{U}\right)$. Since x is connected to a spectral parameter λ via (66) and

$$\operatorname{sh}(2h(x))\operatorname{ch}(2x) = -\frac{U}{4}$$

must be true for all spectral parameters and thus especially for ν we get

$$\begin{aligned} -U &= z_-(\nu) - \frac{1}{z_-(\nu)} + z_+(\nu) - \frac{1}{z_+(\nu)} \\ &= 2i\sin\left(-\frac{\pi}{2} + l_-\right) + 2i\sin\left(\frac{\pi}{2} - l_+\right) \\ &= i\left(l_-^2 - l_+^2\right) + \mathcal{O}\left(U^2\right) \\ &= -4ab + \mathcal{O}\left(U^2\right) \\ \Rightarrow ab &= \frac{U}{4}. \end{aligned} \tag{137}$$

This means that a is a free parameter and b is fixed by a. Furthermore we consider

$$\begin{aligned} z_-(\nu)\, z_+(\nu) &= e^{i(l_- - l_+)} \\ &= 1 + i(l_- - l_+) + \mathcal{O}(U) \\ &\overset{!}{=} e^{4h(\nu)} \\ \Rightarrow e^{2h(\nu)} &= 1 + \mathcal{O}\left(\sqrt{U}\right) \end{aligned} \tag{138}$$

Inserting (135), (136) and (138) into the Bethe ansatz equations for the row-to-row transfer matrix of the Hubbard model with impurity and with boundary factor $(-1)^L i^{L+1}$ we get

$$e^{i\frac{\tilde{k}_j}{\sqrt{\bar{U}}}\sqrt{\bar{U}}Vl}\frac{\tilde{k}_j+l_+}{\tilde{k}_j-l_-}=\prod_{l=1}^{M}\frac{\frac{\tilde{k}_j^2}{U}-\frac{2}{U}\left(\Lambda_l+1\right)+\frac{i}{2}}{\frac{\tilde{k}_j^2}{U}-\frac{2}{U}\left(\Lambda_l+1\right)-\frac{i}{2}},$$
$$\prod_{j=1}^{K}\frac{\frac{2}{U}\left(\Lambda_l+1\right)-\frac{\tilde{k}_j^2}{U}+\frac{i}{2}}{\frac{2}{U}\left(\Lambda_l+1\right)-\frac{\tilde{k}_j^2}{U}-\frac{i}{2}}=-\prod_{m=1}^{M}\frac{\frac{2}{U}\left(\Lambda_l-\Lambda_m\right)+i}{\frac{2}{U}\left(\Lambda_l-\Lambda_m\right)-i},$$

which simplifies to

$$e^{i\frac{\tilde{k}_j}{\sqrt{\bar{U}}}\sqrt{\bar{U}}Vl}\frac{\tilde{k}_j+a-ib}{\tilde{k}_j+a+ib}=\prod_{l=1}^{M}\frac{\frac{\tilde{k}_j^2}{U}-\lambda_l+\frac{i}{2}}{\frac{\tilde{k}_j^2}{U}-\lambda_l-\frac{i}{2}},$$
$$\prod_{j=1}^{K}\frac{\lambda_l-\frac{\tilde{k}_j^2}{U}+\frac{i}{2}}{\lambda_l-\frac{\tilde{k}_j^2}{U}-\frac{i}{2}}=-\prod_{m=1}^{M}\frac{\lambda_l-\lambda_m+i}{\lambda_l-\lambda_m-i}.$$

Identifying $\frac{\tilde{k}^2}{U}$ with $g\left(\bar{k}\right)$ and dropping $e^{-i\frac{\epsilon_d+\frac{U}{2}}{\sqrt{\bar{U}}V}l}$ yields

$$e^{i\bar{k}_jl}\frac{\bar{k}_j-\epsilon_d-\frac{\bar{U}}{2}+\frac{\sqrt{\bar{U}}V}{\sqrt{U}}a-i\frac{\sqrt{\bar{U}}V}{\sqrt{U}}b}{\bar{k}_j-\epsilon_d-\frac{\bar{U}}{2}+\frac{\sqrt{\bar{U}}V}{\sqrt{U}}a+i\frac{\sqrt{\bar{U}}V}{\sqrt{U}}b}=\prod_{l=1}^{M}\frac{g\left(\bar{k}_j\right)-\lambda_l+\frac{i}{2}}{g\left(\bar{k}_j\right)-\lambda_l-\frac{i}{2}},$$
$$\prod_{j=1}^{K}\frac{\lambda_l-g\left(\bar{k}_j\right)+\frac{i}{2}}{\lambda_l-g\left(\bar{k}_j\right)-\frac{i}{2}}=-\prod_{m=1}^{M}\frac{\lambda_l-\lambda_m+i}{\lambda_l-\lambda_m-i}.$$

Setting $a=\frac{\sqrt{\bar{U}U}}{2V}$ and $b=\sqrt{\frac{U}{\bar{U}}}\frac{V}{2}$ satisfies (137) and we get

$$e^{i\bar{k}_jl}\frac{\bar{k}_j-\epsilon_d-i\frac{V^2}{2}}{\bar{k}_j-\epsilon_d+i\frac{V^2}{2}}=\prod_{l=1}^{M}\frac{g\left(\bar{k}_j\right)-\lambda_l+\frac{i}{2}}{g\left(\bar{k}_j\right)-\lambda_l-\frac{i}{2}},$$
$$\prod_{j=1}^{K}\frac{\lambda_l-g\left(\bar{k}_j\right)+\frac{i}{2}}{\lambda_l-g\left(\bar{k}_j\right)-\frac{i}{2}}=-\prod_{m=1}^{M}\frac{\lambda_l-\lambda_m+i}{\lambda_l-\lambda_m-i}.$$

Obviously, these are the Bethe ansatz equations of the Hamiltonian of the Anderson impurity model. Note that there are typing errors in [124], which have been corrected here.

5.2 Limit of the thermodynamical Bethe ansatz equations

In this chapter we want to derive thermodynamical Bethe ansatz equations of the Anderson impurity model by use of the established continuum limit by considering the thermodynamical Bethe ansatz equations of the Hubbard model with impurity.
They are given by (see chapter 3.2) [142, 117]

$$\begin{aligned}
\ln\zeta(k) &= -2\beta\cos k - 4\beta\int_{-\infty}^{\infty}\mathrm{d}y s(\sin k - y)\,\mathrm{Re}\sqrt{1-\left(y-i\frac{U}{4}\right)^2} \\
&\quad + \left(s * \ln\frac{1+\eta_1'}{1+\eta_1}\right)(\sin k), \\
\eta_0(\Lambda) &= \eta_0'(\Lambda) = 0 \\
\ln\eta_n(\Lambda) &= \left(s * \ln\left((1+\eta_{n-1})(1+\eta_{n+1})\right)\right)(\Lambda) - \delta_{1n}\left(s * \ln\left(1+\zeta^{-1}\right)\right)(\Lambda), \\
\ln\eta_n'(\Lambda) &= \left(s * \ln\left((1+\eta_{n-1})(1+\eta_{n+1})\right)\right)(\Lambda) - \delta_{1n}\left(s * \ln(1+\zeta)\right)(\Lambda),
\end{aligned}$$

where $n \in \mathbb{N}$ and

$$s(x) = \frac{1}{U\mathrm{ch}\frac{2\pi x}{U}}.$$

We have the boundary conditions

$$\lim_{n\to\infty}\frac{\ln\eta_n(\Lambda)}{n} = \frac{2B}{T}, \qquad \lim_{n\to\infty}\frac{\ln\eta_n'(\Lambda)}{n} = -\frac{2\mu}{T}.$$

The Gibbs free energy in terms of solutions of (69) is

$$\begin{aligned}
f_\mathrm{h} &= \frac{U}{4} - T\int_{-\pi}^{\pi}\frac{\mathrm{d}k}{2\pi}\ln\left(1+\frac{1}{\zeta(k)}\right) - T\sum_{n=1}^{\infty}\int_{-\infty}^{\infty}\frac{\mathrm{d}\Lambda}{\pi}\ln\left(1+\frac{1}{\eta_n'(\Lambda)}\right)\mathrm{Re}\frac{1}{\sqrt{1-\left(\Lambda-in\frac{U}{4}\right)^2}}, \\
f_\mathrm{i} &= \frac{U}{4} - T\int_{-\pi}^{\pi}\mathrm{d}k\hat{\Delta}(k)\ln\left(1+\frac{1}{\zeta(k)}\right) \\
&\quad - \frac{4T}{\pi}\sum_{n=1}^{\infty}\int_{-\infty}^{\infty}\mathrm{d}\Lambda\left(\partial_\Lambda\hat{\delta}\left(\mathrm{Re}\frac{1}{\sqrt{1-\left(\Lambda-ni\frac{U}{4}\right)^2}}\right)\right)\ln\left(1+\frac{1}{\eta_n'(\Lambda)}\right).
\end{aligned}$$

We define

$$\bar{s}(x) := \frac{1}{2\mathrm{ch}(\pi x)}, \qquad R(x) := \int_0^{\infty}\frac{\mathrm{d}\omega}{\pi}\frac{\cos(\omega x)}{1+e^{\omega}}$$

and use our established continuum limit and set $T = \frac{2\sqrt{U}}{\sqrt{\bar{U}}V}\bar{T}$. Then the thermodynamical

Bethe ansatz equations of the Hubbard model simplify

$$\begin{aligned}
\ln\zeta\left(\tilde{k}-\frac{\pi}{2}\right) &\to -2\beta\tilde{k}-2\beta\int_{-\infty}^{\infty}\mathrm{d}y\frac{\mathrm{Re}\sqrt{1-\left(\frac{U}{2}y-1-i\frac{U}{4}\right)^2}}{\mathrm{ch}\left(\pi\left(\frac{\tilde{k}^2}{U}-y\right)\right)}+\frac{1}{2}\left(s*\ln\frac{1+\eta_1'}{1+\eta_1}\right)\left(\frac{\tilde{k}^2}{U}\right)\\
&\to -\frac{1}{\bar{T}}\left(\bar{k}-\epsilon_d-\frac{\bar{U}}{2}\right)-\frac{1}{\bar{T}}\int_{-\infty}^{\infty}\mathrm{d}pR\left(g\left(\bar{k}\right)-g\left(p\right)\right)pg'\left(p\right)\\
&\quad+\left(\bar{s}*\ln\frac{1+\eta_1'}{1+\eta_1}\right)\left(g\left(\bar{k}\right)\right),\\
\eta_0\left(\lambda\right)&=\eta_0'\left(\lambda\right)=0,\\
\ln\eta_n\left(\frac{U}{2}\lambda\right)&\to\left(\bar{s}*\ln\left(\left(1+\eta_{n-1}\right)\left(1+\eta_{n+1}\right)\right)\right)\left(\lambda\right)-\delta_{1n}\left(\bar{s}*\ln\left(1+\zeta^{-1}\right)\right)\left(\lambda\right)\\
\ln\eta_n'\left(\frac{U}{2}\lambda\right)&\to\left(\bar{s}*\ln\left(\left(1+\eta_{n-1}\right)\left(1+\eta_{n+1}\right)\right)\right)\left(\lambda\right)-\delta_{1n}\left(\bar{s}*\ln\left(1+\zeta\right)\right)\left(\lambda\right)
\end{aligned}$$

with $n=1,2,\ldots$.
Identifying $\epsilon\left(\bar{k}\right)=-\bar{T}\ln\zeta\left(\sqrt{U}\bar{k}-\frac{\pi}{2}\right)$, $\kappa_n\left(\lambda\right)=\bar{T}\ln\eta_n\left(\frac{U}{2}\lambda\right)$ and $\kappa_n'\left(\lambda\right)=\bar{T}\ln\eta_n'\left(\frac{U}{2}\lambda\right)$ yields

$$\begin{aligned}
\epsilon\left(\bar{k}\right)&=\bar{k}-\epsilon_d-\frac{\bar{U}}{2}+\int_{-\infty}^{\infty}\mathrm{d}pR\left(g\left(\bar{k}\right)-g\left(p\right)\right)pg'\left(p\right)\\
&\quad+\bar{T}\left(\bar{s}*\ln\frac{1+e^{\bar{\beta}\kappa_1'}}{1+e^{\bar{\beta}\kappa_1}}\right)\left(g\left(\bar{k}\right)\right),\\
\kappa_0\left(\lambda\right)&=\kappa_0'\left(\lambda\right)=-\infty,\\
\kappa_n\left(\lambda\right)&=\bar{T}\left(\bar{s}*\ln\left(\left(1+e^{\bar{\beta}\kappa_{n-1}}\right)\left(1+e^{\bar{\beta}\kappa_{n+1}}\right)\right)\right)\left(\lambda\right)\\
&\quad-\delta_{1n}\bar{T}\left(\bar{s}*\ln\left(1+e^{-\bar{\beta}\epsilon}\right)\right)\left(\lambda\right),\\
\kappa_n'\left(\lambda\right)&=\bar{T}\left(\bar{s}*\ln\left(\left(1+e^{\bar{\beta}\kappa_{n-1}'}\right)\left(1+e^{\bar{\beta}\kappa_{n+1}'}\right)\right)\right)\left(\lambda\right)\\
&\quad-\delta_{1n}\bar{T}\left(\bar{s}*\ln\left(1+e^{\bar{\beta}\epsilon}\right)\right)\left(\lambda\right).
\end{aligned}\tag{139}$$

For the boundary conditions we choose $\frac{B}{\sqrt{U}}\to\frac{H}{\sqrt{\bar{U}}V}$ and $-\frac{\mu}{\sqrt{U}}\to\frac{2\epsilon_d+\bar{U}}{\sqrt{\bar{U}}V}$. Then we find

$$\lim_{n\to\infty}\frac{\kappa_n\left(\lambda\right)}{n}\to H,\qquad\lim_{n\to\infty}\frac{\kappa_n'\left(\lambda\right)}{n}=2\epsilon_d+\bar{U}.$$

These are the well-known [124] thermodynamical Bethe ansatz equations of the Anderson impurity model.
Furthermore we consider the free energy, use the relations

$$\begin{aligned}
\Delta(k) &= \frac{1}{2\pi}\partial_k\delta(k), \\
a_n(\lambda) &= \frac{1}{2\pi}\frac{n}{\lambda^2+\frac{n^2}{4}}, \\
-\sqrt{\bar{U}}V\mathrm{Re}\frac{1}{\sqrt{\lambda+\frac{in}{2}}} &= \int_{-\infty}^{\infty}\mathrm{d}k a_n(\lambda-g(k)), \\
-\frac{1}{\pi}\partial_\lambda\mathrm{Re}\delta\left(\sqrt{\bar{U}}V\sqrt{\lambda+\frac{in}{2}}\right) &= \int_{-\infty}^{\infty}\mathrm{d}k\Delta(k)a_n(\lambda-g(k))
\end{aligned}$$

and apply our continuum limit, which yields

$$\begin{aligned}
f_\mathrm{h} &= -\bar{T}\int_{-\infty}^{\infty}\frac{\mathrm{d}k}{2\pi}\ln\left(1+e^{-\bar{\beta}\epsilon(k)}\right) \\
&\quad -\bar{T}\sum_{n=1}^{\infty}\int_{-\infty}^{\infty}\frac{\mathrm{d}k}{2\pi}\int_{-\infty}^{\infty}\mathrm{d}\lambda a_n(\lambda-g(k))\ln\left(1+e^{-\bar{\beta}\kappa_n'(\lambda)}\right), \qquad (140) \\
f_\mathrm{i} &= -\bar{T}\int_{-\infty}^{\infty}\mathrm{d}k\Delta(k)\ln\left(1+e^{-\bar{\beta}\epsilon(k)}\right) \\
&\quad -\bar{T}\sum_{n=1}^{\infty}\int_{-\infty}^{\infty}\mathrm{d}k\int_{-\infty}^{\infty}\mathrm{d}\lambda\Delta(k)a_n(\lambda-g(k))\ln\left(1+e^{-\bar{\beta}\kappa_n'(\lambda)}\right), \qquad (141) \\
f &= f_\mathrm{h}+\frac{1}{l}f_\mathrm{i} \qquad (142)
\end{aligned}$$

Equations (142), (140) and (141) together with equations (139) completely describe the thermodynamical properties of the Anderson impurity model. Note that it is easily possible to derive another well-known form for the thermodynamical potential (142) [124]. Note furthermore that (140) together with (139) describe the free fermion gas. This can easily be shown by the use of the dilogarithm trick [122, 42, 123, 95, 94, 124].

As we have seen in the last two subsections, it is possible to derive the Anderson impurity model from the Hubbard model with integrable impurity by the use of a continuum limit. In the Hubbard model with integrable impurity, there are originally four free parameters U, B, μ, ν (i. e. a, because $z_\pm(\nu)=e^{\mp i\left(-\frac{\pi}{2}\pm a-ib\right)}$ holds and b is fixed via $ab=\frac{U}{4}$) and two sets of Bethe numbers $\{k_j\}_{j=1}^K$ and $\{\lambda_\alpha\}_{\alpha=1}^M$. Furthermore T is the temperature and $L+1$ the chain length. These pass into the parameters of the Anderson impurity model in non-trivial ways:

Table 1: Parameters before and after the continuum limit

Hubbard model with impurity	Continuum limit		Anderson impurity model
U	U	0	
L	$\sqrt{U}L$	$\sqrt{\bar{U}}Vl$	l
B	$\frac{B}{\sqrt{U}}$	$\frac{H}{\sqrt{\bar{U}}V}$	H
μ	$-\frac{\mu}{\sqrt{U}}$	$\frac{2\epsilon_d+\bar{U}}{\sqrt{\bar{U}}V}$	$2\epsilon_d+\bar{U}$
a	$\frac{a}{\sqrt{U}}$	$\frac{\sqrt{\bar{U}}}{2V}$	V
T	$\frac{T}{\sqrt{U}}$	$\frac{2\bar{T}}{\sqrt{\bar{U}}V}$	$\bar{T}$
k	$\frac{2(1+\sin k)}{U}$	$g\left(\bar{k}\right)$	$\bar{k}$
Λ	$\frac{2}{U}\left(\Lambda+1\right)$	λ	λ

5.3 Non-linear integral equations of the Anderson impurity model

In the previous subsection we showed that the thermodynamical Bethe ansatz equations of the Anderson impurity model follow from the Hubbard model with integrable impurity. Thus the thermodynamics of the model can be completely described. However, this is a system of infinitely many, coupled, non-linear integral equations, which makes the numerical analysis difficult. For this reason we want to derive a new set of finitely many non-linear integral equations of the Anderson impurity model in this section. In the previous chapters, we showed that the column-to-column transfer matrix is necessary, but does not exist in the continuum. Therefore, we are using our continuum limit to derive the non-linear integral equations of the Anderson impurity model from those of the Hubbard model with impurity

$$
\begin{aligned}
\ln\mathfrak{b}^{+}(s) &= -2\beta B-\left(K_2*\ln\mathfrak{B}^{+}\right)(s)+\left(K_{2,\frac{U}{2}}*\ln\mathfrak{B}^{-}\right)(s)-\left(K_1*\ln\frac{\bar{\mathfrak{c}}^{+}\bar{\mathfrak{C}}^{-}}{\bar{\mathfrak{c}}^{-}\bar{\mathfrak{C}}^{+}}\right)(s),\\
\ln\mathfrak{b}^{-}(s) &= -2\beta B-\left(K_{2,-\frac{U}{2}}*\ln\mathfrak{B}^{+}\right)(s)+\left(K_2*\ln\mathfrak{B}^{-}\right)(s)-\left(K_{1,-\frac{U}{2}}*\ln\frac{\bar{\mathfrak{c}}^{+}\bar{\mathfrak{C}}^{-}}{\bar{\mathfrak{c}}^{-}\bar{\mathfrak{C}}^{+}}\right)(s),\\
\ln\mathfrak{c}^{\pm}(s) &= -\frac{\beta U}{2}+\beta\left(\mu+B\right)\pm 2\beta\sqrt{1-s^2}+\left(K_{1,-\frac{U}{2}}*\ln\bar{\mathfrak{B}}^{+}\right)(s)-\left(K_1*\ln\bar{\mathfrak{B}}^{-}\right)(s)\\
&\quad+\left(K_{1,-\frac{U}{4}}*\ln\frac{\bar{\mathfrak{C}}^{+}}{\bar{\mathfrak{C}}^{-}}\right)(s)\pm\frac{1}{2}\ln\frac{\bar{\mathfrak{C}}^{+}}{\bar{\mathfrak{C}}^{-}}(s),\\
\ln\bar{\mathfrak{c}}^{\pm}(s) &= -\frac{\beta U}{2}-\beta\left(\mu+B\right)\mp 2\beta\sqrt{1-s^2}-\left(K_1*\ln\mathfrak{B}^{+}\right)(s)+\left(K_{1,\frac{U}{2}}*\ln\mathfrak{B}^{-}\right)(s)\\
&\quad-\left(K_{1,\frac{U}{4}}*\ln\frac{\mathfrak{C}^{+}}{\mathfrak{C}^{-}}\right)(s)\pm\frac{1}{2}\ln\frac{\mathfrak{C}^{+}}{\mathfrak{C}^{-}}(s).
\end{aligned}
$$

In the following we assume that $B\ll 1$ and $\mu<0$. Considering our continuum limit $U\to 0$ and $T=\mathcal{O}\left(\sqrt{U}\right)$ and the driving terms of $\mathfrak{c}^{-}(s)$ and $\bar{\mathfrak{c}}^{-}(s)$ yields that $\mathfrak{c}^{-}(s)\to 0$ and $\bar{\mathfrak{c}}^{-}(s)\to\infty$. Using this and dropping the $+$ in the notation of $\mathfrak{c}^{+}(s)$ and $\bar{\mathfrak{c}}^{+}(s)$ we

can simplify the non-linear integral equations

$$\begin{aligned}
\ln \mathfrak{b}^{+}(s) &= -2\beta B - \left(K_2 * \ln \mathfrak{B}^{+}\right)(s) + \left(K_{2,\frac{U}{2}} * \ln \mathfrak{B}^{-}\right)(s) - \left(K_1 * \ln \frac{\bar{\mathfrak{c}}}{\bar{\mathfrak{C}}}\right)(s), \\
\ln \mathfrak{b}^{-}(s) &= -2\beta B - \left(K_{2,-\frac{U}{2}} * \ln \mathfrak{B}^{+}\right)(s) + \left(K_2 * \ln \mathfrak{B}^{-}\right)(s) - \left(K_{1,-\frac{U}{2}} * \ln \frac{\bar{\mathfrak{c}}}{\bar{\mathfrak{C}}}\right)(s), \\
\ln \mathfrak{c}(s) &= \frac{3\beta U}{4} + \frac{5\beta}{2}(\mu + B) + \beta\sqrt{1-s^2} - \frac{\beta}{2}\sqrt{4 + (U+2is)^2} + \left(K_{2,-\frac{U}{4}} * \ln \mathfrak{B}^{+}\right)(s) \\
&\quad - \left(K_{1,\frac{U}{2}} * \ln \mathfrak{B}^{-}\right)(s) + \left(K_{1,-\frac{U}{2}} * \ln \bar{\mathfrak{B}}^{+}\right)(s) - \left(K_1 * \ln \bar{\mathfrak{B}}^{-}\right)(s) + \left(K_2 * \ln \mathfrak{C}\right)(s) \\
&\quad + \left(K_{1,-\frac{U}{4}} * \ln \bar{\mathfrak{C}}\right)(s) + \frac{1}{4}\ln \mathfrak{C}(s) + \frac{1}{2}\ln \bar{\mathfrak{C}}(s), \\
\ln \bar{\mathfrak{c}}(s) &= -\frac{\beta U}{2} - \beta(\mu + B) - 2\beta\sqrt{1-s^2} - \left(K_1 * \ln \mathfrak{B}^{+}\right)(s) + \left(K_{1,\frac{U}{2}} * \ln \mathfrak{B}^{-}\right)(s) \\
&\quad - \left(K_{1,\frac{U}{4}} * \ln \mathfrak{C}\right)(s) + \frac{1}{2}\ln \mathfrak{C}(s).
\end{aligned}$$

Note that the following relations have been used for the simplification of $\ln \mathfrak{c}(s)$

$$\begin{aligned}
\frac{1}{2}K_1(s) + \left(K_{1,-\frac{U}{4}} * K_1\right)(s) &= \begin{cases} K_{2,-\frac{U}{4}}, & \text{for } U \geq 0, \\ -K_{1,-\frac{U}{2}}, & \text{otherwise,} \end{cases} \\
\frac{1}{2}K_{1,\frac{U}{2}}(s) + \left(K_{1,-\frac{U}{4}} * K_{1,\frac{U}{2}}\right)(s) &= \begin{cases} K_{1,\frac{U}{2}}, & \text{for } U \geq 0, \\ 0, & \text{otherwise,} \end{cases}, \\
\frac{1}{2}K_{1,\frac{U}{4}}(s) + \frac{1}{2}K_{1,-\frac{U}{4}}(s) + \left(K_{1,-\frac{U}{4}} * K_{1,\frac{U}{4}}\right)(s) &= -\frac{1}{4}\delta(s) + \begin{cases} K_2, & \text{for } U \geq 0, \\ 0, & \text{otherwise} \end{cases}
\end{aligned}$$

and

$$\begin{aligned}
&\int_{-\infty}^{\infty} \mathrm{d}y K_{1,-\frac{U}{4}}(s-y)\left(-\frac{\beta U}{2} - \beta(\mu + B) + 2\beta\sqrt{1-y^2}\Theta(1+y)\Theta(1-y)\right) \\
&= \begin{cases} -\frac{\beta U}{2} - \beta(\mu + B) + \frac{\beta}{2}\left(\sqrt{4 + (U+2is)^2} - U\right), & \text{for } U > 0, \\ 2is, & \text{for } U = 0, \\ \frac{\beta U}{2} + \beta(\mu + B) + \frac{\beta}{2}\left(\sqrt{4 + (U+2is)^2} - U + 4is\right), & \text{for } U < 0. \end{cases}
\end{aligned}$$

Furthermore we used $U > 0$, because the non-linear integral equations are here formulated for this case.
Now we are considering the convolutions using (94)

$$
\begin{aligned}
\left(K_{n,\alpha} * \ln A\right)(s) &= \int_{-\infty}^{\infty} \mathrm{d}y K_{n,\alpha}(s-y) \ln A(y) \\
&= \frac{n}{4\pi} \int_{-\infty}^{\infty} \frac{\mathrm{d}y}{U} \frac{\ln A(y)}{\left(\frac{s+i\alpha-y}{U}\right)^2 + \left(\frac{n}{4}\right)^2} \\
&= \frac{n}{4\pi} \int_{-\infty}^{\infty} \mathrm{d}y \frac{\ln A(Uy)}{\left(\frac{s+i\alpha}{U} - y\right)^2 + \left(\frac{n}{4}\right)^2} \\
\Rightarrow \left(K_{n,U\alpha} * \ln A\right)(Us) &= \frac{n}{4\pi} \int_{-\infty}^{\infty} \mathrm{d}y \frac{\ln A(Uy)}{(s+i\alpha-y)^2 + \left(\frac{n}{4}\right)^2}.
\end{aligned}
$$

and a similar calculation for functions $\ln \bar{A}$ that vanish outside of $s \in [-1,1]$ (i. e. $\mathfrak{c}(s)$ and $\bar{\mathfrak{c}}(s)$) we find

$$
\left(K_{n,U\alpha} * \ln \bar{A}\right)(s) \to \left(\mathcal{K}_{2n,2\alpha} * \ln \bar{A}\right)\left(\frac{\tilde{k}}{\sqrt{U}}\right).
$$

Note that we used

$$
\mathcal{K}_{n,\alpha}(s) = K_{n,\alpha}(s)|_{U=1} \tag{143}
$$

and $s = \sin k = -1 + \frac{\tilde{k}^2}{2}$ on the right-hand side.
Using this interim results as well as table (1) and defining

$$
\begin{aligned}
\ln b^{\pm}(\lambda) &= \ln \mathfrak{b}^{\pm}\left(-1 + \frac{U\lambda}{2}\right), \\
\ln c^{\pm}(k) &= \ln \mathfrak{c}^{\pm}\left(-1 + \frac{Uk^2}{2}\right), \\
\ln \bar{c}^{\pm}(k) &= \ln \bar{\mathfrak{c}}^{\pm}\left(-1 + \frac{Uk^2}{2}\right)
\end{aligned}
$$

we get for the non-linear integral equations of the Anderson impurity model

$$
\begin{aligned}
\ln b^{+}(\lambda) &= -H\bar{\beta} - \left(\mathcal{K}_4 * \ln B^{+}\right)(\lambda) + \left(\mathcal{K}_{4,1} * \ln B^{-}\right)(\lambda) - \left(\mathcal{K}_2 * \ln \frac{\bar{c}}{\bar{C}}\right)(\lambda), \\
\ln b^{-}(\lambda) &= -H\bar{\beta} - \left(\mathcal{K}_{4,-1} * \ln B^{+}\right)(\lambda) + \left(\mathcal{K}_4 * \ln B^{-}\right)(\lambda) \\
&\quad - \left(\mathcal{K}_{2,-1} * \ln \frac{\bar{c}}{\bar{C}}\right)(\lambda), \\
\ln c(k) &= \frac{5\bar{\beta}}{4}\left(H - 2\epsilon_d - \bar{U}\right) + \left(\mathcal{K}_{4,-\frac{1}{2}} * \ln B^{+}\right)(g(k)) - \left(\mathcal{K}_{2,1} * \ln B^{-}\right)(g(k)) \\
&\quad + \left(\mathcal{K}_{2,-1} * \ln \bar{B}^{+}\right)(g(k)) - \left(\mathcal{K}_2 * \ln \bar{B}^{-}\right)(g(k)) + \left(\mathcal{K}_4 * \ln C\right)(k) \\
&\quad + \left(\mathcal{K}_{2,-\frac{1}{2}} * \ln \bar{C}\right)(k) + \frac{1}{4}\ln C(k) + \frac{1}{2}\ln \bar{C}(k), \\
\ln \bar{c}(k) &= -\frac{\bar{\beta}}{2}(H - 2k) - \left(\mathcal{K}_2 * \ln B^{+}\right)(g(k)) + \left(\mathcal{K}_{2,1} * \ln B^{-}\right)(k) \\
&\quad - \left(\mathcal{K}_{2,\frac{1}{2}} * \ln C\right)(k) + \frac{1}{2}\ln C(k)
\end{aligned}
\tag{144}
$$

There are just six auxiliary functions for the Hubbard model with integrable impurity (99) and just four for the Anderson impurity model (144) in comparison to the infinitely many equations of thermodynamical Bethe ansatz type (139). Note that the functions $b^{\pm}(\lambda)$ can be reduced to just one function similar to (96), but then the integrals are not ordinary convolutions, rather they are contour convolutions.
Considering the free energy per site (111) and using our continuum limit yields the free energy of the Anderson impurity model

$$
f = f_h + \frac{1}{l} f_i, \tag{145}
$$

$$
-\bar{\beta} f_{\mathrm{h}} = -\int_{-\infty}^{\infty} \frac{\mathrm{d}k}{2\pi i g'(k)} \left(\ln C(k) + \ln \frac{1 + c + \bar{c}}{\bar{c}}(k)\right), \tag{146}
$$

$$
\begin{aligned}
-\bar{\beta} f_{\mathrm{i}} &= \frac{\bar{\beta}\bar{U}}{4} + \frac{1}{\pi i}\left(k * \ln B^{+}\right)(0) - \frac{1}{\pi i}\left(k * \ln B^{-}\right)(0) - \frac{1}{2\pi i}\left(k * \ln \frac{\bar{C}}{\bar{c}}\right)(0) \\
&\quad - \frac{2}{\pi i}\int_{-\infty}^{\infty} \frac{\mathrm{d}k}{g(k)} \left(\ln C(k) + \ln \frac{1 + c + \bar{c}}{\bar{c}}(k)\right) \\
&\quad - \int_{-\infty}^{\infty} \frac{\mathrm{d}k}{2\pi i} \ln g(k) \left[\ln \frac{(1 + c + \bar{c}) B^{+}}{1 + \bar{c} B^{+}}(k)\right]'.
\end{aligned}
\tag{147}
$$

Equations (144), (145), (146) and (147) completely describe thermodynamical properties of the Anderson impurity model.
We note that we could have introduced a shift in the chemical potential in table (1), which allows us to shift the chemical potential freely in the Anderson impurity model.

5.4 Continuum limit of the creation and annihilation operators $c_k^\dagger$ and c_k

We consider plane waves

$$|k\rangle := \sum_{j=1}^{L} e^{ikr_j} |r_j\rangle , \qquad r_j := \bar{a}j, \tag{148}$$

for a lattice with L sites with lattice constant $\bar{a}$. The creation and annihilation operators are $c_k^\dagger$ and c_k. There are only discrete k mod $\frac{2\pi}{\bar{a}} \in \frac{2\pi}{\bar{a}L} \cdot \mathbb{Z}$. The vacuum $|0\rangle$ is a state without particles: $c_k |0\rangle = 0$. For $k \neq q$ the $c_k^\dagger$ and c_k must satisfy $\left\{c_k^\dagger, c_q\right\} = 0$. Furthermore we find

$$\begin{aligned}\left\langle 0 \left| \left\{c_k^\dagger, c_k\right\} \right| 0 \right\rangle &= \left\langle 0 \left| c_k c_k^\dagger \right| 0 \right\rangle \\ &= \langle k \mid k \rangle \\ &= L.\end{aligned}$$

This leads to

$$\left\{c_k^\dagger, c_q\right\} = L\delta_{kq}. \tag{149}$$

We can consider these creation and annihilation operators as approximations to the continuum. Setting $l = \bar{a}L$ and

$$\tilde{c}_k^\dagger = \sqrt{\frac{\bar{a}}{l}} c_k^\dagger \tag{150}$$

yields on the interval $[0, l]$

$$\left\{\tilde{c}_k^\dagger, \tilde{c}_q\right\} = \delta_{kq} \tag{151}$$

with discrete $k \in \frac{2\pi}{l} \cdot \mathbb{Z}$.
We want to use $\mathbb{R}$ as interval and we want the following relation for the creation and annihilation operators $\bar{c}_k^\dagger$ and $\bar{c}_k$

$$\left\{\bar{c}_k^\dagger, \bar{c}_q\right\} = \delta\left(k - q\right). \tag{152}$$

Therefore we use

$$\bar{c}_k^\dagger = \lim_{l\to\infty} \sqrt{\frac{l}{2\pi}} \tilde{c}_k^\dagger \tag{153}$$

for the construction, since

$$
\begin{aligned}
1 &= \sum_k \left\{ \tilde{c}_k^\dagger, \tilde{c}_q \right\} \\
&= \frac{1}{\Delta k} \sum_k \Delta k \left\{ \tilde{c}_k^\dagger, \tilde{c}_q \right\} \\
&\to \int_{-\infty}^{\infty} \mathrm{d}k \left\{ \bar{c}_k^\dagger, \bar{c}_q \right\}.
\end{aligned}
$$

Note that in (153) k is continuous and that $\bar{c}_k^\dagger$ and $\bar{c}_k$ are of order $\mathcal{O}\left(\sqrt{\bar{a}}\right)$.
Thus, the Hamiltonian H (in the continuum and with the thermodynamic limit) can be written in second quantization such that integrals over k occur for creation and annihilation operators $\bar{c}_k^\dagger$ and $\bar{c}_k$. The energy scale must be introduced so that $\bar{a}$ disappears.

5.5 Hamiltonian

We note here that we have also shown that the Hamiltonian of the Anderson impurity model (133) follows from the Hubbard model with integrable impurity. The necessary calculations were carried out with Maple. The procedure is analogous to the one described in chapter 6.1. The hybridization is given by

$$
\begin{aligned}
\langle \{k_{\text{out}}, \sigma\} | H | \{d, \sigma\} \rangle &= \langle \{d, \sigma\} | H | \{k_{\text{in}}, \sigma\} \rangle \\
&= V U^{\frac{1}{4}} + \mathcal{O}\left(U^{\frac{3}{4}}\right), \qquad \sigma = \uparrow, \downarrow .
\end{aligned}
$$

There are also on-site matrix elements at the impurity

$$
\begin{aligned}
\langle \{d, 0\} | H | \{d, 0\} \rangle &= 0, \\
\langle \{d, \uparrow\} | H | \{d, \uparrow\} \rangle &= \bar{U}\sqrt{U} + \mathcal{O}(U), \\
\langle \{d, \downarrow\} | H | \{d, \downarrow\} \rangle &= \bar{U}\sqrt{U} + \mathcal{O}(U), \\
\langle \{d, \uparrow\downarrow\} | H | \{d, \uparrow\downarrow\} \rangle &= 0.
\end{aligned}
$$

It should be noted that this is a surprising result. The limit $U \to 0$ is the free fermion limit. This causes the host to have no interaction. The combined limits, however, lead to the fact that the interaction with the impurity does not disappear. This creates the Anderson impurity model, non-interacting host, which interacts with the impurity [138, 42, 94, 123, 122, 95, 124]. The Hubbard model with integrable impurity plus continuum limit is thus absolutely necessary, since otherwise a different impurity model is

generated:

- An impurity interacting with an interacting host.
- An impurity not interacting with a non-interacting host.

The models in chapter 2, 3 and 4 are such special impurity models. Note furthermore that all many-particle terms that appear in the Hamiltonian of the Hubbard model with integrable impurity in chapter 3 disappear in the continuum limit.

5.6 Ground state

We derive analytic expressions for the thermodynamics. For $T \ll 1$ we simplify the non-linear integral equations (144). We set $H \ll 1$ and $\bar{U}, \epsilon_d > 0$, such that $\mathfrak{b}^- (\lambda) \to 0$ and $c(k) \to 0$. $b^+(\lambda)$ and $\bar{c}(k)$ do not disappear. Then we find from equations (144)

$$\begin{aligned} \ln b^+(\lambda) &= -H\bar{\beta} - \left(\mathcal{K}_4 * \ln B^+\right)(\lambda) - \left(\mathcal{K}_2 * \ln \frac{\bar{c}}{\bar{C}}\right)(\lambda), \\ \ln \bar{c}(k) &= -\frac{\bar{\beta}}{2}(H - 2k) - \left(\mathcal{K}_{2,0} * \ln B^+\right)(g(k)). \end{aligned} \tag{154}$$

These formulas are justified at low temperature T. There the corrections are exponentially small $\mathcal{O}\left(e^{-\text{cst.}\bar{\beta}}\right)$. The constant is real and positive.
These equations correspond to the result of Tsvelick and Wiegmann [124] from 1983. In their work they have derived the set of infinitely many equations of thermodynamical Bethe ansatz type, which we have also derived in this work through the continuum limit (139). In their work, Tsvelick and Wiegmann have then performed the limit $T \to 0$, which turns the infinite number of equations into finitely many. In their case they had only two equations left, which correspond to the equations (154).

6 Limit from the modified Hubbard model with integrable impurity to the pseudogap Anderson impurity model

We consider in this chapter the Hubbard model with integrable impurity and shifts on the horizontal lines, which follow the distribution density $\rho_\alpha(y)$, as explained in chapter 4. We combine this model with the continuum limit from chapter 5 and obtain a pseudogap Anderson impurity model. This new model is in principle Anderson-like, which means the host is non-interacting but the impurity interacts with the host. Furthermore we have a new dispersion relation $e(k) = k|k|^\alpha$ $(-1 < \alpha < 0)$, which follows from (124) and table (1).

6.1 Hamiltonian

For calculating the Hamiltonian of the pseudogap Anderson impurity model we have to pay attention to two aspects.
First, we have to consider the modified Hubbard model with integrable impurity. Since we know the effect of the shifts on the horizontal lines on the host (these change the dispersion relation), the old dispersion relation can readily be exchanged with the new one. Nothing else changes in the host.
The more complicated question is how the shifts on the horizontal lines affect the interaction with the impurity. The relevant transition rates occur in the Hamiltonian and must be calculated.
The exact evaluation is based on the fact that the local objects

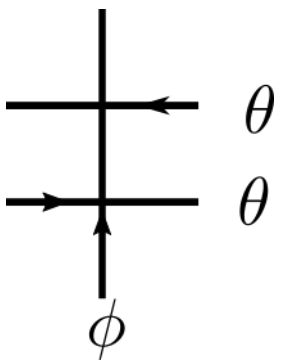

Figure 22: Product of L-matrices with spectral parameters θ and ϕ, which are used for calculations.

leave right hand-sided singlets

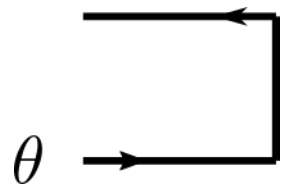

Figure 23: "Ket" singlets.

and "bra" states (which are orthogonal to the right hand-sided singlet) invariant,

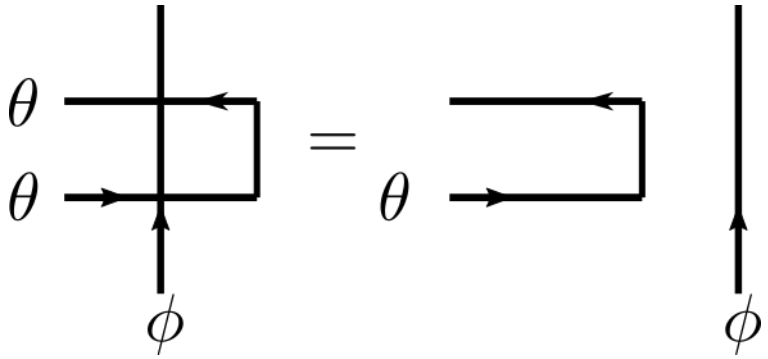

Figure 24: Invariance.

but other states (orthogonal to the right hand-sided singlet) have very small eigenvalues. That reads

$$\begin{aligned} t(\theta)\,\bar{t}(\theta) &= \mathrm{id} + \mathcal{O}\left(e^{-\mathrm{cst.}L}\right), \\ t(\theta)\,\bar{t}(\theta+\epsilon) &= e^{-\epsilon H} + \mathcal{O}\left(e^{-\mathrm{cst.}L}\right). \end{aligned} \tag{155}$$

For L lattice sites of the host we consider the row-to-row transfer matrix with open boundary conditions left and right. An incoming or outgoing plane wave with spectral parameter k and $\sigma = \uparrow, \downarrow$ can be written down graphically.

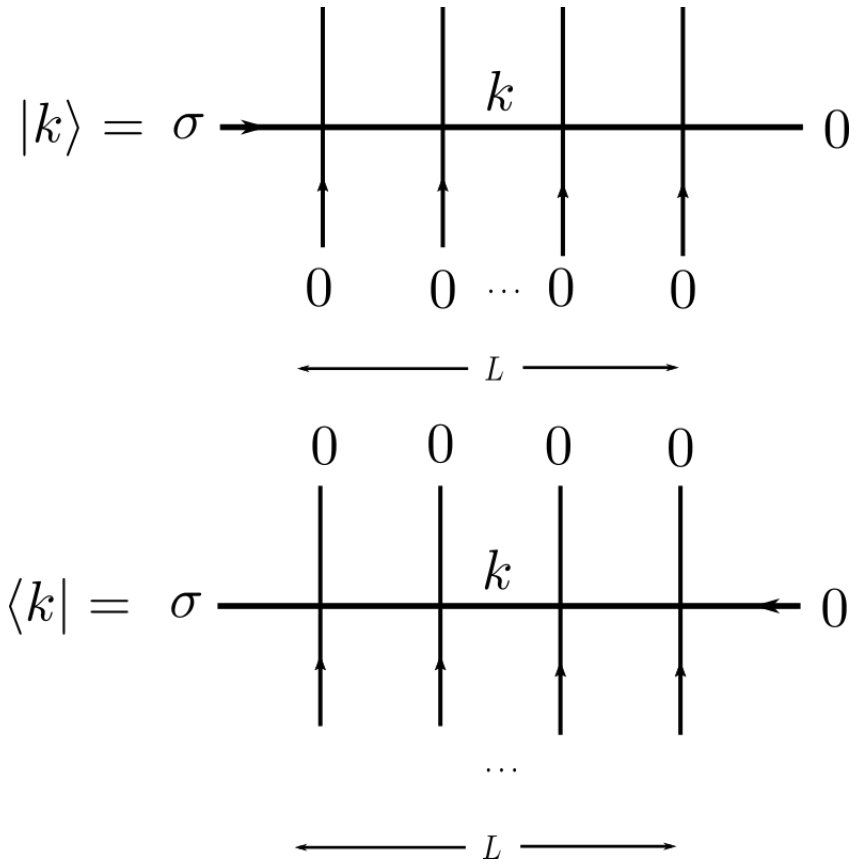

Figure 25: Incoming and outgoing plane wave with $\sigma = \uparrow, \downarrow$. The spectral parameters can be converted into momenta as required. σ on the horizontal line means that there is fermion with spin σ, 0 means there is none. Note furthermore that zeroes on vertical lines belong to the vacuum state $|0\rangle$. This means that zeroes on horizontal and vertical lines do not have the same meaning.

Due to equation (155), we consider two horizontal lines, i.e. the product of two row-to-row transfer matrices. Now we consider the interaction with a plane wave which is generated. Putting everything together we get

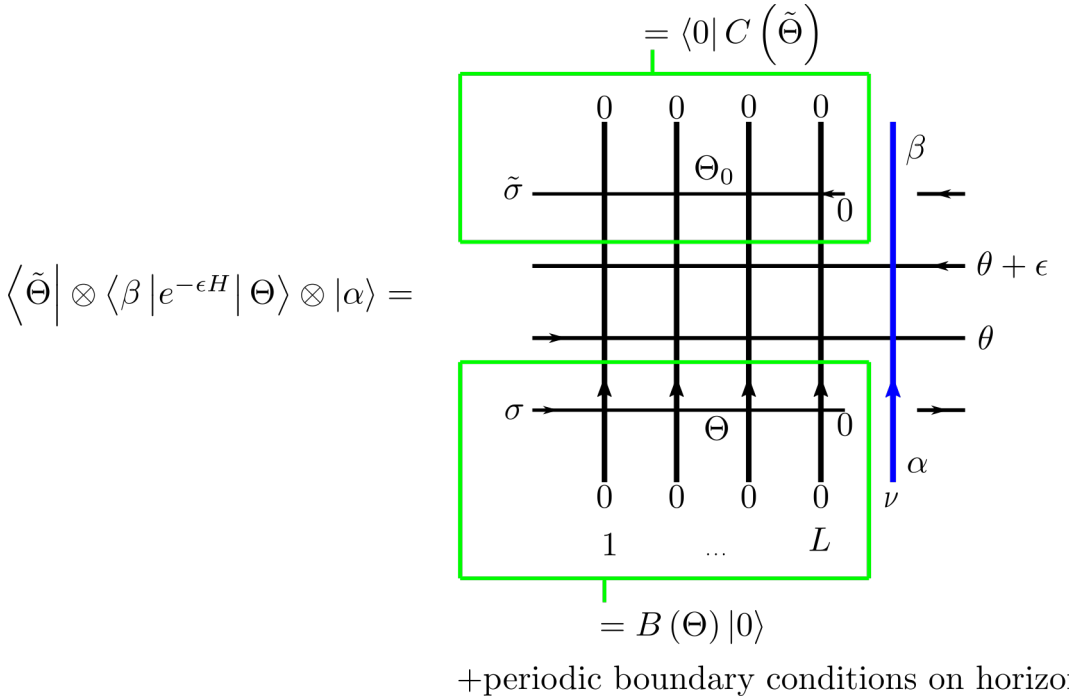

Figure 26: The "effective" partition function on a $(L+1) \times 4$ lattice. Here we can also add a twist angle. We can see two kinds of column-to-column transfer matrices, T the host and T_{i} the impurity. Note that zeroes on the vertical lines belong to the Fock vacuum $|0\rangle$. Operators $B(\Theta)$ and $C(\Theta)$ are defined like drawn. Positions of σ, $\tilde{\sigma}$ and zeroes on the horizontal lines show that there are 4 operators of each kind. Note furthermore that there are periodic boundary conditions on the horizontal lines and open boundary conditions on vertical lines. We also point out that it is enough to just consider two horizontal lines, that yield the Hamiltonoperator, because row-row transfer matrices commute.

The matrix element has a natural interpretation as the partition function on a $(L+1) \times 4$ lattice. The derivative with respect to ϵ at $\epsilon = 0$ yields the desired matrix element of H. As $L \to \infty$ we intend to apply a transfer matrix approach. For this, we define the transfer matrices.

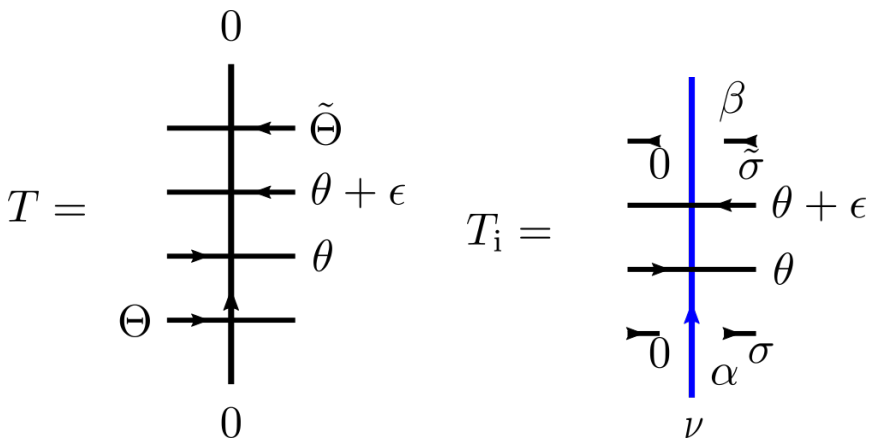

Figure 27: Transfer matrices of the bulk and the impurity. The dimension of the spaces associated with horizontal lines in T with spectral parameters Θ and $\tilde{\Theta}$ is two, which means that there are four creation operators for plane waves, which was explained in the previous figure. The dimension of the spaces associated to the lines with θ and $\theta+\epsilon$ are four. This means that T and T_i are of size $2^2 4^2 \times 2^2 4^2$.

Now we have to calculate

$$\mathrm{tr}\left(T^L T_\mathrm{i}\right) = \sum_{n=1}^{4} \Lambda_n^L \left\langle n \left| T_\mathrm{i} \right| n \right\rangle ,$$

where only four states $|n\rangle$ are relevant in the limit $L \to \infty$ and depend on ϵ. The matrix space has the dimension $2 \cdot 4 \cdot 4 \cdot 2$, but just four eigenvalues have the same absolute value and have larger absolute values than the remaining ones. These statements were shown numerically. Unfortunately, all expressions are quite complicated for $\epsilon \neq 0$. Only for $\epsilon = 0$ everything is simple.
We define graphically the following operators:

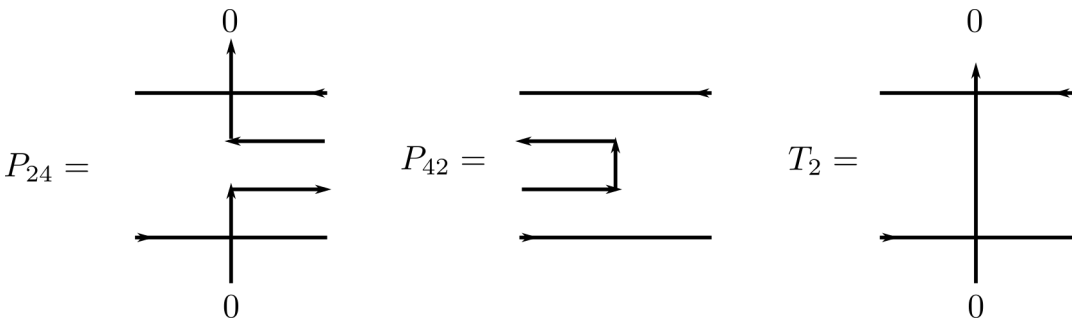

Figure 28: Useful operators.

Obviously the following relations hold

$$TP_{42} = P_{42}T_2,$$
$$P_{24}T = T_2P_{24}.$$

Note that unitarity and the Yang-Baxter equation were used here.
Eigenvalues of T_2 are also eigenvalues of T. The numerics shows that other eigenvalues of T are irrelevant to us. The eigenvalues of T_2 are 1, $e^{ik_{\text{in}}}$, $e^{-ik_{\text{out}}}$ and $e^{i(k_{\text{in}}-k_{\text{out}})}$. In the following we use eigenstates for which k_{in} and k_{out} are multiples of $\frac{2\pi}{L}$. This provides a basis. The projector to the four-dimensional subspace is

$$P_0 = P_{42}T_2^{-1}P_{24}, \tag{156}$$

because $P_{24}P_{42} = T_2$ holds. From this we obtain

$$\begin{aligned} P_0^2 &= P_{42}T_2^{-1}P_{24}P_{42}T_2^{-1}P_{24} \\ &= P_{42}T_2^{-1}P_{24} \\ &= P_0. \end{aligned}$$

The problem to be solved is

$$\frac{\mathrm{d}}{\mathrm{d}\epsilon}\sum_{n=1}^{4}\langle n\left|T_{\text{i}}\right|n\rangle = \frac{\mathrm{d}}{\mathrm{d}\epsilon}\mathrm{tr}\left(PT_{\text{i}}\right),$$

because all other terms in $\frac{\mathrm{d}}{\mathrm{d}\epsilon}\mathrm{tr}\left(T^LT_{\text{i}}\right)$ are proportional to L. Such an expression has to vanish for $k_{\text{in}} \neq k_{\text{out}}$. We do not calculate the individual $|n\rangle$, but the whole P. By definition we have

$$P = \sum_{n=1}^{4}|n\rangle\langle n|,$$

and it fulfills the following relations:

- P has to be the projector onto the four-dimensional space of the leading eigenvalues of T, i.e.

$$\begin{aligned} P^2 &= P, \\ [P,T] &= 0, \\ P|_{\epsilon=0} &= P_0. \end{aligned}$$

We use the ansatz $P = P_0 + \epsilon P_1$, where P_0 is known (156). P_1 has to be determined.

Furthermore we use $T = T_0 + \epsilon T_1$.
From the previous equations we find in first order of ϵ

$$\begin{aligned} P^2 &= P \\ \Rightarrow P_1 &= P_0 P_1 + P_1 P_0 \end{aligned} \tag{157}$$

and

$$\begin{aligned} [P, T] &= 0 \\ \Rightarrow [P_1, T_0] + [P_0, T_1] &= 0. \end{aligned} \tag{158}$$

These are linear equations that uniquely determine P_1.
In $\frac{\mathrm{d}}{\mathrm{d}\epsilon}\mathrm{tr}\left(T^L T_\mathrm{i}\right)$ occurs $\mathrm{tr}\left(P_1 T_\mathrm{i}\right)$. This expression can be rephrased, which makes the calculation easier. Consider all eigenstates $|n\rangle$ for $\epsilon = 0$

$$\begin{aligned} T_0 \left|n\right\rangle &= \Lambda_n \left|n\right\rangle, \\ P_0 \left|n\right\rangle &= \delta_n \left|n\right\rangle, \qquad \delta_n = 0, 1. \end{aligned}$$

Using (157) and (158) this yields

$$\begin{aligned} \Rightarrow 0 &= \left\langle n\right| \left[P_1, T_0\right] \left|m\right\rangle + \left\langle n\right| \left[P_0, T_1\right] \left|m\right\rangle \\ &= \left(\Lambda_m - \Lambda_n\right) \left\langle n\right| P_1 \left|m\right\rangle + \left(\delta_n - \delta_m\right) \left\langle n\right| T_1 \left|m\right\rangle \\ \Rightarrow 0 &= \left\langle n\right| P_0 P_1 + P_1 P_0 - P_1 \left|m\right\rangle \\ &= \left(\delta_n + \delta_m - 1\right) \left\langle n\right| P_1 \left|m\right\rangle. \end{aligned}$$

For $(\delta_n, \delta_m) = (1, 0)$ or $(0, 1)$ we have $\Lambda_m - \Lambda_n \neq 0$. Therefore we find

$$\begin{aligned} \left\langle n\right| P_1 \left|m\right\rangle &= \frac{\delta_m - \delta_n}{\Lambda_m - \Lambda_n} \left\langle n\right| T_1 \left|m\right\rangle \\ \Rightarrow \mathrm{tr}\left(P_1 T_\mathrm{i}\right) &= \sum_{n,m} \left\langle n\right| P_1 \left|m\right\rangle \left\langle m\right| T_\mathrm{i} \left|n\right\rangle \\ &= \sum_{n,m} \frac{\delta_m - \delta_n}{\Lambda_m - \Lambda_n} \left\langle n\right| T_1 \left|m\right\rangle \left\langle m\right| T_\mathrm{i} \left|n\right\rangle. \end{aligned}$$

Using this we find the useful formulas

$$P_0\tilde{P}_1 + \tilde{P}_1 P_0 = \tilde{P}_1, \tag{159}$$

$$\left[\tilde{P}_1, T_0\right] + [P_0, T_\mathrm{i}] = 0. \tag{160}$$

These formulas were used in the computer algebra program based on Maple. If we compare the last two equations with (157) and (158), we find that $[P_0, T_\mathrm{i}]$ can be calculated more easily than $[P_0, T_1]$, but only for $\theta = 0$. In addition, the calculation of $T_\mathrm{i}P_0$ for $\theta \neq 0$ is easier since

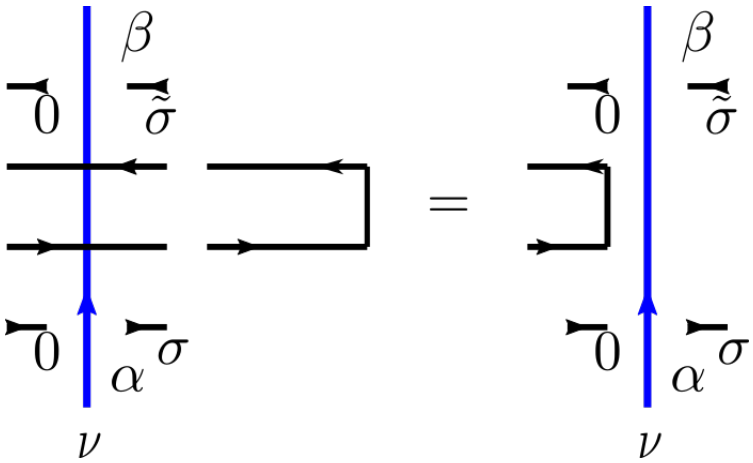

Figure 29: Trivial calculation for $T_\mathrm{i}P_0$. This simple equation is the reason why (160) is used and not (158).

The procedure described has been programmed, the code is given in appendix 8.5.
The calculations were carried out in Maple with spectral parameters. The hybridization is found to be

$$\begin{aligned}
\langle\{k_\mathrm{out}, \sigma\}|H|\{d, \sigma\}\rangle &= (2 + i\cos k_\mathrm{out})\, V e^{3\theta} U^{\frac{1}{4}} + \mathcal{O}\left(U^{\frac{3}{4}}\right), \qquad \sigma = \uparrow, \downarrow, \\
\langle\{d, \sigma\}|H|\{k_\mathrm{in}, \sigma\}\rangle &= (2 - i\cos k_\mathrm{in})\, V e^{3\theta} U^{\frac{1}{4}} + \mathcal{O}\left(U^{\frac{3}{4}}\right), \qquad \sigma = \uparrow, \downarrow .
\end{aligned}$$

There are also on-site matrix elements at the impurity

$$\begin{aligned}
\langle\{d, 0\}|H|\{d, 0\}\rangle &= 0, \\
\langle\{d, \sigma\}|H|\{d, \sigma\}\rangle &= \bar{U} e^{3\theta}\sqrt{U} + \mathcal{O}(U), \qquad \sigma = \uparrow, \downarrow, \\
\langle\{d, \uparrow\downarrow\}|H|\{d, \uparrow\downarrow\}\rangle &= 0, .
\end{aligned}$$

Note that $\sqrt{U}$ is the lattice constant and that the annihilation and creation operators are of order $\mathcal{O}\left(\sqrt{U}\right)$. In the continuum, therefore, all matrix elements are of order

$\mathcal{O}\left(\sqrt{U}\right)$. The energy scale is in (135) introduced so that $\sqrt{U}$ disappears. Remember that we introduced a distribution density $\rho_\alpha(y)$ in Chapter 4 (119). This must also be re-parameterized in the spectral parameter via $y = ie^{2x+2h(x)}$ and (78). Then we get for the hybridization

$$\bar{V}_k = (2 + i\cos k)\, V \int_{-\infty}^{\infty} \mathrm{d}\theta e^{3\theta} \rho_\alpha(\theta), \tag{161}$$

and for the on-site Coulomb repulsion

$$\tilde{U} = \bar{U} \int_{-\infty}^{\infty} \mathrm{d}\theta e^{3\theta} \rho_\alpha(\theta), \tag{162}$$

which are typically not integrable, however, we have to take into account that we must compute for example $\langle \{k_{\text{out}}, \sigma\} | H | \{d, \sigma\} \rangle$ completely, then perform the integral over θ and then expand the result for small U, which can again be integrable. We call this results $\check{V}_k$ and $\check{U}$. This is, however, a question that has remained unresolved in this work.
The Hamiltonian of the modified Anderson impurity model is then be given by

$$\begin{aligned} H_{\text{AIM}} = \frac{l}{2\pi} \sum_{\sigma=\uparrow,\downarrow} \int_{-\infty}^{\infty} \mathrm{d}k \left(k\,|k|^\alpha\, n_{k,\sigma} + \check{V}_k c^\dagger_{k,\sigma} d_\sigma + \check{V}^*_k d^\dagger_\sigma c_{k,\sigma} \right) + \epsilon_d \sum_{\sigma=\uparrow,\downarrow} n_{d,\sigma} \\ + \check{U} n_{d,\uparrow} n_{d,\downarrow}. \end{aligned} \tag{163}$$

6.2 Non-linear integral equations of the pseudogap Anderson impurity model

In chapter 5.3 we showed that the non-linear integral equations of the Anderson impurity model follow from the Hubbard model with integrable impurity by the use of our continuum model. Thus the thermodynamics of the model can be completely described. This is a system of finitely many, coupled, non-linear integral equations, which makes the numerical analysis quite simple. For this reason we also want to derive the non-linear integral equations of the modified Anderson impurity model in this section. We are using our continuum limit (cf. chapter 5) to derive these from those of the modified Hubbard model with integrable impurity (114). The analysis is quite similar and the result reads

$$
\begin{aligned}
\ln b^{+}(\lambda) &= -H\bar{\beta} - \left(\mathcal{K}_4 * \ln B^{+}\right)(\lambda) + \left(\mathcal{K}_{4,1} * \ln B^{-}\right)(\lambda) \\
&\quad - \left(\mathcal{K}_2 * \ln \frac{\bar{c}}{\bar{C}}\right)(\lambda), \\
\ln b^{-}(\lambda) &= -H\bar{\beta} - \left(\mathcal{K}_{4,-1} * \ln B^{+}\right)(\lambda) + \left(\mathcal{K}_4 * \ln B^{-}\right)(\lambda) \\
&\quad - \left(\mathcal{K}_{2,-1} * \ln \frac{\bar{c}^{+}}{\bar{C}^{+}}\right)(\lambda), \\
\ln c(k) &= \frac{5\bar{\beta}}{4}\left(H - 2\epsilon_d - \bar{U}\right) + \frac{\bar{\beta}}{2}\frac{\pi(1+\alpha)}{\sin\frac{\pi\alpha}{2}}\left(k - \epsilon_d - \frac{\bar{U}}{2}\right)\left|k - \epsilon_d - \frac{\bar{U}}{2}\right|^{\alpha} \\
&\quad + \left(\mathcal{K}_{4,-\frac{1}{2}} * \ln B^{+}\right)(g(k)) - \left(\mathcal{K}_{2,1} * \ln B^{-}\right)(g(k)) \\
&\quad + \left(\mathcal{K}_{2,-1} * \ln \bar{B}^{+}\right)(g(k)) - \left(\mathcal{K}_2 * \ln \bar{B}^{-}\right)(g(k)) + \left(\mathcal{K}_4 * \ln C\right)(k) \\
&\quad + \left(\mathcal{K}_{2,-\frac{1}{2}} * \ln \bar{C}\right)(k) + \frac{1}{4}\ln \mathfrak{C}(k) + \frac{1}{2}\ln \bar{C}(k), \\
\ln \bar{c}(k) &= -\frac{\bar{\beta}}{2}\left(H - 2\epsilon_d - \bar{U} + \frac{\pi(1+\alpha)}{\sin\frac{\pi\alpha}{2}}\left(k - \epsilon_d - \frac{\bar{U}}{2}\right)\left|k - \epsilon_d - \frac{\bar{U}}{2}\right|^{\alpha}\right) \\
&\quad - \left(\mathcal{K}_2 * \ln B^{+}\right)(g(k)) + \left(\mathcal{K}_{2,1} * \ln B^{-}\right)(k) - \left(\mathcal{K}_{2,\frac{1}{2}} * \ln C\right)(k) \\
&\quad + \frac{1}{2}\ln C(k)
\end{aligned}
\tag{164}
$$

Since we have not introduced any shifts on the vertical lines in the modified Hubbard model with integrable impurity, the expression for the free energy remains unchanged (145). Together with equations (164) this equation describes the thermodynamical properties of the modified Anderson impurity model completely.

Note that the density of states of this model is given by

$$
\rho(\epsilon) = \frac{(1+r)\,|\epsilon|^{r}}{2^{1+r}\pi}, \tag{165}
$$

where $r = -\frac{\alpha}{1+\alpha}$. Since $\alpha \in (-1, 0)$ holds, we have $r \in (0, \infty)$. Notice furthermore that $r = 0$ for $\alpha = 0$ and $r = 1$ for $\alpha = -\frac{1}{2}$. The comparison with (3) shows that this is a pseudogap system. The particle-hole symmetry requires $\bar{U} = -2\epsilon_d$.

6.3 Low-temperature asymptotics

We derive analytic expressions for the thermodynamics. For $T \ll 1$ we simplify the non-linear integral equations (164). We adopt $H \ll 1$ and $\bar{U}, \epsilon_d > 0$, such that $\mathfrak{b}^{-}(\lambda) \to 0$ and $c(k) \to 0$. $b^{+}(\lambda)$ and $\bar{c}(k)$ do not vanish. Then we find from equations (164)

$$\ln b^{+}(\lambda) = -H\bar{\beta} - \left(\mathcal{K}_4 * \ln B^{+}\right)(\lambda) - \left(\mathcal{K}_2 * \ln \frac{\bar{c}}{\bar{C}}\right)(\lambda),$$
$$\ln \bar{c}(k) = -\frac{\bar{\beta}}{2}\left(H - 2\epsilon_d - \bar{U} + \frac{\pi(1+\alpha)}{\sin\frac{\pi\alpha}{2}}\left(k - \epsilon_d - \frac{\bar{U}}{2}\right)\left|k - \epsilon_d - \frac{\bar{U}}{2}\right|^{\alpha}\right)$$
$$- \left(\mathcal{K}_2 * \ln B^{+}\right)(g(k)).$$

These formulas are justified at low temperatures T. There the correction terms are exponentially small $\mathcal{O}\left(e^{-\text{const.}\bar{\beta}}\right)$. The constant is real and positive. The expression for the free energy also simplifies

$$f = f_h + \frac{1}{l} f_i, \tag{166}$$
$$-\bar{\beta} f_{\mathrm{h}} = -\int_{-\infty}^{\infty} \frac{\mathrm{d}k}{2\pi i g'(k)} \ln \frac{\bar{C}}{\bar{c}}(k), \tag{167}$$
$$-\bar{\beta} f_{\mathrm{i}} = \frac{\bar{\beta}\bar{U}}{4} + \frac{1}{\pi i}\left(k * \ln B^{+}\right)(0) - \frac{1}{2\pi i}\left(k * \ln \frac{\bar{C}}{\bar{c}}\right)(0)$$
$$- \frac{2}{\pi i}\int_{-\infty}^{\infty} \frac{\mathrm{d}k}{g(k)} \ln \frac{\bar{C}}{\bar{c}}(k) \quad - \int_{-\infty}^{\infty} \frac{\mathrm{d}k}{2\pi i} \ln g(k) \left[\ln \frac{\bar{C}B^{+}}{1+\bar{c}B^{+}}(k)\right]' \tag{168}$$

We perform a linearization of the non-linear integral equations similar to Chapter 2.5.2. The functions $-\frac{\ln \mathfrak{b}^{+}(\lambda)}{\beta}$ and $-\frac{\ln \bar{c}(k)}{\beta}$ possess zeroes at $\pm\lambda_0$ and k_0. We find

$$\ln \mathfrak{b}^{+}(\lambda) = -H\bar{\beta} + \frac{\pi^2}{6}\frac{\mathcal{K}_4(\lambda-\lambda_0) + \mathcal{K}_4(\lambda+\lambda_0)}{(\ln b^{+})'(\lambda_0)} + \frac{\pi^2}{6}\frac{\mathcal{K}_2(\lambda - g(k_0))}{\left(\ln \frac{\bar{c}}{\bar{C}}\right)'(k_0)} g'(k_0)$$
$$- \int_{-\lambda_0}^{\lambda_0} \mathrm{d}\lambda' \mathcal{K}_4(\lambda-\lambda') \ln b^{+} - \int_{-k_0}^{k_0} \mathrm{d}p g'(p) \mathcal{K}_2(\lambda - g(p)) \ln \frac{\bar{c}}{\bar{C}}(p),$$
$$\ln \bar{c}(k) = -\frac{\bar{\beta}}{2}\left(H - 2\epsilon_d - \bar{U} + \frac{\pi(1+\alpha)}{\sin\frac{\pi\alpha}{2}}\left(k - \epsilon_d - \frac{\bar{U}}{2}\right)\left|k - \epsilon_d - \frac{\bar{U}}{2}\right|^{\alpha}\right)$$
$$+ \frac{\pi^2}{6}\frac{\mathcal{K}_4(g(k)-\lambda_0) + \mathcal{K}_4(g(k)+\lambda_0)}{(\ln b^{+})'(k_0)} - \int_{-\lambda_0}^{\lambda_0} \mathrm{d}\lambda' \mathcal{K}_4(g(k)-\lambda') \ln b^{+}.$$

Note that the expressions for the free energy do not change in comparison with chapter (145). It should be noted that a comparison with other work [133, 43, 131, 107, 44] is for now hardly possible, because the calculation of $\check{V}_k$ and $\check{U}$ (see chapter 6.1) must be done completely for this.

6.4 Screening of the impurity spin in the modified Anderson impurity model

We now discuss the rich physics of the modified Anderson impurity model.
The case $r = 0$ is the simplest: The density of states of the host is given by $\rho(\epsilon) = \frac{1}{2\pi}$. The density of states for a metallic host is finite at the Fermi energy. In this case we find the results of the Anderson impurity model. For antiferromagnetic $J_0 > 0$ the impurity moment is screened below the Kondo temperature T_K [74, 124]

$$T_K = \sqrt{\pi J_0} e^{-\frac{2\pi}{J_0}},$$

where J_0 is given by (4). Note that the crossovers are described by the single scale T_K at finite energies and temperatures [124]. For example, the impurity susceptibility $\chi_{\mathrm{i}}(T) = \partial_H^2 f_{\mathrm{i}}|_{\bar{T}}$ shows single-parameter scaling. It is a universal function of $\frac{\bar{T}}{T_K}$. The complete phase-diagram is well-known [124].
The case $r > 0$ describes a semimetal with vanishing density of states of the host at the Fermi energy. The bias towards Kondo screening decreases in this case. There is no screening at small Kondo couplings. Hence there exists a quantum phase transition among phases with and without screening. It arises upon increasing the Kondo coupling.
For particle-hole symmetry $\left(\bar{U} = -2\epsilon_d\right)$ there exists a transition between a local-moment phase and a symmetric strong-coupling phase.
Screening is also possible for particle-hole asymmetry. There exists a transition between a local-moment phase and an asymmetric strong-coupling phase, where full screening is obtained.
The density of states of the host with $r = 1$ (3) describes d-wave superconductors and charge-neutral graphene at low energies.
Note that for a quantitative analysis of the discussed phases and the critical points, the equations (164) must be numerically evaluated. This is left for future work.

7 Summary and Outlook

In this work, the construction of a pseudogap Anderson impurity model was investigated. This model describes the Kondo physics in metalloids and in pseudogap systems, especially in graphene, a system whose low-temperature physics in the charge-neutral case is dominated by two-dimensional Dirac electrons.
Since the host density of states of pseudogap systems disappears at the Fermi energy, the dispersion relation of the Anderson impurity model had to be modified. For this modification and for deriving the finitely many non-linear integral equations on the basis of the column-to-column transfer matrix we used a lattice approach. A suitable lattice model had to be identified yielding the Anderson impurity model in a continuum limit.
In chapter 2, a prototype of integrable models, the one-dimensional anisotropic spin-$\frac{1}{2}$ Heisenberg model was considered first. We used this as a warm up exercise to find out which modifications are possible on the lattice. We introduced an integrable spin-$\frac{1}{2}$ impurity on an additional site $L+1$ with the spectral parameter ν and shifts $\theta_1, \ldots, \theta_{\frac{N}{2}}$ and $\vartheta_1, \ldots, \vartheta_L$ on the horizontal and vertical lines, following some distributions ρ_h and ρ_v. These distribution densities depend on the parameters α_h and α_v ($\alpha_h, \alpha_v > 0$). We derived the Bethe ansatz equations for the row-to-row transfer matrix and the column-to-column transfer matrix of this novel model. The shifts on the horizontal lines can only be seen in the Bethe ansatz equations of the column-to-column transfer matrix, whereas the shifts on the vertical lines and the spin-$\frac{1}{2}$ impurity manifest themselves in the other set of Bethe ansatz equations. In the finitely many non-linear integral equations, therefore, the density ρ_h appears only in the equations for the auxiliary functions, while the density ρ_v is found in the expression for the free energy. The fact that the density ρ_h only appears in the driving terms of the finitely many non-linear integral equations is due to integrability. We have shown that by the right choice of distribution densities ρ_h and ρ_v the dispersion relation can be modified in such a way that the density of states disappears at the Fermi energy, characterizing a pseudogap system. Furthermore, we have seen that the use of shifts $\vartheta_1, \ldots, \vartheta_L$ on the vertical lines is not necessary to this end. For pseudogap systems, shifts $\theta_1, \ldots, \theta_{\frac{N}{2}}$ only on the horizontal lines are sufficient. To obtain a complete picture, we have determined the Hamiltonian of this new model, where we neglected additional many-body terms. Naturally, terms of this kind exist because the locality of the one-dimensional anisotropic spin-$\frac{1}{2}$ Heisenberg model was broken by the shifts $\theta_1, \ldots, \theta_{\frac{N}{2}}$ and $\vartheta_1, \ldots, \vartheta_L$ on the horizontal and vertical lines. It should therefore be noted that this a special impurity lattice model with an impurity interacting with an interacting host. Finally, we considered the low-temperature asymptotics of the model for $h = 0$ and $h \neq 0$. For $h = 0$ it was found that the free energy of the host behaves like $T^{1+\frac{\alpha_v}{\alpha_h}}$, but the free energy of the impurity behaves like $T^{1+\frac{1}{\alpha_h}}$. The free energy of the host and the impurity show a T^2 behaviour for the case $h \neq 0$. An open question is if a free fermion limit leads to a model with

non-interacting host, which interacts with the impurity.
In chapter 3 we considered the Hubbard model and introduced an integrable impurity in analogy to chapter 2. The impurity leads to an additional factor in the Bethe ansatz equations of the row-to-row transfer matrix. Regardless of whether the equivalent infinite number of non-linear integral equations derived in the thermodynamic Bethe ansatz or the finitely many non-linear integral equations derived in the quantum transfer matrix approach are used for the description of the thermodynamics, there are integral expressions for the impurity contribution to the free energy. In both cases the auxiliary functions do not change, but new expressions for the impurity part of the free energy arises. These are obtained in chapter 3, where established results [36] for the Hubbard model were generalized. In the thermodynamic Bethe ansatz, we used the string hypothesis and followed the traditional procedure [117]. In the quantum transfer matrix approach [63], it is easy to determine an expression in terms of solutions of the Bethe ansatz equations for the impurity contribution to the free energy (88), but to express it as an integral expression in terms of the auxiliary functions is much more complicated. The further course of this chapter is therefore devoted to the derivation of such an expression.
In chapter 4 on the modified density of states we considered the Hubbard model with integrable impurity and introduced shifts $\theta_1, \ldots, \theta_{\frac{N}{2}}$ on the horizontal lines, which follow a distribution density ρ_α. Right from the start, we did not use any shifts on the vertical lines, as chapter 2 showed that this is not necessary for pseudogap systems. Also the thermodynamic Bethe ansatz was not considered anymore in this chapter. Due to the shifts, the Bethe ansatz equations for the row-to-row transfer matrix of chapter 3 remained unchanged. However, the Bethe ansatz equations for the column-to-column transfer matrix are changed, which is reflected in the finitely many non-linear integral equations for the auxiliary functions, which now also change. The changes depend considerably on the choice of the distribution density function ρ_α. In this chapter, we briefly discussed different distribution densities and then show how to choose one that leads to pseudogap systems. We also showed that in the limit $U \to 0$ the host consists of free fermions now with a new dispersion relation. This is essential as the Anderson impurity model is a model with non-interacting host, interacting with the impurity and it is embedded in the Hubbard model with integrable impurity on the lattice. Finally, in this chapter the connection between the auxiliary functions and the dressed energy functions was deduced. It should again be noted that this is a special impurity lattice model with an impurity interacting in general $U \neq 0$ with an interacting host. An open question is what the shifts $\vartheta_1, \ldots, \vartheta_L$ on the vertical lines would provide.
Chapter 5 is devoted to the continuum limit of the Hubbard model with integrable impurity to the Anderson impurity model in the continuum. We showed that a combined continuum limit exists when the lattice constant is set to $\sqrt{U}$ and sent to zero. In addition, a linearization of the energy takes place in which the momenta k are distributed around

the Fermi points. The energy must also scale like $\sqrt{U}$, as well as the temperature. The parameters of the Hubbard model with integrable impurity pass into the parameters of the Anderson impurity model in non-trivial ways. The reformulation can be found in table (1). We have shown that this choice of parameters and the combined continuum limit yields the well-known Bethe ansatz equations and the infinitely many thermodynamic Bethe ansatz equations [124] of the Anderson impurity model, from the Bethe ansatz equations of the row-to-row transfer matrix and the thermodynamic Bethe ansatz equations of the Hubbard model with integrable impurity of chapter 3. In addition, we derived the finitely many non-linear integral equations of the Anderson impurity model through the continuum limit of the analogues for the Hubbard model. These equations are new and an improvement over previous work [22], as there a different lattice model with same regimes as in the phase diagram of the Anderson impurity model [124] was studied. With respect to the regimes, the models were considered equivalent. Note that in this lattice model the interaction of the host does not disappear. We have shown that the Hamiltonian of the Hubbard model with integrable impurity yields precisely the Hamiltonian of the Anderson impurity model. For the ground state the infinitely many thermodynamic Bethe ansatz equations of the Anderson impurity model reduce to finitely many and provide the same as the finitely many non-linear integral equations. It is noteworthy that the combined continuum limit from a lattice model with interacting host interacting with an impurity yields a continuum model with a non-interacting host still interacting with an impurity.
In the last chapter, the methods developed in the previous chapters were used to derive a pseudogap Anderson impurity model in the continuum. We applied the continuum limit established in chapter 5, to the lattice model in Chapter 4. This leads to a novel model (163) with the dispersion relation $\epsilon(k) = k|k|^{\alpha}$, $-1 < \alpha < 0$. What is remarkable about this model is, first, that $\check{V}_k$ depends on k and is no longer a constant. In addition, $\check{V}_k$ and $\check{U}$ depend on the distribution density ρ_α. However, we have not completely succeeded in calculating these two parameters, since the matrix elements $\langle \{k_{\text{out}}, \sigma\} | H | \{d, \sigma\} \rangle$, $\langle \{d, \sigma\} | H | \{k_{\text{in}}, \sigma\} \rangle$ and $\langle \{d, \sigma\} | H | \{d, \sigma\} \rangle$ must be calculated completely, not just in the limit $U \to 0$. In principle, the Maple program used by us is capable of doing so, but would require a much higher computation time, which is why this calculation was not performed. Therefore, a comparison with other work [133, 43, 131, 107] at this point is not yet possible. Nevertheless, we have described the thermodynamics of the model with finitely many non-linear integral equations and described the screening of the impurity spin. The screening is suppressed for small Kondo couplings. Therefore an impurity quantum phase transition exists among an unscreened and a screened impurity moment in this case. A detailed numerical analysis of the finitely many non-linear integral equations is still an open task.

This work may be followed by other interesting projects in which the open questions described here can be worked out. An attempt can be made to rewrite the Maple program to fully compute the $\check{V}_k$ and $\check{U}$ parameters in chapter 6. In addition, the finitely many non-linear integral equations can be numerically evaluated. The influence of shifts $\vartheta_1, \ldots, \vartheta_L$ on the vertical lines can be examined. These should allow the exponent r in equation (165) to take negative values. A simple free fermion limit for the modified one-dimensional anisotropic spin-$\frac{1}{2}$ Heisenberg model with spin-$\frac{1}{2}$ impurity may also be considered.

8 Appendix

The appendix lists some alternative expressions and the program codes in Maple.

8.1 Alternative expressions for $\ln \Lambda_0^{\mathsf{QTM}}(\lambda)$ in chapter 3.3.4

We derive two alternative formulas for the integrals in (107). We consider the last integral in

$$
\begin{aligned}
I := & \int_{\mathcal{L}} \frac{\mathrm{d}s'}{2\pi i} \left[\ln g\left(s' - i\frac{U}{2}\right)\right]' \ln \mathfrak{C}(s') + \int_{\mathcal{L}} \frac{\mathrm{d}s'}{2\pi i} \left[\ln g(s')\right]' \ln \frac{1+\mathfrak{c}+\bar{\mathfrak{c}}}{\bar{\mathfrak{c}}}(s') \\
= & \int_{\mathcal{L}} \frac{\mathrm{d}s'}{2\pi i} \left[\ln g\left(s' - i\frac{U}{2}\right)\right]' \ln \mathfrak{C}(s') + \int_{\mathcal{L}} \frac{\mathrm{d}s'}{2\pi i} \left[\ln g(s')\right]' \ln (1+\mathfrak{c}+\bar{\mathfrak{c}})(s') \\
& - \int_{\mathcal{L}} \frac{\mathrm{d}s'}{2\pi i} \left[\ln g(s')\right]' \ln \bar{\mathfrak{c}}(s')
\end{aligned}
\tag{169}
$$

use integration by parts and blow up the integration contour $\mathcal{L}$. This yields clockwise loops around the poles and the contour $\mathcal{L} - i\frac{U}{2}$ in reversed sense. Using again integration by parts we find

$$
\begin{aligned}
I = & \frac{N}{4\pi i} \ln \frac{g\left(s_0 - i\frac{U}{2}\right)}{g(s_0)} + \int_{\mathcal{L}} \frac{\mathrm{d}s'}{2\pi i} \left[\ln g(s')\right]' \ln (1+\mathfrak{c}+\bar{\mathfrak{c}})(s') \\
& - \int_{\mathcal{L}} \frac{\mathrm{d}s'}{2\pi i} \left[\ln \frac{g\left(s' - i\frac{U}{2}\right)}{g(s')}\right]' \ln \mathfrak{B}(s')
\end{aligned}
$$

yielding the first alternative expression to (107) in the limit $N \to \infty$

$$
I = \int_{\mathcal{L}} \frac{\mathrm{d}s'}{2\pi i} \left[\ln g(s')\right]' \ln (1+\mathfrak{c}+\bar{\mathfrak{c}})(s') - \int_{\mathcal{L}} \frac{\mathrm{d}s'}{2\pi i} \left[\ln \frac{g\left(s' - i\frac{U}{2}\right)}{g(s')}\right]' \ln \mathfrak{B}(s') \tag{170}
$$

.

Another formula can be derived by considering

$$
\int_{\mathcal{L}} \frac{\mathrm{d}s'}{2\pi i} \left[\ln \frac{g\left(s' + i\frac{U}{2}\right)}{g(s')}\right]' \ln \bar{\mathfrak{B}}(s')
$$

and defourming the contour $\mathcal{L}$ around poles, singularities and branch cuts. Applying this we obtain

$$\int\limits_{\mathcal{L}} \frac{\mathrm{d}s'}{2\pi i} \left[\ln \frac{g\left(s'+i\frac{U}{2}\right)}{g\left(s'\right)}\right]' \ln \bar{\mathfrak{B}}\left(s'\right) = \int\limits_{\mathcal{L}} \frac{\mathrm{d}s'}{2\pi i} \left[\ln \frac{g\left(s'-i\frac{U}{2}\right)}{g\left(s'\right)}\right]' \ln \mathfrak{B}\left(s'\right)$$

and therefore we find

$$\begin{aligned} I = &\int\limits_{\mathcal{L}} \frac{\mathrm{d}s'}{2\pi i} \left[\ln g\left(s'\right)\right]' \ln\left(\mathfrak{1}+\mathfrak{c}+\bar{\mathfrak{c}}\right)\left(s'\right) - \int\limits_{\mathcal{L}} \frac{\mathrm{d}s'}{4\pi i} \left[\ln \frac{g\left(s'-i\frac{U}{2}\right)}{g\left(s'\right)}\right]' \ln \mathfrak{B}\left(s'\right) \\ &- \int\limits_{\mathcal{L}} \frac{\mathrm{d}s'}{4\pi i} \left[\ln \frac{g\left(s'+i\frac{U}{2}\right)}{g\left(s'\right)}\right]' \ln \bar{\mathfrak{B}}\left(s'\right). \end{aligned} \tag{171}$$

8.2 Fractional calculus for another Anderson impurity model

The aim of this work is to construct an Anderson-like model (pseudogap system) and to describe its thermodynamics completely. The simplest such model that can be written down is

$$H = \frac{l}{2\pi} \sum_{\sigma=\uparrow,\downarrow} \int\limits_{-\infty}^{\infty} \mathrm{d}k \left(k^z n_{k,\sigma} + V\left(c^\dagger_{k,\sigma} d_\sigma + d^\dagger_\sigma c_{k,\sigma}\right)\right) + \epsilon_d \sum_{\sigma=\uparrow,\downarrow} n_{d,\sigma} + \bar{U} n_{d,\uparrow} n_{d,\downarrow}, \tag{172}$$

where $z \in \mathbb{R}^+$. Usually one would now try to solve the one- and two-particle problem, but in local space we have to confront the linear operator ∂_x^z, the so-called fractional derivative. The idea of a fractional derivative was first desribed in a letter from 1695 to G. F. A. de l'Hôpital by G. W. Leibniz. The idea for such a theory were described by J. Liouville in a paper from 1832.
For a general function $f\left(x\right)$, which is a monomial, and $0 < z < 1$, the complete fractional derivative is given by

$$\partial_x^z f\left(x\right) = \frac{1}{\Gamma\left(1-z\right)} \frac{\mathrm{d}}{\mathrm{d}x} \int\limits_0^x \mathrm{d}t \frac{f\left(t\right)}{\left(x-t\right)^z}. \tag{173}$$

If $z > 1$, we write $z = z' + \lfloor z \rfloor$ and use $\partial_x^z = \partial_x^{z'} \partial_x^{\lfloor z \rfloor}$, since then $0 < z' < 1$. Note that the derivative of a function $f\left(x\right)$ at a point x is local only when z is an integer. This is obviously not true in the case for non-integer z .
We can try to solve the one- and two-particle case by use of the Schrödinger equation and the corresponding eigenstates. The one-particle and two-particle eigenstates are given by

$$
\begin{aligned}
|\psi_{k,\sigma}\rangle &= \left(\int_{-\infty}^{\infty} \mathrm{d}x g_k(x)\, c_\sigma^\dagger(x) + e_k d_\sigma^\dagger \right) |0\rangle , \\
|\psi\rangle &= \Bigg(\int_{-\infty}^{\infty} \mathrm{d}x_1 \mathrm{d}x_2 g(x_1, x_2)\, c_\uparrow^\dagger(x_1)\, c_\downarrow^\dagger(x_2) \\
&\quad + \int_{-\infty}^{\infty} \mathrm{d}x e(x) \left(c_\uparrow^\dagger(x)\, d_\downarrow^\dagger - c_\downarrow^\dagger d_\uparrow^\dagger \right) + f d_\uparrow^\dagger d_\downarrow^\dagger \Bigg) |0\rangle , \qquad (174)
\end{aligned}
$$

where the vacuum $|0\rangle$ is a state without particles: $c_\sigma(x)|0\rangle = d_\sigma|0\rangle = 0$. Unfortunately, this approach does not lead to a physical solution, since even the fractional derivative of the Euler function is non-trivial for $0 < z < 1$

$$
\begin{aligned}
\partial_x^z x^n &= \frac{1+n-z}{(1-z)\,\Gamma(1-z)} x^{n-z} \\
\Rightarrow \partial_x^z e^x &= \frac{1+x-z}{x^z \Gamma(2-z)} e^x .
\end{aligned}
$$

8.3 Results of the Maple program for the one-dimensional isotropic spin-$\frac{1}{2}$ Heisenberg model with spin-$\frac{1}{2}$ impurity and modification of the density of states

> Im *Folgenden sind* θ *und* θ_0 *Spektralparameter von ebenen Wellen und haben Realteil* $-\frac{1}{2}$,
> Θ *und* ϕ *sind Parameter auf horizontaler Linie und der Verunreinigung und sind rein imaginär.*

>

> *Übergangsrate von ebener Welle mit Spektralparameter* θ *und Verunreinigungsspin* $+$ *nach* $-$:

> $$rate := \frac{2\theta(3\Theta - 2\theta - 1 - \phi)}{(1+\Theta-\phi)(-1+\Theta-\phi)(-\theta+\Theta-1)(\Theta-\theta)}$$

>

> *Übergangsrate von ebener Welle mit Spektralparameter* θ **in** *Welle mit* θ_0 *bei Verunreinigungsspin fest* $+$

> $$rate_{++} := \left(2(1+\theta_0)\theta\left(-3\Theta\theta_0 + 2\theta\theta_0 + \theta_0 + \theta_0\phi + \phi - 2\Theta\phi + 1 + 4\Theta^2 - 3\Theta - 3\theta\Theta + \theta + \theta\phi\right)\right) \Big/ \left((-\theta_0 + \Theta - 1)(\Theta-\theta)(\Theta-\theta_0)(\Theta-1-\theta)(1+\Theta-\phi)(\Theta-1-\phi)\right)$$

>

> *Übergangsrate von ebener Welle mit Spektralparameter* θ **in** *Welle mit* θ_0 *bei Verunreinigungsspin fest* $-$

> $$rate_{--} := -\left(2\theta(1+\theta_0)\left(\theta_0 + 2\theta\theta_0 - 3\Theta\theta_0 + \theta_0\phi + 4\Theta^2 - 1 - 2\Theta\phi + \phi - 3\Theta + \theta - 3\theta\Theta + \theta\phi\right)\right) \Big/ \left((-\theta_0 + \Theta - 1)(\Theta-\theta)(\Theta-\theta_0)(\Theta-1-\theta)(1+\Theta-\phi)(\Theta-1-\phi)\right)$$

8.4 Maple code for the calculation of the Hamiltonian of the Anderson impurity model

```
> restart:
> with(LinearAlgebra):#with(MTM):
> with(plots):
> cin:=1:cout:=1:din:=4:dout:=4:
> if cin≠1 then dim1:=2 else dim1:=1 end if:
> if cout≠1 then dim4:=2 else dim4:=1 end if:
> dim2:=4:dim3:=4:
> dimg:=dim1·dim2·dim3·dim4:
> V:=Vector(dimg):W:=Vector(dim2·dim3):X:=Vector(dim1·dim4):Y
      :=Vector(4):elin:=Vector(dim1):elaus:=Vector(dim4):
> XX:=Matrix(dim1,dim4):
> n:=0:
  for i to dim1 do for j to dim2 do for k to dim3 do for l to dim4 do
  n:=n+1:
  V_n:=i,j,k,l:
  end do:end do:end do:end do:
> n:=0:
  for j to dim2 do for k to dim3 do
  n:=n+1:
  W_n:=j,k:
  end do:end do:
> n:=0:
  for j to dim1 do for k to dim4 do
  n:=n+1:
  X_n:=j,k:XX_{j,k}:=n:
  end do:end do:
> n:=0:
  for j to 2 do for k to 2 do
  n:=n+1:
  Y_n:=j,k:
  end do:end do:
> gewa:=proc(V,Z,Hv,Hz,U)
  ap:=1/2·(V·Z+1/(V·Z)):am:=1/2·(V/Z+Z/V):
  bp:=1/(2·I)·(V·Z-1/(V·Z)):bm:=1/(2·I)·(V/Z-Z/V):
  HV2:=U/(8·I)·(V^2-V^(-2))+((U/(8·I)·(V^2-V^(-2)))^2+1)^(1/2):
  HZ2:=U/(8·I)·(Z^2-Z^(-2))+((U/(8·I)·(Z^2-Z^(-2)))^2+1)^(1/2):
  um:=ap·(HV2+HZ2):up:=am·(HV2-HZ2):
  am,bm,um,ap,bp,up,(U/(8·I)·(V^2-V^(-2)))^2+1,(U/(8·I)·(Z^2-Z^(-2)))^2+1:
  end proc:
```

```
> sz := Vector(2) : sz[1] := 1 : sz[2] := -1 :
> delt := proc(i, j)
  if (i = j) then delt := 1 else delt := 0 end if:
  end proc:
> lm := Array(1..2, 1..2, 1..2, 1..2, 0) : lp := Array(1..2, 1..2, 1..2, 1..2, 0) :
> Lin := Array(1..4, 1..4, 1..4, 1..4, 0) : Lt := Array(1..4, 1..4, 1..4, 1..4, 0) : Ltd
      := Array(1..4, 1..4, 1..4, 1..4, 0) : Lo := Array(1..4, 1..4, 1..4, 1..4, 0) : Lphi
      := Array(1..4, 1..4, 1..4, 1..4, 0) : Lphid := Array(1..4, 1..4, 1..4, 1..4, 0) :
> lm[1, 1, 1, 1] := am: lm[2, 2, 2, 2] := am:
  lp[1, 1, 1, 1] := ap: lp[2, 2, 2, 2] := ap:
> lm[1, 2, 1, 2] := bm: lm[2, 1, 2, 1] := bm:
  lp[1, 2, 1, 2] := bp: lp[2, 1, 2, 1] := bp:
> lm[1, 2, 2, 1] := 1 : lm[2, 1, 1, 2] := 1 :
  lp[1, 2, 2, 1] := 1 : lp[2, 1, 1, 2] := 1 :

> normboltz := um·lm[1, 1, 1, 1]·lm[1, 1, 1, 1] + up·sz[1]·sz[1]·lp[1, 1, 1, 1]·lp[1,
      1, 1, 1] :
  for i to 4 do for j to 4 do for k to 4 do for l to 4 do
  i1, i2 := Y_i:
  j1, j2 := Y_j:
  k1, k2 := Y_k:
  l1, l2 := Y_l:
  #zwi:=um·lm[i1, j1, k1, l1]·lm[i2, j2, k2, l2] + up·sz[k1]·sz[k2]·lp[i1, j1, k1, l1]
      ·lp[i2, j2, k2, l2] :
  zwi := 1/normboltz (um·lm[i1, j1, k1, l1]·lm[i2, j2, k2, l2] + up·sz[i1]·sz[i2]·lp[i1,
      j1, k1, l1]·lp[i2, j2, k2, l2]) :
  Lin[i, j, k, l] := subs({am = ami, bm = bmi, um = umi, ap = api, bp = bpi, up
      = upi}, zwi) :
  Lt[i, j, k, l] := subs({am = amt, bm = bmt, um = umt, ap = apt, bp = bpt, up
      = upt}, zwi) :
  Ltd[i, j, k, l] := subs({am = amtd, bm = bmtd, um = umtd, ap = aptd, bp = bptd,
      up = uptd}, zwi) :
  Lo[i, j, k, l] := subs({am = amo, bm = bmo, um = umo, ap = apo, bp = bpo, up
      = upo}, zwi) :
  Lphi[i, j, k, l] := subs({am = amphi, bm = bmphi, um = umphi, ap = apphi, bp
      = bpphi, up = upphi}, zwi) :
  Lphid[i, j, k, l] := subs({am = amphid, bm = bmphid, um = umphid, ap
      = apphid, bp = bpphid, up = upphid}, zwi) :
  end do: end do: end do: end do:
> ami, bmi, umi, api, bpi, upi, dV0, dV1 := gewa(V1, V0, hV0, hV1, U) :
> amt, bmt, umt, apt, bpt, upt, dV0, dV2 := gewa(V2, V0, hV0, hV2, U) :
> amtd, bmtd, umtd, aptd, bptd, uptd, dV3, dV0 := gewa(V0, V3, hV3, hV0, U) :
> amo, bmo, umo, apo, bpo, upo, dV4, dV0 := gewa(V0, V4, hV4, hV0, U) :
> amphi, bmphi, umphi, apphi, bpphi, upphi, dVphi, dV2 := gewa(V2, Vphi, hVphi,
      hV2, U) :
> amphid, bmphid, umphid, apphid, bpphid, upphid, dV3, dVphi := gewa(Vphi,
```

```
      V3, hV3, hVphi, U) :

> Ltdiff := Array(1..4, 1..4, 1..4, 1..4, 0) :
> for i to 4 do for j to 4 do for k to 4 do for l to 4 do
  Ltdiff[i, j, k, l] := subs(V3 = V2, diff(Ltd[i, j, k, l], V3))
  end do: end do: end do: end do:
> Lphidiff := Array(1..4, 1..4, 1..4, 1..4, 0) :
> for i to 4 do for j to 4 do for k to 4 do for l to 4 do
  Lphidiff[i, j, k, l] := subs(V3 = V2, diff(Lphid[i, j, k, l], V3))
  end do: end do: end do: end do:
> elin[1] := 1 : if dim1 > 1 then elin[2] := cin end if:
> elaus[1] := 1 : if dim4 > 1 then elaus[2] := cout end if:
> alpha := din : beta := dout :
> T := Matrix(dimg, dimg) :
> for i to dimg do for j to dimg do
  li := V_i : lj := V_j :
  T[i, j] := 0 :
  for k to 4 do for l to 4 do for m to 4 do
  T[i, j] := T[i, j] + Lin[elin[li_1], 1, elin[lj_1], k]·Lt[li_2, k, lj_2, l]·Ltd[l, lj_3, m, li_3]
      ·Lo[m, elaus[lj_4], 1, elaus[li_4]] :
  end do: end do:end do:
  end do: end do:
> Ti := Matrix(dimg, dimg) :
> for i to dimg do for j to dimg do
  li := V_i : lj := V_j :
  Ti[i, j] := 0 :
  for l to 4 do
  Ti[i, j] := Ti[i, j] + delt(li_1, 1)·delt(li_4, 1)·Lphi[li_2, alpha, lj_2, l]·Lphid[l, lj_3, beta,
      li_3]·delt(lj_1, dim1)·delt(lj_4, dim4) :
  end do:
  end do: end do:
> T4 := Matrix(dim1·dim4, dim1·dim4) :
> for i to dim1·dim4 do for j to dim1·dim4 do
  li := X_i : lj := X_j :
  T4[i, j] := 0 :
  for k to 4 do
  T4[i, j] := T4[i, j] + Lin[elin[li_1], 1, elin[lj_1], k]·Lo[k, elaus[lj_2], 1, elaus[li_2]] :
  end do:
  end do: end do:
> Ti4 := Matrix(dim1·dim4, dim1·dim4) :
> for i to dim1·dim4 do for j to dim1·dim4 do
  li := X_i : lj := X_j :
  Ti4[i, j] := delt(li_1, 1)·delt(li_2, 1)·delt(alpha, beta)·delt(lj_1, dim1)·delt(lj_2,
      dim4) :
  end do: end do:
> P0 := Matrix(dim1·dim4, dimg) : P1 := Matrix(dim1·dim4, dimg) :
```

```
> for i to dim1·dim4 do for j to dimg do
  li := X_i: lj := V_j:
  P0[i, j] := subs(V0 = V2, Lin[elin[li_1], 1, elin[lj_1], lj_2]·Lo[lj_3, elaus[lj_4], 1,
      elaus[li_2]]) :
  end do: end do:
  Tt2in := subs(V0 = V2, T4)^-1 :
  P0 := Tt2in.P0 :
>
> #ersetzen:={V0 = exp(I·0.0), V1 = exp((I·Pi)/4)·0.1, V2 = exp(I·2.1), V3 = exp(I
      ·0.5), V4 = exp(-(I·Pi)/4)·0.01, Vphi = exp(I·0.7), U = 0.0}
> Ts := Matrix(dimg, dim1·dim4) :
> for i to dimg do for j to dim1·dim4 do
  li := V_i: lj := X_j:
  Ts[i, j] := 0 :
  for k to 4 do for l to 4 do for m to 4 do for n to 4 do
  Ts[i, j] := Ts[i, j] + Lin[elin[li_1], 1, elin[lj_1], k]·Lt[li_2, k, n, l]·Ltdiff[l, n, m, li_3]
      ·Lo[m, elaus[lj_2], 1, elaus[li_4]] :
  end do: end do:end do: end do:
  end do: end do:

> T4s := P0.Ts :
> Tis := Matrix(dimg, dim1·dim4) :
> for i to dimg do for j to dim1·dim4 do
  li := V_i: lj := X_j:
  Tis[i, j] := 0 :
  for l to 4 do for n to 4 do
  Tis[i, j] := Tis[i, j] + delt(li_1, 1)·delt(li_4, 1)·Lphi[li_2, alpha, n, l]·Lphidiff[l, n,
      beta, li_3]·delt(lj_1, dim1)·delt(lj_2, dim4) :
  end do: end do:
  end do: end do:

> for i to dim1·dim4 do for j to dimg do P1_{i,j} := x_{i,j} end do: end do:
> Pnull1 := Matrix(dim1·dim4, dim1·dim4, 0) :
  for i to dim1·dim4 do for j to dimg do
  li := X_i: lj := V_j:
  if (lj_2 = lj_3) then
  Pnull1[i, XX[lj_1, lj_4]] := Pnull1[i, XX[lj_1, lj_4]] + P1[i, j]:
  end if:
  end do: end do:
  eq1 := convert(Pnull1, set) :

> Pnull := Matrix(dim1·dim4, dimg) :
> Pnull := P1.T + P0.Ti - T4.P1 - Ti4.P0 :
```

```
> eq2 := { }:
  for i to dim1·dim4 do for j to dimg do
  li := X_i: lj := V_j:
  if not( (lj_2 = 4) and (lj_3 = 4) ) then
  eq2 := eq2 ∪ {Pnull[i, j]}
  end if
  end do:end do:
> eq := eq1∪ eq2:
> allvar := convert(P1, set) :
Warning, `ap` is implicitly declared local to procedure `gewa`
Warning, `am` is implicitly declared local to procedure `gewa`
Warning, `bp` is implicitly declared local to procedure `gewa`
Warning, `bm` is implicitly declared local to procedure `gewa`
Warning, `HV2` is implicitly declared local to procedure `gewa`
Warning, `HZ2` is implicitly declared local to procedure `gewa`
Warning, `um` is implicitly declared local to procedure `gewa`
Warning, `up` is implicitly declared local to procedure `gewa`
Warning, `delt` is implicitly declared local to procedure
`delt`
```

$$> \ teilloest := \left\{ Vphi = \frac{a2 \cdot b2}{2^{\frac{1}{2}}},\ V1 = I^{\frac{1}{2}} \cdot a2^2 \cdot ki^{-1},\ V4 = I^{\frac{1}{2}} \cdot a2^2 \cdot ko^{-1},\ U = a2^4,\ V0 = 1,\ V2 = \left(1 + \frac{I \cdot a2^2 \cdot t}{2}\right),\ V3 = \left(1 + \frac{I \cdot a2^2 \cdot t}{2}\right) \right\}$$

```
> teilloes := subs(t = 0, teilloest);
> eq3vek := convert(subs(teilloes, eq), list) :
> eq3 := { }:
  for i to nops(eq3vek) do
  eq3 := eq3∪ {convert(series(simplify(eq3vek_i), a2 = 0, 4), polynom)}
  end do:
> loesung := solve(eq3, allvar) :
> Transfer1
```

$$:= convert\left(simplify\left(series\left((Trace(simplify(subs(loesung, subs(teilloes, P1.Ts))))) \Big/ \left(simplify\left(subs\left(teilloes, \left(\frac{Lin[2,1,1,2]}{Lin[2,1,2,1]} \right)^{dim1-1} \cdot \left(\frac{Lo[2,1,1,2]}{Lo[1,2,1,2]} \right)^{dim4-1} \right) \right), a2 = 0, 6 \right) \right), polynom \right)$$

```
> Transfer0
```

$$:= convert\left(simplify\left(series\left((Trace(simplify(subs(loesung, subs(teilloes,\right.\right.\right.\right.$$

```
        P0.Tis)))))/(simplify(subs(teilloes, (Lin[2, 1, 1, 2]/Lin[2, 1, 2, 1])^(dim1 - 1)
        ·(Lo[2, 1, 1, 2]/Lo[1, 2, 1, 2])^(dim4 - 1))), a2 = 0, 6)), polynom)
> Transfer := I·(Transfer1 + Transfer0):
> Transf := factor(convert(convert(simplify(series(series(Transfer, ki = 0, 4), ko
      = 0, 4)), polynom), polynom))
> imppar := {ki = (I·8·cos(pin))^(1/2), ko = (I·8·cos(po))^(1/2)}
```

$$teilloest := \left\{U = a2^4,\ V0 = 1,\ V1 = \frac{(-1)^{1/4}\,a2^2}{ki},\ V2 = 1 + \frac{1}{2}\,\mathrm{I}\,a2^2\,t,\ V3 = 1 + \frac{1}{2}\,\mathrm{I}\,a2^2\,t,\ V4 = \frac{(-1)^{1/4}\,a2^2}{ko},\ Vphi = \frac{1}{2}\,a2\,b2\sqrt{2}\right\}$$

$$teilloes := \left\{U = a2^4,\ V0 = 1,\ V1 = \frac{(-1)^{1/4}\,a2^2}{ki},\ V2 = 1,\ V3 = 1,\ V4 = \frac{(-1)^{1/4}\,a2^2}{ko},\ Vphi = \frac{1}{2}\,a2\,b2\sqrt{2}\right\}$$

$$Transfer1 := 0$$

$$Transfer0 := 0$$

$$Transf := 0$$

$$imppar := \left\{ki = \sqrt{8\,\mathrm{I}\cos(pin)},\ ko = \sqrt{8\,\mathrm{I}\cos(po)}\right\} \quad (1)$$

```
> # keine Wellen, Übergänge nur auf Verunr.platz
> # 1->1, 1->1
  simplify(subs(imppar, Transf))
```

$$0 \quad (2)$$

```
> # 1->1, 2->2
  simplify(subs(imppar, Transf))
```

$$\frac{1}{2}\,\frac{a2^2\,(-1 + 2\,a2^2\,b2^2)}{b2^2} \quad (3)$$

```
> # 1->1, 3->3
  simplify(subs(imppar, Transf))
```

$$\frac{1}{2}\,\frac{a2^2\,(-1 + 2\,a2^2\,b2^2)}{b2^2} \quad (4)$$

```
> # 1->1, 4->4
  simplify(subs(imppar, Transf))
```

$$0 \quad (5)$$

```
> # Streuung Welle in Welle, kein Überg. auf Verunrg.
> # 2->2, 1->1
  simplify(subs(imppar, Transf))
```

$$\cos(pin) - \mathrm{I}\cos(pin) + \cos(po) + \mathrm{I}\cos(po) + 2 \quad (6)$$

```
> # 2->2, 2->2
  simplify(subs(imppar, Transf))
```

$$-2+\cos(pin)+I\cos(pin)+\cos(po)-I\cos(po) \tag{7}$$

```
> # 2->2, 3->3
  simplify(subs(imppar, Transf))
```

$$\cos(pin)-I\cos(pin)+\cos(po)+I\cos(po)+2 \tag{8}$$

```
> # 2->2, 4->4
  simplify(subs(imppar, Transf))
```

$$-2+\cos(pin)+I\cos(pin)+\cos(po)-I\cos(po) \tag{9}$$

```
> # Hybridisierung
> # 1->2, 2->1
  simplify(expand(convert(series(simplify(subs(imppar, Transf)), a2 = 0, 2),
      polynom)))
```

$$-a2\,b2\sqrt{2}\,(1-I+\cos(po)) \tag{10}$$

```
> # 2->1, 1->2
  simplify(expand(convert(series(simplify(subs(imppar, Transf)), a2 = 0, 2),
      polynom)))
```

$$-a2\,b2\sqrt{2}\,(1+I+\cos(pin)) \tag{11}$$

```
>
> # "Nebenrechnungen"
> simplify(solve(8*I*ki^2/(1+sqrt((1+64*ki^4)/ki^4)*ki^2) = EP, ki)[1])
```

$$\frac{1}{2}\,\frac{\sqrt{-I\,EP\,(EP^2+1)}}{EP^2+1} \tag{12}$$

```
> simplify((1/2*sqrt(-I*EP*(EP^2+1))/(EP^2+1))^2 + (I/4)/(EP+1/EP))
```

$$0 \tag{13}$$

```
> simplify(log(subs(ki = (-I/(8*cos(p)))^(1/2), 8*I*ki^2/(1+sqrt((1+64*ki^4)/ki^4)*ki^2))))
```

$$\ln\left(\frac{I}{I\cos(p)+\mathrm{csgn}(\sin(p))\sin(p)}\right) \tag{14}$$

```
> simplify(subs(imppar, -1/8*I*(sqrt(ko^4+64)+ko^2)))
```

$$-I\,\mathrm{csgn}(\sin(po))\sin(po)+\cos(po) \tag{15}$$

```
> simplify(subs(imppar, 8*I/(ki^2+sqrt(ki^4+64))))
```

$$\frac{I}{I\cos(pin)+\mathrm{csgn}(\sin(pin))\sin(pin)} \tag{16}$$

```
> for i to 4 do print(simplify(convert(series(simplify(subs(teilloest, T4[i, i])), y = 0, 2), polynom))) end do
```

$$1$$

$$-\frac{1}{8}I\left(\sqrt{ko^4+64}+ko^2\right)$$

$$\frac{8I}{ki^2+\sqrt{ki^4+64}}$$

$$\frac{\sqrt{ko^4+64}+ko^2}{ki^2+\sqrt{ki^4+64}} \tag{17}$$

8.5 Maple code for the calculation of the Hamiltonian of the pseudogap Anderson impurity model

```
> restart:
> with(LinearAlgebra) :#with(MTM) :
> with(plots) :
> gewa := proc(V, Z, Hv, Hz, U)
  ap := 1/2·(V·Z + 1/(V·Z)) : am := 1/2·(V/Z + Z/V) :
  bp := 1/(2·I)·(V·Z - 1/(V·Z)) : bm := 1/(2·I)·(V/Z - Z/V) :
  HV2 := U/(8·I)·(V^2 - V^(-2)) + ((U/(8·I)·(V^2 - V^(-2)))^2 + 1)^(1/2) :
  HZ2 := U/(8·I)·(Z^2 - Z^(-2)) + ((U/(8·I)·(Z^2 - Z^(-2)))^2 + 1)^(1/2) :
  um := ap·(HV2 + HZ2) : up := am·(HV2 - HZ2) :
  am, bm, um, ap, bp, up, (U/(8·I)·(V^2 - V^(-2)))^2 + 1, (U/(8·I)·(Z^2 - Z^(-2)))^2 + 1 :
  end proc:
> sz := Vector(2) : sz[1] := 1 : sz[2] := -1 :
  Phf := ⟨1, I, I, -1⟩ :
  Y := Vector(4) :
  n := 0 :
  for j to 2 do for k to 2 do
  n := n + 1 :
  Y[n] := j, k:
  end do:end do:
> delt := proc(i, j)
  if (i = j) then delt := 1 else delt := 0 end if:
  end proc:
> lm := Array(1..2, 1..2, 1..2, 1..2, 0) : lp := Array(1..2, 1..2, 1..2, 1..2, 0) :
> Lin := Array(1..4, 1..4, 1..4, 1..4, 0) : Lt := Array(1..4, 1..4, 1..4, 1..4, 0) : Ltd
      := Array(1..4, 1..4, 1..4, 1..4, 0) : Lo := Array(1..4, 1..4, 1..4, 1..4, 0) : Lphi
      := Array(1..4, 1..4, 1..4, 1..4, 0) : Lphid := Array(1..4, 1..4, 1..4, 1..4, 0) :
  Lin2 := Array(1..4, 1..4, 1..4, 1..4, 0) : Lo2 := Array(1..4, 1..4, 1..4, 1..4, 0) :
> lm[1, 1, 1, 1] := am: lm[2, 2, 2, 2] := am:
  lp[1, 1, 1, 1] := ap: lp[2, 2, 2, 2] := ap:
> lm[1, 2, 1, 2] := bm: lm[2, 1, 2, 1] := bm:
  lp[1, 2, 1, 2] := bp: lp[2, 1, 2, 1] := bp:
> lm[1, 2, 2, 1] := 1 : lm[2, 1, 1, 2] := 1 :
  lp[1, 2, 2, 1] := 1 : lp[2, 1, 1, 2] := 1 :
Warning, `ap` is implicitly declared local to procedure `gewa`
Warning, `am` is implicitly declared local to procedure `gewa`
Warning, `bp` is implicitly declared local to procedure `gewa`
Warning, `bm` is implicitly declared local to procedure `gewa`
Warning, `HV2` is implicitly declared local to procedure `gewa`
Warning, `HZ2` is implicitly declared local to procedure `gewa`
```

```
Warning, `um` is implicitly declared local to procedure `gewa`
Warning, `up` is implicitly declared local to procedure `gewa`
Warning, `delt` is implicitly declared local to procedure
`delt`
```

```
> normboltz := um·lm[1, 1, 1, 1]·lm[1, 1, 1, 1] + up·sz[1]·sz[1]·lp[1, 1, 1, 1]·lp[1,
      1, 1, 1] :
  for i to 4 do for j to 4 do for k to 4 do for l to 4 do
  i1, i2 := Y_i:
  j1, j2 := Y_j:
  k1, k2 := Y_k:
  l1, l2 := Y_l:
  zwi := 1/normboltz (um·lm[i1, j1, k1, l1]·lm[i2, j2, k2, l2] + up·sz[i1]·sz[i2]·lp[i1,
      j1, k1, l1]·lp[i2, j2, k2, l2]) :
  Lin[i, j, k, l] := subs({am = ami, bm = bmi, um = umi, ap = api, bp = bpi, up
      = upi}, zwi) :
  Lt[i, j, k, l] := subs({am = amt, bm = bmt, um = umt, ap = apt, bp = bpt, up
      = upt}, zwi) :
  Ltd[i, j, k, l] := subs({am = amtd, bm = bmtd, um = umtd, ap = aptd, bp = bptd,
      up = uptd}, zwi) :
  Lo[i, j, k, l] := subs({am = amo, bm = bmo, um = umo, ap = apo, bp = bpo, up
      = upo}, zwi) :
  Lphi[i, j, k, l] := subs({am = amphi, bm = bmphi, um = umphi, ap = apphi, bp
      = bpphi, up = upphi}, zwi) :
  Lphid[i, j, k, l] := subs({am = amphid, bm = bmphid, um = umphid, ap
      = apphid, bp = bpphid, up = upphid}, zwi) :
   end do: end do: end do: end do:
> ami, bmi, umi, api, bpi, upi, dV0, dV1 := gewa(V1, V0, hV0, hV1, U) :
> amt, bmt, umt, apt, bpt, upt, dV0, dV2 := gewa(V2, V0, hV0, hV2, U) :
> amtd, bmtd, umtd, aptd, bptd, uptd, dV3, dV0 := gewa(V0, V3, hV3, hV0, U) :
> amo, bmo, umo, apo, bpo, upo, dV4, dV0 := gewa(V0, V4, hV4, hV0, U) :
> amphi, bmphi, umphi, apphi, bpphi, upphi, dVphi, dV2 := gewa(V2, Vphi, hVphi,
      hV2, U) :
> amphid, bmphid, umphid, apphid, bpphid, upphid, dV3, dVphi := gewa(Vphi,
      V3, hV3, hVphi, U) :
>
> Ltdiff := Array(1..4, 1..4, 1..4, 1..4, 0) :
> for i to 4 do for j to 4 do for k to 4 do for l to 4 do
  Ltdiff[i, j, k, l] := subs(V3 = V2, diff(Ltd[i, j, k, l], V3))
  end do: end do: end do: end do:
> Lphidiff := Array(1..4, 1..4, 1..4, 1..4, 0) :
> for i to 4 do for j to 4 do for k to 4 do for l to 4 do
  Lphidiff[i, j, k, l] := subs(V3 = V2, diff(Lphid[i, j, k, l], V3))
  end do: end do: end do: end do:
  for i to 4 do for j to 4 do for k to 4 do for l to 4 do
  Lin2[i, j, k, l] := subs(V0 = V2, Lin[i, j, k, l]) :
  Lo2[i, j, k, l] := subs(V0 = V2, Lo[i, j, k, l])
```

```
end do: end do: end do: end do:
> teilloes := { Vphi = a2·b2 / 2^(1/2), V1 = I^(1/2) · a2^2 · ki^(-1), V4 = I^(1/2) · a2^2 · ko^(-1), U = a2^4, V0 = 1,
    V2 = (1 + t), V3 = (1 + t) }
> imax := 5 :
teilloes := { U = a2^4, V0 = 1, V1 = (-1)^(1/4) a2^2 / ki, V2 = 1 + t, V3 = 1 + t, V4 = (-1)^(1/4) a2^2 / ko, Vphi = 1/2 a2 b2 sqrt(2) }   (1)
> Normi := simplify( subs( teilloes, Lin[2, 1, 1, 2] / Lin[2, 1, 2, 1] ) ) :
> Normo := simplify( subs( teilloes, Lo[2, 1, 1, 2] / Lo[1, 2, 1, 2] ) ) :
> for i to 4 do for j to 4 do for k to 4 do for l to 4 do
  Lin[i, j, k, l] := simplify( convert( series( simplify( subs( teilloes, Lin_{i,j,k,l} ) ), a2 = 0, imax ), polynom ) ) :
  Lin2[i, j, k, l] := simplify( convert( series( simplify( subs( teilloes, Lin2_{i,j,k,l} ) ), a2 = 0, imax ), polynom ) )
  end do: end do: end do: end do:
> for i to 4 do for j to 4 do for k to 4 do for l to 4 do
  Lo[i, j, k, l] := simplify( convert( series( simplify( subs( teilloes, Lo_{i,j,k,l} ) ), a2 = 0, imax ), polynom ) ) :
  Lo2[i, j, k, l] := simplify( convert( series( simplify( subs( teilloes, Lo2_{i,j,k,l} ) ), a2 = 0, imax ), polynom ) )
  end do: end do: end do: end do:
> for i to 4 do for j to 4 do for k to 4 do for l to 4 do
  Lt[i, j, k, l] := simplify( convert( series( simplify( subs( teilloes, Lt_{i,j,k,l} ) ), a2 = 0, imax ), polynom ) )
  end do: end do: end do: end do:
> for i to 4 do for j to 4 do for k to 4 do for l to 4 do
  Ltd[i, j, k, l] := simplify( convert( series( simplify( subs( teilloes, Ltd_{i,j,k,l} ) ), a2 = 0, imax ), polynom ) )
  end do: end do: end do: end do:
> for i to 4 do for j to 4 do for k to 4 do for l to 4 do
  Lphi[i, j, k, l] := simplify( convert( series( simplify( subs( teilloes, Lphi_{i,j,k,l} ) ), a2 = 0, imax ), polynom ) )
  end do: end do: end do: end do:
```

```
> for i to 4 do for j to 4 do for k to 4 do for l to 4 do
  Lphid[i, j, k, l] := simplify(convert(series(simplify(subs(teilloes, Lphid[i, j, k, l])),
      a2 = 0, imax), polynom))
  end do: end do: end do: end do:
> for i to 4 do for j to 4 do for k to 4 do for l to 4 do
  #print(i, j, k, l):
  Lphidiff[i, j, k, l] := simplify(convert(series(simplify(subs(teilloes,
      Lphidiff[i, j, k, l])), a2 = 0, imax), polynom))
  end do: end do: end do: end do:
> for i to 4 do for j to 4 do for k to 4 do for l to 4 do
  Ltdiff[i, j, k, l] := simplify(convert(series(simplify(subs(teilloes, Ltdiff[i, j, k, l])),
      a2 = 0, 5), polynom))
  end do: end do: end do: end do:
>
> cin := 1: cout := 1: din := 4: dout := 4:
> if cin ≠ 1 then dim1 := 2 else dim1 := 1 end if:
> if cout ≠ 1 then dim4 := 2 else dim4 := 1 end if:
> dim2 := 4: dim3 := 4:
> dimg := dim1·dim2·dim3·dim4:
> V := Vector(dimg): W := Vector(dim2·dim3): X := Vector(dim1·dim4): elin
      := Vector(dim1): elaus := Vector(dim4):
> XX := Matrix(dim1, dim4):
> n := 0:
  for i to dim1 do for j to dim2 do for k to dim3 do for l to dim4 do
  n := n + 1:
  V[n] := i, j, k, l:
  end do:end do:end do:end do:
> n := 0:
  for j to dim2 do for k to dim3 do
  n := n + 1:
  W[n] := j, k:
  end do:end do:
> n := 0:
  for j to dim1 do for k to dim4 do
  n := n + 1:
  X[n] := j, k: XX[j, k] := n:
  end do:end do:
>
> elin[1] := 1: if dim1 > 1 then elin[2] := cin end if:
> elaus[1] := 1: if dim4 > 1 then elaus[2] := cout end if:
> alpha := din: beta := dout:
> T := Matrix(dimg, dimg):
> for i to dimg do for j to dimg do
  li := V[i]: lj := V[j]:
  T[i, j] := 0:
  for k to 4 do for l to 4 do for m to 4 do
```

```
    T[i, j] := T[i, j] + Lin[elin[li1], 1, elin[lj1], k]·Lt[li2, k, lj2, l]·Ltd[l, lj3, m, li3]
        ·Lo[m, elaus[lj4], 1, elaus[li4]]:
    end do: end do:end do:
    end do: end do:
> Ti := Matrix(dimg, dimg):
> for i to dimg do for j to dimg do
    li := Vi: lj := Vj:
    Ti[i, j] := 0:
    for l to 4 do
    Ti[i, j] := Ti[i, j] + Phf[lj2] / Phf[lj3] · delt(li1, 1)·delt(li4, 1)·Lphi[li2, alpha, lj2, l]
        ·Lphid[l, lj3, beta, li3]·delt(lj1, dim1)·delt(lj4, dim4):
    end do:
    end do: end do:
> T4 := Matrix(dim1·dim4, dim1·dim4): T42 := Matrix(dim1·dim4, dim1·dim4):
> for i to dim1·dim4 do for j to dim1·dim4 do
    li := Xi: lj := Xj:
    T4[i, j] := 0: T42[i, j] := 0:
    for k to 4 do
    T4[i, j] := T4[i, j] + Lin[elin[li1], 1, elin[lj1], k]·Lo[k, elaus[lj2], 1, elaus[li2]]:
    T42[i, j] := T42[i, j] + Lin2[elin[li1], 1, elin[lj1], k]·Lo2[k, elaus[lj2], 1,
        elaus[li2]]:
    end do:
    end do: end do:
> Ti4 := Matrix(dim1·dim4, dim1·dim4):
> for i to dim1·dim4 do for j to dim1·dim4 do
    li := Xi: lj := Xj:
    Ti4[i, j] := delt(li1, 1)·delt(li2, 1)·delt(alpha, beta)·delt(lj1, dim1)·delt(lj2,
        dim4):
    end do: end do:
> P0 := Matrix(dim1·dim4, dimg): P1 := Matrix(dim1·dim4, dimg):
> for i to dim1·dim4 do for j to dimg do
    li := Xi: lj := Vj:
    P0[i, j] := Lin2[elin[li1], 1, elin[lj1], lj2]·Lo2[lj3, elaus[lj4], 1, elaus[li2]]:
    end do: end do:
    Tt2in := T42^-1:
    P0 := Tt2in.P0:
>
> Ts := Matrix(dimg, dim1·dim4):
> for i to dimg do for j to dim1·dim4 do
    li := Vi: lj := Xj:
    Ts[i, j] := 0:
    for k to 4 do for l to 4 do for m to 4 do for n to 4 do
    Ts[i, j] := Ts[i, j] + Lin[elin[li1], 1, elin[lj1], k]·Lt[li2, k, n, l]·Ltdiff[l, n, m, li3]
```

```
      ·Lo[m, elaus[lj2], 1, elaus[li4]]:
   end do: end do:end do: end do:
   end do: end do:
>
>  T4s := P0.Ts:
>  Tis := Matrix(dimg, dim1·dim4):
>  for i to dimg do for j to dim1·dim4 do
   li := Vi: lj := Xj:
   Tis[i, j] := 0:
   for l to 4 do for n to 4 do
   Tis[i, j] := Tis[i, j] + delt(li1, 1)·delt(li4, 1)·Lphi[li2, alpha, n, l]·Lphidiff[l, n,
      beta, li3]·delt(lj1, dim1)·delt(lj2, dim4):
   end do: end do:
   end do: end do:
>
>  for i to dim1·dim4 do for j to dimg do P1i,j := xi,j end do: end do:
>  Pnull1 := Matrix(dim1·dim4, dim1·dim4, 0):
    for i to dim1·dim4 do for j to dimg do
   li := Xi: lj := Vj:
   if (lj2 = lj3) then
   Pnull1[i, XX[lj1, lj4]] := Pnull1[i, XX[lj1, lj4]] + P1[i, j]:
   end if:
   end do: end do:
   eq1 := convert(Pnull1, set):
>  Pnull := Matrix(dim1·dim4, dimg):
>   for i to dim1·dim4 do for j to dimg do
    P0[i, j] := simplify(convert(series(simplify(subs(teilloes, P0[i, j])), a2 = 0,
      imax), polynom)):
    end do: end do:
   for i to dimg do for j to dimg do
    T[i, j] := simplify(convert(series(simplify(subs(teilloes, T[i, j])), a2 = 0, imax),
      polynom)):
   end do: end do:
   for i to dimg do for j to dimg do
    Ti[i, j] := simplify(convert(series(simplify(subs(teilloes, Ti[i, j])), a2 = 0,
      imax), polynom)):
   end do: end do:
    for i to dim1·dim4 do for j to dim1·dim4 do
    T4[i, j] := simplify(convert(series(simplify(subs(teilloes, T4[i, j])), a2 = 0,
      imax), polynom)):
   end do: end do:
    for i to dim1·dim4 do for j to dim1·dim4 do
    Ti4[i, j] := simplify(convert(series(simplify(subs(teilloes, Ti4[i, j])), a2 = 0,
      imax), polynom)):
   end do: end do:
   for i to dimg do for j to dim1·dim4 do
```

```
    Tis[i, j] := simplify(convert(series(simplify(subs(teilloes, Tis[i, j])), a2 = 0,
        imax), polynom)) :
    end do: end do:
> Pnull := P1.T + P0.Ti − T4.P1 − Ti4.P0 :
> eq2 := { } :
    for i to dim1·dim4 do for j to dimg do
    li := Xi: lj := Vj:
    #if not( (lj2 = 4) and (lj3 = 4) ) then
    eq2 := eq2 ∪ {Pnull[i, j]}
    #end if
    end do:end do:
> eq := eq1 ∪ eq2:
> allvar := convert(P1, set) :
> #eq3vek:=convert(subs(teilloes, subs(teilloes0, eq)), list) :
    eq3vek := subs(teilloes, eq) :
> # fuer Welle-in-Welle
    eq3 := { } :
    for i from 1 to nops(eq3vek) do
    #print(i) :
    #expkiko:=convert( convert( series( series( simplify( subs( t = 0, eq3vek_i) ), ki = 0,
        9), ko = 0, 9), polynom), polynom) :
    expkiko := convert( convert( series( series( simplify( convert( series( ( subs( { },
        eq3vek_i) ), a2 = 0, 3), polynom) ), ki = 0, 9), ko = 0, 9), polynom),
        polynom) :
    #ldko:=ldegree(expkiko, ko) :
    #ldki:=ldegree(expkiko, ki) :
    eq3 := eq3 ∪ {expkiko} :
    #eq3:=eq3∪{convert( taylor( convert( taylor( expkiko·ki^(−ldki)·ko^(−ldko), ki = 0, 5),
        polynom), ko = 0, 5), polynom) }
    #eq3:=eq3∪{convert( series( subs( t = 0, eq3vek_i), a2 = 0, 3), polynom) }
    #eq3:=eq3∪{subs( t = 0, eq3vek_i) }
    end do:
> # fuer einfache Faelle
    eq3 := eq3vek :
> loesung := solve(eq3, allvar) :
> t0 := t :
    loesung0 := simplify( subs( {t = t0}, loesung) ) :
> Transfer1
        := (Trace(simplify(subs(loesung0, subs({t = t0}, subs(teilloes, P1
        .Ts))))))/(simplify(subs({t = t0}, subs(teilloes, (Normi)^(dim1 − 1)
        ·(Normo)^(dim4 − 1))))) :
> Transfer0
        := (Trace(simplify(subs(loesung0, subs({t = t0}, subs(teilloes, P0
```

```
      .Tis))))))/(simplify(subs({t = t0}, subs(teilloes, (Normi)^(dim1 - 1)
      ·(Normo)^(dim4 - 1)))))):
> Transfer := I·(Transfer1 + Transfer0):
> Transf := simplify(expand(subs({t = t0}, convert(simplify(series(Transfer, a2
      = 0, 5)), polynom)))):
> Transfn := convert(convert(simplify(series(series(simplify(numer(Transf)), ki
      = 0, 8), ko = 0, 8)), polynom), polynom):
  Transfd := convert(convert(simplify(series(series(simplify(denom(Transf)), ki
      = 0, 8), ko = 0, 8)), polynom), polynom):
  Transf44 := convert(convert(simplify(series(series(simplify((Transfn/Transfd)), ki
      = 0, 3), ko = 0, 3))), polynom), polynom);
> imppar := {ki = (I·8·cos(pin))^(1/2), ko = (I·8·cos(po))^(1/2)}:
> #Trf:=simplify(expand(convert(series(simplify(subs(imppar, Transf44)), a2
      = 0, imax), polynom))) - subs(t = t0,
      (cos(pin) + cos(po))/((1/2) + (5/2)·t + 5·t^2 + 5·t^3 + (5/2)·t^4 + (1/2)·t^5))
> #0→2,1→1/16, 2→2/243, 3→1/512, 4→2/3125, 5→1/3888, 6→2/16807, 10
      →2/161051, 100→2/10510100501, 1000→2/1005010010005001
> Transfer1 := Trace(simplify(subs(loesung, subs(teilloes, P1.Ts))))/
      simplify(subs(teilloes, (Normi)^(dim1 - 1)·(Normo)^(dim4 - 1))):
> Transfer0 := Trace(simplify(subs(loesung, subs(teilloes, P0.Tis))))/
      simplify(subs(teilloes, (Normi)^(dim1 - 1)·(Normo)^(dim4 - 1))):
> Transfer := I·(Transfer1 + Transfer0):
> imppar := {ki = (I·8·cos(pin))^(1/2), ko = (I·8·cos(po))^(1/2)}:
> Transf := subs(imppar,
      convert(convert(simplify(series(series(simplify((convert(simplify(series(
      Transfer, a2 = 0, 6)), polynom))), ki = 0, 3), ko = 0, 3)), polynom),
      polynom))
```

$$Transf := 0 \tag{2}$$

```
> subs(t = t0, (cos(pin) + cos(po))/((1/2) + (5/2)·t + 5·t^2 + 5·t^3 + (5/2)·t^4 + (1/2)·t^5))
```

$$\frac{2}{243}\cos(pin) + \frac{2}{243}\cos(po) \tag{3}$$

```
> Nenner := t→1/2+5/2*t+5*t^2+5*t^3+5/2*t^4+1/2*t^5
```

$$Nenner := t \to \frac{1}{2} + \frac{5}{2}\,t + 5\,t^2 + 5\,t^3 + \frac{5}{2}\,t^4 + \frac{1}{2}\,t^5 \tag{4}$$

```
> # keine Wellen, Übergänge nur auf Verunr.platz
> # 1->1, 1->1
  simplify(taylor(simplify(expand(convert(series(simplify(subs(imppar,
      Transf)), a2=0, imax), polynom))), a2))
```

$$0 \tag{5}$$

```
> # 1->1, 2->2
   factor(simplify(taylor(simplify(expand(convert(series(simplify(subs(imppar,
       Transf)), a2=0, imax), polynom))), a2)))
```

$$-\frac{1}{2\,(1+t)^3\,b2^2}\,a2^2 + \frac{1}{(1+t)^5}\,a2^4 \tag{6}$$

```
> # 1->1, 3->3
  factor(simplify(taylor(simplify(expand(convert(series(simplify(subs(imppar,
      Transf)), a2=0, imax), polynom))), a2)))
```

$$-\frac{1}{2\,(1+t)^3\,b2^2}\,a2^2 + \frac{1}{(1+t)^5}\,a2^4 \tag{7}$$

```
> # 1->1, 4->4
  simplify(taylor(simplify(expand(convert(series(simplify(subs(imppar,
      Transf)), a2=0, imax), polynom))), a2))
```

$$0 \tag{8}$$

```
> # Hybridisierung
> # 1->2, 2->1
  H1221 := simplify(taylor(subs(imppar, Transf), a2=0, 4))
```

$$H1221 := -\frac{b2\sqrt{2}\,(2+\mathrm{I}\cos(po))}{(1+t)\,(1+2\,t+t^2)}\,a2 + \frac{1}{8}\,\frac{1}{(1+2\,t+t^2)^3\,(1+t)\,b2}\left(\sqrt{2}\,(2\,\mathrm{I}\,t^4 + 8\,\mathrm{I}\,t^3 + 12\,\mathrm{I}\,t^2 + 8\,\mathrm{I}\,t + 8\,b2^4 + 8\,\mathrm{I}\cos(po)\,b2^4\,t + 4\,\mathrm{I}\cos(po)\,b2^4\,t^2 - \cos(po)\,t^4 + 4\,\mathrm{I}\cos(po)\,b2^4 + 2\,\mathrm{I} - 4\cos(po)\,t + 16\,b2^4\,t + 8\,b2^4\,t^2 - 6\cos(po)\,t^2 - 4\cos(po)\,t^3)\right)a2^3 \tag{9}$$

```
> H1221 := factor(-b2*sqrt(2)*(2+I*cos(po))/((1+t)*(1+2*t+t^2))*a2)
      + factor(1/8*1/((1+2*t+t^2)^3*(1+t)*b2)*(sqrt(2)*(2*I*t^4+8*I*t^3+12*I*t^2+8*I*t
      +8*b2^4+8*I*cos(po)*b2^4*t+4*I*cos(po)*b2^4*t^2-cos(po)*t^4+4*I*cos(po)*b2^4
      +2*I-4*cos(po)*t+16*b2^4*t+8*b2^4*t^2-6*cos(po)*t^2-4*cos(po)*t^3))*a2^3)
```

$$H1221 := -\frac{\mathrm{I}\sqrt{2}\,(-2\,\mathrm{I}+\cos(po))\,a2\,b2}{(1+t)^3} + \frac{1}{8}\,\frac{1}{b2\,(1+t)^7}\left(\sqrt{2}\,(2\,\mathrm{I}\,t^4 + 8\,\mathrm{I}\,t^3 + 12\,\mathrm{I}\,t^2 + 8\,\mathrm{I}\,t + 8\,b2^4 + 8\,\mathrm{I}\cos(po)\,b2^4\,t + 4\,\mathrm{I}\cos(po)\,b2^4\,t^2 - \cos(po)\,t^4\right) \tag{10}$$

$$+4\,\mathrm{I}\cos(po)\,b2^4+2\,\mathrm{I}-4\cos(po)\,t+16\,b2^4\,t+8\,b2^4\,t^2-6\cos(po)\,t^2$$
$$-4\cos(po)\,t^3)\,a2^3)$$

```
> simplify(taylor(simplify(subs(t = 0, H1221)), a2 = 0, 4))
```

$$-\sqrt{2}\;b2\,(2+\mathrm{I}\cos(po))\,a2+\frac{1}{4}\,\frac{\sqrt{2}\,(4\,b2^4+\mathrm{I}+2\,\mathrm{I}\cos(po)\,b2^4)}{b2}\,a2^3 \qquad (11)$$

```
> # 2->1, 1->2
  H2112 := simplify(taylor(subs(imppar, Transf), a2 = 0, 4))
```

$$H2112 := \frac{(-2+\mathrm{I}\cos(pin))\,\sqrt{2}\;b2}{t^3+3\,t^2+3\,t+1}\,a2 \qquad (12)$$
$$-\frac{1}{8}\,\frac{1}{(1+2\,t+t^2)^2\,b2\,(t^3+3\,t^2+3\,t+1)}\,(\sqrt{2}\,(8\,\mathrm{I}\,t^3-16\,b2^4\,t+8\,\mathrm{I}\,t$$
$$-8\,b2^4+2\,\mathrm{I}\,t^4+12\,\mathrm{I}\,t^2+8\,\mathrm{I}\cos(pin)\,b2^4\,t+4\,\mathrm{I}\cos(pin)\,b2^4\,t^2+2\,\mathrm{I}$$
$$+4\,\mathrm{I}\cos(pin)\,b2^4-8\,b2^4\,t^2+4\cos(pin)\,t^3+6\cos(pin)\,t^2+\cos(pin)\,t^4$$
$$+4\cos(pin)\,t))\,a2^3$$

```
> H2112 := factor((-2+I*cos(pin))*sqrt(2)*b2/(t^3+3*t^2+3*t+1)*a2)
      - factor(1/8*1/(1+2*t+t^2)^2/b2/(t^3+3*t^2+3*t+1)*(sqrt(2)*(8*I*t^3-16*b2^4*t
      +8*I*t-8*b2^4+2*I*t^4+12*I*t^2+8*I*cos(pin)*b2^4*t+4*I*cos(pin)*b2^4*t^2+2*I
      +4*I*cos(pin)*b2^4-8*b2^4*t^2+4*cos(pin)*t^3+6*cos(pin)*t^2+cos(pin)*t^4
      +4*cos(pin)*t))*a2^3)
```

$$H2112 := \frac{\mathrm{I}\sqrt{2}\,(2\,\mathrm{I}+\cos(pin))\,a2\,b2}{(1+t)^3}-\frac{1}{8}\,\frac{1}{b2\,(1+t)^7}\,(\sqrt{2}\,(8\,\mathrm{I}\,t^3-16\,b2^4\,t \qquad (13)$$
$$+8\,\mathrm{I}\,t-8\,b2^4+2\,\mathrm{I}\,t^4+12\,\mathrm{I}\,t^2+8\,\mathrm{I}\cos(pin)\,b2^4\,t+4\,\mathrm{I}\cos(pin)\,b2^4\,t^2+2\,\mathrm{I}$$
$$+4\,\mathrm{I}\cos(pin)\,b2^4-8\,b2^4\,t^2+4\cos(pin)\,t^3+6\cos(pin)\,t^2+\cos(pin)\,t^4$$
$$+4\cos(pin)\,t)\,a2^3)$$

```
> simplify(taylor(simplify(subs(t = 0, H2112)), a2 = 0, 4))
```

$$(-2+\mathrm{I}\cos(pin))\,\sqrt{2}\;b2\,a2-\frac{1}{4}\,\frac{\sqrt{2}\,(\mathrm{I}+2\,\mathrm{I}\cos(pin)\,b2^4-4\,b2^4)}{b2}\,a2^3 \qquad (14)$$

```
> simplify(subs({I = -I, pin = po}, H2112) - H1221)
```

$$0 \qquad (15)$$

```
> # Streuung Welle in Welle, kein Überg. auf Verunrg.
> # 2->2, 1->1
  simplify(taylor(simplify(expand(convert(series(simplify(subs(imppar,
      Transf44)), a2 = 0, imax), polynom))), a2))
```

$$0 \qquad (16)$$

```
> # 2->2, 2->2
```

```
simplify( (cos(pin) + cos(po)) / ((1/2 + 5/2 t + 5 t^2 + 5 t^3 + 5/2 t^4 + 1/2 t^5)) )
```

$$\frac{2\,(\cos(pin)+\cos(po))}{1+5\,t+10\,t^2+10\,t^3+5\,t^4+t^5} \tag{17}$$

```
> # 2->2, 3->3
simplify(taylor(simplify(expand(convert(series(simplify(subs(imppar,
    Transf44)), a2 = 0, imax), polynom))), a2))
```

$$0 \tag{18}$$

```
> # 2->2, 4->4
simplify( (cos(pin) + cos(po)) / ((1/2 + 5/2 t + 5 t^2 + 5 t^3 + 5/2 t^4 + 1/2 t^5)) )
```

$$\frac{2\,(\cos(pin)+\cos(po))}{1+5\,t+10\,t^2+10\,t^3+5\,t^4+t^5} \tag{19}$$

References

[1] I. Affleck. Conformal Field Theory Approach to the Kondo Effect. *Acta Physica Polonica*, B26:1869–1932, December 1995.

[2] I. Affleck and A. W. W. Ludwig. Critical theory of overscreened Kondo fixed points. *Nuclear Physics B*, 360(2 - 3):641 – 696, August 1991.

[3] P. W. Anderson. Localized Magnetic States in Metals. *Physical Review Letters*, 124(1):41 – 53, October 1961.

[4] P. W. Anderson. A poor man's derivation of scaling laws for the Kondo problem. *Journal of Physics C: Solid State Physics*, 3(12):2436 – 2441, April 1970.

[5] P. W. Anderson. Local moments and localized states. *Reviews of Modern Physics*, 50(2):191 – 201, April 1978.

[6] P. W. Anderson and A. M. Clogston. Antiferromagnetic contribution to the polarization of free electrons by inner shell spins. *Bulletin of the American Physical Society*, 6(2):124, November 1961.

[7] N. Andrei. Diagonalization of the Kondo Hamiltonian. *Physical Review Letters*, 45(5):379 – 382, August 1980.

[8] N. Andrei and C. Destri. Solution of the Multichannel Kondo Problem. *Physical Review Letters*, 52(5):364 – 367, January 1984.

[9] N. Andrei and J. H. Lowenstein. Scales and Scaling in the Kondo Model. *Physical Review Letters*, 46(5):356 – 360, February 1981.

[10] H. Asakawa and M. Suzuki. Elementary excitations in the Hubbard model with boundaries. *Journal of Physics A: Mathematical and General*, 30(11):3741 – 3756, June 1997.

[11] R. Z. Bariev, A. Klümper, and J. Zittartz. A New Integrable Two-Parameter Model of Strongly Correlated Electrons in One Dimension. *Europhysics Letters*, 32(1):85 – 90, October 1995.

[12] R. J. Baxter. *Exactly Solved Models in Statistical Mechanics*. Academic Press, 1982.

[13] G. Bedürftig and H. Frahm. Thermodynamics of an integrable model for electrons with correlated hopping. *Journal of Physics A: Mathematical and General*, 28(16):4453 – 4468, August 1995.

[14] G. Bedürftig and H. Frahm. Spectrum of boundary states in the open Hubbard chain. *Journal of Physics A: Mathematical and General*, 30(12):4139 – 4149, June 1997.

[15] N. Beisert. The analytic Bethe ansatz for a chain with centrally extended $su(2 \mid 2)$ symmetry. *Journal of Statistical Mechanics: Theory and Experiment*, P01017:1 – 63, January 2007.

[16] N. Beisert and P. Koroteev. Quantum deformations of the one-dimensional Hubbard model. *Journal of Physics A: Mathematical and Theoretical*, 41(25):255204, June 2008.

[17] G. Benkart, S.-J. Kang, and M. Kashiwara. Crystal bases for the quantum superalgebra $U_q(gl(m,n))$. *Journal of the American Mathematical Society*, 13(2):295 – 331, January 2000.

[18] H. Bethe. Zur Theorie der Metalle. *Zeitschrift für Physik*, 71(3 - 4):205 – 226, 1931.

[19] M. Bortz and A. Klümper. Lattice path integral approach to the one-dimensional Kondo model. *Journal of Physics A: Mathematical and General*, 37(25):6413 – 6436, June 2004.

[20] M. Bortz and A. Klümper. The anisotropic multichannel spin-S Kondo model: Calculation of scales from a novel exact solution. *European Physical Journal B - Condensed Matter and Complex Systems*, 40(1):25 – 42, July 2004.

[21] M. Bortz and A. Klümper. Crossover from Anderson- to Kondo-like models. *Physica B: Physics of Condensed Matter*, 359:765 – 767, April 2005.

[22] M. Bortz, A. Klümper, and C. Scheeren. Crossover from Anderson-like to Kondo-like behavior: Universality induced by spin-charge separation. *Physical Review B: Condensed Matter and Materials Physics*, 71(14):144421–1 – 144421–11, April 2005.

[23] A. J. Bracken, M. D. Gould, J. R. Links, and Y.-Z. Zhang. New Supersymmetric and Exactly Solvable Model of Correlated Electrons. *Physical Review Letters*, 74(14):2768 – 2771, April 1995.

[24] J. Brundan. Kazhdan-Lusztig Polynomials and Character Formulae for the Lie superalgebra $gl(m \mid n)$. *Journal of the American Mathematical Society*, 16:185 – 231, October 2002.

[25] R. Bulla, T. Glossop, D. E. Logan, and T. Pruschke. The soft-gap Anderson model: comparison of renormalization group and local moment approaches. *Journal of Physics: Condensed Matter*, 12(23):4899 – 4921, June 2000.

[26] R. Bulla, T. Pruschke, and A. C. Hewson. Anderson impurity in pseudo-gap Fermi systems. *Journal of Physics: Condensed Matter*, 9(47):10463 – 10474, November 1997.

[27] A. Cavaglià, M. Cornagliotto, M. Mattelliano, and R. Tateo. A Riemann-Hilbert formulation for the finite temperature Hubbard model . *Journal of High Energy Physics*, 2015(6):15, June 2015.

[28] S.-J. Cheng, N. Lam, and W. Wang. Brundan-Kazhdan-Lusztig conjecture for general linear Lie superalgebras. *Duke Mathematical Journal*, 164(4):617–695, March 2015.

[29] S.-J. Cheng, W. Wang, and R. B. Zhang. Super duality and Kazhdan-Lusztig polynomials. *Transactions of the American Mathematical Society*, 360(11):5883 – 5924, June 2008.

[30] T. A. Costi, L. Bergqvist, A. Weichselbaum, J. von Delft, T. Micklitz, A. Rosch, P. Mavropoulos, P. H. Dederichs, F. Mallet, L. Saminadayar, and C. Bäuerle. Kondo decoherence: Finding the right spin model for iron impurities in gold and silver. *Physical Review Letters*, 102(5):056802–1 – 056802–4, February 2009.

[31] J. Dalibard. *Collisional dynamics of ultra-cold atomic gases*. IOS Press, 1999.

[32] T. Deguchi, F. H. L. Essler, F. Göhmann, A. Klümper, V. E. Korepin, and K. Kusakabe. Thermodynamics and excitations of the one-dimensional Hubbard model. *Physics Reports*, 331(5):197 – 281, July 2000.

[33] H.-U. Desgranges and K. D. Schotte. Specific heat of the Kondo model. *Physics Letters A*, 91(5):240 – 242, September 1982.

[34] M. Duflo and V. Serganova. On associated variety for Lie superalgebras. *ArXiv Mathematics e-prints*, 0507198:1 – 21, July 2005.

[35] H. Eckle, A. Punnoose, and R. A. Rømer. Absence of backscattering at integrable impurities in one-dimensional quantum many-body systems. *Europhysics Letters*, 39(3):293, August 1997.

[36] F. H. L. Essler, H. Frahm, F. Göhmann, A. Klümper, and V. E. Korepin. *The One-Dimensional Hubbard Model*. Cambridge University Press, February 2005.

[37] F. H. L. Essler and V. E. Korepin. Higher conservation laws and algebraic Bethe Ansätze for the supersymmetric $t - J$ model. *Physical Review B: Condensed Matter and Materials Physics*, 46(14):9147 – 9162, October 1992.

[38] F. H. L. Essler and V. E. Korepin. Scattering matrix and excitation spectrum of the Hubbard model. *Physical Review Letters*, 72(6):908 – 911, February 1994.

[39] F. H. L. Essler and V. E. Korepin. $SU(2)\times SU(2)$-invariant scattering matrix of the Hubbard model. *Nuclear Physics B*, 426(3):505 – 533, September 1994.

[40] V. A. Fateev and P. B. Wiegmann. Thermodynamics of the $s - d$ Exchange Model with Arbitrary Impurity Spin (Kondo Problem). *Physical Review Letters*, 46(24):1595 – 1598, June 1981.

[41] S. Ferrara, R. Fioresi, and V. S. Varadarajan. *Supersymmetry in Mathematics and Physics*, volume 2027 of *0075-8434*. Springer-Verlag, 2011.

[42] V. M. Filyov, A. M. Tsvelick, and P. B. Wiegmann. Low-temperature thernodynamics of the Anderson model. I. Symmetric case. *Physics Letters A*, 89(3):157 – 162, May 1982.

[43] L. Fritz and M. Vojta. Phase transitions in the pseudogap Anderson and Kondo models: Critical dimensions, renormalization group, and local-moment criticality. *Physical Review B: Condensed Matter and Materials Physics*, 70(21):214427–1 – 214427–24, December 2004.

[44] L. Fritz and M. Vojta. The Physics of Kondo Impurities in Graphene. *Reports on Progress in Physics*, 76(3):1 – 15, March 2013.

[45] F. Gebhard. *The Mott Metal-Insulator Transition*. Springer-Verlag, 1997.

[46] A. Georges, G. Kotliar, W. Krauth, and M. J. Rozenberg. Dynamical mean-field theory of strongly correlated fermion systems and the limit of infinite dimensions. *Reviews of Modern Physics*, 68(1):13 – 125, January 1996.

[47] T. Giamarchi. *Quantum Physics in One Dimension*. Oxford University Press, 2003.

[48] F. Göhmann. Algebraic Bethe ansatz for the gl(1|2) generalized model and Lieb-Wu equations. *Nuclear Physics B*, 620(3):501 – 518, January 2002.

[49] F. Göhmann, A. Klümper, , and A. Seel. Integral representations for correlation functions of the XXZ chain at finite temperature. *Journal of Physics A: Mathematical and Theoretical*, 37(31):7625 – 7651, August 2004.

[50] F. Göhmann and V. E. Korepin. Solution of the quantum inverse problem. *Journal of Physics A: Mathematical and General*, 33(6):1199 – 1220, February 2000.

[51] F. Göhmann and V. E. Korepin. A Quantum Version of the Inverse Scattering Transformation. *Physics of Atomic Nuclei*, 65(6):968 – 975, June 2002.

[52] F. Göhmann and S. Murakami. Fermionic representations of integrable lattice systems. *Journal of Physics A: Mathematical and General*, 31(38):7729 – 7749, September 1998.

[53] F. Göhmann and H. Schulz. The exact susceptibility of a Kondo spin-$\frac{1}{2}$ for ferromagnetic coupling and $T = 0$. *Journal of Physics: Condensed Matter*, 2(16):3841 – 3854, April 1990.

[54] F. Göhmann and A. Seel. A note on the Bethe ansatz solution of the supersymmetric t-J model. *Czechoslovak Journal of Physics*, 53(11):1041 – 1046, November 2003.

[55] F. Göhmann and A. Seel. Algebraic Bethe ansatz for the gl(1|2) generalized model: II. the three gradings. *Journal of Physics A: Mathematical and Theoretical*, 37(8):2843 – 2862, February 2004.

[56] C. Gonzalez-Buxton and K. Ingersent. Renormalization-group study of Anderson and Kondo impurities in gapless Fermi systems. *Physical Review B: Condensed Matter and Materials Physics*, 57(22):14 254 – 14 293, June 1998.

[57] G. Götz, T. Quella, and V. Schomerus. Representation theory of $sl\,(2 \mid 1)$. *Journal of Algebra*, 312(2):829 – 848, June 2007.

[58] C. Gruson and V. Serganova. Cohomology of generalized supergrassmannians and character formulae for basic classical Lie superalgebras. *Proceedings London Mathematical Society*, 101(3):852 – 892, March 2010.

[59] I. U. Heilmann, G. Shirane, Y. Endoh, R. J. Birgeneau, and S. L. Holt. Neutron study of the line-shape and field dependence of magnetic excitations in $CuCl_2 \cdot 2N(C_5D_5)$. *Physical Review B: Condensed Matter and Materials Physics*, 18(7):3530 – 3536, October 1978.

[60] M. T. Hutchings, G. Shirane, R. J. Birgeneau, and S. L. Holt. Spin Dynamics in the One-Dimensional Antiferromagnet $(CH_3)_4NMnCl_3$. *Physical Review B: Condensed Matter and Materials Physics*, 5(5):1999 – 2014, March 1972.

[61] K. Ingersent and Q. Si. Critical Local-Moment Fluctuations, Anomalous Exponents, and ω/T Scaling in the Kondo Problem with a Pseudogap. *Physical Review Letters*, 89(7):076403–1 – 076403–4, August 2002.

[62] D. Jacob and G. Kotliar. Orbital selective and tunable Kondo effect of magnetic adatoms on graphene: Correlated electronic structure calculations. *Physical Review B: Condensed Matter and Materials Physics*, 82(8):085423–1 – 085423–11, August 2010.

[63] G. Jüttner, A. Klümper, and J. Suzuki. The Hubbard chain at finite temperatures: ab initio calculations of Tomonaga-Luttinger liquid properties. *Nuclear Physics B*, 522(3):471 – 502, July 1998.

[64] V. Kac. *Representations of classical lie superalgebras*, volume 676 of *0075-8434*. Springer-Verlag, July 1977.

[65] S.-J. Kang and J.-H. Kwon. Tensor Product of Crystal Bases for $U_q(gl(m,n))$-Modules. *Communications in Mathematical Physics*, 224(3):705 – 732, December 2001.

[66] N. Kawakami and A. Okiji. Exact expression of the ground-state energy for the symmetric anderson model. *Physics Letters A*, 86(9):483 – 486, December 1981.

[67] N. Kawakami and A. Okiji. Ground State of Anderson Hamiltonian. *Journal of Physical Society of Japan*, 51(4):1145, April 1982.

[68] N. Kawakami, T. Usuki, and A. Okiji. Thermodynamic properties of the one-dimensional Hubbard model. *Physics Letters A*, 137(6):287 – 290, May 1989.

[69] A. Klümper. Thermodynamics of the anisotropic spin-1/2 Heisenberg chain and related quantum chains. *Physica B: Physics of Condensed Matter*, 91(4):507 – 519, December 1993.

[70] A. Klümper. Integrability of Quantum Chains: Theory and Applications to the Spin-1/2 XXZ Chain. *Quantum Magnetism*, 645:349 – 379, 2004.

[71] A. Klümper, M. T. Batchelor, and P. A. Pearce. Central charges of the 6- and 19-vertex models with twisted boundary conditions. *Journal of Physics A: Mathematical and General*, 24(13):3111 – 3133, July 1991.

[72] A. Klümper and O. I. Pâţu. Efficient thermodynamic description of multicomponent one-dimensional Bose gases. *Physical Review A: Atomic, Molecular, and Optical Physics*, 84(5):051604–1 – 051604–4, November 2011.

[73] A. Klümper and K. Sakai. The thermal conductivity of the spin-$\frac{1}{2}$ XXZ chain at arbitrary temperature. *Journal of Physics A: Mathematical and General*, 35(9):2173 – 2182, March 2002.

[74] J. Kondo. Resistance Minimum in Dilute Magnetic Alloys. *Progress of Theoretical Physics*, 32(1):37 – 49, July 1964.

[75] V. E. Korepin, N. M. Bogoliubov, and A. G. Izergin. *Quantum Inverse Scattering Method and Correlation Functions*. Cambridge Monographs on Mathematical Physics, March 1997.

[76] H. Kühne, M. Günther, S. Grossjohann, W. Brenig, F. J. Litterst, A. P. Reyes, P. L. Kuhns, M. M. Turnbull, C. P. Landee, and H.-H. Klauss. Low frequency spin dynamics in the quantum magnet copper pyrazine dinitrate. *Physica Status Solidi (B)*, 247(3):671 – 675, February 2010.

[77] J. Kujawa. Crystal structures arising from representations of $GL(m \mid n)$. *Representation Theory*, 10:49 – 85, February 2006.

[78] P. P. Kulish. Integrable graded magnets. *Journal of Soviet Mathematics*, 35(4):2648 – 2662, November 1986.

[79] E. H. Lieb and F. Y. Wu. Absence of Mott Transition in an Exact Solution of the Short-Range One-Band Model in One Dimension. *Physical Review Letters*, 20(25):1445 – 1448, June 1968.

[80] J. Links. Extended integrability regime for the supersymmetric U model. *Journal of Physics A: Mathematical and General*, 32(27):L315 – L319, July 1999.

[81] M. Lüscher. Dynamical Charges in the Quantized, Renormalized Massive Thirring Model. *Nuclear Physics B*, 117(2):475 – 492, December 1976.

[82] Z. Maassarani. Hubbard Models as Fusion Products of Free Fermions. *International Journal of Modern Physics B*, 12(19):1893 – 1906, 1998.

[83] M. J. Martins and P. B. Ramos. The algebraic Bethe ansatz for rational braid-monoid lattice models. *Nuclear Physics B*, 500(1):579 – 620, February 1997.

[84] M. J. Martins and P. B. Ramos. The quantum inverse scattering method for Hubbard-like models. *Nuclear Physics B*, 522(3):413 – 626, July 1998.

[85] K. M. McCreary, A. G. Swartz, W. Han, J. Fabian, and R. K. Kawakami. Magnetic Moment Formation in Graphene Detected by Scattering of Pure Spin Currents. *Physical Review Letters*, 109(18):186604–1 – 186604–5, November 2012.

[86] W. Metzner and D. Vollhardt. Correlated Lattice Fermions in $d = \infty$ Dimensions. *Physical Review Letters*, 62(3):324 – 327, January 1989.

[87] H.-J. Mikeska and M. Steiner. Solitary excitations in one-dimensional magnets. *Advances in Physics*, 40(3):191 – 356, July 1991.

[88] P. Millet, F. Mila, F. C. Zhang, M. Mambrini, A. B. Van Oosten, V. A. Pashchenko, A. Sulpice, and A. Stepanov. Biquadratic Interactions and Spin-Peierls Transition in the Spin-1 Chain $LiVGe_2O_6$. *Physical Review Letters*, 83(20):4176 – 4179, November 1999.

[89] Y. Nagaoka. Self-Consistent Treatment of Kondo's Effect in Dilute Alloys. *Physical Review Letters*, 138(4A):A1112 – A1120, May 1965.

[90] R. R. Nair, M. Sepioni, I.-L-Tsai, O. Lehtinen, J. Keinonen, A. V. Krasheninnikov, T. Thomson, A. K. Geim, and I. V. Grigoviera. Spin-half paramagnetism in graphene induced by point defects. *Nature Physics*, 8:199 – 202, January 2012.

[91] A. H. Castro Neto, F. Guinea, N. M. R. Peres, K. S. Novoselov, and A. K. Geim. The electronic properties of graphene. *Reviews of Modern Physics*, 81(1):109 – 162, January 2009.

[92] K. S. Novoselov, A. K. Geim, S. V. Morozov, D. Jiang, M. I. Katsnelson, I. V. Grigoviera, S. V. Dubonos, and A. A. Firsov. Two-dimensional gas of massless Dirac fermions in graphene. *Nature*, 438:197 – 200, November 2005.

[93] K. S. Novoselov, A. K. Geim, S. V. Morozov, D. Jiang, Y. Zhang, S. V. Dubonos, I. V. Grigoviera, and A. A. Firsov. Electric Field Effect in Atomically Thin Carbon Films. *Science*, 306(5696):666 – 669, October 2004.

[94] A. Okiji and N. Kawakami. Exact expression of magnetic susceptibility for the Anderson model. *Solid State Communications*, 43(5):365 – 367, August 1982.

[95] A. Okiji and N. Kawakami. Magnetic Properties of Anderson Model at Zero Temperature. *Journal of the Physical Society of Japan*, 51(10):3192 – 3196, June 1982.

[96] O. I. Pâţu and A. Klümper. Correlation lengths of the repulsive one-dimensional Bose gas. *Physical Review A: Atomic, Molecular, and Optical Physics*, 88(3):033623–1 – 033623–24, September 2013.

[97] I. Penkov and V. Serganova. Cohomology of G/P for classical complex Lie supergroups G and characters of some atypical G-modules. *Annales de l'institut Fourier*, 39(4):845 – 873, 1989.

[98] I. Penkov and V. Serganova. Generic irreducible representations of classical Lie superalgebras. *Differential Geometric Methods in Theoretical Physics*, 375:311 – 319, June 1990.

[99] V. Rajan, J. H. Lowenstein, and N. Andrei. Thermodynamics of the Kondo Model. *Physical Review Letters*, 49(7):497 – 500, August 1982.

[100] P. B. Ramos and M. J. Martins. Algebraic Bethe ansatz approach for the one-dimensional Hubbard model. *Journal of Physics A: Mathematical and General*, 30(7):L195, 1997.

[101] A. N. Rudenko, F. J. Keil, M. I. Katsnelson, and A. I. Lichtenstein. Adsorption of cobalt on graphene: Electron correlation effects from a quantum chemical perspective. *Physical Review B: Condensed Matter and Materials Physics*, 86(7):075422–1 – 075422–11, August 2012.

[102] P. D. Sacramento and P. Schlottmann. Low-temperature properties of a two-level system interacting with conduction electrons: An application of the overcompensated multichannel Kondo model. *Physical Review B: Condensed Matter and Materials Physics*, 43(16):13 294 – 13 304, June 1991.

[103] S. Das Sarma, S. Adam, E. H. Hwang, and Enrico Rossi. Electronic transport in two-dimensional graphene. *Reviews of Modern Physics*, 83(2):407 – 470, June 2011.

[104] M. Scheunert, W. Nahm, and V. Rittenberg. Irreducible representations of the osp(2,1) and spl(2,1) graded Lie algebras. *Journal of Mathematical Physics*, 18(1):155 – 162, January 1977.

[105] P. Schlottmann. Impurity-induced critical behaviour in antiferromagnetic Heisenberg chains. *Journal of Physics: Condensed Matter*, 3(34):6617 – 6634, March 1991.

[106] P. Schlottmann. Overcompensated impurities in antiferromagnetic Heisenberg chains. *Journal of Applied Physics*, 70(10):6071 – 6073, 1991.

[107] I. Schneider, L. Fritz, F. B. Anders, A. Benlagra, and M. Vojta. Two-channel pseudogap Kondo and Anderson models: Quantum phase transitions and non-Fermi liquids. *Physical Review B: Condensed Matter and Materials Physics*, 84(12):125139–1 – 125139–13, September 2011.

[108] J. R. Schrieffer and P. A. Wolff. Relation between the Anderson and Kondo Hamiltonians. *Physical Review Letters*, 149(2):491 – 492, September 1966.

[109] A. Seel, T. Bhattacharyya, F. Göhmann, and A. Klümper. A note on the spin-$\frac{1}{2}$ XXZ chain concerning its relation to the Bose gas. *Journal of Statistical Mechanics: Theory and Experiment*, 2007:1 – 10, August 2007.

[110] V. Serganova. Kazhdan-Lusztig Polynomials and Character Formula for the Lie Superalgebra $gl\,(m \mid n)$. *Selecta Mathematica*, 2(4):607 – 651, September 2001.

[111] B. S. Shastry. Exact Integrability of the One-Dimensional Hubbard Model. *Physical Review Letters*, 56(23):2453 – 2455, June 1986.

[112] B. S. Shastry. Infinite Conservation Laws in the One-Dimensional Hubbard Mode. *Physical Review Letters*, 56(15):1529 – 1531, April 1986.

[113] S. Shastry. Decorated Star-Triangle Relations and Exact Integrability of the One-Dimensional Hubbard Model. *Journal of Statistical Physics*, 50(1 - 2):57 – 79, January 1988.

[114] M. Shiroishi and M. Wadati. Yang-Baxter Equation for the R-Matrix of the One-Dimensional Hubbard Model. *Journal of the Physical Society of Japan*, 64(1):57 – 63, 1995.

[115] J. Suzuki, Y. Akutsu, and M. Wadati. A New Approach to Quantum Spin Chains at Finite Temperature. *Journal of the Physical Society of Japan*, 59(8):2667 – 2680, 1990.

[116] M. Suzuki and M. Inoue. The ST-Transformation Approach to Analytic Solutions of Quantum Systems. I: General Formulations and Basic Limit Theorems . *Progress of Theoretical Physics*, 78(4):787 – 799, October 1987.

[117] M. Takahashi. One-dimensional Hubbard model at finite temperature. *Progress of Theoretical Physics*, 47(1):69 – 82, January 1972.

[118] M. Takahashi. Low-Temperature Specific-Heat of One-Dimensional Hubbard Model. *Progress of Theoretical Physics*, 52(1):103 – 114, July 1974.

[119] C. Trippe and A. Klümper. Quantum phase transitions and thermodynamics of quantum antiferromagnets with competing interactions. *Low Temperature Physics*, 30(11):920 – 926, November 2007.

[120] H. Tsunetsugu. Temperature Dependence of Spin Correlation Length of Half-Filled One-Dimensional Hubbard Model. *Journal of the Physical Society of Japan*, 60(5):1460 – 1463, 1991.

[121] A. M. Tsvelick. The thermodynamics of multichannel Kondo problem. *Journal of Physics C: Solid State Physics*, 18(1):159 – 170, January 1985.

[122] A. M. Tsvelick and P. B. Wiegmann. Exact solution of the degenerate exchange model (Kondo problem for alloys with rare earth impurities). *Journal of Physics C: Solid State Physics*, 15(8):1707 – 1712, March 1982.

[123] A. M. Tsvelick and P. B. Wiegmann. Low-temperature properties of the asymmetric Anderson model (exact solution) II. *Physics Letters A*, 89(7):368 – 372, May 1982.

[124] A. M. Tsvelick and P. B. Wiegmann. Exact results in the theory of magnetic alloys. *Advances in Physics*, 32(4):453 – 713, July 1983.

[125] B. Uchoa, T. G. Rappoport, and A. H. Castro Neto. Erratum: Kondo Quantum Criticality of Magnetic Adatoms in Graphene. *Physical Review Letters*, 106(15):159901–1, April 2011.

[126] B. Uchoa, T. G. Rappoport, and A. H. Castro Neto. Kondo Quantum Criticality of Magnetic Adatoms in Graphene. *Physical Review Letters*, 106(1):016801–1 – 016801–4, January 2011.

[127] B. Uchoa, L. Yang, S.-W. Tsai, N. M. R. Peres, and A. H. Castro Neto. Theory of Scanning Tunneling Spectroscopy of Magnetic Adatoms in Graphene. *Physical Review Letters*, 103(20):206804–1 – 206804–4, November 2009.

[128] B. Uchoa, L. Yang, S.-W. Tsai, N. M. R. Peres, and A. H. Castro Neto. Orbital symmetry fingerprints for magnetic adatoms in graphene. *ArXiv e-prints*, 1105.4893:1 – 15, May 2011.

[129] Y. Umeno, M. Shiroishi, and A. Klümper. Correlation length of the 1D Hubbard model at half-filling: Equal-time one-particle Green's function. *Europhysics Letters*, 62(3):384, 2003.

[130] T. Usuki, N. Kawakami, and A. Okiji. Thermodynamic Quantities of the One-Dimensional Hubbard Model at Finite Temperatures. *Journal of Physical Society of Japan*, 59(4):1357 – 1365, 1990.

[131] M. Vojta. Impurity quantum phase transitions. *Philosophical Magazine*, 86(13 - 14):1807 – 1846, 2006.

[132] M. Vojta and R. Bulla. A fractional-spin phase in the power-law Kondo model. *European Physical Journal B - Condensed Matter and Complex Systems*, 28(3):283 – 287, August 2002.

[133] M. Vojta and L. Fritz. Upper critical dimension in a quantum impurity model: Critical theory of the asymmetric pseudogap Kondo problem. *Physical Review B: Condensed Matter and Materials Physics*, 70(9):094502–1 – 094502–4, September 2004.

[134] Y. Wang and J. Dai. Kondo effect in a quantum critical ferromagnet. *Physical Review B: Condensed Matter and Materials Physics*, 59(21):13561 – 13564, June 1999.

[135] T. O. Wehling, A. V. Balatsky, M. I. Katsnelson, A. I. Lichtenstein, and A. Rosch. Orbitally controlled Kondo effect of Co adatoms on graphene. *Physical Review B: Condensed Matter and Materials Physics*, 81(11):115427–1 –115427–6, March 2010.

[136] T. O. Wehling, A. I. Lichtenstein, and M. I. Katsnelson. Transition metal ad-atoms on graphene: Influence of local Coulomb interactions on chemical bonding and magnetic moments. *Physical Review B: Condensed Matter and Materials Physics*, 84(23):35110–1 – 235110–7, December 2011.

[137] M. F. Weiss and K. D. Schotte. Lattice approach to the spectrum of the massive thirring model. *Nuclear Physics B*, 225(2):247 – 260, October 1983.

[138] P. B. Wiegmann. Exact solution of the s-d exchange model (Kondo problem). *Journal of Physics C: Solid State Physics*, 14(10):1463 – 1478, April 1981.

[139] P. B. Wiegmann and A. M. Tsvelick. Exact solution of the Anderson model: I. *Journal of Physics C: Solid State Physics*, 16(12):2281, 1983.

[140] K. G. Wilson. The renormalization group: Critical phenomena and the Kondo problem. *Reviews of Modern Physics*, 47(4):773 – 840, October 1975.

[141] D. Withoff and E. Fradkin. Phase transitions in gapless Fermi systems with magnetic impurities. *Physical Review Letters*, 64(15):1835 – 1838, April 1990.

[142] C. N. Yang and C. P. Yang. Thermodynamics of a One-Dimensional System of Bosons with Repulsive Delta-Function Interaction. *Journal of Mathematical Physics*, 10(7):1115 – 1122, July 1969.

[143] W.-L. Yang, Y.-Z. Zhang, and S.-Y. Zhao. Drinfeld twists and algebraic Bethe ansatz of the supersymmetric $t - J$ model. *Journal of High Energy Physics*, 12(032):1 – 23, December 2004.

[144] R. Yue and T. Deguchi. Analytic Bethe ansatz for 1D Hubbard model and twisted coupled XY model. *Journal of Physics A: Mathematical and General*, 30(3):849, 1997.

[145] R. B. Zhang. Finite dimensional irreducible representations of the quantum supergroup $U_q\left(gl\left(m/n\right)\right)$. *Journal of Mathematical Physics*, 34(3):1236 – 1254, September 1992.

[146] R. B. Zhang. Bott-Borel-Weil construction for quantum supergroup $U_q\left(gl\left(m \mid n\right)\right)$. *Journal of Mathematical Physics*, 38(7):3863 – 3884, April 1997.

[147] R. B. Zhang. Structure and Representations of the Quantum General Linear Supergroup. *Communications in Mathematical Physics*, 195(3):525 – 547, August 1998.

[148] Z.-G. Zhu, K.-H. Ding, and J. Berakdar. Single- or multi-flavor Kondo effect in graphene. *Europhysics Letters*, 90(6):67001–p1 – 67001–p5, June 2010.

Erklärung

Ich versichere hiermit, gemäß § 7 (2) der Promotionsordnung zur Verleihung der akademischen Grade Dr. rer. nat. und Dr. paed. (Fassung vom 18.02.2008), dass ich die eingereichte Arbeit selbständig verfasst, bei der Abfassung der Arbeit nur die in der Dissertation angegebenen Hilfsmittel benutzt und alle wörtlich oder inhaltlich übernommenen Stellen als solche gekennzeichnet habe. Außerdem versichere ich, dass ich die Dissertation in der gegenwärtigen oder einer anderen Fassung nicht schon einem anderen Fachbereich einer wissenschaftlichen Hochschule vorgelegt habe.

Ort: Wuppertal

Datum: 30.11.2017

Unterschrift: Yahya Öz

Danksagung

Das selbstständige Verfassen der Arbeit ist nur reinen Gewissens zu unterschreiben, wenn allen, die am Entstehen beteiligt waren, angemessener Dank ausgesprochen wird.
So stehe ich tief in der Schuld von Prof. Andreas Klümper, der die Arbeit von Beginn an betreute, mir die Möglichkeit gab, an dieser interessanten Aufgabe zu arbeiten und an Engstellen das Vorankommen sicherte. Seine intensive Unterstützung, vielen hilfreichen Anregungen und Diskussionen während der Arbeit an der Dissertation waren von unschätzbarem Wert.
Weiterhin gilt mein Dank Priv.-Doz. Frank Göhmann, der die Fortschritte mit Herz verfolgte und Fragen mit Sachverstand zu beantworten wusste.
Kolleginnen und Kollegen des gesamten Lehrstuhls in früherer und aktueller Besetzung trugen bewusst oder unbewusst zu neuen Ideen innerhalb einer angenehmen Atmosphäre bei. Unter ihnen befinden sich Priv.-Doz. Michael Karbach, Prof. Hermann Boos, Priv.-Doz. Andreas Fledderjohann, Dr. Khazretali Nirov sowie Dr. Michael Brockmann, Dr. Maxime Dugave, M. Sc. Raphael Kleinemühl, M. Sc. Christina Ballnus, M. Sc. Dennis Wagner, M. Sc. Eyzo Stouten, M. Sc. Arthur Hutsalyuk, M. Sc. Rubina Zadourian und Dipl.-Phys. Win Nuding.
Für die jahrelange Unterstützung meiner Arbeit bedanke ich mich bei der Studienstiftung des deutschen Volkes. Ich spreche hier erneut meinen Dank an Herrn Prof. Andreas Klümper aus, der an dieser Stelle auch als Vertrauensdozent tätig war.
Besonders danke ich meinen Freunden und meiner Familie für ihre liebevolle Unterstützung und Geduld.